NBS SPECIAL PUBLICATION 580

U.S. DEPARTMENT OF COMMERCE / National Bureau of Standards

The State-of-the-Art of Thermal Analysis

NATIONAL BUREAU OF STANDARDS

The National Bureau of Standards[1] was established by an act of Congress on March 3, 1901. The Bureau's overall goal is to strengthen and advance the Nation's science and technology and facilitate their effective application for public benefit. To this end, the Bureau conducts research and provides: (1) a basis for the Nation's physical measurement system, (2) scientific and technological services for industry and government, (3) a technical basis for equity in trade, and (4) technical services to promote public safety. The Bureau's technical work is performed by the National Measurement Laboratory, the National Engineering Laboratory, and the Institute for Computer Sciences and Technology.

THE NATIONAL MEASUREMENT LABORATORY provides the national system of physical and chemical and materials measurement; coordinates the system with measurement systems of other nations and furnishes essential services leading to accurate and uniform physical and chemical measurement throughout the Nation's scientific community, industry, and commerce; conducts materials research leading to improved methods of measurement, standards, and data on the properties of materials needed by industry, commerce, educational institutions, and Government; provides advisory and research services to other Government agencies; develops, produces, and distributes Standard Reference Materials; and provides calibration services. The Laboratory consists of the following centers:

Absolute Physical Quantities[2] — Radiation Research — Thermodynamics and Molecular Science — Analytical Chemistry — Materials Science.

THE NATIONAL ENGINEERING LABORATORY provides technology and technical services to the public and private sectors to address national needs and to solve national problems; conducts research in engineering and applied science in support of these efforts; builds and maintains competence in the necessary disciplines required to carry out this research and technical service; develops engineering data and measurement capabilities; provides engineering measurement traceability services; develops test methods and proposes engineering standards and code changes; develops and proposes new engineering practices; and develops and improves mechanisms to transfer results of its research to the ultimate user. The Laboratory consists of the following centers:

Applied Mathematics — Electronics and Electrical Engineering[2] — Mechanical Engineering and Process Technology[2] — Building Technology — Fire Research — Consumer Product Technology — Field Methods.

THE INSTITUTE FOR COMPUTER SCIENCES AND TECHNOLOGY conducts research and provides scientific and technical services to aid Federal agencies in the selection, acquisition, application, and use of computer technology to improve effectiveness and economy in Government operations in accordance with Public Law 89-306 (40 U.S.C. 759), relevant Executive Orders, and other directives; carries out this mission by managing the Federal Information Processing Standards Program, developing Federal ADP standards guidelines, and managing Federal participation in ADP voluntary standardization activities; provides scientific and technological advisory services and assistance to Federal agencies; and provides the technical foundation for computer-related policies of the Federal Government. The Institute consists of the following centers:

Programming Science and Technology — Computer Systems Engineering.

[1]Headquarters and Laboratories at Gaithersburg, MD, unless otherwise noted; mailing address Washington, DC 20234.
[2]Some divisions within the center are located at Boulder, CO 80303.

The State-of-the-Art of Thermal Analysis

Proceedings of a Workshop
Held at the National Bureau of Standards,
Gaithersburg, Maryland, May 21-22, 1979

Edited by:

Oscar Menis *
Harry L. Rook

National Measurement Laboratory
National Bureau of Standards
Washington, D.C. 20234

and

Paul D. Garn

University of Akron
Akron, Ohio 44304

* deceased

* Special publication

U.S. DEPARTMENT OF COMMERCE, Philip M. Klutznick, Secretary

Luther H. Hodges, Jr., Deputy Secretary
Jordan J. Baruch, Assistant Secretary for Productivity, Technology and Innovation

NATIONAL BUREAU OF STANDARDS, Ernest Ambler, Director

Issued August 1980

Library of Congress Catalog Card Number: 80-600099

National Bureau of Standards Special Publication 580

Nat. Bur. Stand. (U.S.), Spec. Publ. 580, 265 pages (Aug. 1980)
CODEN: XNBSAV

U.S. GOVERNMENT PRINTING OFFICE
WASHINGTON: 1980

For sale by the Superintendent of Documents, U.S. Government Printing Office, Washington, D.C. 20402
Price $7.00
(Add 25 percent for other than U.S. mailing)

IN MEMORIUM

We of the Center for Analytical Chemistry would like to dedicate this book to Dr. Oscar Menis who died December 12, 1979. Dr. Menis joined NBS in 1965 as Chief of the Analytical Coordination Chemistry Section of the Analytical Chemistry Division. At the time of his passing he was Senior Scientist, Gas and Particulate Science Division, Center for Analytical Chemistry. This book and the workshop held in May 1979 were his last major contributions to the chemical world. In working with Dr. Menis to prepare these papers for print we felt that it took a great effort on his part to find the time and energy needed for an undertaking of this sort. We hope that those of you who attended the workshop and those reading this book for information will enjoy Dr. Menis' book.

J. J. Shoemaker and Co-workers
of the Text Editing Facility

FOREWORD

Thermal analysis has long been an important technique to characterize materials such as clays, minerals, inorganic systems, metals, and alloys. G. K. Burgess, second director of the National Bureau of Standards, is credited as being the first American to use or mention differential thermal analysis (DTA).

His contribution is described in the following excerpt from A History of Analytical Chemistry, Eds., H. A. Laitinen and G. W. Ewing (Division of Analytical Chemistry, American Chemical Society, 1977); p. 46.

"The first American to use or to mention DTA was G. K. Burgess of the National Bureau of Standards, who published a classic paper on cooling curves in 1908. He discussed the various methods of recording cooling curves, including the use of differential curves, derivative curves, and so on. This article is an excellent review of the state-of-the-art up to 1908."

They further point out that the 1960's saw the introduction of elaborate DTA instruments and after 1960, DTA became an important technique in most branches of chemistry.

During this time the need for dynamic temperature standards was recognized and the Committee on Standardization of the International Confederation for Thermal Analysis (ICTA) was formed in 1966. The National Bureau of Standards, as a member of this Committee, participated in the planning and implementation of a test program designed to screen proposed standards. By 1967, priorities had been established and a number of materials were tested with first priority being given to inorganic specimens in the temperature range, ambient to 1000 °C.

This program has fulfilled many of its objectives. The NBS Office of Standard Reference Materials announced in 1978 the availability of five Special Reference Materials that have been certified by ICTA for dynamic measurement of temperature by differential thermal analysis and differential scanning calorimetry.

To focus attention on the recent trends and needs in the field of thermal analysis, NBS, in 1970, organized a Symposium on the Current Status of Thermal Analysis, joint with the American Society for Testing Materials (ASTM). The papers from this symposium were published as Status for Thermal Analysis, NBS Special Publication 338, 185 pages (1970). The first volume reviewed the progress on development of standards for temperature calibration based on dynamic measurements and thermal analysis applications for characterization of materials.

The present volume contains texts of invited lectures presented at the workshop on the State-of-the-Art in Thermal Analysis, held at NBS May 21-22, 1979. In contrast to the first publication, this second volume represents an advanced and sophisticated field of thermoanalytical techniques for solving problems related to current national issues including conservation of energy and environmental health and safety.

The workshop considered practical applications of thermal analysis which are just beginning to appear in many industrial processes. The applications summarized here are discussed in detail in the workshop proceedings. In the glass manufacturing industry thermal methods are used to study the behavior of glass during heating and devitrification. Thermal analysis techniques are used by steel industries for second phase determination to find the physical properties of steel such as its ductility and its behavior at freezing temperatures, an important consideration for the Alaskan pipeline. In the rubber industry thermoanalytical techniques are used to determine the basic thermal stability of elastomers, the qualitative and quantitative analysis of elastomers, the heat of vulcanization, and the low temperature properties of elastomeric products. Other areas utilizing thermal analysis for qualitative and quantitative determinations and for monitoring technological processes include studies on polymer ignition, ceramic processes and energy conservation, chemical complexes, measurements at high pressures, and analyses of ancient paper technology.

Thermal analysis has made it possible to undertake analyses of complex systems, on a routine basis, which are not possible by other techniques. In many cases the full potential of thermal analysis is just beginning to be achieved. Major advances may be possible through use of computer techniques for data reduction and analysis, and through increased acceptance by industries of thermal analysis as a practical as well as a research tool.

It is gratifying to see a field which started as a disipline in 1908, lead to a research program in the 1960's, and come to fruition for innovative and useful applications which can only increase in the 1980's.

With sadness we note the death of Oscar Menis. Colleague and co-editor of these workshop proceedings, Paul D. Garn, has stated in the Preface that this was Oscar Menis' last completed project. Surely it must have been satisfying to Oscar Menis to be part of a successful program to provide temperature standards for thermal analysis and to see the application of the thermoanalytical techniques to solving problems of national concern.

C. W. Reimann, Director
Center for Analytical Chemistry

PREFACE

The purpose in having this type of workshop from time to time is to provide for interchange of information between the diverse segments of science and technology which are involved in thermoanalytical studies. Advances made in one field may be also useful in a quite different area. In the proliferation of literature, two groups (for an example, ceramic and polymer chemists) may fail to notice each others contributions.

In an earlier meeting of this kind at NBS in 1970, a small step was made toward that goal. At that time an effort was made to look at a variety of sciences ranging from biochemistry to high temperature technology. But limitations of available speakers and shortness of time left many areas untouched. Similarly, this Workshop is not an absolute milestone, but an attempt to collect into one meeting the progress and innovations of a number of fields, and thus – through sharing – provide a synergistic effect on the use of thermoanalytical techniques for solving some of the current problems that are of real concern to all.

One of these, the conservation of energy, is a timely theme that warranted examination by a number of speakers, while another theme related to environmental problems. Pertaining to major users of energy, Dollimore dealt with the issue of how thermoanalytical data can be utilized in interpreting and controlling the process in the chemical industry, and Ott specifically examined the means of saving energy in the ceramic industry. Conservation of energy is also accomplished by minimization of waste and control of the quality of product. One aspect of it is process control; another is product or material evaluation. These two areas were covered respectively by Brazier in the rubber, and by Bandi in the steel industry. Another method of conserving energy is by lowering processing temperature, or increasing the rate of reaction through catalysis. The problem of producing catalysts reproducibly requires thorough knowledge of decomposition processes. Garn described one important method for obtaining catalysts by thermal decomposition of coordination compounds whose thermal behavior in many cases depends upon their thermodynamic environment. In a more direct way, the utilization of an energy source – coal – called for the development of a special high pressure thermogravimetric apparatus, by Gardiner et al., that might be useful in related technologies wherein data on centigram samples cannot be related with confidence to working batches a million times larger.

A second area of current concern is environmental health and safety. Three lecturers dealt with separate aspects. The emission of noxious materials from industrial processing is a major irritant. Very often, these noxious substances are collected – from stacks or other effluents – by adsorption. This use requires reproducible production, which in turn requires good knowledge of the physical-chemical properties, as described by Rouquerol, of the adsorbent as functions of the method of production. In another area, for the last decade, flame retardance has been investigated very intensively with a goal of avoiding active flame. Understanding of the ignition process itself (Miller and Martin) is critical to progress in this field. In another public concern, enthalpimetric analysis, as described by Jordan et al., is valuable in health-related studies because a very nonspecific property, heat, can be used for very specific measurements when enzymes are involved.

Not all uses of thermal analysis are technological; some are investigative, as in forensic science or archeology. An example of the latter is the examination and comparison of papyri of different cultures, by Wiedemann.

Finally, utilization of up-to-date knowledge may be impracticable without up-to-date instruments; hence Wendlandt's summing up of recent developments in instrumentation is very pertinent.

The constraints of meeting time and the unavailability of speakers eliminated some themes of lesser priority. Hopefully, progress in those areas will be aided by these summations in their more limited fields.

The editors are grateful to the Analytical Chemistry Center of the National Bureau of Standards for supporting this meeting, furnishing physical facilities and personnel for conducting it, in providing for the publication of these proceedings, and to the University of Akron for its support in services and communications. Finally, we acknowledge the contributions of distinguished rapporteurs in conducting the Workshop.

We also note with sadness the death of an esteemed colleague, W. R. Bandi, a few weeks after his contribution to our meeting.

Editors:

Oscar Menis

Paul D. Garn

This was Oscar Menis's last completed project. He died 12 December 1979 just after turning in the last of these papers for setting into the production-ready format. Our world is better for his having gone through it.

Paul D. Garn

Abstract

A workshop on the State-of-the-Art in Thermal Analysis was held at the National Bureau of Standards, May 21-22, 1979. This volume contains the texts of the invited lectures with summaries by the rapporteurs. Topics covered include the variety of uses of thermal analysis in industrial processing, such as the measurement of the temperature coefficients needed for pilot plant design in the chemical industry, quality control and product testing in the rubber industry, a review of instrumental developments, descriptions of enthalpimetry, high pressure thermogravimetry using large samples, reports on polymer ignition, energy conservation in ceramic processing, industrial adsorbents, coordination compounds, and studies of ancient paper technology. Also, a poster session was provided for contributed presentation; these included a dynamic mechanical analysis system, high pressure DTA to study glass transitions, aluminum alloy microstructure, characterization of thermoplastics, and simultaneous thermogravimetry and differential scanning calorimetry. Abstracts of the poster presentations are included.

Key Words: Adsorbents; chemical processing; coordination compounds; enthalpimetry; glass processing; instrumentation; paper technology; polymer ignition; rubber processing; thermal analysis; thermogravimetry.

TABLE OF CONTENTS

National Bureau of Standards Special Publication 580. Proceedings of the Workshop on the State-of-the-Art of Thermal Analysis held at NBS, Gaithersburg, MD, May 21-22, 1979. (Issued May 1980)

THERMAL ANALYSIS IN CHEMICAL PROCESSING

David Dollimore

Department of Chemistry and Applied Chemistry
University of Salford, Salford,
M5 4WT, England

Abstract

The interpretation of the science and technology of chemical processing must be dominated by the simple knowledge that the particular process is kinetically or thermodynamically dominated. This in turn decides how thermal analysis data on the subject is to be treated. The subject is made complicated by the fact that both types of process are described by the same basic equation, namely,

$$\log k = A - \frac{C}{T}$$

where k is a particular property based upon either thermodynamic or kinetic principles depending upon the process investigated and the environmental conditions of the investigation.

In thermodynamically dominated processes the Vant Hoff equation describes the conditions;

$$\log_e K_p = \frac{-\Delta H}{RT} + \text{constant}$$

where K_p is the equilibrium constant, ΔH is the heat of reaction, R the gas constant and T the temperature in degrees kelvin.

For a description of kinetic processes the Arrhenius equation is used in the form,

$$\log_e k = \frac{-E}{RT} + \text{constant},$$

where k is the specific reaction rate and E the activation energy.

It can be demonstrated that rising temperature data can be used to calculate the specific reaction rate in the Arrhenius equation. If, however, the rising temperature data is not a reflection of kinetic changes, then it would be erroneous to apply the kinetic interpretation. It would also be in error to interpret data as representing the equilibrium condition if the data did not comply with thermodynamic principles.

Some simple observations are made indicating the characteristic phenomena if the rising temperature regime applied to a particular system under specified conditions is a reflection of the changing equilibrium conditions or represents kinetic parameters. Further conditions are then laid down to ensure that kinetic parameters calculated under particular experimental restraints actually refer to the chemical reaction itself and not to a diffusion-controlled kinetic process.

Various technological processes drawn from the fields of glass manufacture, ceramics, and catalysis are then discussed with reference to the information provided by thermal analysis methods on these subjects.

1. Introduction

Many chemical processes of industrial importance involve an alteration in the temperature during the course of the reaction or reactions that are taking place. This is in contrast to classical laboratory investigations which either allow equilibrium to be established at a particular temperature or follows the rate of change of the chemical system again with the temperature constant. There is thus often a divergence between industrial chemical processes and the nature of the corresponding laboratory experiments. The methods of thermal analysis, however, follow industrial processes by allowing temperatures to change and could if needed follow a temperature regime which matched the process under consideration. One then, however, has to evolve methods of interpreting the data in terms of equilibrium or kinetic parameters, depending on which is appropriate.

An example that can be quoted is the carbonization of coal to produce coke. Van Krevelen and co-workers [1,2][1], and Fitzgerald [3] treated this as a system responding to kinetic parameters based on three successive reactions,

Step One,
$$\text{Coking coal(P)} \xrightarrow{k_1} \text{Metaplast(M)},$$

Step Two,
$$\text{Metaplast(M)} \xrightarrow{k_2} \text{Semi-Coke(R)} + \text{Primary Gas}(G_1),$$

Step Three,
$$\text{Semi-Coke(R)} \xrightarrow{k_3} \text{Coke(S)} + \text{Secondary Gas}(G_2),$$

where k_1, k_2, and k_3 denote the respective velocity constants. Van Krevelen considered that step one is a depolymerization reaction whilst the second is a coking process. Both of these are normally considered to be first order. The third reaction is more complex, but Van Krevelen simplifies the problem by dealing with it as a first-order reaction.

Thus,

$$-\frac{dP}{dt} = k_1 P \tag{1}$$

$$\frac{dM}{dt} = k_1 P - k_2 M \tag{2}$$

and

$$\frac{dG}{dt} = \frac{dG_1}{dt} + \frac{dG_2}{dt} \tag{3}$$

$$= k_2 M + k_3 R$$

[1]Figures in brackets indicate the literature references at the end of this paper.

Van Krevelens treatment is restricted to temperatures below that at which the degasification rate reaches a maximum (T_{md}) so that

$$\left(\frac{dG_2}{dt}\right)_{T < T_{md}} = 0 \tag{4}$$

or

$$\left(k_3\right)_{T < T_{md}} = 0. \tag{5}$$

Van Krevelen also assumed that the specific reaction rate constants were of the same magnitude, so that,

$$k_1 \Omega k_2 \Omega k_3.$$

This treatment produces a final equation of the form,

$$\frac{G}{P_o} = 1 - (kt + 1)\cdot e^{-kt} \tag{6}$$

where G = amount of gas produced

and P_o = original material

so that $\frac{G}{P_o}$ = the fraction decomposed (α) in time t,

and k is a rate constant.

Hence,

$$(1 - \alpha) = (kt + 1)\cdot e^{-kt} \tag{7}$$

$$\frac{d\alpha}{dt} = k' \cdot t \cdot e^{-kt} \tag{8}$$

and

$$(1 - \alpha) = (kt + 1) \cdot \frac{1}{k't} \cdot \frac{d\alpha}{dt} \tag{9}$$

Krevelen and Schuyer [2] then went on to produce one of the earlier solutions to the determination of kinetic parameters (i.e., the pre-exponential term and the activation energy in the Arrhenius Equation) from rising temperature data.

2. Thermodynamically Dominated Systems

In practice, thermodynamics relates to those properties which describe equilibrium conditions. It is possible that under appropriate experimental restraints the thermal analysis techniques with a programmed temperature regime will produce equilibrium properties.

The Vant Hoff equation describes the equilibrium condition,

$$\ln \cdot K_p = \frac{-\Delta H}{RT} + \text{constant} \tag{10}$$

where K_p is the equilibrium constant, ΔH is the heat of reaction, R the gas constant, and T the temperature in degrees kelvin.

In a typical application of this equation to a solid state thermal decomposition, the effect of heat on calcium carbonate may be considered. This is the basis of the industrially important process where limestone is heat treated to produce quick-lime. The equation for this reaction is,

$$CaCO_3(s) = CaO(s) + CO_2(g).$$

Le Chateliers principle may be quoted to indicate qualitatively what may happen. This notes that if a change occurs in one of the factors, such as temperature or pressure, under which a system is in equilibrium, the system will tend to adjust to annul as far as possible the effect of that change. Thus, if equilibrium is set up at a particular temperature and pressure of carbon dioxide in the calcium carbonate system and the temperature is increased, then the equilibrium pressure of carbon dioxide will be adjusted to a higher value to attain a fresh equilibrium position.

Equation 10 describes this situation quantitatively, and in this particular case under consideration, $K_p = P_{CO_2}$ where p_{CO_2} is the equilibrium pressure of carbon dioxide. In principle, the equipment required is relatively simple, being a fixed volume container with the calcium carbonate in a furnace and a pressure measurement device attached. Starting with the calcium carbonate under vacuum, the solid is heated and the equilibrium pressure at various temperatures noted. Such equipment can have various degrees of sophistication, but can only be applied to a single step reaction such as is represented by the decomposition of calcium carbonate. The data are usually shown plotted as log p_{CO_2} against 1/T where T is the temperature in degrees kelvin. The data are shown in figure 1. The equation in this instance is,

$$\ln p_{CO_2} = \frac{-\Delta H}{RT} + \text{constant}, \qquad (11)$$

and similar equations should be shown for all systems of the kind,

$$A(s) \rightarrow B(s) + C(g).$$

There are, however, other patterns of experimental behavior. The first is that the dissociation pressure does not depend on the temperature, but remains more or less invariant. The second variation in behaviour is that the system is obeyed in the rising temperature mode only and is not reversible on the decreasing temperature mode. Various aspects of the application of the Vant Hoff equation have been discussed previously [4,5], but here the practical interpretation of these two behavior patterns are mentioned. Both variant behavior patterns are probably best explained on the basis of the formation of an impervious layer of solid product over the solid reactant, thus preventing in some cases further reaction or the reversibility of the process. An interesting example of some industrial importance is the thermal decomposition of the mineral dolomite ($CaMg(CO_3)_2$). This decomposes in two stages [6]:

$$CaMg(CO_3)_2 \rightarrow CaCO_3 + MgO + CO_2,$$

followed at a higher temperature by

$$CaCO_3 \rightarrow CaO + CO_2.$$

The first reaction represents the breakdown of the dolomite lattice into the two carbonates at a temperature above the normal decomposition temperature of the magnesium carbonate and this explains the fact that its decomposition pressure is invariant with temperature. The second stage represents the decomposition of calcium carbonate and can be shown to obey the Vant Hoff equation.

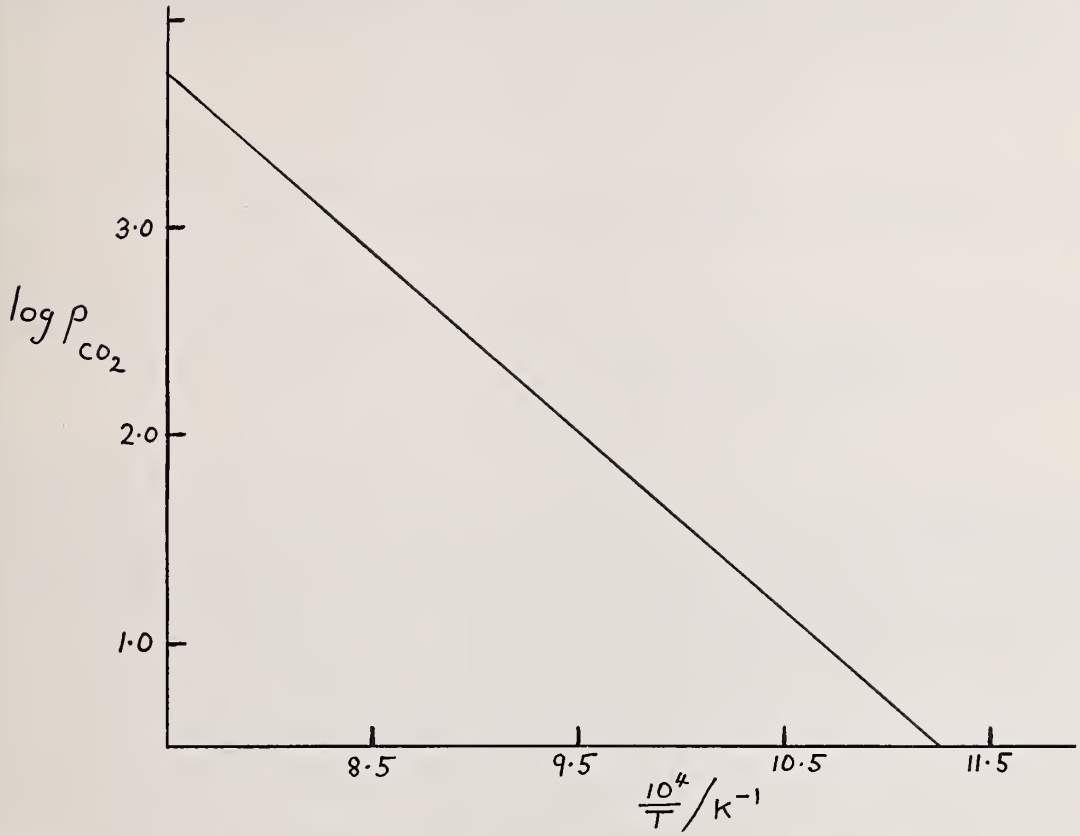

Figure 1. The variation of the equilibrium pressure of carbon dioxide with the temperature for the heat treatment of calcium carbonate.

Ordinate: $\log p_{CO_2}$ where p_{CO_2} is the dissociation pressure of carbon dioxide over calcium carbonate.

Abscissae: $\left(\frac{10^4}{T}\right) \Big/ K^{-1}$ where T is the temperature of heat treatment in degrees kelvin.

An alternative and often much easier method of establishing such data is by the methods of thermal analysis. Thus, if calcium carbonate is decomposed in a differential thermal analysis (DTA) unit under various pressures of carbon dioxide, then the onset of the endothermic decomposition peak can be shown to be dependent upon the pressure. The method is especially useful where there are a series of dissociation processes. Thus, manganese dioxide prepared by the thermal decomposition of manganese nitrate goes through a series of dissociation reactions with the liberation of oxygen [7,8],

$$MnO_2 \underset{T_1}{\rightarrow} Mn_2O_3 \underset{T_2}{\rightarrow} Mn_3O_4 \underset{T_3}{\rightarrow} MnO.$$

Apart from any crystal transformations that may occur, the three dissociations may be observed at any stated partial pressure of oxygen such that,

$$T_1 < T_2 < T_3.$$

If the partial pressure of oxygen is increased, then these temperatures are increased T_1 to $T_1 + \Delta T_1$, T_2 to $T_2 + \Delta T_2$, etc., so that,

$$T_1 + \Delta T_1 < T_2 + \Delta T_2 < T_3 + \Delta T_3.$$

Then for each transition the Vant Hoff equation (eq. 10) holds, and plots of log p against 1/T are linear.

Dehydration reactions may be studied in this way using DTA runs carried out in the presence of controlled pressures of water vapor, and the stages involved may be many. The dehydration of copper sulphate may be quoted as an example [9,10,11,12],

$$CuSO_4 \cdot 5H_2O \rightleftharpoons CuSO_4 \cdot 3H_2O + \text{vapor}$$

$$CuSO_4 \cdot 5H_2O \rightleftharpoons CuSO_4 \cdot 3H_2O + \text{soln. (96 °C)}$$

$$\text{Soln.} \rightleftharpoons CuSO_4 \cdot 3H_2O + \text{vapor}$$

$$CuSO_4 \cdot 3H_2O \rightleftharpoons CuSO_4 \cdot H_2O + \text{vapor}$$

$$CuSO_4 \cdot H_2O \rightleftharpoons CuSO_4 + \text{vapor}.$$

To study this system over a wide range of water vapor pressure (p_{H_2O}) involves difficulties, but the system is reported in detail and plotted in the form of $\ln p_{H_2O}$ against 1/T by Berg and co-workers [9,10]. The main difficulty is that with an ambient temperature of about 25 °C, the various concentrated salt solutions can be used to produce a maximum saturated vapor pressure equivalent to only 2.2 cms of mercury. To reach a saturated vapor pressure of one atmosphere and thus increase the range of observations, the ambient temperature has to be raised to 100 °C. This can be achieved by placing the DTA head, furnace, and ancillary equipment into an oven and operating the oven at controlled constant temperatures between room temperature and 100 °C. With the water storage system also in the oven, this controls the saturated vapor pressure.

In all these systems, to apply the data collected to the Vant Hoff equation the DTA system must record equilibrium conditions.

3. Kinetically Dominated Systems

Kinetic systems are studied by measuring the rate of change against time at a constant temperature. This experiment is then repeated at a series of temperatures. The form of the rate of change against time must first be elucidated and the specific reaction rate determined. The data collected in this way can then be fitted to the Arrhenius equation,

$$k = A.e^{-E/RT} \tag{12}$$

or

$$\ln k = \frac{-E}{RT} + \ln A \tag{13}$$

where k is the specific reaction rate,
A is the pre-exponential factor,
and E is the Activation Energy.

In homogeneous liquid phase reactions, the rate of change can be expressed in concentration terms, whilst in homogeneous gaseous phase reactions the rate of change can be expressed in units of pressure, if the volume of the system remains the same. This is also true for heterogeneous reactions involving a solid-state decomposition producing a gaseous reaction product, but again the volume of the system must remain the same. However, the progress of a solid-state decomposition is often monitored by noting the change in weight of the solid phase, and the system may not be such that the volume remains the same. Often the pressure is constant or the reaction may be carried out with constant pumping to maintain a vacuum condition, or the system may be dynamic and the experimental environment consist of a flowing stream of inert gas usually at atmospheric pressure. In such systems the rate of change is monitored in terms of the change in weight of the solid residue and expressed as the fractional decomposition (α) against time (t). If the conditions of experimentation are suitable then the rate of reaction ($\frac{d\alpha}{dt}$) is based on the changing geometry of a reaction interface. Under other conditions the rate of reaction may be determined by a diffusion mechanism modified by the geometry of the system. In this way, for solid state decompositions various theoretical expressions [13] may be derived of the form,

$$\frac{d\alpha}{dt} = kf(\alpha) \tag{14}$$

where $f(\alpha)$ is some function of α and k is a specific reaction rate. By analogy with homogeneous reaction rate treatments, when the reaction rate equals the specific reaction rate at unit concentration, then,

$$\frac{d\alpha}{dt} = k$$

when $1-\alpha \rightarrow 1$
or $\alpha \rightarrow 0$
and $f(\alpha) \rightarrow 1.$

In rising temperature experiments, the temperature program is imposed on the system and can be represented by,

$$T = T_o + \beta t \tag{15}$$

where T_o is the initial temperature and a linear heating rate β is imposed, while t is the time of heating.

In theory these three basic equations (i.e. eq. 13, 14, and 15) can be used to determine the kinetic parameters, but it should be noted that the constant k in the Arrhenius equation is given by,

$$k = \frac{RT}{Nh} \cdot K^{\neq} \tag{16}$$

where h is Plancks constant and $K^{\neq}$ is the equilibrium constant for the activated complex. This may be developed in terms of thermodynamic functions, namely,

$$\Delta G^{\neq} = -RT \ln K^{\neq} \tag{17}$$

and

$$\Delta G^{\neq} = \Delta H^{\neq} - T\Delta S^{\neq} \tag{18}$$

where the suffix refers to the formation of the activated complex. Comparison with the Arrhenius equation allows,

$$E \text{ to be identified with } \Delta H^{\neq}$$

and

$$A \text{ with } \frac{RT}{Nh} \cdot e^{\Delta S^{\neq}/R}$$

where $\Delta S^{\neq}$ is the entropy change associated with the change to the activated complex. The pre-exponential term A can also be written in terms of the partition functions, as,

$$A = \frac{RT}{Nh} \frac{Q^{\neq}}{Q} \tag{19}$$

where $Q^{\neq}$ is the complete partition function for the activated complex, excluding that for the reaction coordinate, and Q is the complete partition function for the reactant. Both forms of the equation have been used in solid state reactions [14,15].

The correct form of the specific reaction rate should be chosen (i.e., it fulfills the limiting conditions set out above). Rate equations may be expressed in integral forms or differential forms. It follows from the above that it is the constant appearing in the differential form that represents the true specific reaction rate constant, and it is this which should be used. Table 1 indicates that only in the first and second order expressions is the constant the same in the integral and differential form. In solid state processes, the rate equation is expressed in the form,

$$kt = 1(\alpha) \tag{20}$$

where $1(\alpha)$ is some function of α and, for example, in the third equation in Table 1, the integral form is,

$$kt = 1 - (1-\alpha)^{2/3} \tag{21}$$

while the differential form is

$$\frac{d\alpha}{dt} = \frac{3k}{2} (1-\alpha)^{1/3} \tag{22}$$

and the specific reaction rate is $3/2 \cdot k$. In Table 1 the equations all show the formal requirement already mentioned for a specific reaction rate, and for the above example this is,

$$\frac{d\alpha}{dt} = \frac{3k}{2} \quad \text{, when } 1-\alpha \to 1$$

$$\text{or} \quad \alpha \to 0$$

$$\text{and } f(\alpha) \to 1$$

It is this constant which is used in the Arrhenius equation. However, in solid state kinetics the equations are either based on a phase boundary rate controlling mechanism or

Table 1. Kinetic Expressions for Solid State Decompositions which Produce "Order" Type Equations.

Integral Form	Differential Form	n
$kt = -\ln(1-\alpha)$	$\frac{d\alpha}{dt} = k(1-\alpha)$	1
$kt = (1-\alpha)^{-1}$	$\frac{d\alpha}{dt} = k(1-\alpha)^{2}$	2
$kt = 1-(1-\alpha)^{2/3}$	$\frac{d\alpha}{dt} = \frac{3}{2} k(1-\alpha)^{1/3}$	1/3
$kt = 1-(1-\alpha)^{1/2}$	$\frac{d\alpha}{dt} = 2k(1-\alpha)^{1/2}$	1/2
$kt = 1-(1-\alpha)^{1/3}$	$\frac{d\alpha}{dt} = 3k(1-\alpha)^{2/3}$	2/3

Notes:

1. The traditional 1st and 2nd order expressions are included because they occur frequently in polymer degradation reactions.
2. The form of the 1st order expression found in solid state reactions is dependent upon a particular mechanism being involved.
3. To a first approximation all deceleratory processes may be represented by the 1st order decay equation.

a diffusion rate controlling mechanism. Many of these are not compatible with the above definition. A selection of such expressions are given in Table 2. It can be seen that there are three forms to these differential rate equations, namely,

$$\frac{d\alpha}{dt} = k\alpha^{m} \tag{23}$$

$$\frac{d\alpha}{dt} = k(1-\alpha)^{n} \tag{24}$$

and

$$\frac{d\alpha}{dt} = k(-\ln(1-\alpha))^{p} \tag{25}$$

which can be combined into one general expression,

$$\frac{d\alpha}{dt} = k\alpha^{m}(1-\alpha)^{n}\cdot(-\ln(1-\alpha))^{p}. \tag{26}$$

The form corresponding to equation 24 meets the formal requirement for use in the Arrhenius equation (Table 1), but equations 23 and 25 do not, and neither does equation 26 if m or p are finite numbers. However, the k term in these equations, although not fulfilling the requirements for a true specific reaction rate constant, is temperature dependent. It would seem advisable, however, to use the constant appearing in the differential form of the equation.

Table 2. Differential Forms for Solid State Kinetic Equations not Showing Traditional Order Form.

Integral Form	Differential Form	m	n	p
	for $\frac{d\alpha}{dt} = k\alpha^m(1-\alpha)^n(-\ln(1-\alpha))^p$			
$kt = \alpha^2$	$\frac{d\alpha}{dt} = \frac{1}{2}\cdot k\,\alpha^{-1}$	-1	0	0
$kt = \ln\alpha$	$\frac{d\alpha}{dt} = k\alpha$	1	0	0
$kt^2 = \alpha$	$\frac{d\alpha}{dt} = 2k^{1/2}\cdot\alpha^{1/2}$	1/2	0	0
$kt^3 = \alpha$	$\frac{d\alpha}{dt} = 3k^{1/3}\alpha^{2/3}$	2/3	0	0
$kt^4 = \alpha$	$\frac{d\alpha}{dt} = 4k^{1/4}\alpha^{3/4}$	3/4	0	0
$kt = (-\ln(1-\alpha))^{1/2}$	$\frac{d\alpha}{dt} = 2k(-\ln(1-\alpha))^{1/2}(1-\alpha)$	0	1	1/2
$kt = (-\ln(1-\alpha))^{1/3}$	$\frac{d\alpha}{dt} = 3k(-\ln(1-\alpha))^{2/3}(1-\alpha)$	0	1	2/3
$kt = (1-\alpha)\ln(1-\alpha)$	$\frac{d\alpha}{dt} = k(-\ln(1-\alpha)^{-1}$	0	0	-1

Note:
Alternative expressions have been put forward for,

$$kt = (-\ln(1-\alpha))^{1/n'}$$

namely,

$$\frac{d\alpha}{dt} = k\alpha^m(1-\alpha)^n$$

n´	m	n
2	1/2	0.774
3	2/3	0.700
4	3/4	0.664
5	4/5	0.642
.	.	.
.	.	.
.	.	.
	1	0.556

There are two parameters in the Arrhenius equation, E and A, and both should be reported, even if the data are considered to be empirical, to enable the kinetics to be properly described. If the data refer to the rate controlling step as the chemical reaction itself, it is possible to place a theoretical interpretation on these parameters. There is a very general treatment by Cordes [14]. However, the easiest treatment to understand is that of Shannon [15], which is based on an earlier treatment by Polanyi and Wigner [16]. In this treatment the activated complex theory of reaction rates is evoked,

$$k_r = \frac{RT}{Nh} \cdot \frac{Q^{\ddagger}}{Q} \cdot \exp(-E/RT) \tag{27}$$

$$= A \cdot \exp(-E/RT)$$

where K_r is a nominal first order type reaction rate constant. This can be rewritten as,

$$k_r = \frac{RT}{Nh} \cdot a \cdot \exp(-E/RT) \tag{28}$$

where,

$$a = A \quad \frac{RT}{Nh} = \frac{Q^{\ddagger}}{Q} = \exp\frac{(\Delta S^{\ddagger})}{R} \tag{29}$$

Experimental kinetic data for "a" show values ranging from less than unity to values greater than one. Expressing the data in this way enables "a" to be calculated from spectroscopic data via Q and $Q^{\ddagger}$, and this can be compared with the value of "a" calculated directly from the kinetic data. However, the calculation of $Q^{\ddagger}$ from the spectroscopic data is open to speculation.

It should be noted that in many related problems in kinetics where the reactions have similarities, i.e., the thermal decomposition of carbonates [17], that there is a linear relationship between log. A and E (or alternatively between $T\Delta S^{\ddagger}$ and $\Delta H^{\ddagger}$), termed the compensation effect. This takes the form,

$$\log A = mE + C \tag{30}$$

where m is the slope and C the intercept. The effect is thought by some to reflect experimental conditions, but Cremer [18] and Constable [19] suggest that the compensation effect will be shown in a heterogeneous model where the reaction will occur simultaneously at different reaction sites.

In rising temperature experiments, kinetically dominated, the question of the distribution of sites of varying energy arises. It would therefore seem possible that the Arrhenius parameters calculated from rising temperature experiments may be different from the same parameters calculated in the traditional way from a series of isothermal experiments.

There are of course many ways of calculating the Arrhenius parameters from rising temperature data [20]. In normal circumstances, an integral method would be chosen. However, this involves the integration of $e^{-E/RT}$ with respect to temperature, i.e. $\int e^{-E/RT} dT$, and this is analytically impossible. Approximate methods have to be resorted to, or one may make use of numerical integration. Differential methods are, however, straightforward. Combination of equations 14 and 15 gives,

$$\frac{d\alpha}{dT} = \frac{kf(\alpha)}{\beta}$$

or

$$k = \left[\frac{\frac{d\alpha}{dT} \cdot \beta}{f(\alpha)}\right] \tag{31}$$

where k is the specific reaction rate constant. Using the Arrhenius equation then gives,

$$\log \left[\frac{\frac{d\alpha}{dT} \cdot \beta}{f(\alpha)} \right] = \log k = \log A - \frac{E}{RT} \qquad (32)$$

and a normal Arrhenius plot of log k against 1/T is possible. The slope $\frac{d\alpha}{dt}$ may be calculated accurately by use of a computer method of fitting an empirical equation to a limited portion of the curve of α against T. An appropriate choice of $f(\alpha)$ has to be made and in many circumstances a preknowledge of related systems allows a suitable choice to be made. Typical data on carbonate decompositions often lead to two linear regions on the Arrhenius plots from rising temperature data, and it is often seen that these plots differ from the same plots collected from traditional isothermal experiments. This is shown schematically in figure 2. The data are believed to be a true representation of Arrhenius parameters as the values of A and E all show a compensation effect [17,21]. It can be noted that in many deceleratory systems it is a good approximation to use a first order expression when $f(\alpha) \underline{\Omega} 1-\alpha$.

4. Factors Controlling Kinetically or Thermodynamically Dominated Processes.

Most industrial processes involve solid starting materials and many require a non-isothermal heating regime. The investigator deciding to investigate such processes by methods of thermal analysis must conclude if the operation of any particular chemical process is kinetically or thermodynamically dominated. The thermal analysis experiments must then be designed so that if the chemical process is thermodynamically dominated, then the corresponding thermal methods of investigation are also thermodynamically dominated. Similarly, if the chemical process is kinetically dominated, then the corresponding thermal analysis experiments must be designed so that they likewise are kinetically dominated.

The problem requires the essential features of both types of process to be recognized.

Consider first thermodynamically dominated processes. Simply, this requires the thermal analysis experiment to exhibit the equilibrium condition at each temperature. In a thermogravimetric (TG) experiment, the test is simply that if the temperature is kept constant then there should be no further change in weight. This is favored by a slow change in the temperature during the TG experiment. Under vacuum conditions it is doubtful if equilibrium is ever seen, especially at relatively low temperatures.

This can be demonstrated by a further consideration of the basic equation governing the equilibrium condition, namely the Vant Hoff equation, which it is convenient to requote here (eq. 10):

$$\ln K_p = \frac{-\Delta H}{RT} + \text{constant.}$$

In a reaction of this type,

$$A_{(s)} \rightarrow B_{(s)} + C_{(g)}$$

then $$K_p = P_{C_{(g)}},$$

and equation 11 results, and again it is convenient to requote this:

$$\ln p_{C_{(g)}} = \frac{-\Delta H}{RT} + \text{constant.}$$

If the reaction is carried out into a fixed pressure of reactant gas, then a high value of the pressure of product gas will mean a high decomposition temperature, i.e., a high value of T, and a low value of 1/T. Conversely, a low value of the pressure of product gas will mean a low decomposition temperature or a high value of 1/T. Taking limits, this means that the predicted equilibrium at $1/T \rightarrow \alpha$, $T \rightarrow 0$, and $P \rightarrow 0$. In other words, at zero temperature and zero pressure and an infinite gas space, then the material should tend to

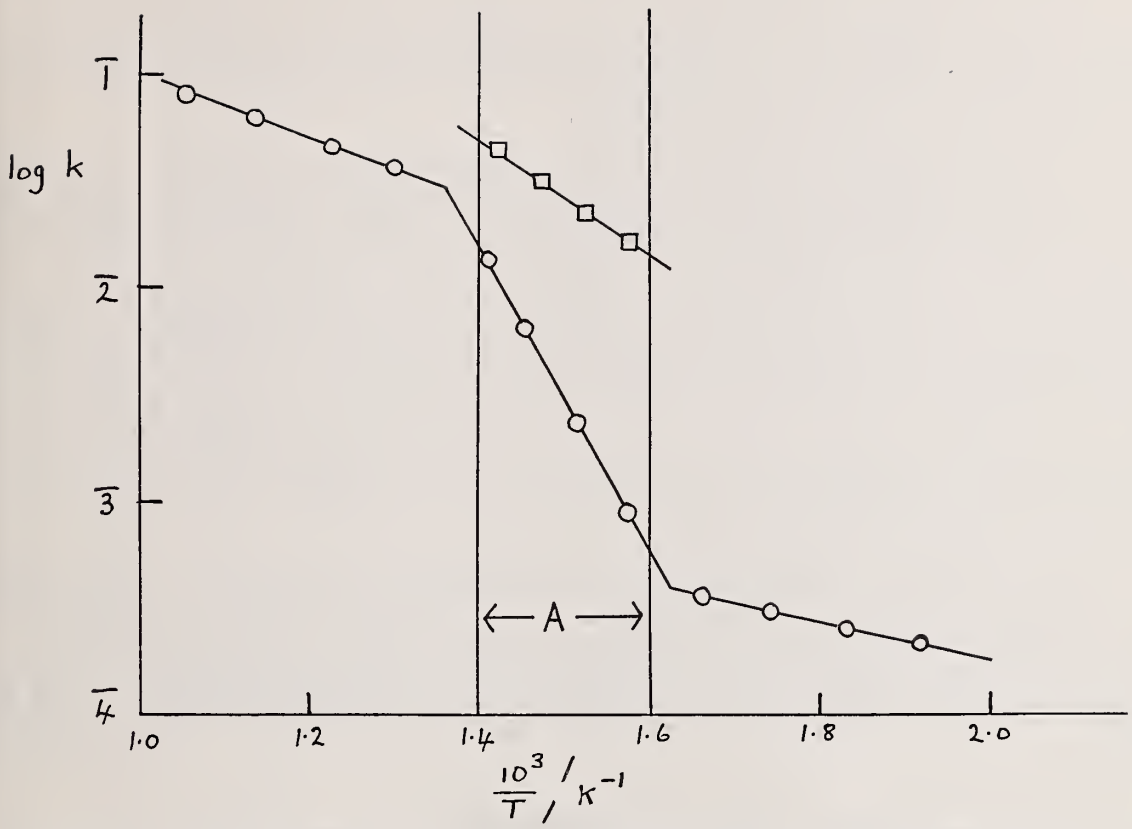

Figure 2. Arrhenius plots for carbonate decompositions. Schematic representation of data for isothermal and rising temperature experiments.

—□—□—□— Isothermal experiments — range A;

—○—○— Rising temperature experiments.

Ordinate: log k — log of specific reaction rate constant.

Abscissae: $\left(\frac{10^3}{T}\right) / K^{-1}$

decompose, and if the pressure is maintained at zero, then decomposition is complete. Actually, there is a choice (in theory at least) depending on the experimental conditions. The two limits concern the volume of gas space above the solid phases. Obviously, if this volume is infinite, then the driving force towards equilibrium pressure at any temperature will result in complete decomposition. If the volume is finite, decomposition will be conditioned by the fact that the temperature recorded determines the equilibrium gas pressure, and, as this temperature is raised, then the equilibrium gas pressure is also raised. The extent of decomposition is then conditioned by the amount of gas required to reach the equilibrium pressure in the gas space available.

The above restraints imply that the product gas comes from the process of decomposition. If, however, the product gas is supplied in the form of a continuous supply, then this corresponds thermodynamically to the concept of an infinite volume of gas space above the sample. In a rising temperature experiment under continuously pumped vacuum condition, or in a flowing nitrogen atmosphere or a flowing atmosphere of some other inert gas, then the pressure of the product gas will be zero and, according to the thermodynamic relationship outlined in equation 11, the material should decompose at zero temperature. This does not happen because an absolute vacuum is never achieved, but more importantly because kinetic factors intervene and become the dominant controlling factor. It should be noted too that because kinetic factors are now dominant, then TG results in vacuum and inert gases are different. At higher partial pressures of product gas in the flowing atmosphere, then the decomposition will be noted when in a rising temperature experiment the equilibrium pressure exceeds the partial pressure of the product gas and it should proceed to complete decomposition.

Before proceeding to the consideration of the kinetic factors, however, another aspect of the equilibrium condition should be noted. In homogeneous reactions the equilibrium process is represented as reversible, and the equilibrium condition at any one temperature can be established by approaching that temperature from a higher temperature or from a lower temperature. However, this is not always the case in solid state decompositions. This may be because a layer of product solid may become interposed between the reactant solid and product gas and thus allow an equilibrium to be established only on a rising temperature program.

The kinetic factors, if dominant, modify the application of the thermodynamic equations. At high temperatures the specific reaction rate is fast and so equilibrium is established and seen on a TG curve rather than the TC curve representing the effect of kinetic parameters. At lower temperatures the kinetic process is slower and takes some time so a TG curve in this region is probably controlled by kinetic factors. The actual temperatures concerned in this argument are determined by the system under investigation. Thus, a generalization is that at high temperatures there is a greater tendency for any system to show a TG result representing the equilibrium condition, whilst at lower temperatures the tendency will be for the shape of the TG curve to be determined by kinetic parameters. A further logical generalization would then be that slow heating rates in a TG experiment will favor the curve being determined by equilibrium conditions whilst faster heating rates will favor a greater dominance by kinetic factors.

These generalizations ignore the effect of the pressure of the environmental gas, and in particular the pressure of product gas. Any decomposition process will proceed towards an equilibrium condition and the observed rate is the rate at which the process proceeds towards equilibrium. However, by removing product gas as formed (e.g., in a flowing atmosphere of inert gas) then the reaction can proceed to completion and a back reaction is avoided. If the rate of decomposition is observed with the sample under a given pressure of product gas, then the process depends on the volume of space above the solid sample. If the volume is finite, then the process of decomposition must produce in a closed system an increase in pressure. If the volume is large and the sample size small, then the pressure change may be small and decomposition complete. At low pressures there will be a smaller tendency for the reverse process to dominate, whilst at higher pressures of product gas the reverse process must be considered and the observed rate will represent the net sum of the forward and reverse rates. It also follows that the reverse rate becomes more important as more product is produced and allowed to accumulate around the decomposing sample.

Consideration must be given to the case where product gas is present, but the volume above the sample is infinite. This corresponds to a flowing stream of product gas being passed over the decomposing solid at a controlled pressure. The decomposition process is not then going to be observed until the thermodynamic temperature of decomposition at the pressure of product gas is reached. At temperatures higher than this value the reaction will proceed, and the higher the temperature the greater the specific reaction rate.

Certain experimental factors must be considered with regard to the kinetic aspects of solid state decomposition. It must first be noted that most solid state processes occur with a reaction boundary – the interface separating the solid reactant from the solid product. It is the process taking place at this interface which is the kinetic feature of interest, and the rate of decomposition usually reflects the changing geometry of the movement of this interface. However, if the sample is too large or the container for the sample badly designed, then the slowest rate process may be the diffusion of product gas away from the interface and then this becomes the factor relevant to the observed kinetics.

In most cases the reaction interface movement (phase boundary controlled) is the rate determining step required, and the experiment must be designed so that this may be measured. To ensure that this is the case, an open type reactant container must be used to allow access of product gas to the environment. Further, the size of the sample should be progressively reduced in a series of experiments to find an optimum limiting size below which the kinetics of decomposition are not altered.

A further point which needs investigating is the possibility that as the temperature range of observation is increased then the actual mechanism of decomposition may alter. In such circumstances the isokinetic data at various temperatures must be established. Methods of doing this using reduced time parameters have been described elsewhere [13,22,23]. The same methods will also serve to identify the kinetic law obeyed.

In subsequent sections of this article, examples of the application of these principles to industrial processes are discussed. The areas chosen to illustrate these principles are the glass manufacturing industry, ceramic processes, and catalysis processes. The areas could have been extended into other fields, but these three serve to illustrate the points already raised.

5. Glass Manufacturing Industry

The glass manufacturing industry may be cited as involving a chemical process which may be studied using thermal methods. The basic materials are silica, alkali, and lime, but there are many variations. These mixtures are heated up beyond a certain temperature to where the materials fuse and the liquid is then cooled and the viscosity rises to give it rigidity. The structure is not that of a solid, however, but the long-range disordered structure of a liquid, whilst retaining a short range structure. Sand is used as a source of silica; it must be free from iron oxide if colorless glass is required. The alkali used is normally sodium carbonate, although sodium hydroxide may also be used. The sodium carbonate used is that obtained from the Solvay process, but the demands of the polymer-based industries in particular have caused an increase in the production of hydrogen chloride and chlorine with a consequent increase in caustic soda production. The reason for caustic soda being used in glass production may therefore be the result of changes in the economics of the alkali industry. The lime constituents of glass may be chalk or limestone, and a certain amount of dolomite is also usually included. These are all quarried materials. All these materials are mixed into "batches" and used in powdered form. The batch usually contains added water up to about 3 percent by weight.

Silica is the glass forming oxide, but needs a very high temperature (ca. 1800 °C) for melting and working. Fluxes are therefore added to reduce the melting temperature. Sodium carbonate is the basic fluxing material, but it decomposes and it is the soda (Na_2O) which is really the fluxing agent. The lowest melting mixture of soda and silica results from a reaction to produce sodium disilicate which with silica melts at 783 °C [24,25]. This can

be demonstrated by the use of TG and DTA runs on these mixes [26,27,28,29]. Wilburn and coworkers [27,28,29] identify several steps in a two-phase mixture of Na_2CO_3-SiO_2,

1. Loss of water – around 100 °C, an endothermic process,

2. Endothermic inversion of silica at 573 °C,

3. Weight loss due to formation of sodium disilicate, also endothermic,

4. Endothermic melting of sodium carbonate, of sodium disilicate and silica,

5. The melted sodium carbonate decomposes.

Reactions 3 and 4 can occur usually around 850 °C, but are highly dependent upon the particle size. In general the smaller particle sizes lead to the production at lower temperatures of melts that can be supercooled to produce a glass. The glass produced by chilling the eutectic mixtures from above 783 °C is readily dissolved in water.

Lime (CaO) is usually added as limestone, and is added to increase the durability of such a glass. The amount to be added is important as too large an addition results in a glass which is difficult to melt and certain to devitrify.

The sand-sodium carbonate-calcined calcium carbonate system has been investigated by Oldfield [29] and by Wilburn and co-workers [30]. The main endothermic peak in the Na_2CO_3-SiO_2 system investigated by Wilburn and Thomasson [26] shows up on the DTA unit at 787 °C. When the silica is progressively replaced by calcium carbonate in the Na_2CO_3-SiO_2 mixture (90% SiO_2·10% Na_2O), the peak occurs at a higher temperature. Thus for a mixture, 10.5 percent Na_2O, 28.5 percent CaO, 61 percent SiO_2, a single peak at 820 °C on the DTA is shown. According to Wilburn and Dawson [27], this is due to the ternary eutectic $Na_2O{\cdot}SiO_2$ + $Na_2O{\cdot}2SiO_2$ + $CaO{\cdot}2Na_2O{\cdot}3SiO_2$. The presence of small amounts of sodium chloride in commercial materials used in batch compositions produces a eutectic melting with sodium carbonate at 630 °C and the liquid phase produced enhances the reaction between the other components which occur at lower temperatures than when pure materials are used [30]. DTA and TG has been used by Wilburn and coworkers [30] to indicate the formation of double carbonates of sodium and calcium at relatively low temperatures. Two of these double salts melt as a eutectic at 780 °C [31] and again the liquid phase ensures a more rapid reaction with the silica.

The combination of TG and DTA can be extended to investigate the behavior of the other components of glass both singly and in mixtures. Finally, the actual batch can be investigated. Wilburn and coworkers [27,30] identified the reactions in a sheet glass mixture consisting of sand, sodium carbonate, dolomite, and limestone, using TG and DTA by this approach of gradually increasing the complexity of the mixture in a series of separate experiments. They decided that on heating the batch the sodium carbonate reacts with both dolomite and calcium carbonate to form the sodium carbonates (mentioned above) at around 500 °C. As already noted, a eutectic melt at 780 °C can be attributed to two of these double carbonates, and this produces a liquid phase which increases the rate to reaction between sodium carbonate and silica at 850 °C. Liquid phases which can be chilled to a glass appear at 900 °C. Silica can be identified by the a⇌b quartz inversion at 573 °C, and it dissolves slowly in the liquid formed. This liquid appears upon the formation of sodium disilicate in the region of 900 °C. The temperatures of many of the chemical reactions can be affected by varying the powder size in the batch composition. In addition to these studies on reaction pathways, thermal methods may be used to study,

1. The behavior of glass during heating (annealing peaks appear in the DTA) and,

2. The devitrification of glass.

Since no weight loss is involved on heating a glass, then DTA is used for this kind of study. The physical properties of a glass have to be repeatable, and to achieve this it is cooled slowly (annealed) from the "transformation range" or temperature region where the appropriate liquid form appears. This transformation range can be recognized by a small endothermic effect [32] as the temperature is raised. The temperature at

which this effect occurs depends on the glass composition and its magnitude on the previous thermal history. In general the effect is small for a poorly annealed sample, but greater for well annealed samples (figure 3).

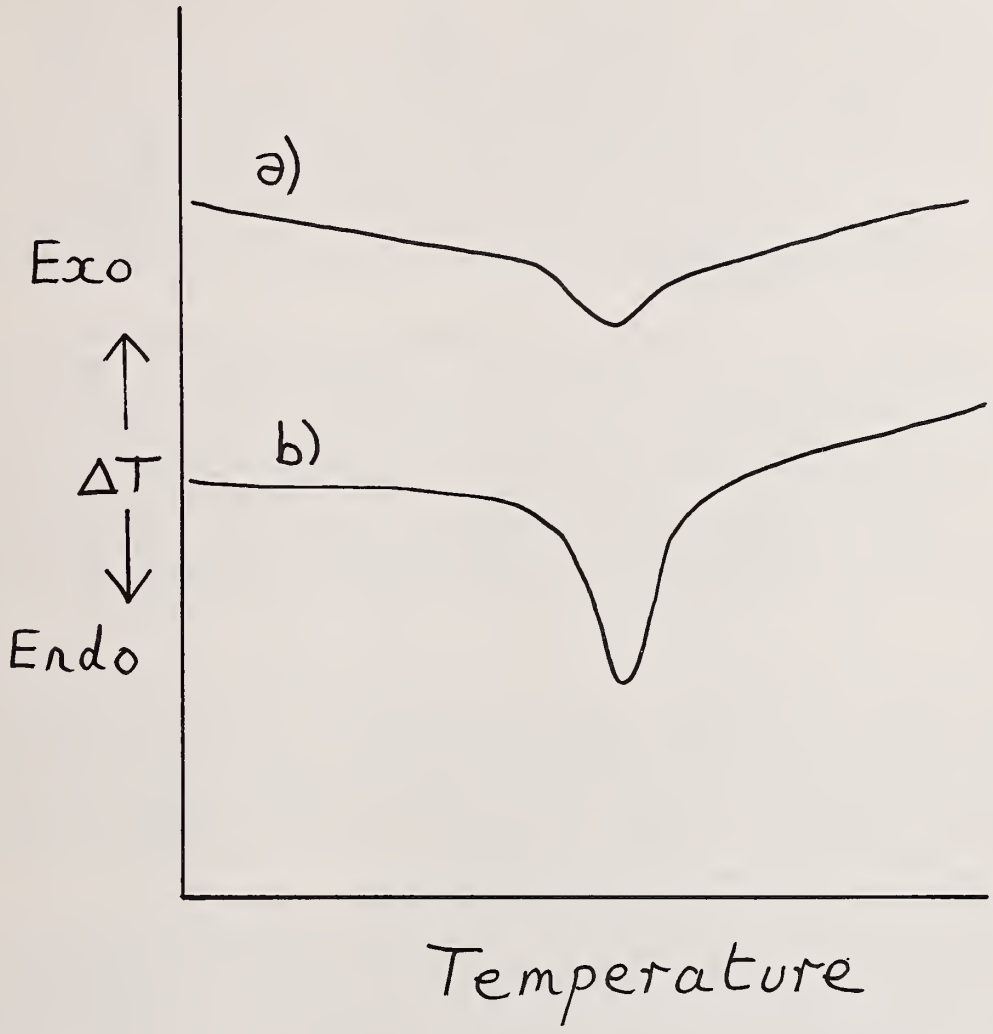

Figure 3. DTA curve for a glass: a) poorly annealed, and b) well annealed. The area of the peak is greater for a well-annealed sample.

Ordinate: ΔT signal
Abscissae: Temperature

A DTA trace for some glasses may show an exothermic peak at a higher temperature than the endothermic peak associated with the annealing process. This exothermic peak is due to the growth of solid phase crystals from the glass – i.e., devitrification. The temperature at which such a peak occurs and its magnitude depends on the rate of crystal growth.

6. Ceramic Processes

Ceramic processes involve the heat treatment of clays and clay mixes. Clays are defined in mineralogical sciences as certain earths which are highly plastic when wet and which, when heated to beyond or around 900 °C, lose their plasticity and are converted into a hard mass unaffected by water. The clays can be identified as various alumino-silicates with variations in composition and replacement by other metal ions. However, commercially used clays are generally mixtures. Engineers and geologists define clays in terms of particle size. Wentworth [33] defines the clay grade as material finer than 4 micrometers, although in solid investigations it is more usual to use 2 μm as the upper limit of the clay size grade. Most of the clays defined by the first definition occur in nature in a form which satisfies the second definition. Clays are generally found mixed with very fine particles of quartz, felspar, mica, etc. This is because they result from the decomposition of a variety of igneous rocks (e.g. granite). These fine particles are bound together by a sticky material – the clay – which as a first approximation may be represented as $Al_2O_3 \cdot 2SiO_2 \cdot 2H_2O$. The clays formed in this way may either be found in their original position or may be carried by water and deposited at a distance.

When moist clay is dried at 100 °C it loses most of its physically retained water and becomes hard and brittle. If the product however is soaked in water, the water is taken up again and it once more becomes soft and plastic. This process can be demonstrated using TG equipment and the reversibility can be demonstrated using suitably designed units. In the temperature range 500 - 600 °C a further loss of water takes place and can also be demonstrated using TG equipment. The loss of water will show as an endothermic peak on DTA units [34,35]. The water lost in this stage is combined water and generally its loss is irreversible, and a hard porous mass results which does not soften in water. At temperatures in the region 900 - 1000 °C there is often an exothermic phase change, the clay becomes less porous and more stony in consistence. This process also can be demonstrated with the aid of the DTA equipment. At higher temperatures between 1400 - 1850 °C, this solid phase will melt to a glassy mass.

Commercially available clays vary from one locality to another. Kaolin or china clay is the purest form. It is a white earthy substance, less plastic and sticky than most clays. An ideal formula for the material would be $Al_2Si_2O_5(OH)_4$, i.e. $Al_2O_3 \cdot 2SiO_2 \cdot 2H_2O$. The quartz sand and micas are removed from the quarried material by washing. A typical DTA and TG plot for kaolin is shown in figure 4. Ball clay is a less pure material used for the manufacture of earthenware. Common clay contains more impurities, often iron oxide which gives a red color to the fired material. Fireclay contains a great deal of silica and very little iron; it has a high fusion point somewhere beyond 1500 °C.

Some of the regions of behavior are of technological importance [36]. In the drying of clays around 100 °C, i.e., the reversible region, the critical moisture content is important. This is an important parameter in relating the shrinkage occurring on drying with the water content. The shrinkage occurs because the water is contained in the voids between the clay particles, and they are drawn closer together upon removal of the water. Once a close packed assembly has been achieved, then further loss of water occurs without further shrinkage. A thermomechanical analysis unit will be required together with either a calibrated DTA unit or a TG unit. It can, however, be achieved using less-sophisticated equipment. Typical data obtained in this way is shown in figure 5. The moisture content where no further shrinkage occurs is the critical moisture content.

There are various factors which affect the critical moisture content. Flocculated clay systems are generally loosely packed and of a low density, and thus have a comparatively high critical moisture content. A deflocculated clay will show a lower critical moisture content. In order to avoid or minimize shrinkage, the initial moisture content must be decreased while the critical moisture content must be increased.

Detailed TG and DTA studies on the many different clay minerals show that they conform to the general behavior, but the exact temperatures recorded for the exothermic and endothermic peaks on DTA vary from material to material and prove to be very useful in identification procedures [34,35].

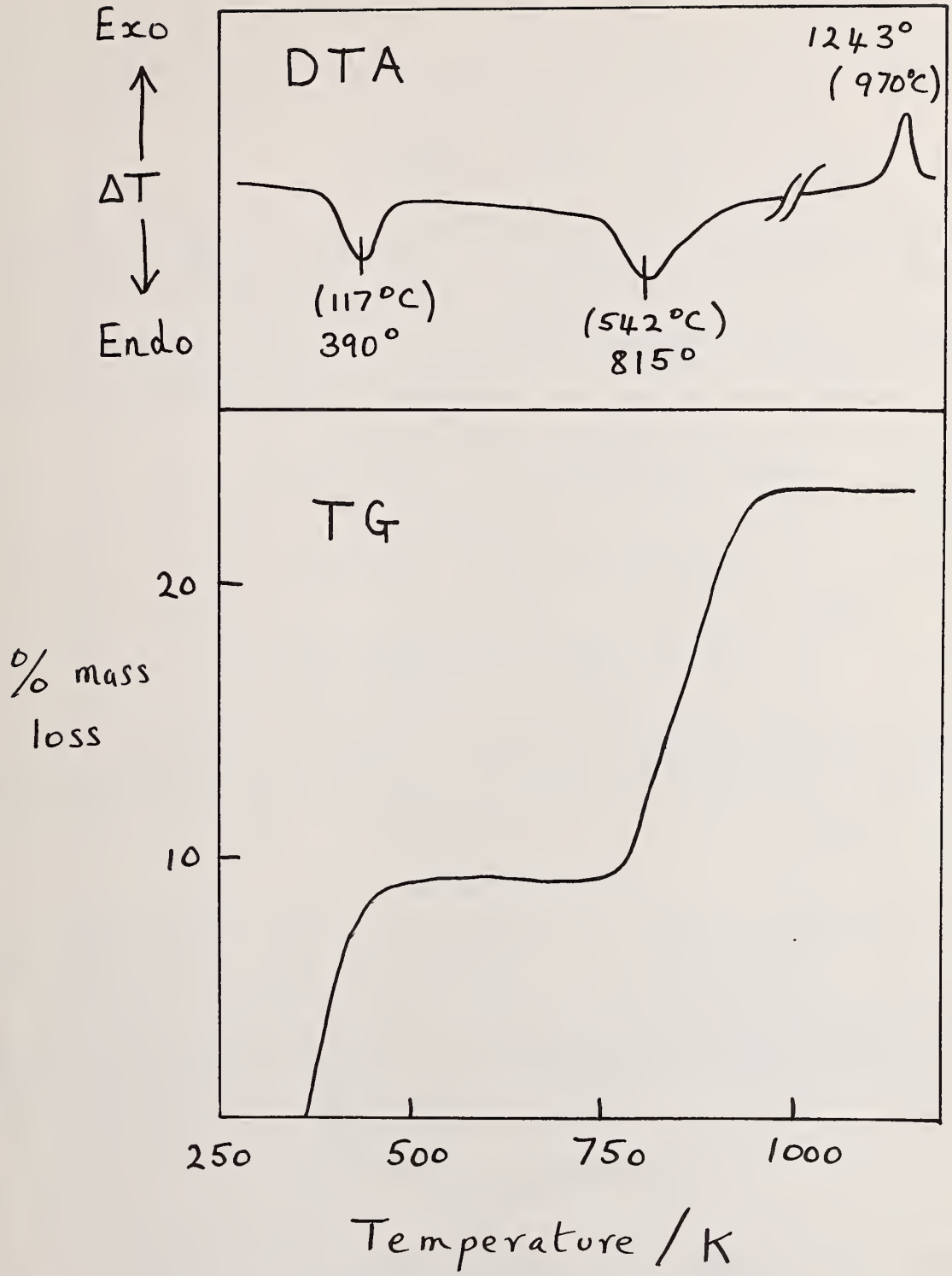

Figure 4. A typical DTA and TG plot for kaolin.

Top Graph:	Ordinate:	ΔT signal
	Abscissae:	Temperature
Bottom Graph:	Ordinate:	% mass loss
	Abscissae:	Temperature / K.

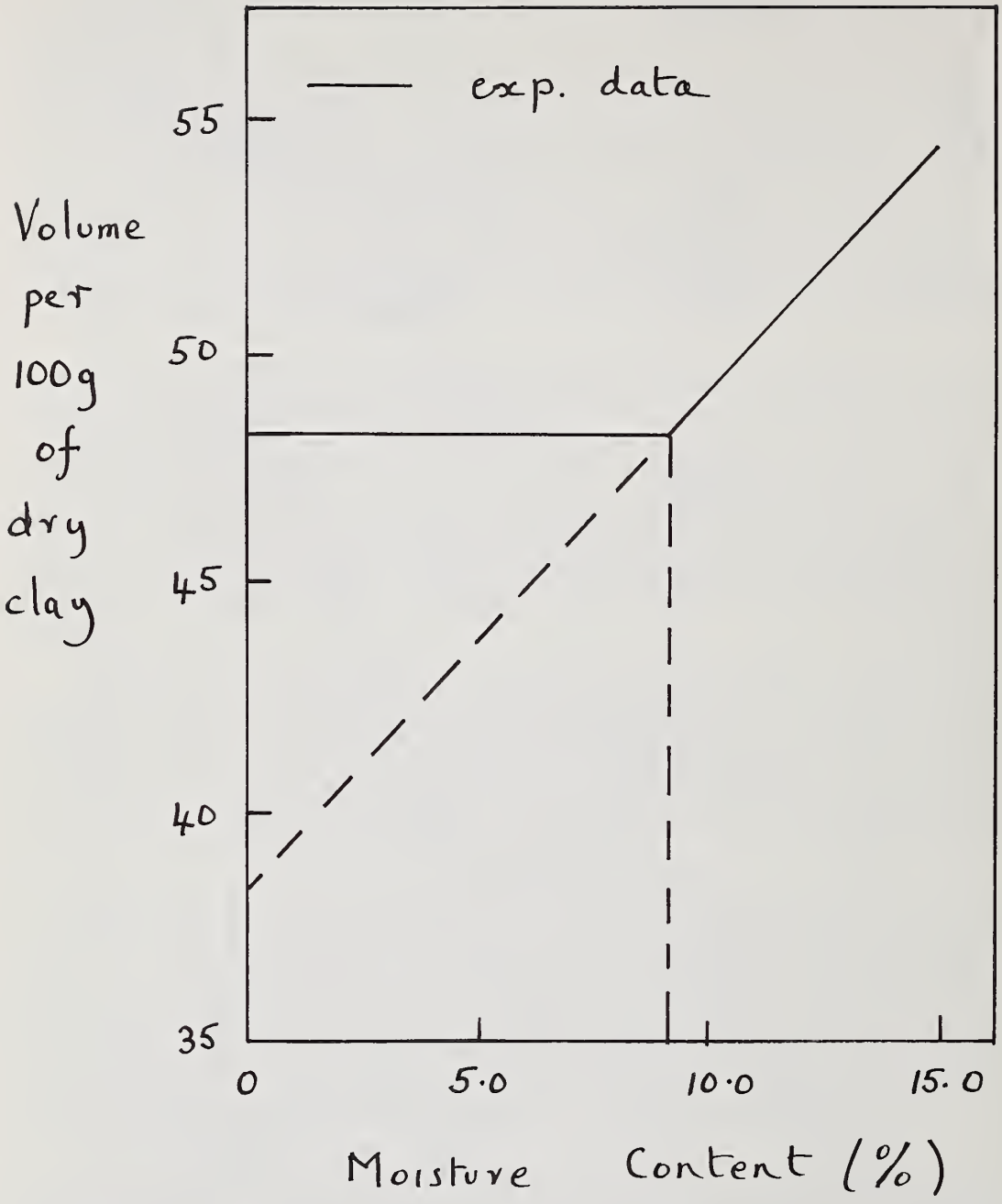

Figure 5. Moisture content plotted against shrinkage for clays on drying (schematic representation – typical data)

Ordinate: Volume per 100 g of dry clay

Abscissae: Moisture content (%).

The effect of heat on pure kaolin may be quoted in some detail. A typical DTA and TG plot has already been described (figure 4). In this instance the removal of adsorbed water takes place endothermically at 117 °C. A further endotherm at 542 °C is shown by the TG results to be associated with the loss of hydroxyl groups as water. This dehydration process has been shown to follow a first-order reaction. The residue from this dehydration is called metakaolinite, is almost non-crystalline to x-rays, but does retain a certain amount of order [37,38]. The ideal equation for this dehydroxylation reaction is,

$$Al_2Si_2O_5(OH)_4 \rightarrow Al_2Si_2O_7 + 2H_2O.$$

With disordered kaolinites, this dehydration product is less well defined. For a well crystallized kaolinite this endotherm will occur on a DTA trace at around 600 °C, but is depressed to a lower temperature for a disordered kaolinite. The conditions of flocculation also cause a variation in the temperature of this endothermic peak [39].

At temperatures just below 1000 °C the metakaoline undergoes an exothermic process. The end products are free silica (cristobalite) and mullite, $3Al_2O_3 \cdot 2SiO_2$. The processes in this region are represented by Worrall [36] as,

$$2\ [Al_2O_3 \cdot 2SiO_2] \xrightarrow{925\ °C} 2Al_2O_3 \cdot 3SiO_2 + SiO_2$$

metakaolin — silicon spinel

$$2\ Al_2O_3 \cdot 3SiO_2 \xrightarrow{1100\ °C} 2\ [Al_2O_3 \cdot SiO_2] + SiO_2$$

silicon spinel — "pseudo-mullite"

$$3\ [Al_2O_3 \cdot SiO_2] \xrightarrow{1400\ °C} 3Al_2O_3 \cdot 2SiO_2 + SiO_2$$

"pseudo mullite" — mullite — cristobalite

The silica appears as cristobolite. The exothermic reaction would then be associated with the formation of silicon spinel. An exothermic peak at 1200 - 1300 °C can be attributed to the rapid crystallization of mullite and/or cristobalite [40]. The matter would seem to be still open to speculation.

7. Catalysis Processes

Thermal methods may be used to follow the catalysis process or may be used to identify and characterize materials used as catalysts or catalyst supports. In certain cases thermal methods can be used to identify catalyst processes not previously detected.

The example of the identification of catalyst processes may be taken from the decomposition of oxalates. These have been studied in a series of papers by Dollimore et al. [41,42,43]. The thermal decomposition of oxalates follow a variety of routes. Zinc oxalate dihydrate in both air or nitrogen first dehydrates and then decomposes to zinc oxide. Schematically this is represented as,

$$ZnC_2O_4 \cdot 2H_2O \xrightarrow[\text{endothermic}]{} ZnC_2O_4 + 2H_2O$$

$$ZnC_2O_4 \xrightarrow[\text{exothermic}]{\text{Air}} ZnO + CO + CO_2$$

$$ZnC_2O_4 \xrightarrow[\text{endothermic}]{\text{Nitrogen}} ZnO + CO + CO_2$$

It will be observed that an endothermic decomposition in nitrogen becomes an exothermic decomposition in air.

Nickel oxalate thermally decomposes in the following manner:

$$NiC_2O_4 2H_2O \xrightarrow[\text{endothermic}]{} NiC_2O_4 + 2H_2O$$

then,

$$Ni \cdot C_2O_4 \xrightarrow[\text{exothermic}]{\text{Air}} [Ni] + 2CO_2$$
$$\downarrow \text{ Air}$$
$$NiO$$

$$NiC_2O_4 \xrightarrow[\text{endothermic}]{\text{Nitrogen}} Ni + 2CO_2$$

Again it will be observed that an endothermic decomposition in nitrogen becomes exothermic in air.

Calcium oxalate shows a three-stage decomposition. This can be shown to be:

$$CaC_2O_4 \cdot 2H_2O \xrightarrow[\text{endothermic}]{} CaC_2O_4 + 2H_2O$$

$$CaC_2O_4 \longrightarrow CaCO_3 + CO$$

i) endothermic in nitrogen but

ii) sometimes exothermic in air

$$CaCO_3 \xrightarrow[\text{endothermic}]{} CaO + CO_2$$

A variable valency metal oxalate shows the following decomposition sequence:

$$MnC_2O_4 \cdot 2H_2O \xrightarrow[\text{endothermic}]{} MnC_2O_4 + 2H_2O$$

$$MnC_2O_4 \xrightarrow[\text{endothermic}]{\text{Nitrogen}} MnO + CO + CO_2$$

$$MnC_2O_4 \xrightarrow[\text{exothermic}]{\text{Air}} MnO_2$$

or Mn_2O_3
Mn_3O_4

(depending on temperature and conditions)

All these facts can be ascertained by the use of TG and DTA and have been reported in detail [42,43,44,45]. The point which is of interest here, however, is the change from an endothermic decomposition observed in nitrogen to an exothermic decomposition in air. The basic decomposition process is endothermic and it is this which is observed in nitrogen. In the case of nickel oxalate the exothermic decomposition peak in air is caused by the vigorous oxidation of a high surface area metal product at the temperature of formation. The exothermic character of the zinc oxalate decomposition in air is caused by the catalytic conversion of carbon monoxide product gas to carbon dioxide at the zinc oxide surface. If either of these two exothermic do not coincide with the basic endothermic process, then a complex

DTA signal is produced. In the case of calcium oxalate decomposition to calcium carbonate it would seem that the exothemic nature of the decomposition in air is probably due to the container material acting as the catalyst surface rather than the catalyst surface being the product calcium carbonate. This further points out a cause of some "accidental catalysis," namely that the container material or indeed the thermocouple material may act as a catalyst.

A second feature of thermal analysis used in catalyst processes is the investigation of procedures which are precursors to the actual catalyst process. One of these kind of studies is the investigation of the drying temperature necessary in the preparation of catalysts and catalyst supports prior to their use. These materials are usually oxides and attract water by adsorption or "pick it up" during their preparation. The water is held by physical adsorption and also in combined form linked to the surface by valency forces. The nature of these valency links varies from oxide to oxide; in any one oxide indeed there may also exist a variety of such linkages, depending on the oxide surface structure, which is rarely homogeneous. The nature of these valency bonds can be ascertained using infrared spectroscopy hydroxyl groups is lost between 115 - 600 °C. Above this temperature there is a loss of surface area simultaneously with the loss of water, but the number of remaining hydroxyl groups remains constant [48]. It is found that

$$\text{Hydroxyl groups per square millimicron} = \frac{660 \cdot W}{S}, \tag{33}$$

where W is the percent by weight of bound water and S is the specific surface area in $m^2 g^{-1}$. Iler gives the full coverage number of hydroxyl groups as 8 per square millimicron. Other investigators [49] set the temperature for the removal of adsorbed water above 115 °C and many chose 200 °C. Dollimore and Heal [49] investigated a fine-pored silica showing Type 1 nitrogen adsorption isotherms. The monolayer capacity was calculated from the BET equation and then using the accepted value of the cross-sectional area, the surface areas for these silicas can be shown to be around 200 $m^2 g^{-1}$. The number of hydroxyls per nm^2 for these oxides was found to be between 20 and 30 in contrast to the accepted value of 8. The method of estimating this hydroxyl content was to record the weight lost between 200 °C and 1000 °C using a thermobalance to collect these data. It can then be claimed that this anomaly is due to the fine pored structure not reflected in the calculation of the surface area from the BET equation. Thus, in the extreme case (figure 6) the molecule of nitrogen just fits into the pore and thus one molecule covers the walls of a circumscribed cylinder. The area associated with the molecule is then $2r \times 2\pi r = 4\pi r^2$. The BET value is that of the molecules covering a planar surface when the area is given by πr^2. Then,

$$\frac{\text{True Area}}{\text{Apparent Area}} = 4. \tag{34}$$

Actually the apparent area is a little greater than given here due to packing of the molecules and the ratio is really 3.63. Therefore, if the number of OH groups per nm^2 is calculated to be 20 to 30, this is because the apparent surface area was too small by a factor of 3 to 4, and making allowance for this would produce normal values for the OH population on a silica surface, namely 8 per nm^2. This kind of proposition has been extended to pores of somewhat greater size [50,51].

The second application of thermal analysis work in relation to catalyst precursors concerns the need to reduce catalysts supplied as oxides *in situ* to the metal which then acts as the actual catalyst. In a study of the reduction of uranium oxide (U_3O_8) and nicklous oxide (NiO) by hydrogen (H), Clough and Dollimore [52] used a Cahn RG electrobalance.

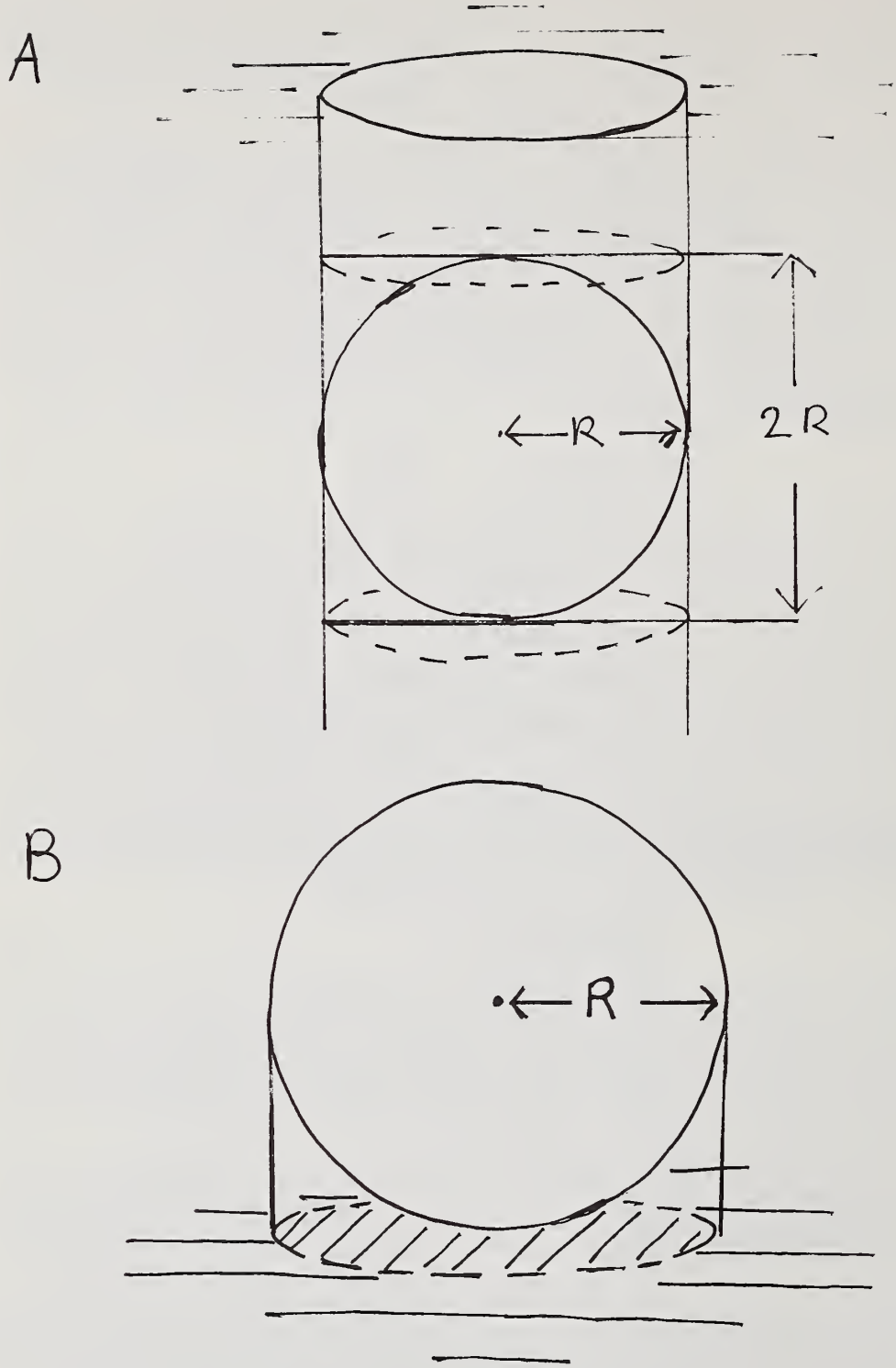

Figure 6. Area occupied by adsorbate molecules in small pores, extreme cases:
A – Molecule just fits into pore;
B – Molecule on a planar surface.

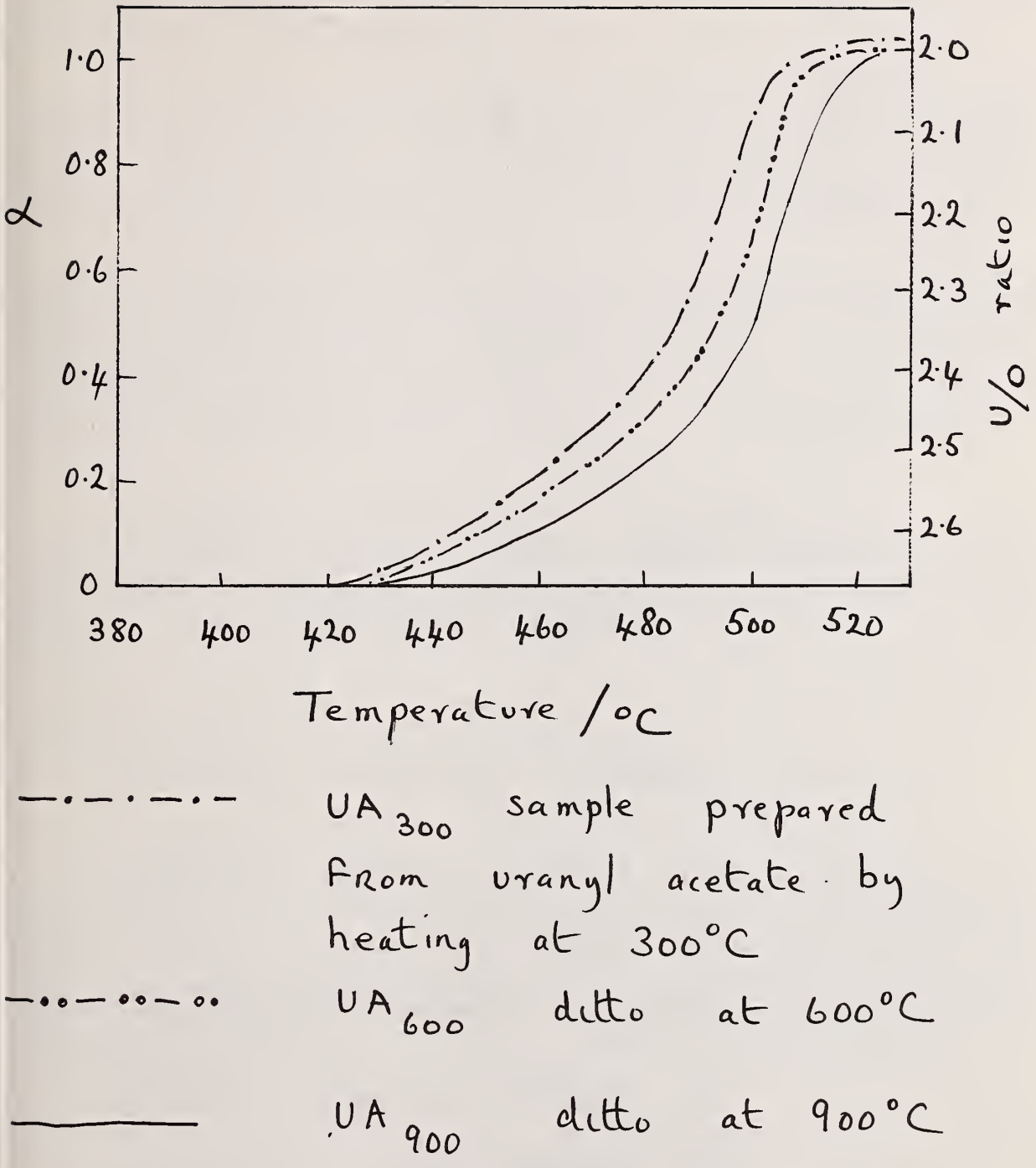

Figure 7. The TG data for the reduction of U3O8 samples with hydrogen
Ordinate: α fraction decomposed
Abscissae: Temperature / °C.

A typical set of thermal analysis data for U_3O_8 reduction is shown in figure 7 while similar data for nickel oxide is shown in figure 8. The U_3O_8 is reduced to UO_2 whilst the nickel oxide is reduced to the metal.

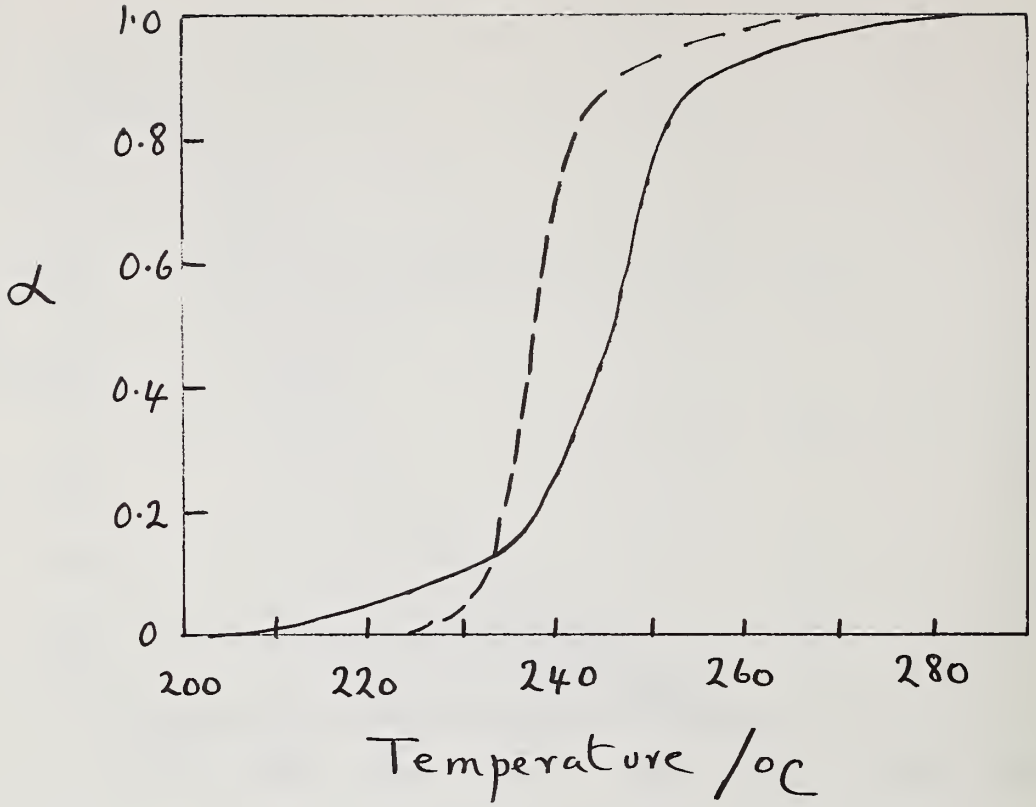

Figure 8. The TG data for the reduction of NiO samples with hydrogen.
Ordinate: α fraction decomposed
Abscissae: Temperature / °C.

The isothermal reduction of U_3O_8 with hydrogen showed linear plots of the fraction decomposed (α) against time (t), and this has been previously noted in other studies [53,54]. An explanation of such linear rates could be due to the presence of micropores ~20A present as fissures and cracks in the reacting solid surface.

These pores widen as the reaction proceeds and the resultant increased surface could theoretically balance the decrease in surface of the bulk solid, so that an almost constant reaction interface is presented up to quite high conversion ratios. However, on the basis of data on density determinations which show a decrease in molar volume of 30 percent on transition from U_3O_8 to UO_2, it is considered more probable that the linearity of the α versus time plots is due to cracks appearing in the product layer owing to this volume contraction permitting constant unrestricted access to the reacting solid surface.

Nickel oxide samples also investigated by Clough and Dollimore were reduced in an atmosphere of hydrogen, but the manner of their reduction depended upon the parent oxysalt. Samples of oxide produced from the nitrate showed an induction period prior to reduction, whereas oxide samples prepared from nickel acetate did not show any induction period. The length of this induction period was a clear function of the temperature of reduction, becoming progressively longer as the temperature was increased. Avrami-Erofeev plots of $(\ln[1/1-\alpha])^{1/3}$ against time were linear for the oxide prepared from the nitrate, but plots of log.log $[1/1-\alpha]$ against log t, where t = time, showed a linear region for α values up to 0.25, where n = 1, whereas for α in the range $0.25 \sim 0.75$, n = 3 in the equation,

$$(\log[1/1-\alpha])^{1/n} = kt + \text{constant} \qquad (35)$$

Clough and Dollimore believe these data indicates nucleation is complete before growth of nuclei begins in the reduction of oxide samples prepared from nickel nitrate. The same authors relate the different behavior of the reduction of nickel oxide from nickel acetate decomposition to the fact that such oxides contain a considerable excess of oxygen in defects in the nickel oxide lattice, with a large number of the defects at or near the crystal surface.

TG data has also been used in investigating the decomposition of formic acid on manganese (II) oxide [55]. Two processes are possible, namely,

$$HCOOH \longrightarrow H_2O + CO \quad \text{dehydration}$$

and

$$HCOOH \longrightarrow H_2 + CO_2 \quad \text{dehydrogenation}$$

These data obtained indicated that dehydrogenation reaction was preferred at 250 °C, becoming progressively less important than the dehydration process at higher temperatures. Figure 9 indicates the selectivity of the manganese (II) oxide towards dehydrogenation (line A), and dehydration (line B) in the temperature range 250 - 300 °C. TG data were obtained (line C) to determine the fraction of manganese (II) formate present after catalysis in the temperature range 200 - 350 °C. Dollimore and Tonge [56] have shown, using thermal methods, that the decomposition of manganese formate proceeds initially by a dehydration reaction which becomes less predominant than the dehydrogenation reaction as the decomposition proceeds, i.e,

$$Mn(HCOO)_2 \longrightarrow MnO + 2CO + H_2O$$

dehydration

$$Mn(HCOO)_2 \longrightarrow MnO + CO + CO_2 + H_2$$

dehydrogenation

This would imply an apparent correlation between the catalytic process and the solid state decomposition of manganese (II) formate; at temperatures where the catalytic process is accompanied by the formation of relatively large amounts of the formate, the catalytic decomposition of formic acid appears to follow the selectivity trends observed during the final stages of the decomposition of the bulk phase. This is probably associated with the

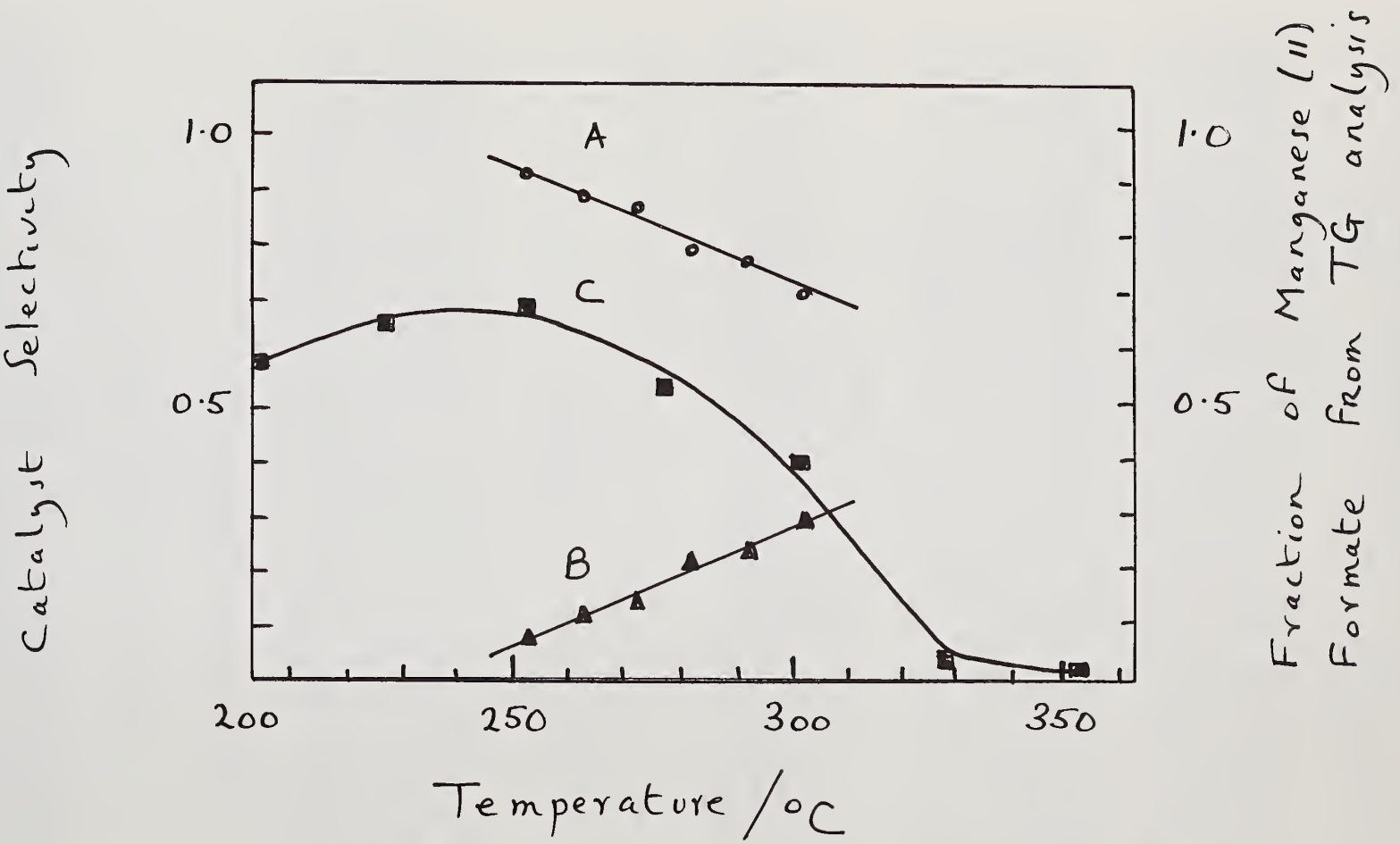

Figure 9. Selectivity of manganese (II) oxide toward dehydrogenation (A) and dehydration (B) in the temperature range 250 °C to 300 °C. Curve C represents the fraction of manganese (II) formate present after catalysis in the temperature range 200 °C to 350 °C.

Ordinate: L.H.S. Catalyst selectivity
R.H.S. fraction of manganese (II) formate from TG analysis.

Abscissae: Temperature / °C.

stability of the formate species since Criado et al. [57] have shown that between 400 and 470 °C the dehydration process dominates and corresponds to the presence of the formate as an unstable surface species.

In an investigation into the constitution and oxidizing properties of materials in the copper (II) oxide manganese (III) oxide system, Dollimore and Tonge [58] made extensive use of TG data to identify the phases present in the heat-treated samples of this system. They showed that the formation of the compound $CuMn_2O_4$ in the Mn_2O_3-CuO system is accompanied by a change in the oxidation state of the manganese and changes of activity in the oxidation of cinnamyl alcohol in neutral solution and in the oxidation of carbon monoxide in air. The results were interpreted as supporting the view that $CuMn_2O_4$ contains the resonance system,

$$Cu^{2+} + Mn^{3+} \rightleftharpoons Cu^{+} + Mn^{4+}.$$

The same authors also used TG data to establish the nature of the manganese oxide in a study on the oxidizing capacities of these oxides in the oxidation of cinnamyl alcohol in neutral solution [59].

8. References

[1] Van Krevelen, D. W., Van Beerden, C., and Hutjens, F. T., Fuel 30, 253 (1951).

[2] Van Krevelen, D. W., and Schuyer, J., Coal Science, Ch. XV, 312 (1957).

[3] Fitzgerald, D., Trans. Farad. Soc. 42, 362 (1956).

[4] Dollimore, D., J. Thermal Analysis 11, 185 (1977).

[5] Dollimore, D., J. Thermal Analysis 13, 455 (1978).

[6] Davies, P., Dollimore, D., and Heal, G. R., Proc. First European Symposium on Thermal Analysis, D. Dollimore (ed.), Heyden, 348 (1976).

[7] Matsushima, T., and Thoburn, W. J., Can J. Chem. 43, 602 (1965).

[8] Dollimore, D., and Tonge, K. H., 5th Int. Symp. React. Solids, Munich, 497 (1964).

[9] Berg, L. G., and Rassonskaya, I. S., Dokl. Akad. Nauk SSSR 73, 113 (1950).

[10] Berg, L. G., Rassonskaya, I. S., and Buris, E. V., Izv. Sekt. fiz-khim. Analiza Inst. Obshchei neorg. Khim. 27, 239 (1956).

[11] Borchardt, H. J., and Daniels, F., J. Phys. Chem. 61, 917 (1957).

[12] Dollimore, D., Differential Thermal Analysis, Vol. 1, R. C. Mackenzie (ed.), Academic Press, 395 (1970).

[13] Keattch, C. J., and Dollimore, D., An Introduction to Thermogravimetry, 2nd Edition, Heyden, 57 (1975).

[14] Cordes, H. F., J. Phys. Chem. 72, 2185 (1968).

[15] Shannon, R. D., Trans. Farad. Soc. 60, 1902 (1964).

[16] Polanyi, M., and Wigner, E., Z. Phys. Chem. A139, 439 (1928).

[17] Dollimore, D., and Rodgers, P. F., Thermochimica Acta 30, 273 (1979).

[18] Cremer, E., Advan. Catal. 7, 75 (1955).

[18] Cremer, E., Advan. Catal. 7, 75 (1955).

[19] Constable, F. H., Proc. Roy. Soc. A108, London, 75 (1925).

[20] Wendlandt, W. W., Sestak, J., and Satava, V., Thermochimica Acta 7, 333 (1973).

[21] Dollimore, D., Heal, G. R., and Krupay, B. W., Thermochimica Acta 24, 293 (1978).

[22] Jones, L. F., Dollimore, D., and Nicklin, T., Thermochimica Acta 13, 240 (1975).

[23] Sharp, J. H., Brindley, G. W., and Narahaki Achar, B. N., J. Amer. Ceram. Soc. 49, 379 (1966).

[24] Morey, G. W., J. Phys. Chem 28, 1167 (1924).

[25] Kracek, F. C., J. Phys. Chem. 34, 1583 (1930).

[26] Wilburn, F. W., and Thomasson, C. V., J. Soc. Glass Technol. 42, 158T (1958).

[27] Wilburn, F. W., and Dawson, J. B., Differential Thermal Analysis, Vol. 2, R. C. MacKenzie (ed.), Academic Press, Ch. 34, 229 (1972).

[28] Wilburn, F. W., Thomasson, C. V., and Cole, H., "Symposium sur la Fusion de Verre," Union Scientifique Continentale du Verre, Brussels, 373 (1958).

[29] Oldfield, L. F., "Symposium sur la Fusion de Verre," Union Scientifique Continentale du Verre, Brussels, 383 (1958).

[30] Wilburn, F. W., Metcalfe, S. A., and Warburton, R. S., Glass Technol. 6, 107 (1965).

[31] Niggli, P., Z. Anorg. Allg. Chem. 98, 241 (1916).

[32] Tool, A. Q., and Eichlin, C. G., J. Opt. Soc. Am. 4, 340 (1920).

[33] Wentworth, C. K., J. Geol. 30, 377 (1922).

[34] MacKenzie, R. C., The Differential Thermal Investigation of Clays, R. C. MacKenzie (ed.), Min. Soc. London, 456 (1957).

[35] MacKenzie, R. C., Differential Thermal Analysis, Vol. 1, R. C. MacKenzie (ed.), Academic Press, London, Ch. 18, 498 (1970).

[36] Worrall, W. E., Clays-their nature, origin and general properties, MaClaren and Sons, London, 128 (1968).

[37] Brindley, G. W., The X-ray Identification and Crystal Structures of Clay Minerals, G. Brown, (ed.), Mineralogical Society, London, 51 (1961).

[38] Taylor, H. F. W., Clay Miner. Bull. 5, 45 (1962).

[39] Dollimore, D., Heal, G. R., and Horridge, T. A., Clay Minerals 8, 479 (1970).

[40] Holdridge, D. A., and Walker, E. G., Trans. Brit. Ceram. Soc. 67, 243 (1968).

[41] Dollimore, D., and Nicholson, D., J. Chem. Soc., 960 (1962).

[42] Dollimore, D., Griffiths, D. L., and Nicholson, D., J. Chem. Soc., 2617 (1963).

[43] Dollimore, D., and Griffiths, D. L., J. Thermal Analysis 2, 229 (1970).

[44] Brown, M. E., Dollimore, D., and Galwey, A. K., Thermochimica Acta 21, 103 (1977).

[45] Brown, M. E., Dollimore, D., and Galwey, A. K., J. Chem. Soc., Farad Trans. I, 70, 1316 (1974).

[46] Linsen, B. G., (ed.), Physical and Chemical Aspects of Adsorbents and Catalysts, Academic Press, London, 650 (1970).

[47] Iler, R. K., Colloid Chemistry of Silica and the Silicates, New York, Cornell University Press, 235 (1955).

[48] Dzisko, V. A., Vishevskaya, A. A., and Chesalova, V. S., Zhur. Fiz. Khim. 24, 1416 (1950).

[49] Dollimore, D., and Heal, G. R., Trans. Farad. Soc. 59, 2386 (1963).

[50] Dollimore, D., and Heal, G. R., Nature 208, 1092 (1965).

[51] Dollimore, D., and Turner, A., Chem. and Ind., 535 (1970).

[52] Clough, P. S., and Dollimore, D., Vacuum Microbalance Techniques 7, 51 (1970).

[53] Dell, R. M., and Wheeler, V. J., Trans. Farad. Soc. 58, 1590 (1962).

[54] Notz, K. J., and Mendel, M. G., J. Inorg. Nucl. Chem. 14, 55 (1960).

[55] Dollimore, D., Krupay, B. W., and Ross, R. A., Proc. First European Symp. Thermal Analysis, Salford, D. Dollimore (ed.), Heyden, 125 (1976).

[56] Dollimore, D., and Tonge, K. H., J. Inorg. and Nuclear Chem. 29, 261 (1967).

[57] Trillo, J. M., Munuera, G., and Criado, J. M., Catal. Rev. 7, 51 (1972).

[58] Dollimore, D., and Tonge, K. H., J. Chem. Soc. A, 1728 (1970).

[59] Dollimore, D., and Tonge, K. H., J. Chem. Soc. B, 1380 (1967).

THERMAL ANALYSIS IN CHEMICAL PROCESSING

RAPPORTEUR'S COMMENTS BY

Oscar Menis
Center for Analytical Chemistry
National Bureau of Standards
Washington, D.C. 20234

Dr. Dollimore developed a basic approach which should, if generally followed, lead to much more productive utilization of thermoanalytical data in interpretation and understanding of technological processes and chemical reaction principles. He illustrated the unique advantages of both thermogravimetry and differential thermal analysis in translating practically useless information from "bench top" experiments into usable form as applied to large production batches. However, his key contribution was in his focusing attention on the need to understand and be able to differentiate between the kinetic and the thermodynamic data derived in the experiment before these can be applied to the interpretation and controlling of the reaction process. It is to be hoped that greater attention will be given to reporting in literature the essential parameter, whether kinetics of thermodynamic, and thus improve the usefulness of the information.

In addition, from the wealth of his experience, he guided his listeners through a series of examples in industrial applications, ranging from the production of glass to the production and understanding of catalytic processes, encompassing a wealth of information of great use to the practitioner and learner in this field.

National Bureau of Standards Special Publication 580. Proceedings of the Workshop on the State-of-the-Art of Thermal Analysis held at NBS, Gaithersburg, MD, May 21-22, 1979. (Issued May 1980)

PROGRESS IN THE USE OF DIFFERENTIAL THERMAL ANALYSIS - EVOLVED GAS ANALYSIS (DTA-EGA) FOR THE ANALYSIS OF SECOND PHASES IN STEEL

W. R. Bandi[1]

U.S. Steel Research
125 Jamison Lane
Monroeville, Pennsylvania 15146

Abstract

For the past 15 years, U. S. Steel Research has applied differential thermal analysis - evolved gas analysis (DTA-EGA) to the identification and quantitative determination of second phases in steels and other alloys. Often existing equipment had to be modified, or special instruments had to be built to attain project objectives.

The procedure has been used for the qualitative identification of at least 35 second-phase compounds which can be chemically or electrochemically isolated from steels and other alloys. Small amounts of a particular phase, or in some instances new phases, have been identified even though they were not detected by other methods. Often phases which have similar diffraction patterns have been easily differentiated using EGA methods. In addition to the progress in identification, the quantitative determination of the precipitated phases has been a valuable aid in studying the rate of precipitation of a phase at a specific temperature; in determining changes in the type of crystal structure of precipitates as a result of heat-treating changes; and in observing the change in physical properties of the steel as a function of phase precipitation.

Introduction

More than 15 years ago the author proposed the use of DTA-EGA as a method of quantitatively determining carbides, nitrides, carbonitrides, sulfides, carbosulfides, and like compounds [1,2,3][2] in steel. Since the original idea for the analysis of these second-phase compounds, at least 35 such compounds have been determined by the DTA-EGA method. In many instances the results determined by this method have been the first quantitative values for those specific compounds in the steel. Although the quantitative determination of such phases is more difficult than was originally believed, it is often easy to identify and quantitatively determine small quantities of phases that are not detected by microscopy, microchemistry, microprobe, and x-ray diffraction methods. It should be understood that DTA-EGA is not ideal for determining all second phases in steel. However, it is a valuable quantitative tool and provides a method for discovering phases not previously detected in steels and alloys.

The DTA method is limited to those phases that can be quantitatively isolated by chemical or electrochemical procedures from the steel matrix. Such isolated residues often contain 20 distinct second-phase compounds. The basis of the carbide analysis is the assumption that the various carbides in an isolated residue will burn and evolve CO_2 at

[1]Professor Bandi passed away in July 1979. Any inquiries concerning this paper may be sent to George Krapf of the same address.

[2]Figures in brackets indicate the literature references at the end of this paper.

different temperatures when program-heated in an oxygen atmosphere in a DTA instrument. The measurement of CO_2 can be used to quantitatively determine the amount of that carbide. In a like manner it is possible to measure by chromatographic procedures the amount of nitrogen evolved when nitrides in an isolated residue are decomposed in a DTA instrument. Sulfides can also be identified by monitoring SO_2 evolution.

One of the distinct advantages of the method is that carbides can be easily distinguished from nitrides or carbonitrides by the amount and type of gas evolved. For example, many alloying elements form a cubic carbide, a cubic carbonitride, and a cubic nitride in the same steel. Diffraction patterns of these are very similar, and thus cannot be used to identify the phases. The evolved gases from DTA-EGA are very different and thereby permit an analysis for the carbides and nitrides.

DTA-EGA Methodology

Only milligram quantities of residue, which contain microgram amounts of a carbide, can be conveniently isolated from the steel and inserted into the DTA apparatus. To gain the desirable EGA sensitivity, it is necessary to use a very small O_2 gas flow (3 mL/min) so that changes in thermal conductivity caused by the evolution of a small amount of CO_2 from the combustion of a carbide can be detected [2,3,4]. Also, to achieve the best DTA-EGA analysis of the chemically isolated residue, it is necessary to modify most commercially available thermal instruments or to build an instrument from components. Existing instruments usually have too large a gas volume in the exit side of the sample compartment, making detection of the minute quantity of gas evolved from a few milligrams of a metal carbide impossible without instrument modifications. It is also important that the evolved gas flow upward through the sample compartment and out the top of the sample holder. In this manner, better "plug" flow characteristics, which yield better-defined gas responses, can be maintained. The lower gas volume and shorter gas flow times result in less elapsed time between the DTA recording and the corresponding EGA response [5].

Figure 1 depicts one of several modifications of the sample compartment which have been made on an R. L. Stone Co. (Columbia Scientific Corp.) thermal apparatus by U. S. Steel Research [2,3.4]. This modification works very well for carbides. Only a thermal conductivity detector is needed for detecting CO_2 in the evolved gas. However, the sample holder is not good for EGA measurement of nitrogen because of the adsorption and desorption of nitrogen by the metal during heating and cooling of the sample holder.

To eliminate the interaction between the evolved nitrogen and the metal sample holder, as well as to maintain a small exit-gas volume, the ceramic tube shown in figure 2 was fitted to a home-built DTA-EGA unit [6]. This instrument has been effectively used for more than 10 years for EGA nitrogen determinations. More recently we have included ceramic tubes as part of the modifications made to a DuPont 990 instrument to improve performance [7]. The conventional arrangement of the differential thermocouples in the DuPont instrument makes it easier to achieve a flat DTA baseline, but the recording and programming instrumentation is not as good for the EGA as the home-built or Columbia Scientific instrumentation shown in figure 1.

Figure 3 shows a modification of the sample compartment of the DuPont instrument which was made at British Steel Corporation [8]. In this modification a small ceramic funnel was inverted and then inserted through the top of the regularly supplied DuPont ceramic tube to reduce the gas volume. An EAI quadrupole mass spectrometer was then attached to measure nitrogen evolved from the decomposition of nitrides present in the chemically isolated residue. Results obtained with this arrangement are in good agreement with those obtained by using chromatographic columns.

Both U. S. Steel and British Steel have used a simple gas-chromatographic separation of O_2 and N_2 in the evolved gas before determining nitrogen evolved from the decomposition of nitrides [3,9]. The EGA apparatus shown schematically in figure 4 employs a molecular sieve 5A column and an eight-port valve which provides gas-flow paths so that the current gas sample is being collected while the previous evolved gas is being analyzed. Oxygen is used as the carrier gas in the gas sample collection system and helium flowing at approximately 75 mL/min is used in the chromatographic part of the analytical system. Figure 5 shows a typical EGA recording for the decompositon of Cr_2N.

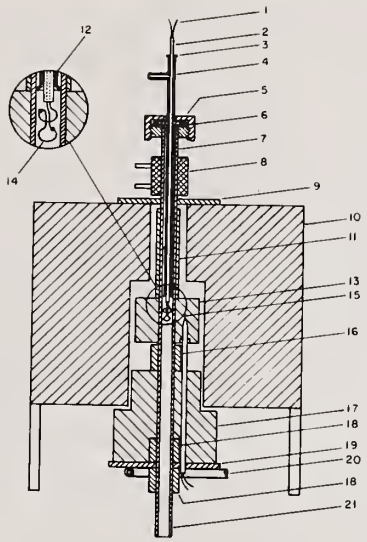

LEGEND:

1. DTA thermocouple leads
2. Thermocouple insulator
3. Epoxy cement seal
4. Gas exit to EGA cell
5. Hexagonal screw cap
6. O-ring seal
7. Outer gas outlet tube (Inconel)
8. Split water jacket (copper)
9. Asbestos washer (split)
10. Furnace
11. Asbestos sleeve
12. Inner gas collecting tube
13. One piece sample block (Inconel)
14. Platinel thermocouple and sample holding wire
15. Control thermocouple
16. Asbestos sleeve
17. Ceramic insulator
18. Sleeve nut
19. Water-cooled flange
20. Cooling coil (copper)
21. Gas inlet tube

Figure 1. Sample holder used in stone DTA instrument.

Figure 2. Ceramic tube modification used in research-designed DTA-EGA unit.

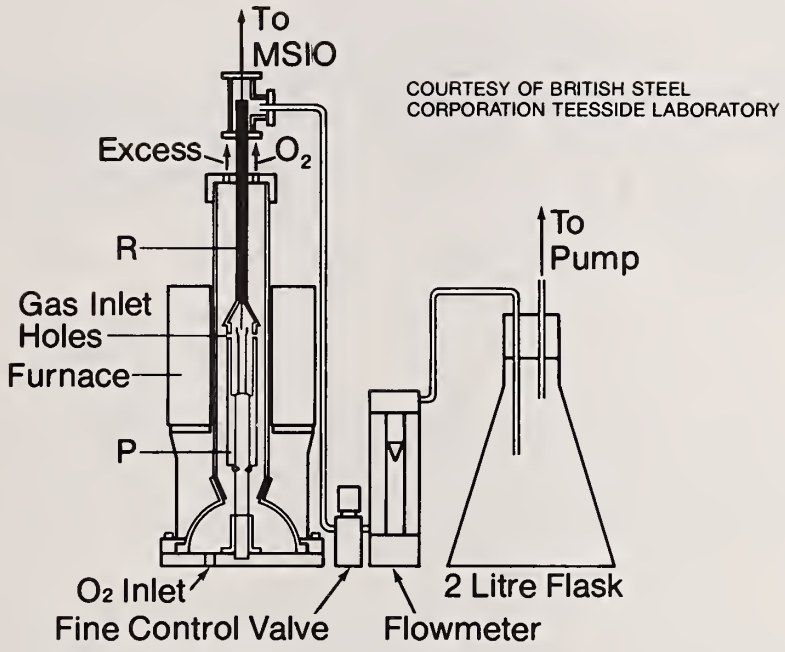

Figure 3. Modified Dupont DTA high-temperature cell. (Courtesy of British Steel Co., Teesside Lab.)

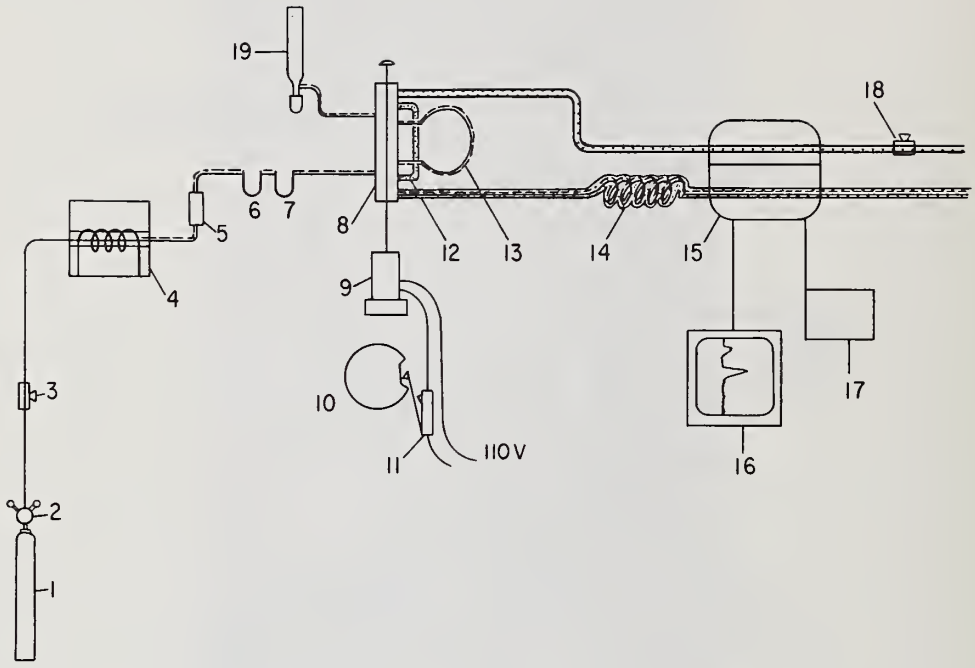

1. Oxygen
2. Regulator
3. Needle valve
4. DTA furnace
5. Catalyst tube
6. CO_2 and SO_2 absorber
7. H_2O absorber
8. Eight-port valve
9. Solenoid-operated pneumatic valve
10. Cam
11. Micro switch
12. Helium by-pass loop
13. Sample loop
14. Chromatographic column
15. Thermal conductivity detector
16. Recorder
17. Detector power supply
18. Helium needle valve
19. Vent to soap bubble flowmeter

Figure 4. Schematic diagram of EGA used in N_2 determination.

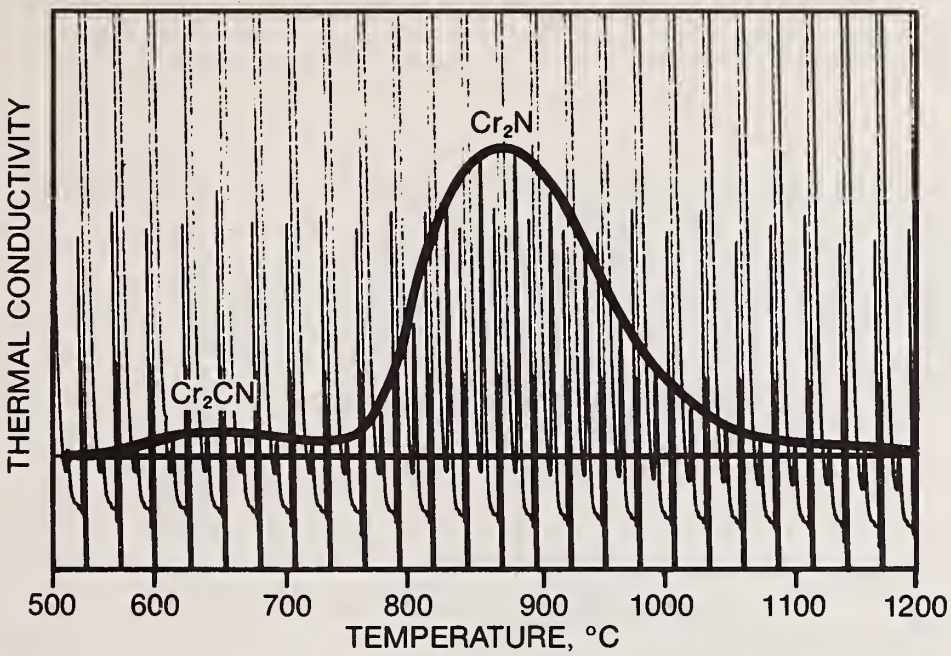

Figure 5. EGA nitrogen response for $Cr_2(CN)$ and Cr_2N.

Besides thermal conductivity, chromatography, and mass spectrometry which have already been mentioned, other EGA detection methods have also been used. At U. S. Steel, the SO_2 evolved from the oxidation of sulfides has been coulometrically monitored with an iodine concentration cell such as that used in organic pyrolysis or air-pollution analysis [10]. In Japan a conductometric unit has been used to monitor the CO_2 obtained from the combustion of carbides [11].

Calibration of EGA in Some Typical DTA-EGA Results

Table 1 shows typical operating parameters which can be used to obtain the DTA-EGA data. Figure 5 shows the chromatographic peaks obtained in the evolution of nitrogen from Cr_2N. By drawing a curve through the family of peaks, an area is obtained which can be related to the amount of nitrogen present. The EGA response of the instrument can be calibrated by use of several weights of a nitride [3].

Table 1. Typical DTA-EGA Operating Parameters.

Heating rate	= 10 °C/min
DTA sensitivity	= 0.33 °C/min
Thermocouples	= Platinel for Stone or Pt-Rh for DuPont
Gas Flow	= 3 mL/min O_2
Reference	= Al_2O_3
Sample holder	= 6-mm platinum dish
Sample size	= 1 to 3 mg of isolated residue
EGA-CO_2 calibration	= $CaCO_3$
EGA-N_2 calibration	= TiN
EGA time lag	= 40-80 °C depending on instrument
EGA-CO_2 sensitivity	= 5 micrograms
EGA-N_2 sensitivity	= 5 micrograms
Column	= molecular sieve 5A
Chromatographic carrier gas	= helium 75 mL/min
Volume of EGA-N_2 sample loop	= 7 mL
EGA-N_2 sampling cycle	= 3 min

The EGA thermal-conductivity unit can be easily calibrated for monitoring the evolution of CO_2 by using the decomposition of $CaCO_3$ in a 3 mL/min O_2 gas flow [2]. An example of this procedure is shown in figure 6.

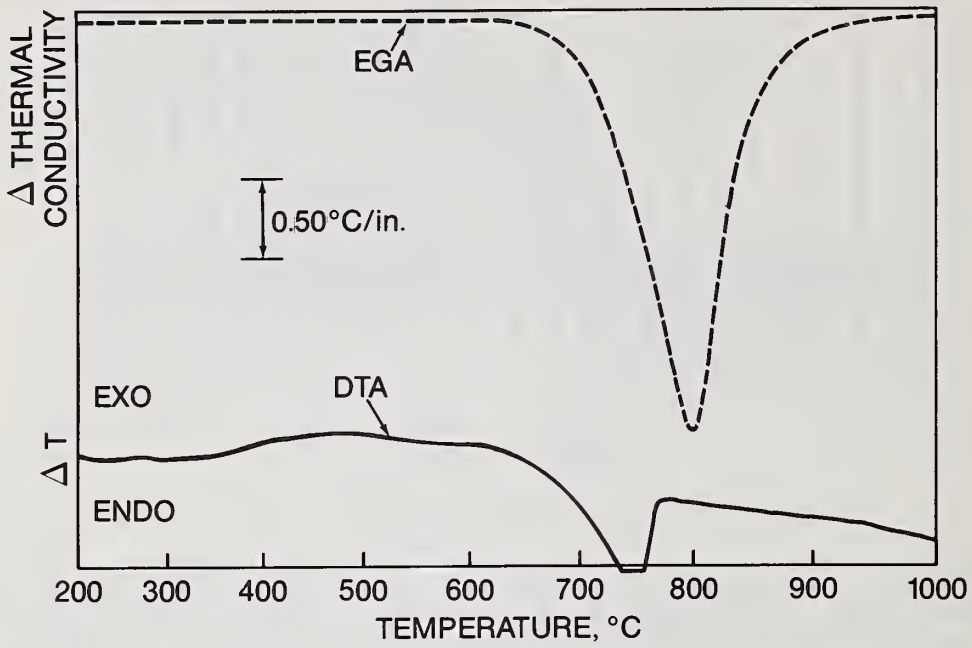

Figure 6. DTA/EGA response for the decomposition of 1 mg of $CaCO_3$.

DTA exotherms resulting from the decomposition and oxidation of nitrides are usually small rounded peaks. In contrast, combustion of carbides often causes very distinctive exotherms. Figure 7 shows the DTA and EGA responses for fractional milligram quantities of M_7C_3 and $M_{23}C_6$ isolated from a stainless steel. However, figure 8 shows a more complicated response for a steel that contains carbides of niobium, molybdenum, and titanium. The molybdenum carbides and Fe_3C are not quantitatively isolated, so no attempt was made to quantitatively determine these carbides.

Even the determination of niobium carbide and titanium carbide requires deconvolution of the EGA response for evolution of CO_2. In this instance a DuPont 310 Curve Resolver (a visual analog computer) is used [4,5,6,12,13,14]. In resolving overlapping EGA responses, it is necessary to consider the composition of the steel and the residue, the heat treatment given the steel, the known EGA temperature peaks of the carbides that could possibly be present in the isolated residue, and the shape of the peaks in the simultaneous DTA thermogram. Other easily recognizable DTA features such as a melting point or volatilization temperature are also useful, as are any corollary x-ray diffraction or microchemical data. Much of this knowledge is only attained by hands-on experience, and it is for this reason that it was stated earlier that quantitative determination of carbides was more difficult than was originally believed.

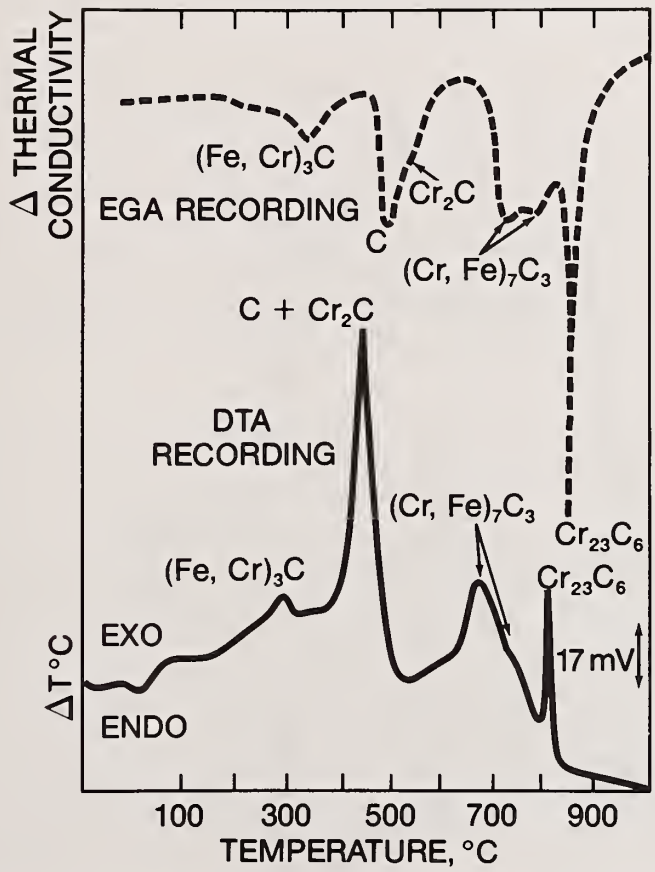

Figure 7. DTA/EGA response for 6 mg of residue obtained from stainless steel using the iodine-methanol isolation method.

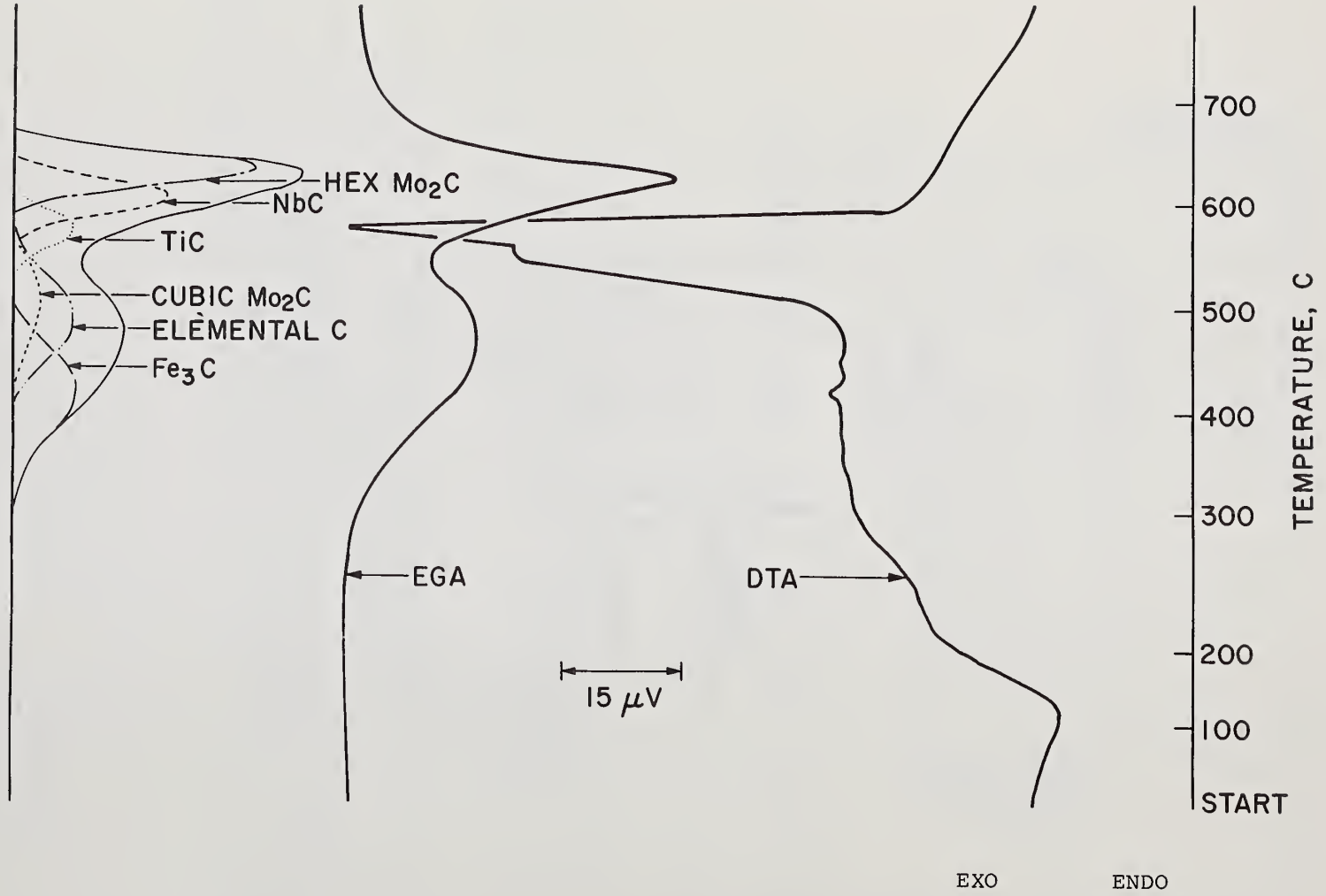

Figure 8. Deconvolution of EGA carbide response using the Dupont curve resolver.

Some Considerations in Chemical Isolation of Second-Phase Compounds

As stated previously, the accuracy of the DTA-EGA result depends on quantitative chemical isolation of the particular second-phase compounds from the steel or alloy matrix. Past experience indicates the DTA-EGA is more easily applied to the chemically stable carbides and nitrides of metals such as titanium, niobium, and vanadium [3,7,12], because chemically unstable compounds such as Fe_3C, MnS, and AlN, which represent a large proportion of the second-phase compounds, are dissolved in acid.

To isolate a residue, typically 2 to 4 grams of fine steel millings are dissolved in 10 percent hydrochloric acid at 40 °C under an inert atmosphere such as argon [3]. The resulting residue is filtered onto a preweighed 100- to 500-Å pore-size organic membrane also under an inert-gas atmosphere. After the organic membrane is dried in a desiccator under an inert atmosphere, it is reweighed. A residue weight is obtained after correction for any membrane weight change, as determined with a blank membrane. An aliquot weight (0.5 to 3 mg) of the residue is then transferred to the DTA instrument and heated in O_2 at a rate of 10 °C/min.

When acid isolation is not possible because the particular second phase is soluble in this medium [6,12], residues are isolated by dissolving the steel in an alcohol-iodine solution or by anodic dissolution in a neutral salt anolyte. Both the potential and the pH in the electrolytic cell are carefully controlled [12]. Such electrochemical dissolution is also used when the alloy cannot be dissolved in dilute hydrochloric acid [5,12,14]. The use of bromine-methanol, bromine-methylacetate, and like reagents for isolation of residues is not desirable because these reagents dissolve too much of the iron carbide or other carbides in the steel and leave large quantities of amorphous carbon in the residue [3,9,12,15]. This amorphous carbon causes errors in the determination of small quantities of both carbides and nitrides. It should be emphasized that because some compounds such as Fe_3C and Fe_4N cannot always be quantitatively isolated, the DTA-EGA procedures cannot be applied [12].

An important consideration in quantitative chemical separation of second-phase compounds is the need to retain particles smaller than 100 angstroms on organic filter membranes. Usually this is not a serious problem because in most isolation procedures at least part of the Fe_3C in the steel decomposes to amorphous carbon and the very small particles of nitrides and carbides adhere to the amorphous carbon and are thus retained during filtration [16-20]. In figure 9 the amount of niobium nitride precipitate at equilibrium at various temperatures is compared with the amount of niobium nitride found in the isolated residue by a DTA-EGA nitrogen determination. Amorphous carbon was present in the residue when the niobium nitride was isolated. The EGA results are slightly in excess of the equilibrium amount because the nitride is most likely $Nb_{0.9}N$. The nonstoichiometric compound is formed because the DTA-EGA samples were not heat-treated for long time periods to ensure an equilibrium precipitate. The results do show complete recovery of the nitride and are in agreement with data acquired by workers [16-20] using microchemical methods. Table 2 presents results for an Fe-Nb-N alloy having very little carbon. At low heat-treating temperature, some of the nitrogen was not believed to be precipitated, but it is also possible that minor amounts of the finer particles may not have been totally recovered.

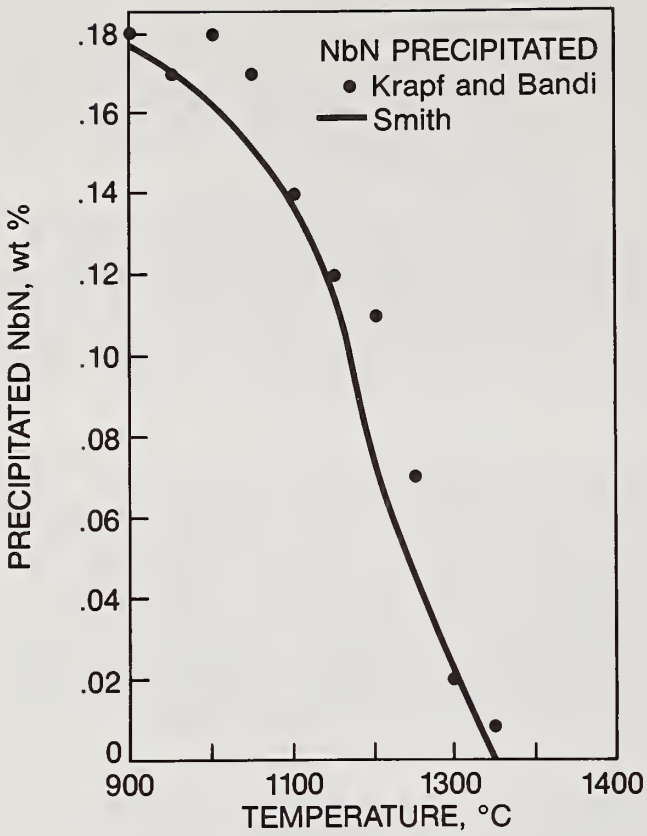

Figure 9. Comparison of results obtained from two methods for measuring niobium nitride precipitate.

Table 2. Recovery of NbN.

[Amount of NbN Isolated and Determined by EGA in Fe-Nb-N Alloy (% 0.17 NbN)]

Heat Treatment °C/3 Hr	% NbN Recovered
As rolled	0.14
900	0.18
950	0.17
1000	0.18
1050	0.17
1100	0.14
1150	0.12
1200	0.11
1250	0.07
1300	0.02
1350	0.008

At most temperatures at which complete precipitation of the nitride was expected, quantitative recovery of the nitrides was achieved. Table 3 presents data from isolation of several chromium carbides and/or nitrides in iodine-methanol. In this case the isolation is quantitative because all the carbon (or nitrogen) in the steel was recovered in the residue as second-phase compounds.

Table 3. EGA Determination of Chromium Phases - Percent.

C in Steel	C in Residue: M_3C	Cr_2C	Cr_2CN	M_7C_3	Amor. C	N in Steel	N in Residue: CrN	Cr_2N	$Cr_2(CN)$
0.065	0.036	0.028	N.D.	N.D.	N.D.	0.002	N.D.	N.D.	N.D.
0.16	0.017	0.052	0.003	0.076	N.D.	0.017	N.D.	N.D.	Trace
0.17	0.11	0.021	0.003	N.D.	0.025	0.022	0.0005	0.007	Trace
0.007	0.004	N.D.	N.D.	N.D.	N.D.	0.045	N.D.	0.044	N.D.
0.14	---------- Not Analyzed ----------					0.010	0.007	0.003	N.D.
0.14	0.048	0.006	Trace	N.D.	0.063	0.010	0.006	Trace	Trace

Use of DTA-EGA Results

Some second phases precipitate in steel as a result of heat treatment, and they almost always influence the mechanical properties of the steel. Therefore, it is important to determine how heat treatments affect steels so that desirable second phases can be precipitated and undesirable second phases can be minimized. Examples of changes in the amount of NbN in a steel as the heat treatment is changed have already been shown in figure 9 and Table 2. Such precipitates tend to control the austenitic grain size when the steel is hot. Thus, when the steel is cooled and transformed to ferrite, a fine-grained crystal is obtained. The fine-grained ferrite exhibits higher strength than coarse-grained ferrite and therefore the niobium nitride indirectly contributes to the strength of the steel and also minimizes strain aging.

The data in Table 4 show that changes occur in the amount of carbon and nitrogen in niobium carbonitride when heat treatment is varied. This is also true for titanium carbonitride. To understand the significance of such changes, consider a titanium-boron low-alloy steel. For the boron to be effective in promoting hardenability of the steel, it must remain in solid solution in the steel during rolling and other processing steps [21,22]. To achieve this end, titanium is first added in the molten metal to combine with nitrogen and thus prevent the formation of boron nitride. Often some titanium carbonitride is also formed with the titanium nitride. When the steel is heat-treated, DTA-EGA results show that some of the nitrogen in the carbonitride can be replaced by carbon, and this nitrogen is then able to combine with effective boron to form a noneffective boron nitride, and proper hardenability of the steel is not achieved. Because other methods do not readily detect changes in the composition of a carbonitride, the DTA-EGA method of analysis is useful in promoting a better understanding of what happens during heat treatment of steels.

Table 4. Changes in Composition of NbC_xN_y - Percent.

Sample	C Found as NbC_xN_y	N Found as NbC_xN_y	Nb As NbC_xN_y
1 As rolled	0.0021	0.0011	0.027
1 Solution annealed; 1000 °C for 3 hr then water quench	0.0044	0.0007	0.034
2 As rolled	0.0017	0.0012	0.027
2 Solution annealed; isothermally transformed 728 °C - 24 h	0.0014	0.0024	0.026

Figure 10 is an example of how changes in carbide precipitates caused by heat treatment of a high-temperature alloy can be observed. When a residue from the heat-treated sample of this alloy was examined by x-ray diffraction, it was difficult to distinguish minor amounts of one cubic phase in the presence of a large amount of another cubic phase. Also, the $M_{23}C_6$ carbide shown in figure 11 was not observed by many members of a group working on the identification of second phases by chemical isolation and x-ray diffraction analysis.

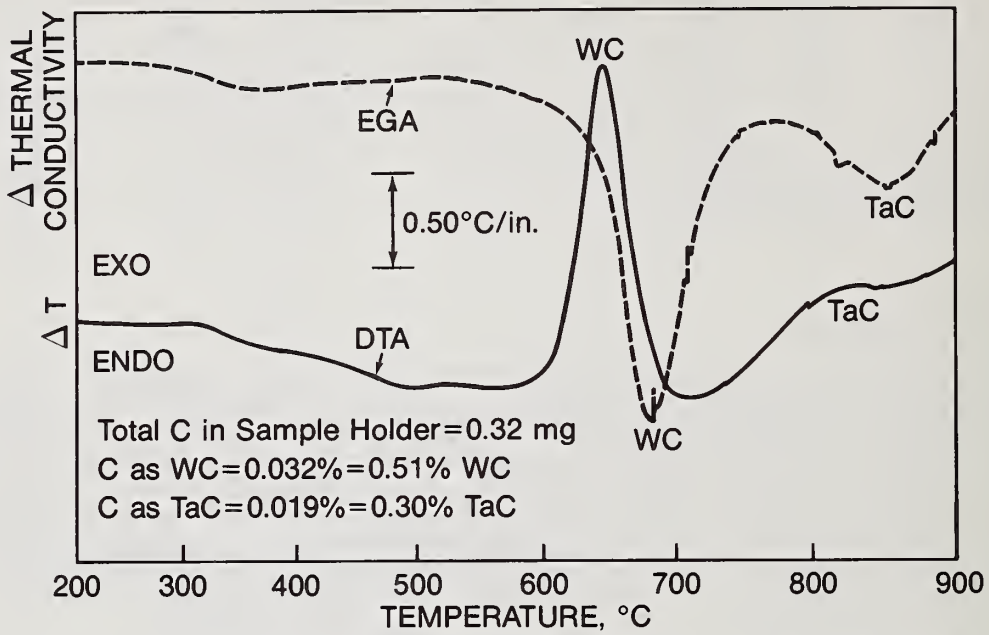

Figure 10. DTA/EGA response obtained from 5 mg of residue isolated from a high-temperature alloy using HCL-methanol isolation method.

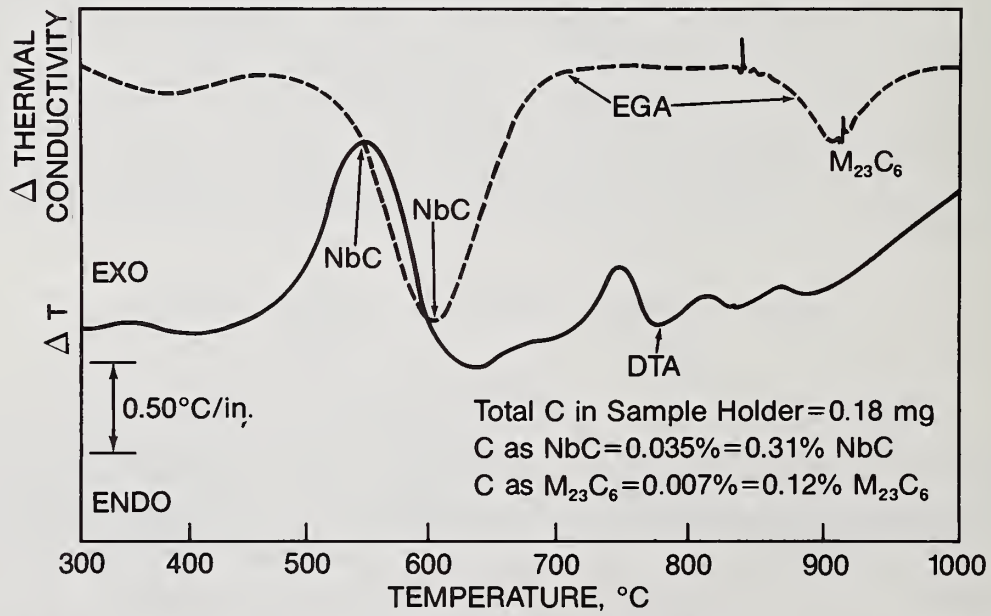

Figure 11. DTA/EGA recording obtained from 5.25 mg of residue isolated from high-temperature alloy using HCl-methanol isolation method.

DTA-EGA examination of niobium and vanadium carbides showed that it was relatively easy to distinguish Nb_4C_3 and V_4C_3 from NbC and VC. Usually, diffraction patterns indicated one carbide having a formula of $NbC_{0.8}$ or $NbC_{0.9}$, but the DTA-EGA analysis nearly always showed two distinct responses (figure 12), one for a carbide having the formula Nb_4C_3 and the second for a carbide with the formula NbC. DTA-EGA work has also identified a cubic (NbMo)C [23] which had been reported previously only by a Japanese worker [24]. A fourth cubic niobium phase containing carbon is NbC_xN_y. This carbonitride decomposes differently from most carbonitrides because it does not evolve CO^2 and nitrogen simultaneously [7,14,23]. NbON is first formed (CO_2 is evolved at 380-390 °C) and then NbO_2 is formed with the evolution of nitrogen at about 580 °C. Cubic NbN also precipitates in steel, and therefore five cubic niobium compounds can be distinguished by DTA-EGA. Figure 12 also shows a peak for combustion of Nb_2C. This compound has not been previously reported in alloy steels.

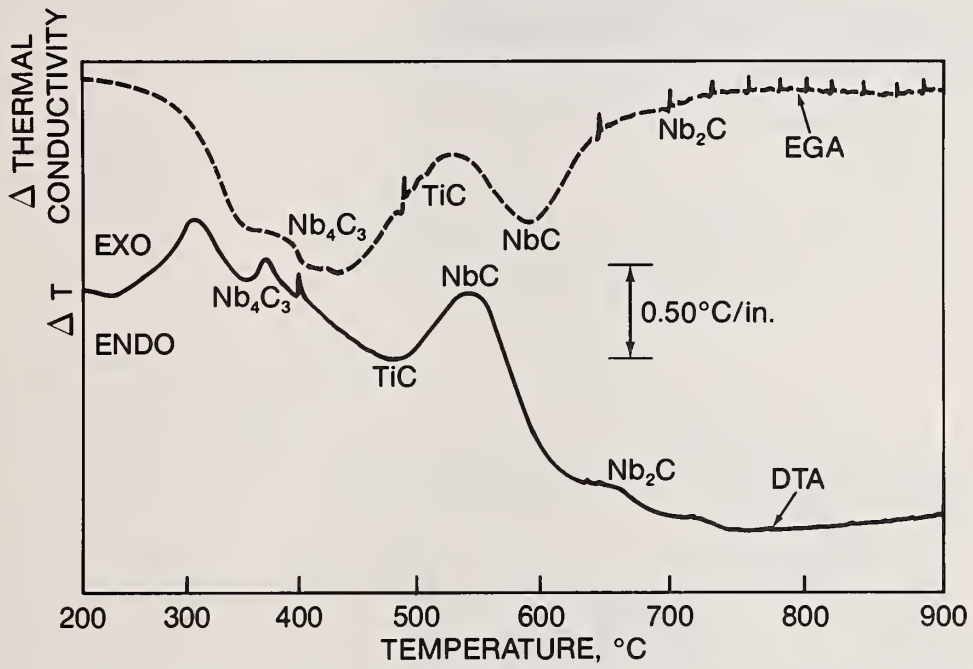

Figure 12. DTA/EGA response obtained from 4.65 mg of residue isolated from a high-temperature alloy using HCl-methanol isolation method.

Details on the precipitation of nitride phases in steel have also been discovered by use of DTA-EGA. As an example, it was previously believed that only cubic NbN was precipitated in steel. Figure 13 clearly indicates three nitrogen peaks which represent three forms of NbN [4]. Only one investigator has previously reported three forms [25].

Cr_2C and Cr_2CN are also easily identified by DTA-EGA. Figure 14 shows that these two compounds can be distinguished from Cr_2N, which is the nitride most often found in 18-8 stainless steel [6].

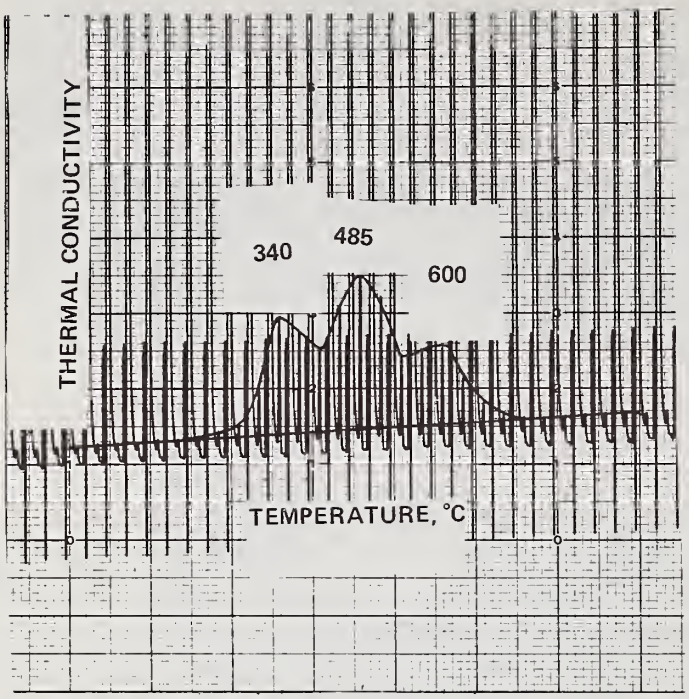

Figure 13. EGA-N_2 response obtained from a residue isolated from Fe-Nb-N alloy.

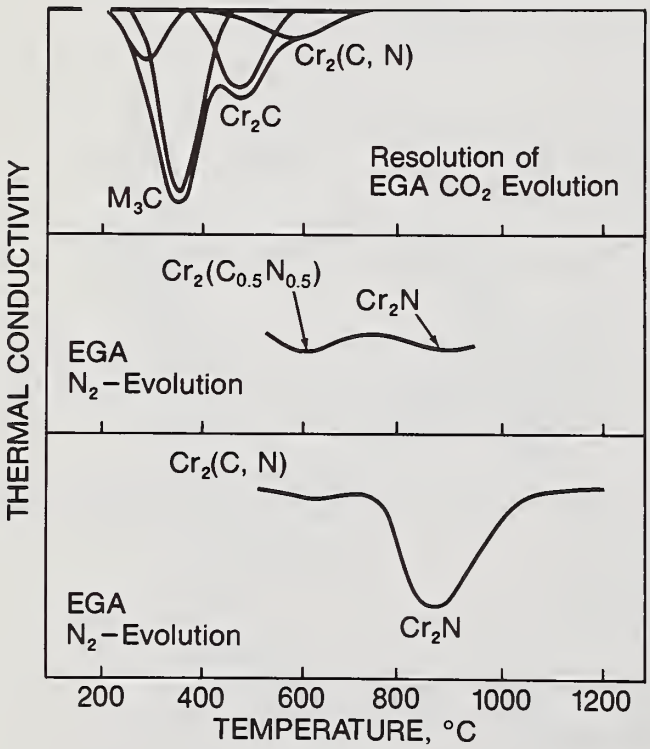

Figure 14. Response for CO_2 and N_2 evolved during the decomposition of Cr_2C, $Cr_2(C,N)$, and Cr_2N.

$Ti_4C_2S_2$ has been identified in steels as another nitride, as a mixture of TiC and TiS, and as γ-Ti_2S, depending on the method used for detecting second-phase compounds. One problem is the similarity in diffraction patterns of γ-Ti_2S and $Ti_4C_2S_2$. However, $Ti_4C_2S_2$ is easily distinguished from γ-Ti_2S by DTA-EGA since the compounds oxidize at different temperatures, and both CO_2 and SO_2 are evolved from the carbosulfide (figure 15). Only SO_2 is evolved from the combustion of the sulfide [26]. It appears that the carbosulfide may often occur in low-alloy titanium-bearing steels commonly produced in this country, yet it has not been previously identified.

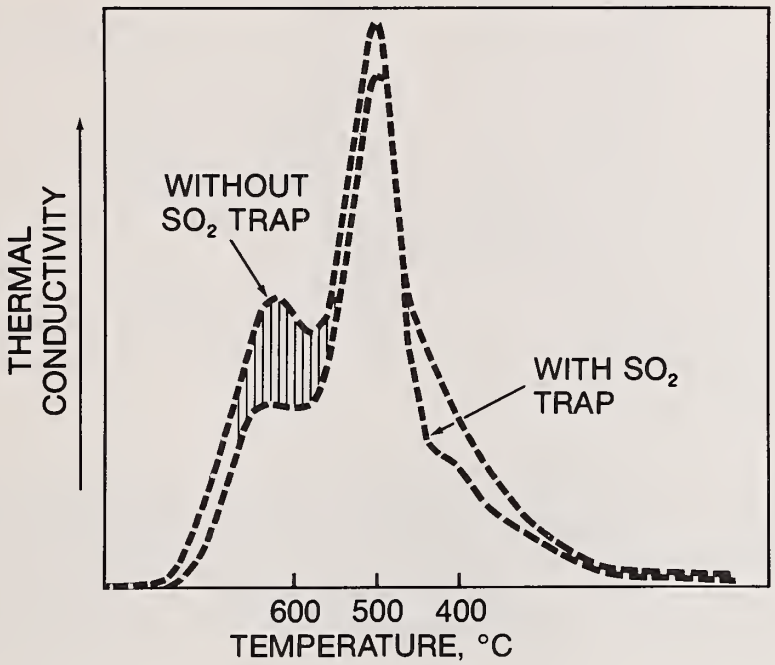

Figure 15. EGA-CO_2 response obtained at 610 to 630 °C with and without an in-line sulfur trap.

The DTA-EGA method has been used in other studies similar to those described in this paper. As an example, Table 5 summarizes the results obtained recently by workers studying the oxidation of NiS at the Western Australia Institute of Technology [27]. In this study a Stanton DTA and TG instrument was used, along with a quadrupole mass spectrometer, to obtain EGA data. X-ray diffraction was also used to characterize the structural changes.

Table 5. A TG/DTA/MS Study of the Oxidation of Nickel Sulfide.
[Dunn & Kelly, J. of Thermal Anal., 1977(43)]

Reaction	Temperature °C
$NiS + 2O_2 \rightarrow NiSO_4$	400 - 785
$NiO + SO_2 + 1/2O_2 \rightarrow NiSO_4$	500 - 785
$NiS + 1.5/2O_2 \rightarrow NiO + SO_2$	540 - 522 and 682 - 692
$3NiS + 2NiSO_4 \rightarrow Ni_3S_2 + 2NiO + 3SO_2$	682 - 692 and possibly
$10NiS + 2O_2 \rightarrow Ni_7S_6 + Ni_3S_2 + 2SO_2$	682 - 692
$Ni_7S_6 + 9.5O_2 \rightarrow 7NiO + 6SO_2$	682 - 780 and/or
$Ni_7S_6 + 12.5O_2 \rightarrow 6NiSO_4 + NiO$	
$Ni_3S_{2(\ell)} \rightarrow Ni_3S_{2(\ell)}$	793
$Ni_3S_{2(\ )} \rightarrow 3\text{-}1/2O_2 \rightarrow 3NiO + 2SO_2$	793
$NiSO_4 \rightarrow NiO + SO_2 + 1/2O_2$	>800

In another similar study at Chalmers Technical School, University of Göteborg, Sweden, Mettler instrumentation is being used to study the formation and decomposition of $MnSiN_2$ and Si_3N_4 (figure 16) [28]. $MnSiN_2$ has only recently been identified in steels, although it has probably been present in many steels studied in the past and may often have been interpreted as another nitride. Si_3N_4 is a nitride which occurs in 3 percent Si-Fe alloy and is involved in preferred grain orientation in steels during rolling and recrystallization of the material.

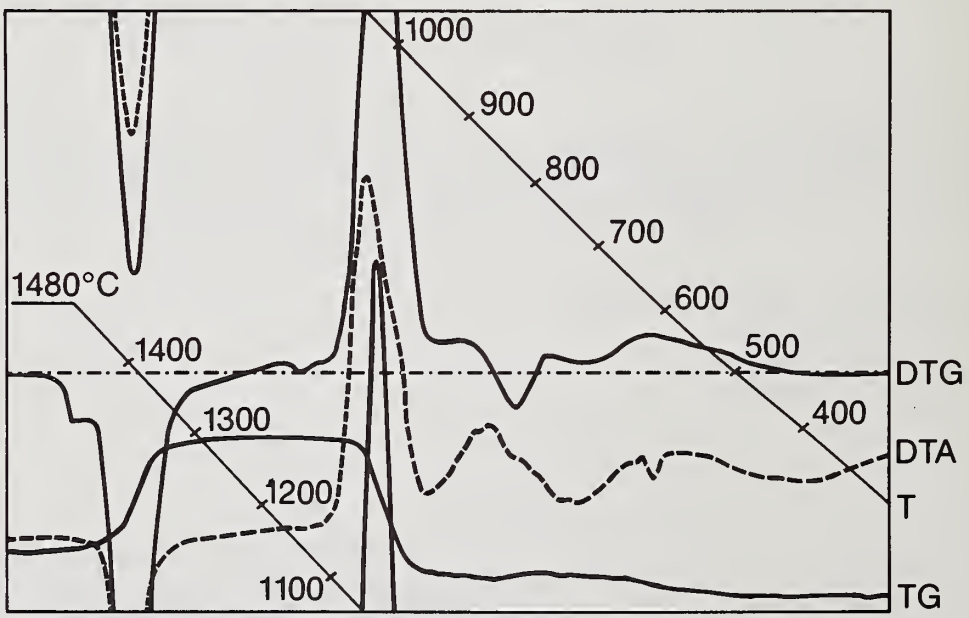

Courtesy R. Pompe Chalmers University of Technology, University of Göteborg, Göteborg, Sweden

Figure 16. DTG, DTA, and TG responses for the nitriding of the powder mixture of Mn and Si in nitrogen.

Figures 17 and 18 are examples of some work published by scientists in the Metallurgical Department of the Polytechnic Institute in Mons, Belgium [15]. The work confirms much of the work done at U. S. Steel Research Laboratory. Some of the DTA results are much better defined than those which we have published, and it is simpler to interpret their thermograms and EGA responses.

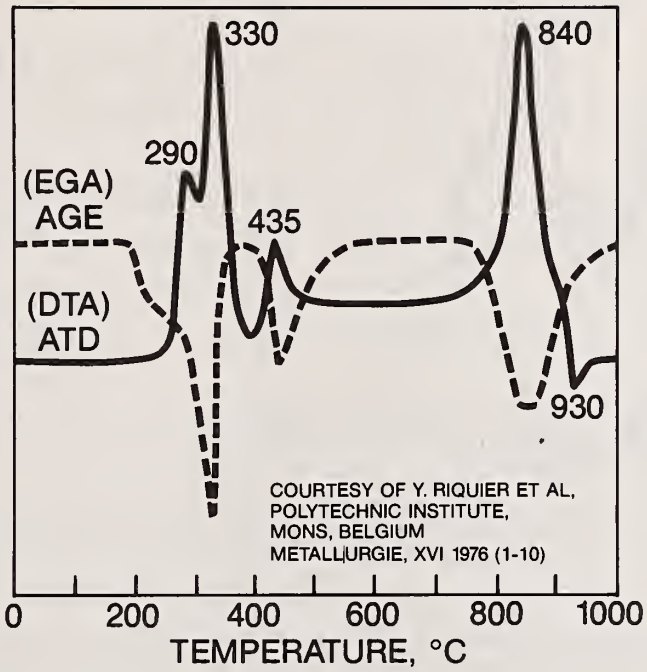

290 - Fe_3C

330 - amorphous C in H_2SO_4

435 - MoC

840 - $M_{23}C_6$

930 - volatilization of MoO_3

Figure 17. DTA/EGA response obtained from a residue isolated from steel using 10 percent H_2SO_4.

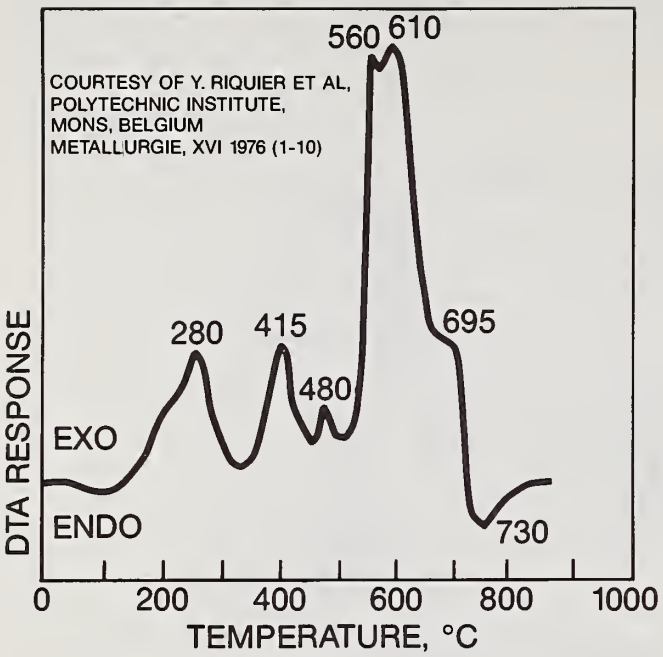

280 - Fe_3C

415 - MoC

480 - TiC

560 - $Ti_4C_2S_2$

610 - Mo_2C

695 - TiN

730 - volatilization of MoO_3

Figure 18. DTA response obtained from a residue isolated from steel using 10 percent H_2SO_4.

Literature in Japan indicates they are using a DTA-type apparatus to program-heat isolated residues from steels and are determining titanium carbide and like compounds by conductometric measurement of evolved CO_2 [11]. It is also known that China Steel in Taiwan intends to study second phases by this method.

There has been little progress in the use of this method in the American steel industry, mostly because second-phase work is usually performed by the more conventional methods of identification such as microscopy and diffraction. However, recently some of the American university metallurgy departments have shown an increased interest and have used this technique with some success. It is probable that as future metallurgists realize the potential of the method, use of the DTA-EGA procedures to study second phases in steels will increase.

References

[1] Bandi, W. R., Karp, H. S. Straub, W. A., Melnick, L. M., Talanta, 11, 1327 (1964).

[2] Karp, H. S., Bandi, W. R., and Melnick, L. M., Ibid., 13, 1679 (1966).

[3] Bandi, W. R., Straub, W. A., Buyok, E. G., and Melnick, L. M., Anal. Chem., 38, 1336 (1966).

[4] Bandi, W. R., Buyok, E. G., Krapf, G., and Melnick, L. M., Thermal Analysis, Vol. 2, R. F. Schwenker, Jr. and P. D. Garn (eds.), Academic Press, New York, NY, 1363-1376 (1969).

[5] Krapf, G., Bandi, W. R., and Melnick, L. M., J. Iron Steel Inst., London, 211, 890 (1973).

[6] Bandi, W. R. and Krapf, G., Anal. Chem., 49, 649 (1977).

[7] Bandi, W. R., Science, 196, 136 (1977).

[8] White, G., Fisher, R., Bradshaw, G., The Thermal Analysis of Nitride Phases in Steel, Corporate Development Laboratory, British Steel Corporation, Sheffield, England (1974).

[9] Lloyd, M. H. and Shanahan, C. E. A., J. of Thermal Anal., 12, 321 (1977).

[10] Bandi, W. R., Straub, W. A., Karp, H. S., and Melnick, L. M., ASTM Special Technical Publication No. 393, American Society for Testing and Materials, Philadelphia, PA (1966).

[11] Ishii, T. and Ihida, M., Tetsu-to-Hagane, 13, 60 (1974).

[12] Krapf, G., Lutz, J. L., Melnick, L. M., and Bandi, W. R., Thermochim. Acta., 4, 257 (1972).

[13] Krapf, G., Buyok, E. G., Bandi, W. R., Ibid., 13, 47 (1975).

[14] Krapf, G., Buyok, E. G., Bandi, W. R., and Melnick, L. M., J. Iron Steel Inst., 211, 353 (1973).

[15] Riquier, Y., Vanthournhaut, M., Levert, J. M., and Vandael, C., Metallurgie, 16 10 (1976). (Mons, Belgium)

[16] Fisher, R. and White, G., A Critical Evaluation of Methods for the Determination of Free Nitrogen in Carbon and Low-Alloy Steels, Corporate Advance Process Laboratory, British Steel Corp., Sheffield, England (1973).

[17] Koch, W. and Sauer, K. H., Archiv. Eisenhuttenw., 36, 591 (1965).

[18] Beeghly, H. F., Anal. Chem., 21, 1513 (1949).

[19] Dahl, W., Schwab, P., and Hergstenberg, P., Archiv. Eisenhuttenw., 32, 475 (1961).

[20] Bandi, W. R., AIME Open Hearth Proceedings 1976, 59, New York, NY, 131-141 (1976).

[21] Kapadia, B. M., AIME Symposium on Hardenability Concepts with Applications to Steel, October (1977).

[22] Ueno, M. and Inoue, T., Trans. ISIJ, 13, 210 (1973).

[23] Krapf, G., Buyok, E. G., Bandi, W. R., and Melnick, L. M., paper Pittsburgh Conference on Analytical Chemistry and Applied Spectroscopy, Cleveland, OH, March 2-7 (1969).

[24] Kanazawa, S., Nakashima, A., Okamoto, K., Tanabe, K., and Nakazawa, S., Nippon Kinzoku Gakkai-shi, 31, 71-76 (1967).

[25] Mori, T., Fujita, K., Tokizane, M., and Yamaguchi, K., Tetsu-to-Hagane, 30, 911 (1964).

[26] Bandi, W. R. and Krapf, George, Analyst, 101, 812 (1979).

[27] Dunn, J. C., and Kelly, C. E., J. of Thermal Anal., 12, 43 (1977).

[28] Pompe, R., Thermochimica Acta, 16, 295 (1976); Pompe, R., Proceedings Nortemps 75, 1, 177-187.

ANALYSIS OF SECOND PHASES IN STEEL

RAPPORTEUR'S COMMENTS BY

W. E. Clark
Delco Products Division
General Motors Corporation
1555 Lyell Avenue
Rochester, New York 14606

This paper offers a very good example of the application of thermal analysis to a practical everyday problem. As a member of the manufacturing community it is gratifying to review a paper dedicated to applying what has been a research tool, to practical problem solving.

In his paper, William Bandi discusses the application of differential thermal analysis and evolved gas analysis (DTA and EGA) to the study of second phases in steel. Second phase determination is particularly important when one is concerned with the resultant physical properties of the steel, i.e., ability to withstand freezing temperatures (Alaskan Pipeline) and ductility to name a few. Bandi's paper deals with methodology which while unique is within everyones grasp to use.

One of the major difficulties in trying to identify some second phases in steel through the use of classical means, i.e., microscopy, x-ray diffraction, microchemistry, etc. is the inability to distinguish between different phases of, say, the cubic type. A good example was cited in the cubic carbide, cubic carbonitride, and the cubic nitride phases. As indicated in the paper, the evolved gases from DTA-EGA are very different and permit an analysis for carbides and nitrides, and allow us to determine the different cubic structures noted above. This method is also useful in determining sulfide phases. Accuracy of this method is quite high but does depend on the quantitative procedures used to isolate the compounds. This chemical isolation step appears to be the only drawback to this method.

The versatility of this method makes one wonder why it is not in wider spread use in this country as one means of controlling critical properties of steel. Discussions with Bandi revealed that the U.S. steel industry is lagging behind the rest of the world, particularly the Japanese, in the application of this method. When queried about the potential uses of this method as an inspection tool for the steel customer, Bandi reiterated his position that if one is interested in the mechanical properties of steel, you have to be able to measure those attributes that affect them. I feel that as a high volume user of steel, the automotive industry should investigate this procedure for inclusion in their material specifications.

National Bureau of Standards Special Publication 580. Proceedings of the Workshop on the State-of-the-Art of Thermal Analysis held at NBS, Gaithersburg, MD, May 21-22, 1979. (Issued May 1980)

THERMAL ANALYSIS IN THE RUBBER INDUSTRY

D. W. Brazier

Dunlop Research Centre
Sheridan Park Research Community
Mississauga, Ontario, Canada L5K 1Z8

Abstract

In this review an attempt will be made to outline just some of the applications of thermoanalytical procedures (TG, DSC, TMA) in the rubber industry. Despite the extensive use of these procedures in the study of high molecular weight polymers, relatively little has been published on commercial elastomers and complex elastomeric compounds. For ease of presentation, each procedure is considered separately; however, the total characterization of a system by several methods often provides insight not apparent from one procedure.

The major areas considered are:

TG/DTG
- basic thermal stability of elastomers
- qualitative identification of elastomers and elastomer blends
- quantitative analysis of rubber compounds (elastomers, carbon black, fillers, etc.)

DSC
- basic features of DSC data on elastomer compounds
- the heat of vulcanization and characterization of curative systems.

TMA/DTMA
- characteristic feature of TMA curves
- low temperature properties of elastomeric products.

The above is by no means exhaustive and it is hoped that the areas chosen will illustrate the versatility and usefulness of thermal analysis in all aspects of the industry.

Introduction and Rubber Technology

Procedures such as thermogravimetric analysis (TG), differential thermal analysis (DTA), differential scanning calorimetry (DSC), and more recently, thermomechanical analysis (TMA and DMA) have found extensive use in the study of high molecular weight polymers. In all polymer applications, be they thermoplastic or thermoset, temperature and its effect, either alone or in conjunction with the ambient chemical environment, determine the limits of the product's performance. Elastomers, a special class of high molecular weight polymers, which exhibit the property of elasticity, are no exception, and temperature plays an important role throughout the entire lifetime of an elastomeric product. In the production plant, elastomers are mixed at elevated temperatures in the solid state with a variety of ingredients (fillers, anti-oxidants, oils, plasticizers, curatives, etc.), each of which plays an important role in the final product in-field performance. After mixing, the compound may be further processed; for example, calendered or extruded, formed into one component of a product, or combined with other materials such as textiles or steel as, for example, in the case of tires, hoses, and belting products. Finally, the unvulcanized composite is cured by a thermal process either as is, or after a final shaping operation under pressure and at elevated temperature. Vulcanization is a very complex chemical process by which crosslinks are introduced between the polymer chain, and the nature and

distribution of these crosslinks primarily determines the physical properties of the vulcanized product. Once produced, the product must often perform adequately over a wide range of temperature (low and high), offer good resistance to chemicals and solvents, and resist oxidation. Additionally, the product should maintain constancy in both chemical composition and physical properties as a function of time.

The above very brief introduction shows some aspects of elastomer technology and is necessary in order to appreciate the wide range of applications for thermal analytical procedures within the industry. Time does not permit an exhaustive discussion and we shall only cover selected areas. The complexity of elastomeric compounds is illustrated in Table 1, which shows typical tire component formulations, based on blends of natural rubber and polybutadiene.

Table 1. Compound Formulations - Typical Tire Components.

Compound	A	B	C
	(Parts per hundred rubber)		
Natural Rubber	80	80	60
Polybutadiene	20	20	40
Carbon Black	50[a]	50[a]	55[b]
Stearic Acid	3	1.8	2.5
Zinc Oxide	3	3	3
Anti-oxidant	3	-	2.25
Oil/Plasticizer	17	11.5	16
Bonding Agent	-	2.7	-
Sulfur	2.2[c]	2.2[c]	1.5
Accelerator (MOR)	1.2	1.2	1.0
Inhibitor	-	-	0.3

[a] N326 (HAF-LS) carbon black.

[b] N339 carbon black.

[c] Added as 2.75 phr. oiled Crystex (80% sulphur in oil).

In general, the experimental procedures to be described are applicable regardless of the type of elastomer, or the elastomers present. Table 2 summarizes the types of elastomers generally encountered in rubber formulations. In each class, numerous variations exist, e.g., for styrene butadiene rubbers, over 200 types are commercially available. Differences can be in styrene: butadiene ratio, random vs. block co-polymerization, solution, and emulsion polymerization, type of oil extender used, etc. In practice, most compounds are blends of two or more elastomers, e.g., NR:BR or SBR:BR EPDM. All results discussed here were obtained on commercial raw materials and products, and not purified laboratory samples.

Table 2. Nomenclature for Elastomer Types.

NR	Natural Rubber - polyisoprene
IR	Synthetic polyisoprene
BR	Polybutadiene
SBR	Styrene-butadiene rubber
NBR	Nitrile-butadiene rubber
EPDM	Ethylene-propylene-diene terpolymer
EPM	Ethylene-propylene copolymer
IIR	Butyl (isobutene-isoprene)
CIIR	Chlorobutyl
BIIR	Bromobutyl
ACM	Copolymer of ethyl or other acrylates
CR	Chloroprene
CSM	Chlorosulphonyl polyethylene
CM	Chloropolyethylene
FKM	Fluoro rubbers of polyethylene type
CO	Epichlorohydrins
ECO	Epichlorohydrin-ethylene oxide copolymers

For ease of presentation, the material is divided into discussion under the analytical procedure used rather than the application area. In the past decade, two reviews of the use of thermoanalytical methods with particular reference to commercial elastomeric systems, have been published [1,2][1]. Despite considerable developments over the last five years, practical routine applications of thermal methods to elastomer systems are still in their infancy. However, the introduction of reliable, robust and cheaper instrumentation is predicted to result in renewed industrial interest. It is the objective of this presentation to illustrate applications as used in our laboratory – many of which require further development and these will be indicated as we proceed.

Thermogravimetry

A. Elastomers

1) The Identification and Analysis of Elastomers:

The identification and determination of elastomers in compounds is often a tedious and time-consuming task. Pyrolysis methods such as pyrolysis-infrared spectroscopy and pyrolysis-gas chromatography are widely used. In this section, we consider the potential of thermogravimetry, or, more important, derivative thermogravimetry as a method for fingerprinting elastomer types. The basic concept is to determine the DTG degradation profile in nitrogen and/or oxygen (or air) and to match it with a profile obtained on an authentic sample under identical experimental conditions. Careful attention to experimental parameters (sample size and geometry in relation to the thermocouple, heating rate, gas flow rate, etc.) is mandatory. However, both the reproducibility and reliability with modern instrumentation is excellent.

Table 3 summarizes DTG characteristics of a variety of elastomer types all obtained under identical experimental conditions in a nitrogen atmosphere [3].

[1]Figures in brackets indicate the literature references at the end of this paper.

Table 3. DTG Characteristics of Elastomers [3].

Polymer	T_{max}, °C[a]	Comments
Natural rubber	373	single peak, shoulder high-temperature side
Polyisoprene (Natsyn 220)	373	
Polybutadienes		
Taktene 1220	461,372	372° peak 4–10% of 460° peak for BR's at 10 °C/min; occasional split peaks at 460 °C
Budene 101	460,372	
Cisdene	460,372	
trans-Polybutadiene	461,372	laboratory sample[b]
MW 81,500	457,376	laboratory sample[b]
MW 365,000	451,367	laboratory sample[b]
Arco 45M	462,375	hydroxyl-terminated liquid BR
Nisso G-2000	455,353	
Hystl B-3000	450,345	non-functional end groups
Hystl B-1000	457 –	
Styrene-butadiene rubbers		
1500	449,261	23.5% styrene; All T_{max} below 300 are small and broad
1502	444,236	23.5% styrene
1515	442,424,228	28% styrene
1516	429,405,220	40% styrene
1712	445,309 (oil)	23.5% styrene, 37.5% aromatic oil
1778	445,285 (oil)	23.5% styrene, 37.5% naphthenic oil
Solprene 300	445	25% styrene, random solution polymer
Solprene 1205	445,373	25% styrene block copolymer
Kraton 101	449,381	block copolymer
Butyl rubbers		
Butyl 301	386	symmetrical single peak
Bromobutyl	386,221	221° peak: 2.2% wt. loss
Chlorobutyl HT-1068	386,245	245° peak: 1% wt. loss
EPDM		
Royalene 301T	461	single symmetrical peak
EPR		
V404	460	symmetrical peak

[a] T_{max} is the temperature at which maximum degradation rates are observed under the given experimental conditions. Scan rate 10 °C/min. Nitrogen flow 50 cm^3/min.

[b] Laboratory samples prepared to investigate effect of molecular weight distribution.

The T_{max} temperatures are the temperatures at which maximum rates of weight loss are observed. Identification of an elastomer on the basis of Tmax alone is difficult because of similar degradation patterns observed for many types. Observation of the complete DTG profile often reveals details which assist in the differentiation of the various elastomers. This can be illustrated by reference to SBR copolymers, the DTG profiles of which are shown in figure 1. SBR 1500, 1712, and 1778 are all 23.5 percent bound styrene random copolymers, 1712 containing 37.5 parts per hundred rubber (phr) of aromatic oil, and 1778 containing 37.5 phr naphthenic oil. The volatilization of the oils from 1712 and 1778 is readily apparent and the greater volatility of naphthenic oil is seen by the lower T_{max}

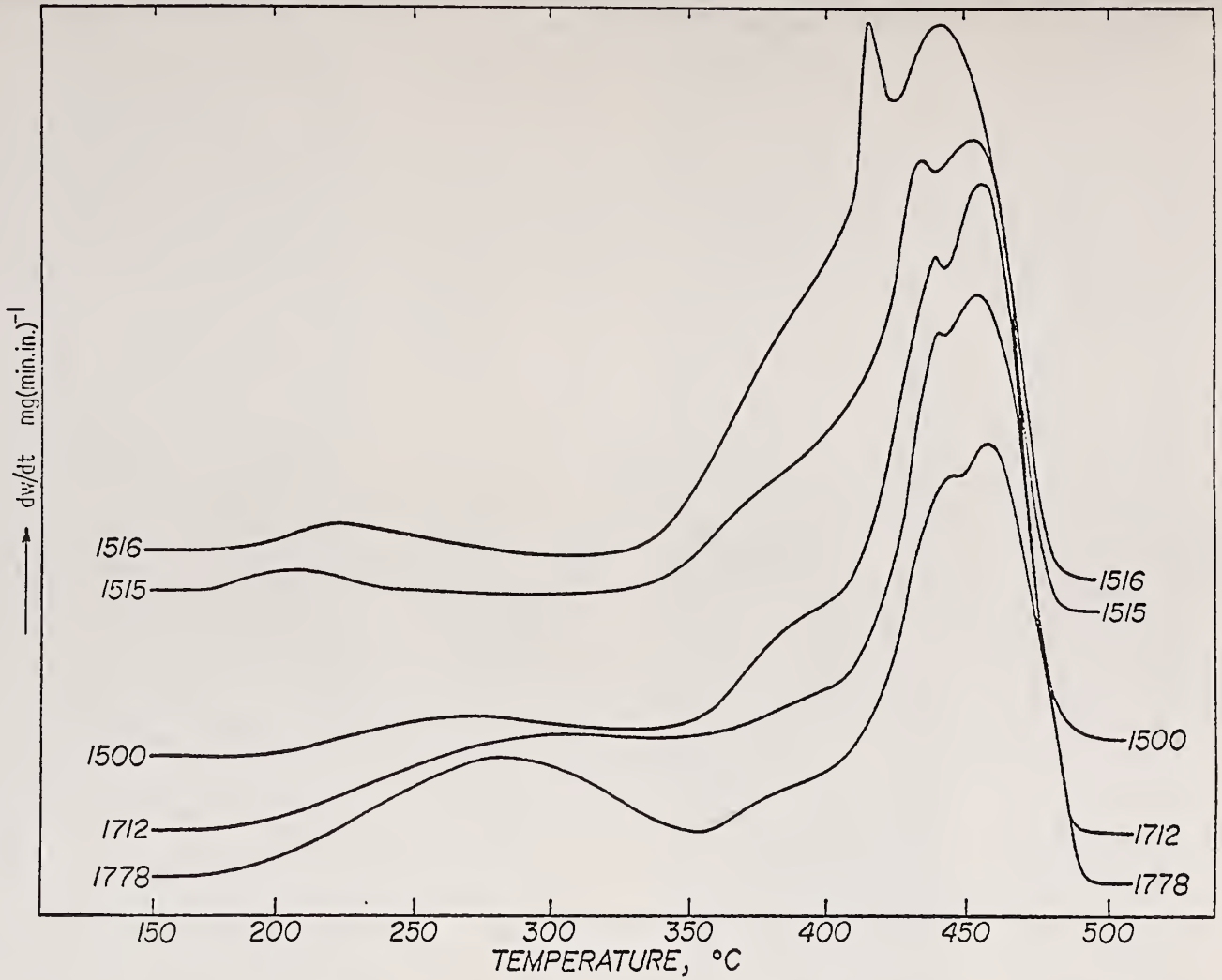

Figure 1. DTG profiles of commercial raw SBR elastomers [3]. Ten °C/min heating rate in nitrogen. Styrene and oil contents of each grade given in Table 3.

for this material. The non-oil extended SBR elastomers also exhibit weight loss at temperatures between 200 and 270 °C as shown for SBR 1500, 1515, and 1516. These weight losses are related to residual emulsifiers in the copolymer (1500 - rosin acid, 1515 - fatty acid, and 1516 - mixed fatty acid-rosin acid emulsified). Apart from differences in the loss of residuals or additives, differences in the main plasticizer degradation patterns are also observed as styrene/butadiene ratio charges (1515, 28% bound styrene, and 1516, 40% bound styrene).

Similar observations on all elastomers, thermoplastic rubbers, and polymer systems can be made leading to the conclusion that the DTG profile can provide a fingerprint of the material of interest. For quality control purposes, this fingerprint can be compared directly to a master curve obtained on a specific sample. In our laboratory, virtually all commerical materials used in the rubber industry have been characterized by DTG, including, in addition to the polymeric component, extender oils, plasticizers, textiles, adhesives, resins, and curatives. Further examples will be given later when considering the quantitative analysis of compounds.

Published information on the DTG studies of elastomers is rather limited. The first DTG curves were obtained manually from the TG curve, following extensive work by D. A. Smith and coworkers at the National College of Rubber Technology [4-8]. The quantitative aspects of DTG for analysis was described by Maurer in 1973 [9,10] and Sircar and Lamond [11-16] have reported DTG studies on the identification of a wide range of elastomers and elastomer blends used in tire components. The approach adopted by Sircar and Lamond, termed "Total Thermal Analysis," involves comparing DTG curves obtained in nitrogen and DSC curves obtained in both nitrogen and in air, for the unknown elastomer system with profiles obtained for blends of known composition. A typical example of this is shown in figure 2. Although an exact profile match for such complex blends containing many other ingredients which affect the weight loss events cannot be anticipated, the evidence obtained rapidly eliminates certain types of elastomers, making subsequent analysis, if required, considerably simpler.

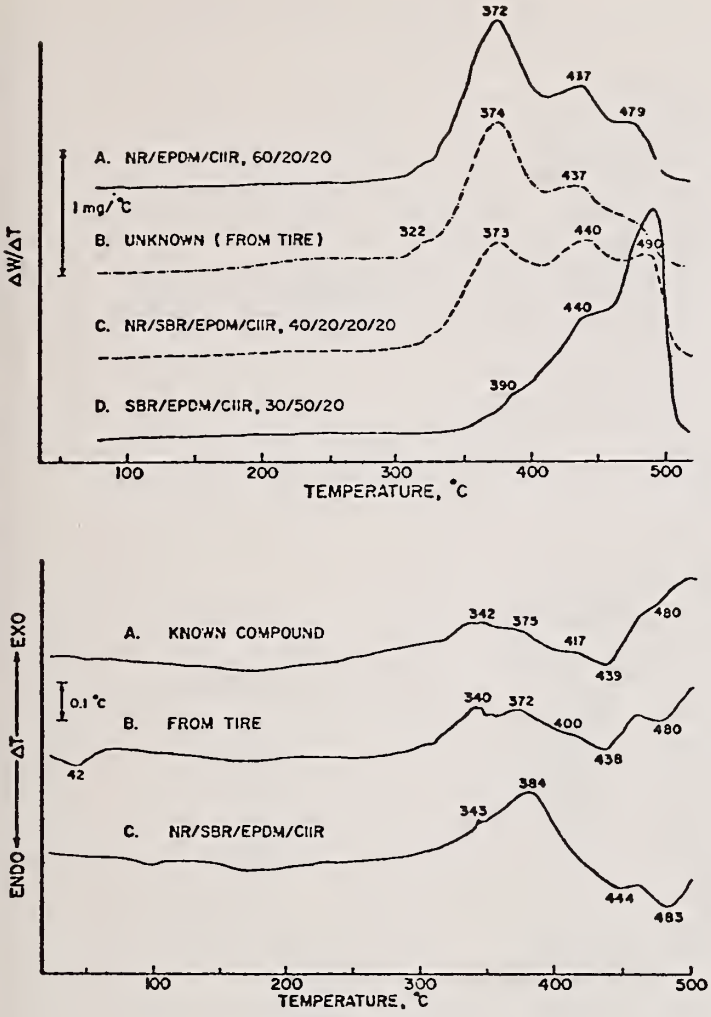

Figure 2. Total thermal analysis of rubber compound by DTG and DSC. NR:EPDM:CIIR Sidewall Blend [14]. Top: DTG curves. Bottom: DSC curves. All in nitrogen atmosphere.

To this point we have discussed only the use of TG/DTG for the identification of elastomers; however, the techniques have extreme importance in the study of the fundamental thermal stability problems associated with polymers. Although basic studies on purified polymers are numerous, little attention has been paid to commercial samples which contain not only residual impurities, but also intentionally added anti-oxidents and stabilizers. Often residual impurities play a significant role in the overall degradation pattern of the system. One example is natural rubber and synthetic polyisoprene (IR) [17], both of which are chemically identical as far as the main polymer chain is concerned. Figure 3 illustrates DTG curves for NR and IR which, in the raw state, appear identical (the degradation of natural resins and proteins in NR is not observed as a separate weight loss stage). The addition of certain high surface area carbon blacks significantly changes the DTG characteristics of IR, whereas no effect is observed for NR. An extensive investigation of the degradation products using DTG/GC combination has shown that residual catalyst in the IR drastically affects the ratio of depolymerization to cyclization of the polyisoprene chain, and alters the volatility characteristics of the degradation products. The overall heat of degradation of NR and IR compounds, as measured in DSC, are also very different [17,18], and it has been shown that other ingredients, and in particular sulphur, added to IR compounds can change the degradation profile.

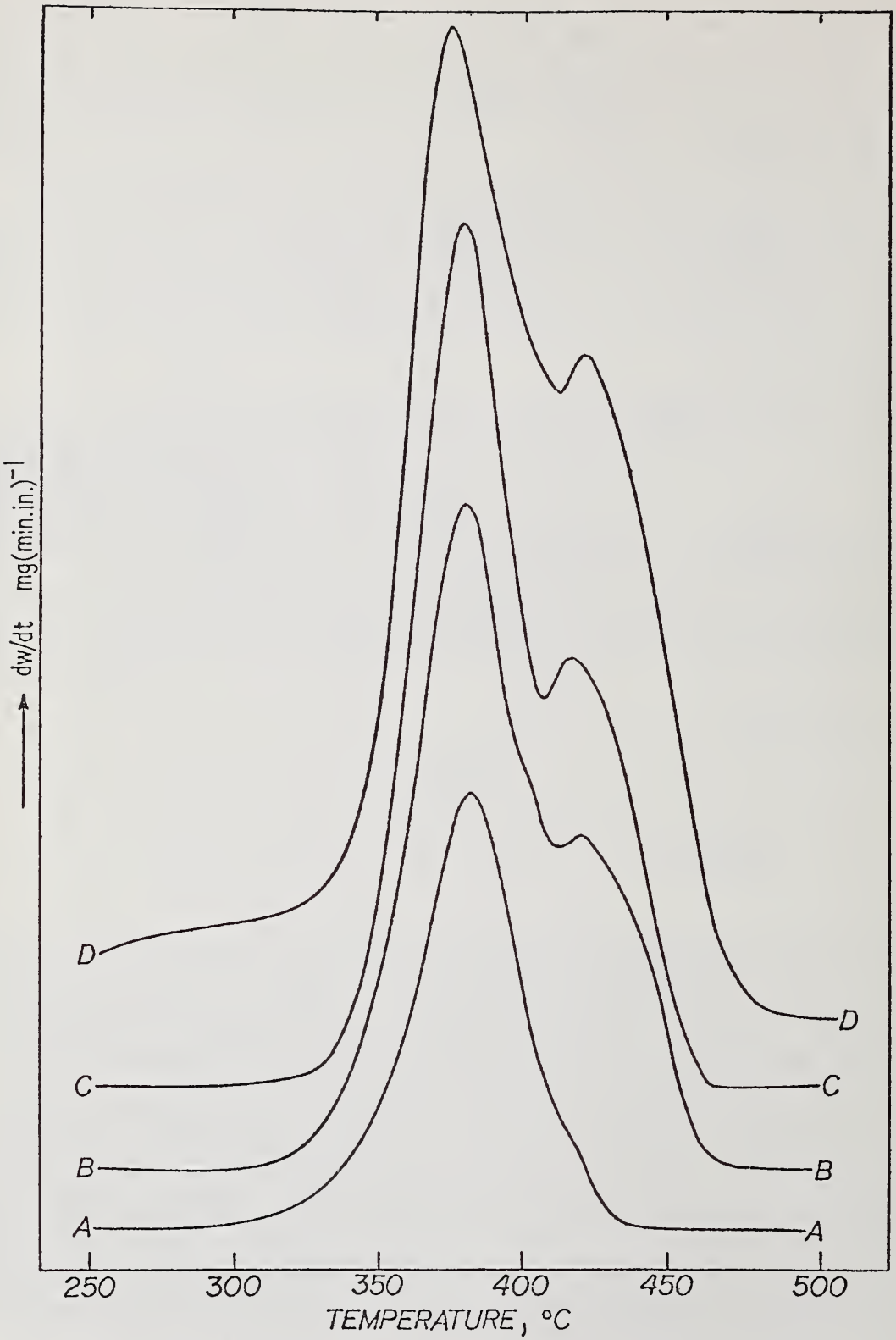

Figure 3. DTG curves of natural rubber and synthetic polyisoprene in nitrogen [3]. Heating rate 10 °C/min, nitrogen atmosphere. A — raw NR and IR (identical); B — raw IR plus 50 phr HAF-LS carbon black; C — raw IR plus 75 phr HAF-LS; D — vulcanized IR compound containing carbon black.

The DTG/GC approach to analysis of complex elastomer compounds holds considerable promise. First published by Chiu [19,20], the potential of this technique does not seem to have been realized. In conventional pyrolysis techniques (pyrolysis-GC or infrared) the total degradation products of all ingredients are collected, and analysis of a very complex mixture is required. Using DTG/GC, the volatiles at any specific time during degradation can be collected, resulting in a considerably simpler mixture for analysis. The DTG/GC proved very useful in studying the two-stage degradation of polybutadiene [21]. Figure 4 illustrates the TG/DTG curves of polybutadiene and typical points at which volatiles were collected. Interest in polybutadiene degradation arose because of a Russian publication [22] describing the potential danger of rapid exothermic decomposition of polybutadiene. The nature of the degradation depends upon the heating rate and this is illustrated by the data in Table 4. As heating rate increases, the first stage of degradation (depolymerization) increases. Numerous applications of DTG/GC in rubber compounds can be foreseen, particularly as the need for environmental screening increases.

Table 4. Polybutadiene Degradation. Effect of Heating Rate as Observed by TG and DSC [21].

Degradation of Polybutadiene - Effect of Heating Rate and Sample Size

	First-Stage		
	Maximum Degradation Rate, min^{-1}	Temperature of Maximum Degradation Rate, °C	Weight Loss, %
Scan rate, °C/min[a]			
2	0.00312	352	6
5	0.0991	375	7
10	0.0230	387	7
20	0.052	402	10
50	1.03	418	33
100	1.85	431	51
Sample size, mg[b]			
5.50	0.023	387	7
9.45	0.022	387	8
19.50	0.031	387	8
50.20	0.896	nonreproducible	37-47

[a] All 5.50-mg sample.

[b] Heating rate 10 °C/min.

Exothermicity of Polybutadiene Degradation - Effect of Heating Rate

Polybutadiene	Heating Rate °C/min	Sample size, mg	T_{max}, °C	ΔH, kJ/g(±10%)
Taktene 1220	2	8.89	350	0.88
	5	8.59	365	0.88
	10	8.60	377	0.92
	20	8.30	388	0.92
	50	6.82	407	0.85
	100	6.57	425	0.89
trans-Polybutadiene	20	5.50	388	0.85
Krylene 1500	20	3.35	390	0.66
Hystl C-3000	20	6.76	358	1.07

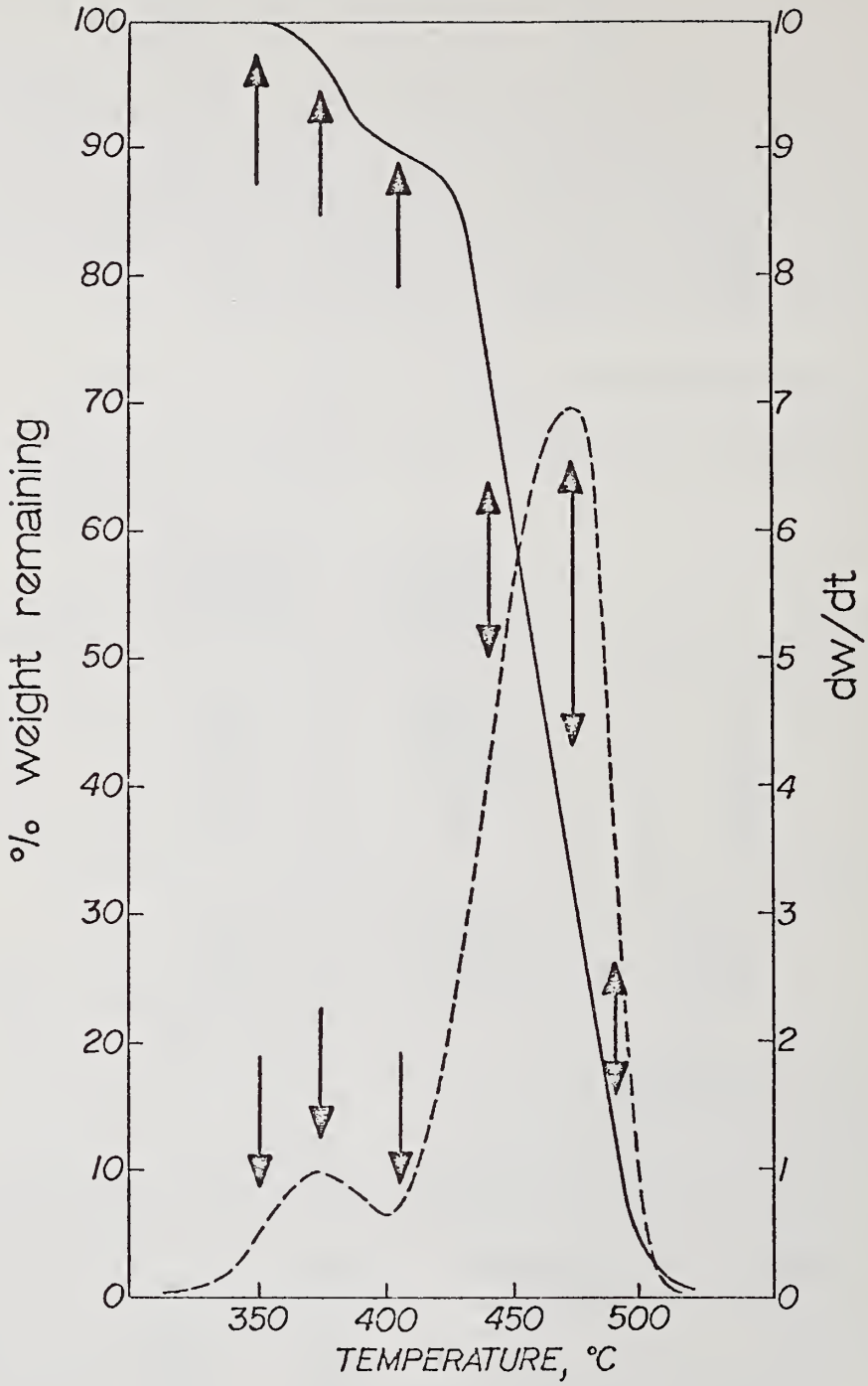

Figure 4. TG/DTG of polybutadiene degradation at 10 °C/min heating rate [3,21]. Arrows indicate typical points along the degradation curve where samples collected for GC analysis using the TG/GC interface.

2) Analysis of Rubber Compounds:

The general principles of TG analysis of rubber compounds are illustrated in figure 5 [1]. The sample is run in a nitrogen atmosphere up to 500-550 °C, which results in the degradation of most organic components – oils, elastomer(s), and minor organic components. The latter can rarely be seen as separate weight loss events. With many elastomers, and in particular, halogenated types (Hypalon, neoprenes, etc.), a carbonaceous residue is formed at 550 °C in nitrogen, thus the residue at 550 °C consists of carbon black, inorganic fillers and other inorganic additives, and, depending upon the elastomer present, carbonaceous residue. The introduction of air or oxygen at 550 °C results in the rapid exothermic oxidation of the organic components and carbon black, leaving only the inorganic components. Fortunately, most general purpose elastomers leave little or no carbonaceous residue and carbon black levels can be calculated directly from the TG data. A major problem with the TG data alone is that difficulties are encountered in separating blend components, and although two components may be detected, rarely can they be separated by TG. In 1973, Maurer [9,10] pointed out the use of DTG to differentiate elastomers of different thermal stability in a blend. The practical application of the TG/DTG thermogram is illustrated in figure 6 for an NR:BR tire tread formulation (Table 1). For the NR and BR components, two separated and discrete peaks are observed. In order to make quantitative use of such data, calibration is performed with blends of known composition. Figure 7 illustrates response factors for each component as the blend ratio is changed. The blend ratio is immediately available from the ratio of NR to BR peak heights. The response factors are dependent upon the blend ratio, indicating that at the T_{max} of each component there is a contribution to the peak height arising from the other component. This contribution can arise from similar degradation temperatures of the two components, and/or from one component interfering with the degradation characteristics of the second. The latter is the case with NR and BR because the response factors are independent of the amount of each component if they are run simultaneously but not blended. In other blends, only a single peak may be observed if the components have similar thermal stabilities. Since response factors are quite different for each elastomer, a given blend ratio will often yield a single composite response factor whose value depends only upon the blend ratio. Such an example is SBR:EPDM blends [9,10] and rapid quality control analysis is still possible. Some terblends can also be analyzed. In NR:SBR:EPDM, for example, NR yields a single peak whilst SBR and EPDM combine into a second peak [3]. Obviously, the method cannot be used to identify an unknown composition.

The use of the TG curve to determine carbon black levels in compounds has received considerable attention [22-26]. Provided the elastomer component is non-carbonizing, carbon black content can generally be obtained to within 1 percent. This accuracy has been reported by Maurer [22] for the analysis of carbon black in butyl rubber compounds. Pautrat et al. [23] have examined a wide range of carbon blacks (HAF, SRF, and MT) in EPDM, butyl, NR, and SBR and found somewhat larger discrepancies. Harris [24] has published results obtained using TG to determine carbon blacks in commercial oil-extended carbon black masterbatch of SBR and BR rubbers.

Several studies [9,10,23,27,28] have been published on the identification of carbon black types recovered from rubber compounds. The concept is to determine the rate of oxidation of the recovered carbon black as judged by the rate of weight loss in an isothermal TG experiment. Initial results supported the view that a correlation should exist between the rate of oxidation and the surface area (particle size of the carbon black), thus allowing its type (ASTM D-1765) to be determined. Maurer [9,10] was also able to demonstrate the difference in oxidation rates of blends of different carbon blacks.

Examination of a wide range of carbon blacks [28] has shown, however, that carbon blacks of different surface area yield very similar oxidation rates. Further, this also applies to virgin blacks (i.e. prior to adding to a compound) and even to different sources of the same black type. Figure 8 illustrates the oxidation characteristics of a variety of carbon black types as observed at 525 °C in a 7 percent oxygen-in-nitrogen stream. Using a controlled oxidative atmosphere, it has been shown that carbonaceous residues derived from a carbonizing elastomer and the carbon blacks initially present in the compound can be separated, e.g. N326 and N990 in natural rubber/neoprene blend.

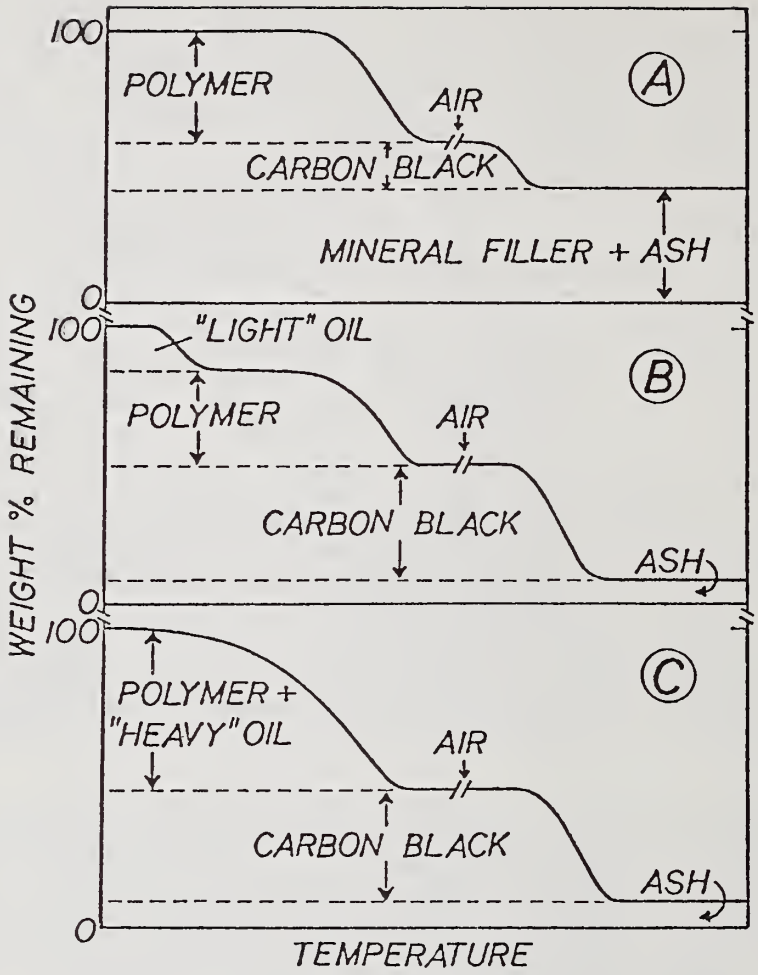

Figure 5. Generalized TG curves for various elastomer formulations. Degraded in nitrogen and then air [1].

A — Elastomer-carbon black-mineral filled system.

B — Compound A type with addition of light oil (or plasticizer) volatilized prior to elastomer degradation.

C — Similar to B except low volatility oil or plasticizer.

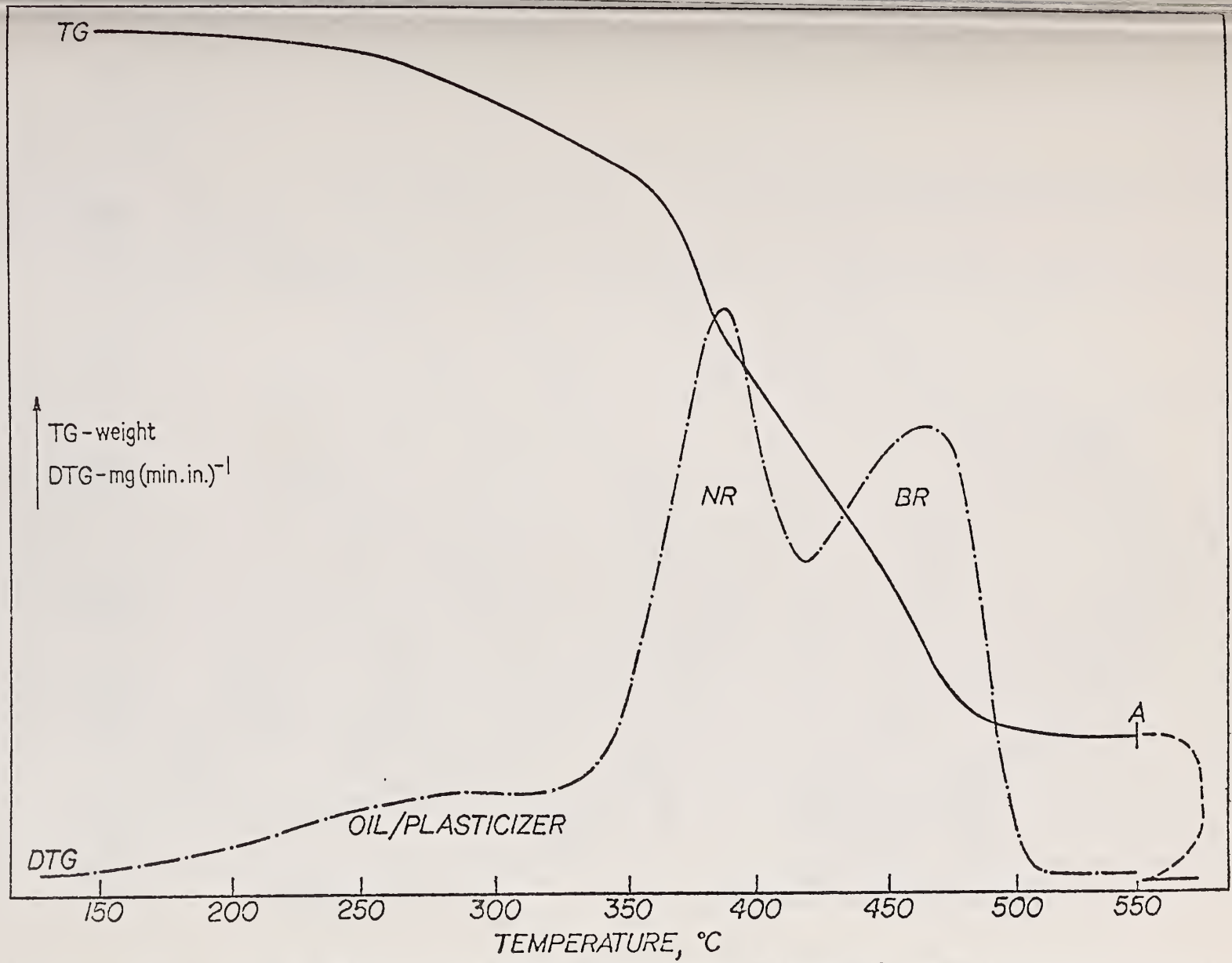

Figure 6. TG/DTG curves for analysis of tire tread compound based on NR and BR [3]. Formulation given in Table 1 — compound 10 °C/min heating rate in nitrogen to 550 °C then air introduced.

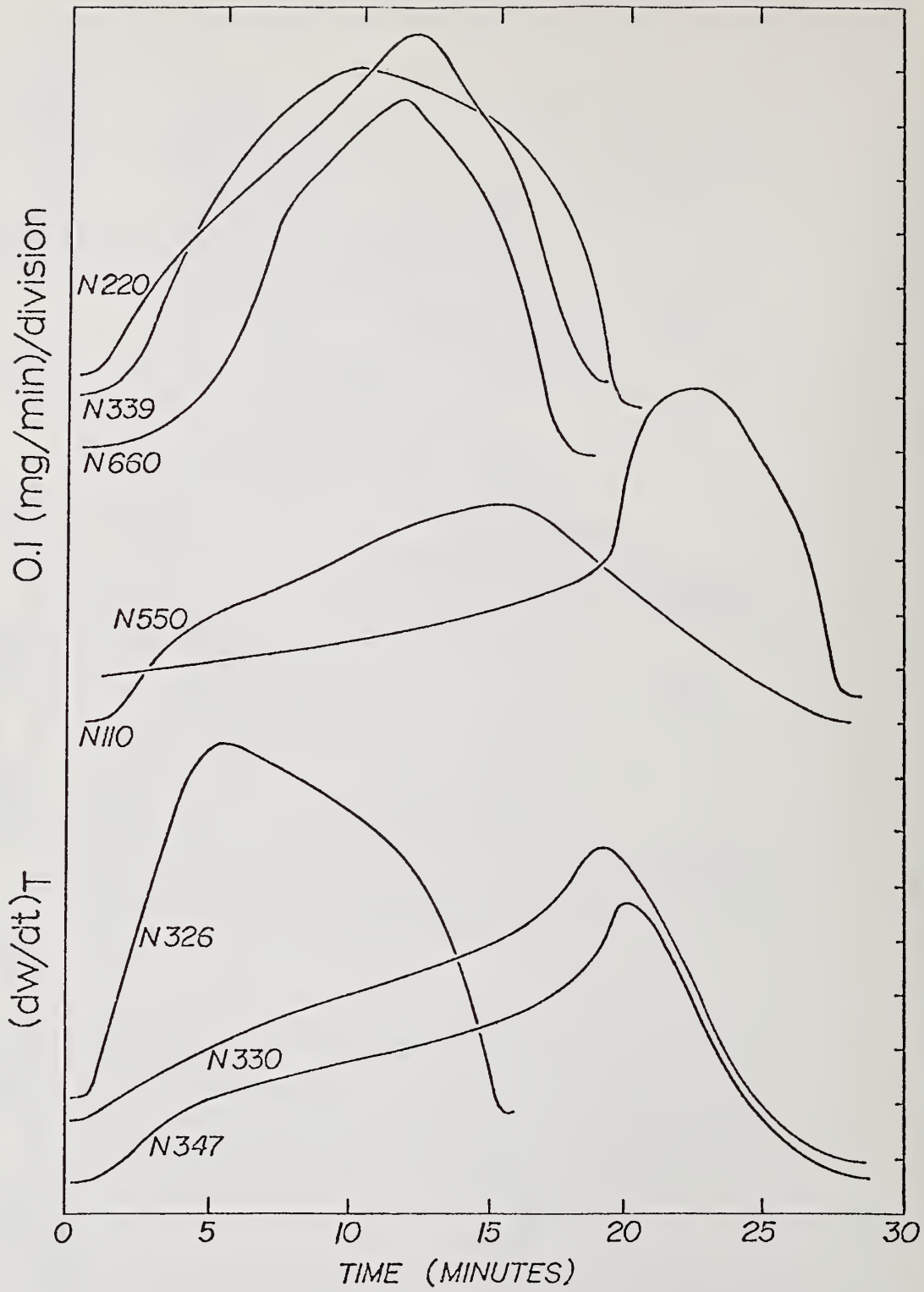

Figure 7. Typical DTG calibration curves for the analysis of NR:BR tire tread compound [3]. Ten °C/min heating rate/nitrogen atmosphere. Top: Peak height NR/peak height BR. Bottom: Response factors for each component as a function of blend ratio.

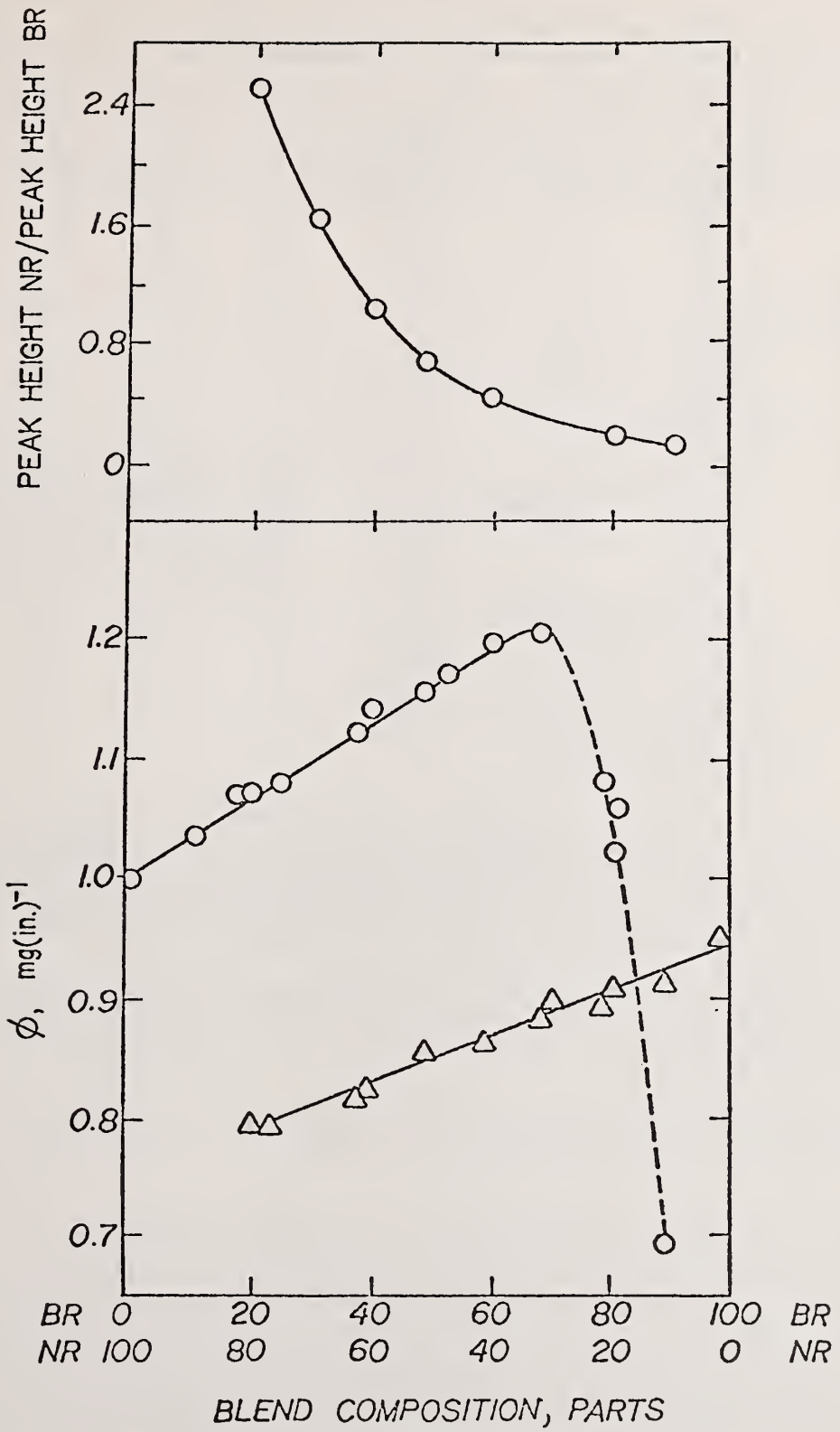

Figure 8. Isothermal oxidation rates of various carbon blacks as observed in DTG [28]. All blacks recovered from SBR vulcanizate oxidized at 525 °C in 7 percent oxygen in nitrogen.
ASTM classification of carbon blacks: N110 — SAF (153).

The final component which can be determined by TG/DTG is the oil and plasticizer level. The restriction here is that the oil/plasticizer must be volatile at lower temperatures than those at which the degradation of the elastomers occurs. This is generally true except for polymeric plasticizers. Swarin and Wims [29] have investigated the loss of plasticizer from EPDM and NBR in O-ring, gasket and hose compounds, and found excellent correlation between the observed temperature of maximum rate of weight loss (T_{max}) and the ASTM distillation range temperature. A good correlation was also shown (figure 9) between the GC retention time for a monomeric plasticizer and its T_{max} value observed in DTG.

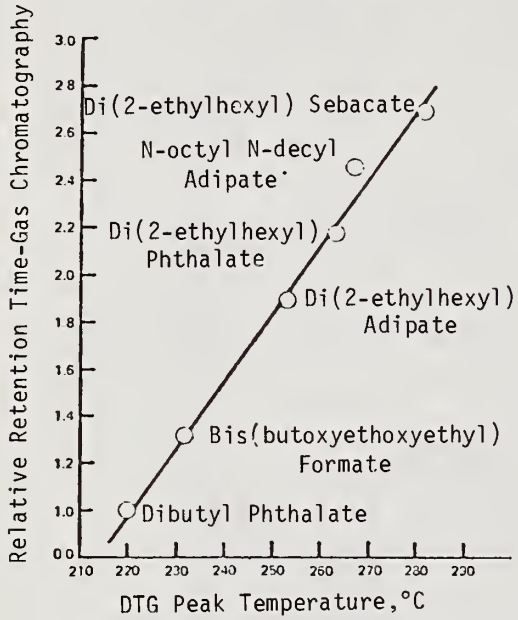

Figure 9. DTG vulcanization temperature versus GC retention data for plasticizers [29]. The DTG temperature is the temperature of maximum volatilization rate from a nitrile (NBR) rubber vulcanizate. Note: N-octyl-N-decyl Adipate contains three peaks.

Finally, Table 5 illustrates typical results obtained for the analysis of a series of factory batches of the same compound, utilizing the methods discussed above [3]. (The determination of sulphur and accelerator is described in the next section.) Analysis of each compound sample was achieved in ~50 minutes at a heating rate of 10 °C/min, and this can be reduced by increasing the heating rate. Each compound must be examined individually to determine the maximum heating rate which will give reproducible results.

In conclusion, DTG is very useful in the identification and analysis of complex rubber compounds provided a sufficient data bank is available on the wide variety of materials encountered. At this time, no comprehensive text contains the necessary data and it must be generated in house.

Table 5. Analysis of Factory Compounds for Quality Control [3].

Combined DTG/DSC Analysis for Compound C, Table 1

Batch No.	% NR[a]	% Br[a]	Oil[b]	% Carbon black[c]	% Ash[d]	% Sulfur[a]	% Accelerator[a]
1	31.3	21.4	8.6	31.7	2.1	0.82	0.55
2	32.8	23.1	8.0	31.1	2.3	0.80	0.55
3	31.7	21.0	8.9	32.2	2.2	0.71	0.50
4	31.6	21.4	8.8	31.6	2.4	0.79	0.55
5	32.9	21.9	8.9	31.8	2.2	0.95	0.55
6	31.1	21.9	8.5	32.5	2.4	0.89	0.55
7	30.7	21.4	8.1	31.9	2.5	0.81	0.60
8	30.8	22.4	8.9	32.3	2.1	0.86	0.60
9	31.4	22.5	8.5	32.2	2.2	0.82	0.60
10	31.6	22.4	8.7	32.2	2.3	0.88	0.44
11	32.4	22.7	9.4	32.1	2.1	0.81	0.44
12	31.6	22.0	8.9	32.2	2.2	0.84	0.50
13	33.2	22.4	9.3	31.9	2.2	0.81	0.50
14	32.2	22.5	8.5	31.8	2.4	0.90	0.55
15	33.2	23.3	8.6	32.5	2.5	0.76	0.55
16	31.0	22.3	8.6	31.7	2.2	0.82	0.50
17	32.0	23.4	8.3	32.5	2.1	0.74	0.55
18	31.9	22.6	8.4	32.5	2.1	0.71	0.55
19	33.2	22.2	8.4	32.0	2.3	0.80	0.55
20	32.0	23.3	8.5	32.1	2.4	0.85	0.50
Nominal	33.0	22.0	8.8	30.3	1.65	0.82	0.55

[a] ±0.5%.

[b] Wt. % loss at 300 °C.

[c] Wt. % loss at 550 °C in nitrogen less ash.

[d] Residual weight at 575 °C in oxygen.

B. Differential Scanning Calorimetry

1) General Observations:

Prior to considering specific applications of DSC in the study of elastomer compounds, figure 10 illustrates the general nature of a DSC scan obtained on a fully compounded stock of the type shown in Table 1. Not all of the events shown will necessarily be observed in a given compound.

On the low temperature side, the first event observed is the glass transition or transitions of the elastomeric components. The glass transition is observed as a shift in baseline corresponding to the heat capacity difference of the sample before and after the transition. The generally quoted glass transition temperature is the extrapolated value obtained by constructing tangents as shown in figure 10. In our laboratory, we prefer to run the derivative curve (DDSC) as shown, however, on vulcanized elastomer samples, thermomechanical analysis (TMA) is the preferred method for determining the glass transition. The importance of differential thermal analysis (DTA) and more recently, DSC, in the study of the glass transition region and the microstructure of polymers cannot be overemphasized; however, this is well covered in the literature and will not be discussed here.

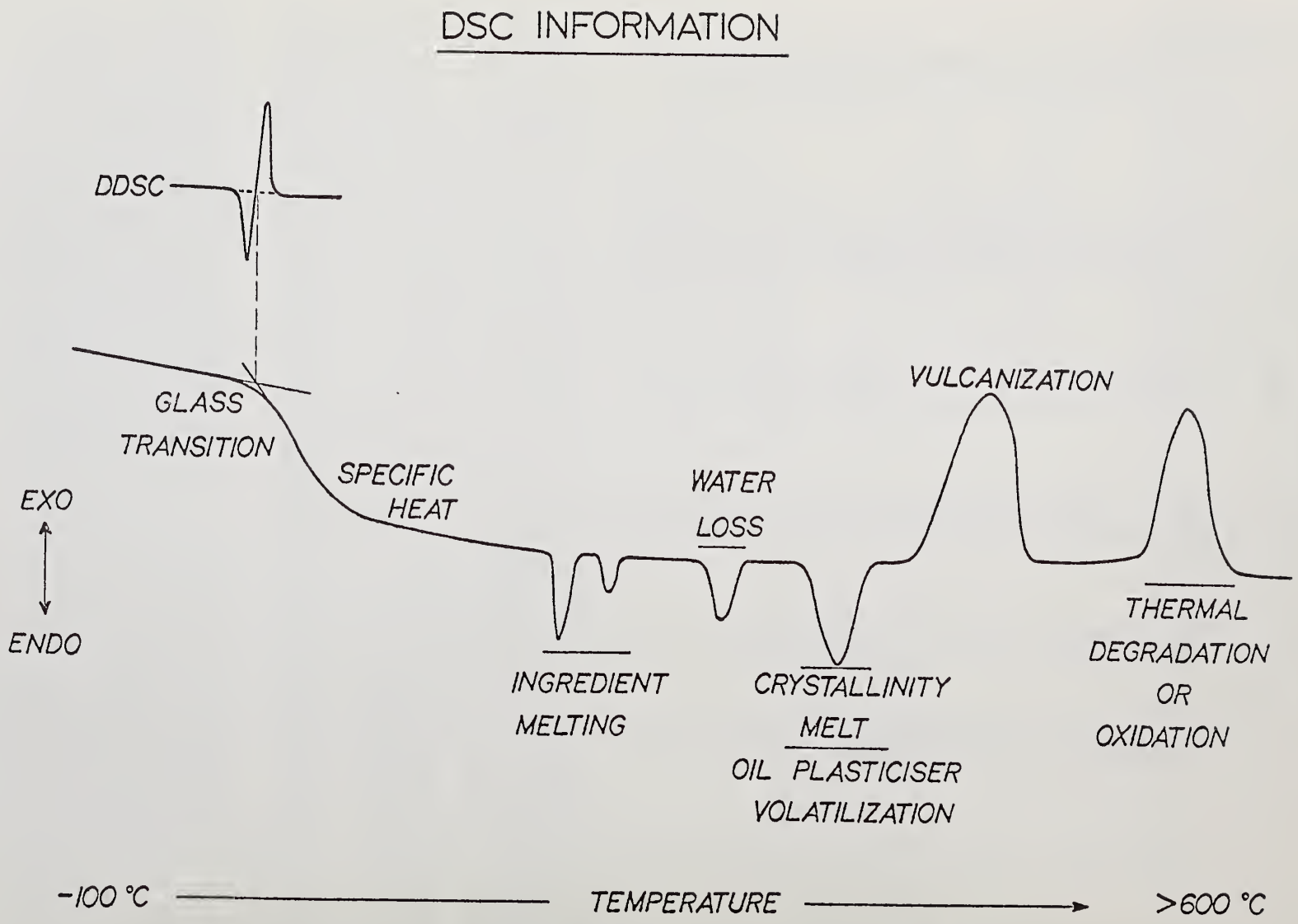

Figure 10. Generalized DSC curve of typical unvulcanized elastomer compound. Sulphur cure system, 20 °C/min heating rate.

As the temperature rises above the glass transition range, the baseline continues to exhibit a slope which reflects the temperature dependence of the specific heat of the elastomer compound. Although useful for determining the temperature dependence of the specific heat, the concomitant baseline slope often causes problems in determining the baseline for events observed at higher temperatures, particularly when a small event needs to be scanned at high sensitivity. For an unvulcanized compounded sample, the various melting temperatures of the ingredients can often be observed in the 80 to 100 °C range. Included here at ~100 °C will be the endothermic loss of water for the sample, if present. Over the same temperature range, melt of any crystalline phase of thermoplastics and plastics will be observed (e.g. ionomeric materials such as Surlyns, polypropylene, polyethylene, etc.).

At approximately 180 °C, depending upon the cure system, the exothermic vulcanization process is observed, and this will be dealt with in detail later in this section. The final event observed corresponds to the degradation of the system. In a nitrogen atmosphere, the degradation can be endothermic or exothermic (or mixed) depending upon the elastomer system. The DSC degradation characteristics of elastomers have been extensively studied by Sircar and Lamond [1116] as part of their total thermal analysis schemes for the identification of elastomers. In an oxygen-containing atmosphere, the oxidative degradation is exothermic and complex. Observed at lower temperatures than the thermal degradation process, several authors [30,31] have attempted to use the oxidation exotherm as an indication of oxidative stability and subsequently evaluate the effectiveness of added anti-oxidants. Although an isothermal method has been developed to determine anti-oxidant efficiency in plastics, experiments in our laboratory, to date, have failed to give good results with elastomer systems.

Time does not permit an extensive discussion of all DSC applications and only two have been chosen for extensive discussion. The first is the identification of impurities and the purity of critical ingredients and the second, the vulcanization process itself.

2) DSC of Impurities and Various Curatives:

No discussion of rubber compounds would be complete without mention of sulphur – the largest used vulcanizing agent in the industry for many years. Figure 11 illustrates the DSC curve of rubber makers' sulphur. Three transitions are apparent, starting from the rhombic allotrope. In an unvulcanized rubber compound, the λ-π liquid-liquid transition at 186 °C is never observed as it falls in the vulcanization range. Reproducibility in the sum of the rhombic-monoclinic and monoclinic melt events is sufficient to allow purity determinations to be made. Since sulphur is used in the 0.5 to 1 percent level (Table 1), it is difficult to determine in compounded systems; however, as shown later, the reactions with the elastomer can be determined and give an excellent indication of the active sulphur present. In order to obtain homogeneous properties throughout the bulk of a rubber product, good dispersion of sulphur in the compound is essential. Often small imperfections, usually as hard spots, can be observed in the product, and many times this can be identified as a sulphur agglomerate by running DSC on even a few tenths of a milligram of material.

Organic accelerators are extensively used in elastomeric sulphur vulcanization. These materials have a drastic effect on the cure rate and the nature of the final sulphidic crosslink structure. Thus, an indication of the purity of a commercial accelerator is of interest. Basically, a single recrystallization of most accelerators results in large changes in the observed DSC melt endotherm, and results in our laboratory suggest many materials as supplied are no better than 95 percent of the required material. For improved dispersion on compounding, it has become common practice to disperse the curatives at high levels (60-80%) in an elastomeric binder. The solid sample is then weighed for mixing rather than the "pure" powdered sample. DSC can then be used to determine the concentration of the active accelerator (or sulphur) in the binder. Figure 12 illustrates typical DSC melt endotherms for ethylene thiourea, both pure and in a binder. As expected, the melt endotherm is considerably broadened; however, the absolute area (or heat of melt if required) can be readily calculated and accelerator determined. Free elemental sulphur which can affect vulcanization characteristics can be an impurity in some accelerators; however, it is rarely observed in DSC as it is hidden below the broad accelerator melt.

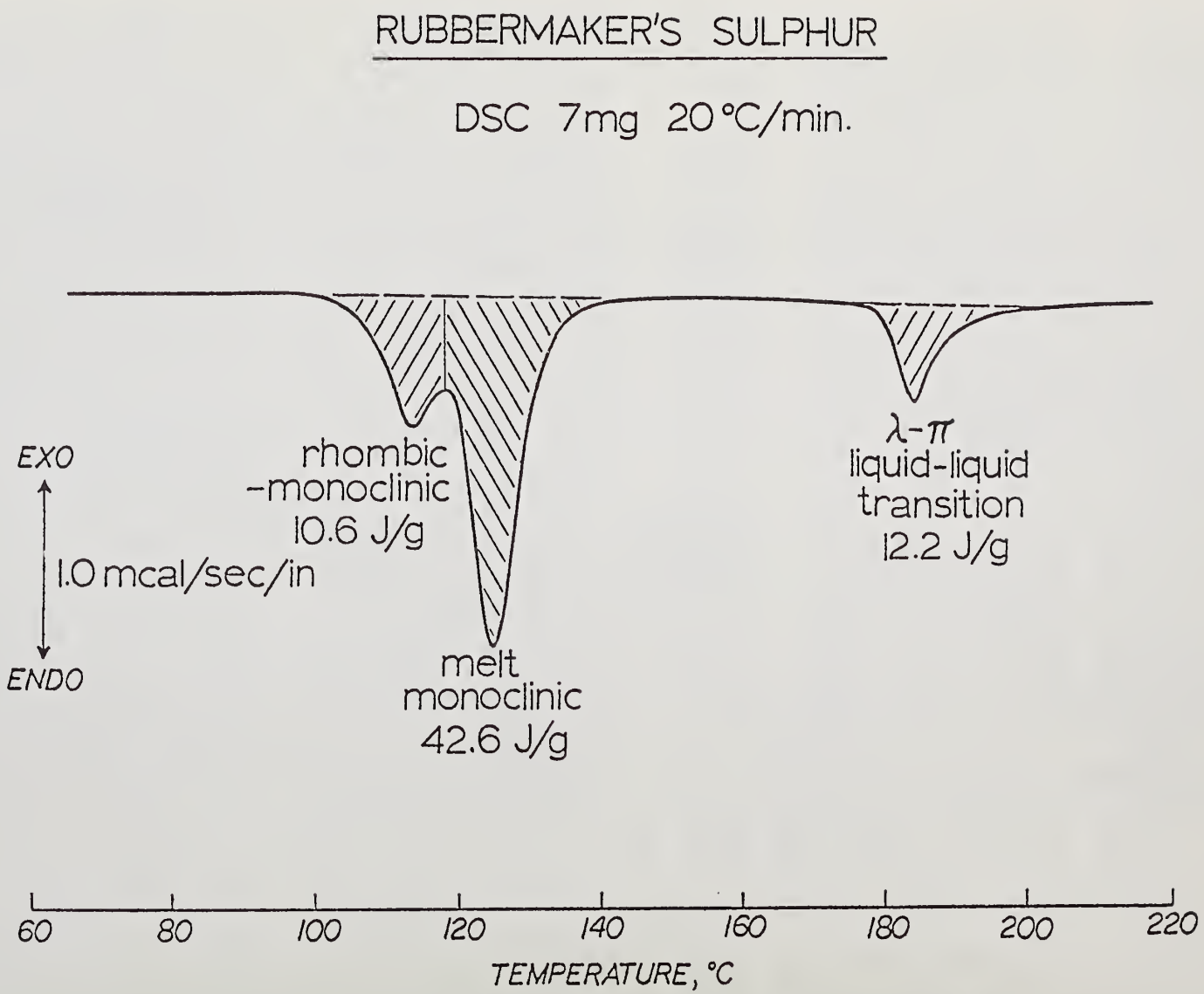

Figure 11. DSC curve of Rubbermaker's sulphur. 20 °C/min scan rate, nitrogen atmosphere. Unpublished data.

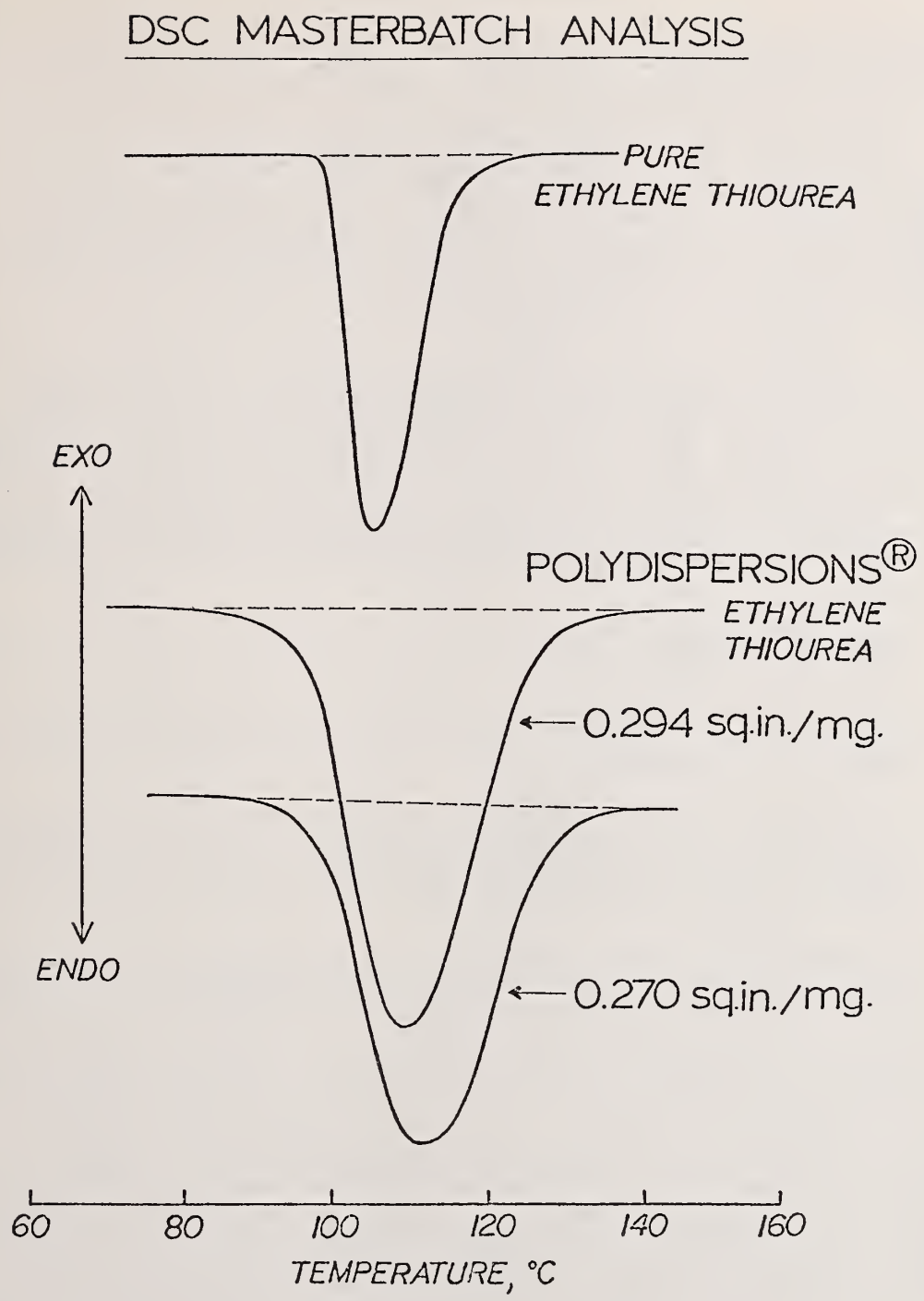

Figure 12. DSC melt endotherms of ethylene thiourea in SBR binder. Materials supplied ex. Wyrough & Loser Inc for analytical purposes. Scan rate 20 °C/min. Unpublished data.

DSC and Vulcanization

Vulcanization – the process whereby sulphidic crosslinks are introduced into unsaturated elastomers, is of tantamount importance in the rubber industry. Accelerated sulphur vulcanization [32] is chemically very complex, resulting not only in crosslinks between elastomer chains, but in non-crosslinking products such as cyclic sulphides and extraneous residues. Sulphur crosslinks are formed containing various numbers of sulphur atoms (polysulphides – tri, di, mono, etc.) and the distribution of sulphur depends upon the nature of the accelerating species. The distribution is also of prime importance in determining the initial physical properties of the vulcanized sample and its subsequent performance on aging in the application. An understanding of the rate at which crosslinks are introduced by a given curative system is essential in the industrial vulcanization process. Normally, the vulcanization characteristics are determined under isothermal conditions by monitoring the change in shear viscosity of the stock (rheometry).

As shown in figure 10, sulphur vulcanization is an exothermic process. Until the careful work of Bekkedahl and Weeks [33] at the National Bureau of Standards, it was not clear that sulphur vulcanization was an overall exothermic reaction at all sulphur levels. Early DTA studies [34] suggested that an exothermic reaction was only observed at 5 percent sulphur or greater in natural rubber. In studies reported from 1975 [35-36] it was shown that even at levels of sulphur used in conventional rubber compounds, the overall reaction was exothermic. DSC vulcanization curves of several tire tread compounds (Table 1) are illustrated in figure 13. The use of this exotherm to determine vulcanization characteristics is being extensively investigated in our laboratory with the following major conclusions reported to-date:

- Sulphur vulcanization (accelerated or unaccelerated) is an overall exothermic process at all sulphur levels.

  Figure 14 illustrates a typical calibration curve used to determine sulphur in a production stock. The range concerned is ~0.5 percent to ~1.9 percent sulphur by weight in the compound.

- The addition of common accelerators in the normal concentration range has little or no affect on the observed heat of vulcanization, but moves the DSC curve to lower temperatures as expected. Under standard experimental conditions, the decrease in the temperature of the maximum heat evolution rate can be used to estimate accelerator level.

The data shown in Table 6 illustrates typical results obtained for a tire tread compound as sulphur and accelerators are varied. The temperature dependence of the observed DSC cure profile for several thiazole type accelerators is also shown, T_o, T_p, and T_c are the temperatures at which the first onset of the cure reactions are observed, the temperatures of maximum heat evolution rate, and the temperatures of return to baseline, respectively. For complex elastomer systems, determining T_o, T_p, and T_c is often difficult as illustrated in figure 13 for compound B. The change in baseline with temperature because of specific heat changes has already been mentioned; however, oil and plasticizer loss by volatilization also occurs in the vulcanization temperature range. Other chemical reactions can occur because of additives – Compound B, for example, contains a bonding agent system of resorcinol and hexmethylenetetramine and the reaction of this system is observed just prior to the sulphur vulcanization exotherm. On the other hand, the observation of the bonding agent reaction can be used to confirm the presence of the system for quality control reasons. We have studied the reactions in the absence of sulphur vulcanization and the formation of the resin matrix within the elastomer system is readily monitored. The procedure adopted to determine the baseline for quality control analysis varies from compound to compound. For a compound like A or C (figure 13) T_o, and T_c are easily estimated. For quality control analysis of systems like B, a baseline was drawn from the onset of the vulcanization exotherm at 187 °C (the known onset temperature for this cure system) to the conclusion of the exotherm. This yields only a very qualitative estimate of the area, but is sufficiently reproducible for quality control.

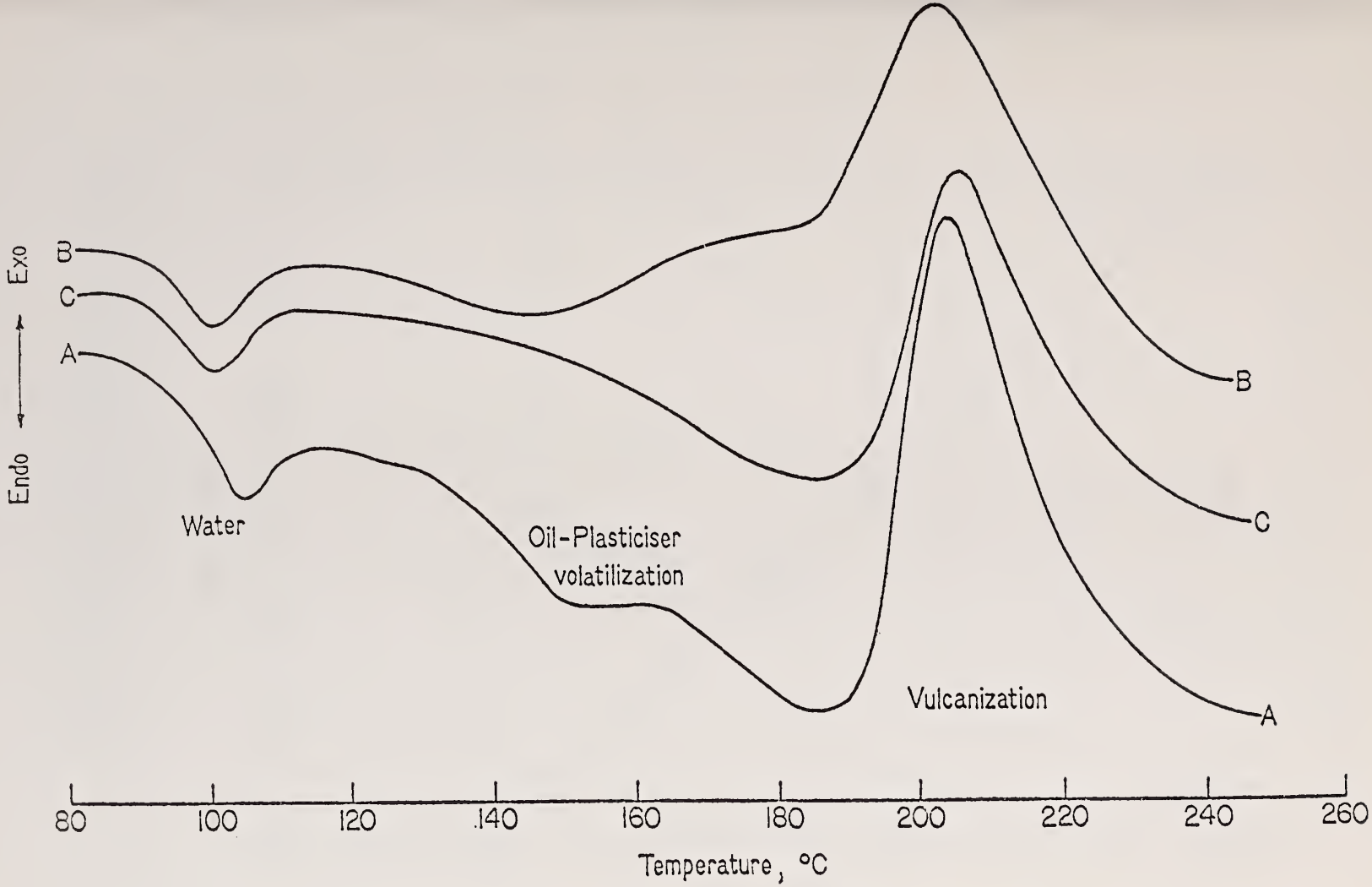

Figure 13. DSC curves for the vulcanization of typical tire compounds [35,36]. Formulations given in Table 1. Scan rate 20 °C/min. Compound B contains dry bonding agents.

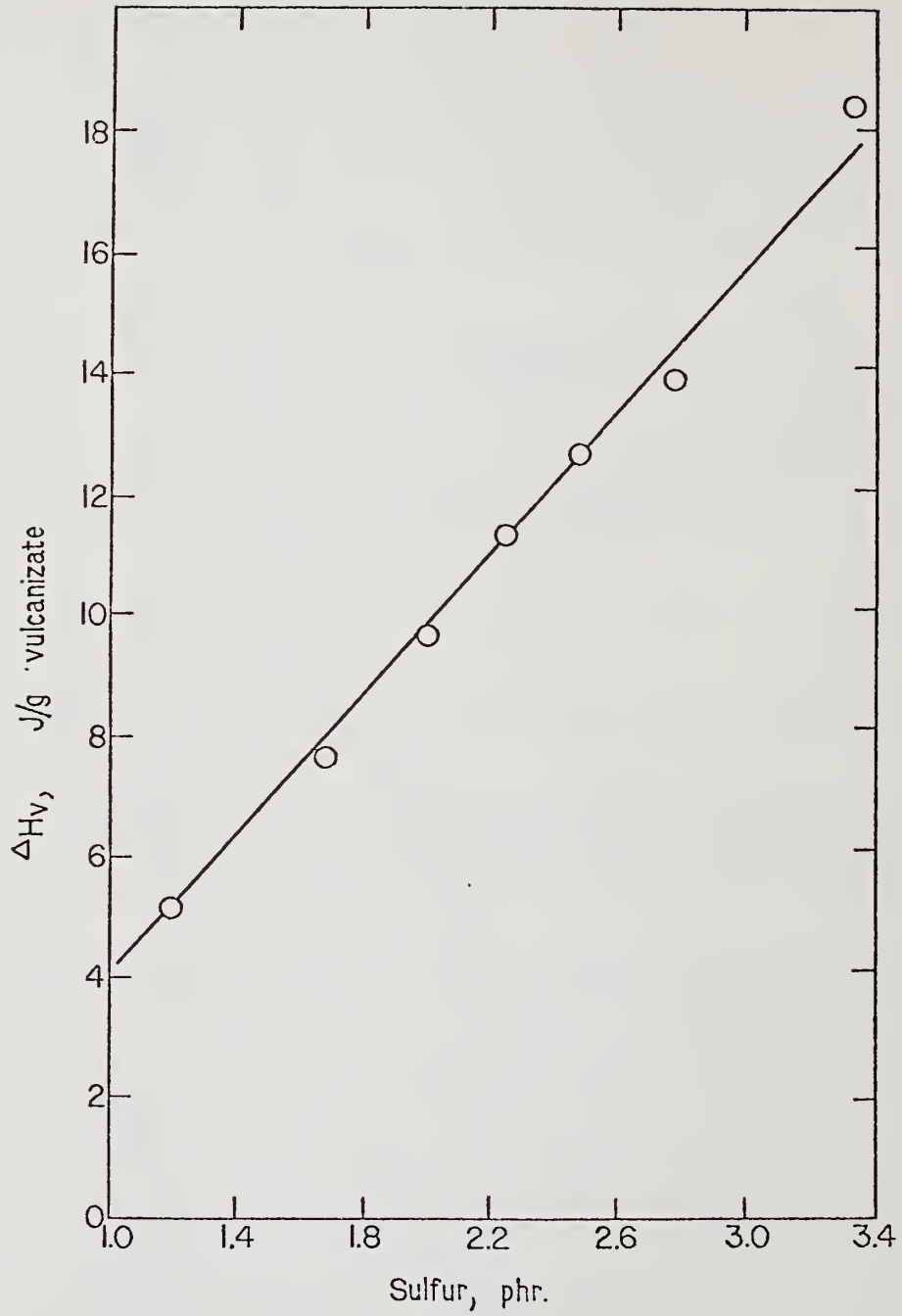

Figure 14. Heat of vulcanization versus sulphur loading in tire tread formulation [35]. 20 °C/min heating rate, compound A, Table 1. Sulphur in formulation added as oiled Crystex (80% sulphur in oil).

Table 6. Effect of Thiazole Accelerators on DSC Vulcanization Characteristics [36].

Formulation: Natural Rubber 100, HAF-LS 50, Zinc Oxide 5, Stearic Acid 3, Sulphur 2, Accelerator 1.2

Accelerator	T_o (°C)	T_p (°C)	T_c (°C)	$\Delta H_v (Jg^{-1})$
None	192	222	245	9.4
MBTS	168	201	238	6.6
MBT	168	201	240	7.4
MOR	164	193	218	7.2

Formulation: Compound A Table 1

Sulphur variation—MOR Constant 1.2 phr

Sulphur, phr	1.20	1.68	2.24	2.80	3.36
$\Delta H_v (Jg^{-1})$	5.02	7.45	11.25	13.43	18.36
T_p (°C)	207	207	207.5	207.5	207
Rheometer, 150 °C:					
$t_s(2)$, min[a]	6.5	6.0	5.5	5.5	5.0
$t_c(90\%)$, min[b]	11.5	11.0	11.5	11.5	11.0
ΔM in lb[c]	28	41	40	43	57

MOR variation—sulphur constant 2.24 phr

MOR, phr	0.4	0.8	1.2	1.6	2.0
$\Delta H_v (Jg^{-1})$	10.75	10.88	11.25	10.88	11.25
T_p (°C)	221	210	207	205	203
Rheometer, 150 °C:					
$t_s(2)$, min[a]	5	6	6	6	5
$t_c(90\%)$, min[b]	17	13	12	10	9
ΔM in lb[c]	34	39	42	44	43

---

[a] Time to 2 in. lb rise after minimum viscosity.

[b] Time for 90% of ΔM to be developed.

[c] ΔM difference in initial and final viscosity.

The absolute magnitude of the heat of vulcanization can vary with other ingredients in the compound, but generally the variation is small and can be ignored. Zinc oxide, for example, has a small effect on the observed Δ_H and if necessary, corrections can be made for zinc oxide variation after analysis using the DTG method. The heat of vulcanization is different for different elastomer systems and this can present problems in blends. An example of the effect of blend ratio is shown in Table 7 for natural rubber/polybutadiene systems. Polybutadiene liberates over twice as much heat as natural rubber when vulcanized with the same curative levels. Thus, it is necessary to analyze for variation of NR:BR ratio before using calibration data of the type previously illustrated. It is interesting to note that the heats of vulcanization of natural rubber and synthetic polyisoprene are quite different and in our laboratory this has been used as a method to differentiate these two materials.

Table 7. Effect of NR and BR Blend Ratio on DSC Heat of Vulcanization.

Formulation: NR and BR - as shown.
HAF-LS 50, Zinc Oxide 5, Stearic Acid 3,
Sulphur 1.5, MOR 1.0

DSC 20 °C/min Nitrogen Atmosphere

Ratio NR:BR	100:0	0:100	80:20	60:40
ΔH_v, J/g	5.8	13.1	6.2	7.1
T_p, °C	196	218	202	204
Rheometer 150 °C:				
$t_s(2)$, min	4.8	7.5	5.8	6.5
$t_c(90\%)$, min	10.0	22.0	11.5	12.0
ΔM, in lb.	42	44	43	44

Carbon blacks [35-37] and inorganic fillers [34] can also affect the magnitude of the observed DSC exotherm; however, this has not been explored in any detail in the study of interreactions between fillers and elastomer-curative systems. In general, the first additions of carbon black reduce the observed heat of vulcanization but the reduction plateaus as levels encountered in conventional rubber compounds (50 phr and greater) are reached.

In industrial practice, rubber products are vulcanized under approximately isothermal conditions. As a result of the low inherent thermal conductivity of elastomers in the vulcanization of thick articles, a significant temperature gradient occurs and it is not uncommon for vulcanization to be complete (or overcured) near the surface before the centre has reached vulcanization temperatures. Rheometers are used to assess the isothermal cure parameters and it is interesting to compare rheometer data and calorimetric data obtained under isothermal conditions. Figure 15 illustrates the vulcanization process as observed in the DSC operated isothermally compared on the same time scale as the rheometer. Experimentally, the calorimeter data can only be obtained over a limited temperature range. If the curative system is very fast, or the temperature too high, vulcanization can be well under way before equilibrium can be reattained in the calorimeter. On the other hand, if the vulcanization rate is slow or the temperature too low, the rate of heat evolution is too slow to be determined accurately. For many curative systems we have studied, a temperature window has been found over which these effects can be balanced, allowing reproducible exotherms to be obtained. Considerable work will be needed to interpret the exotherms in terms of actual chemistry occurring during vulcanization, and this is an interesting challenge for the future.

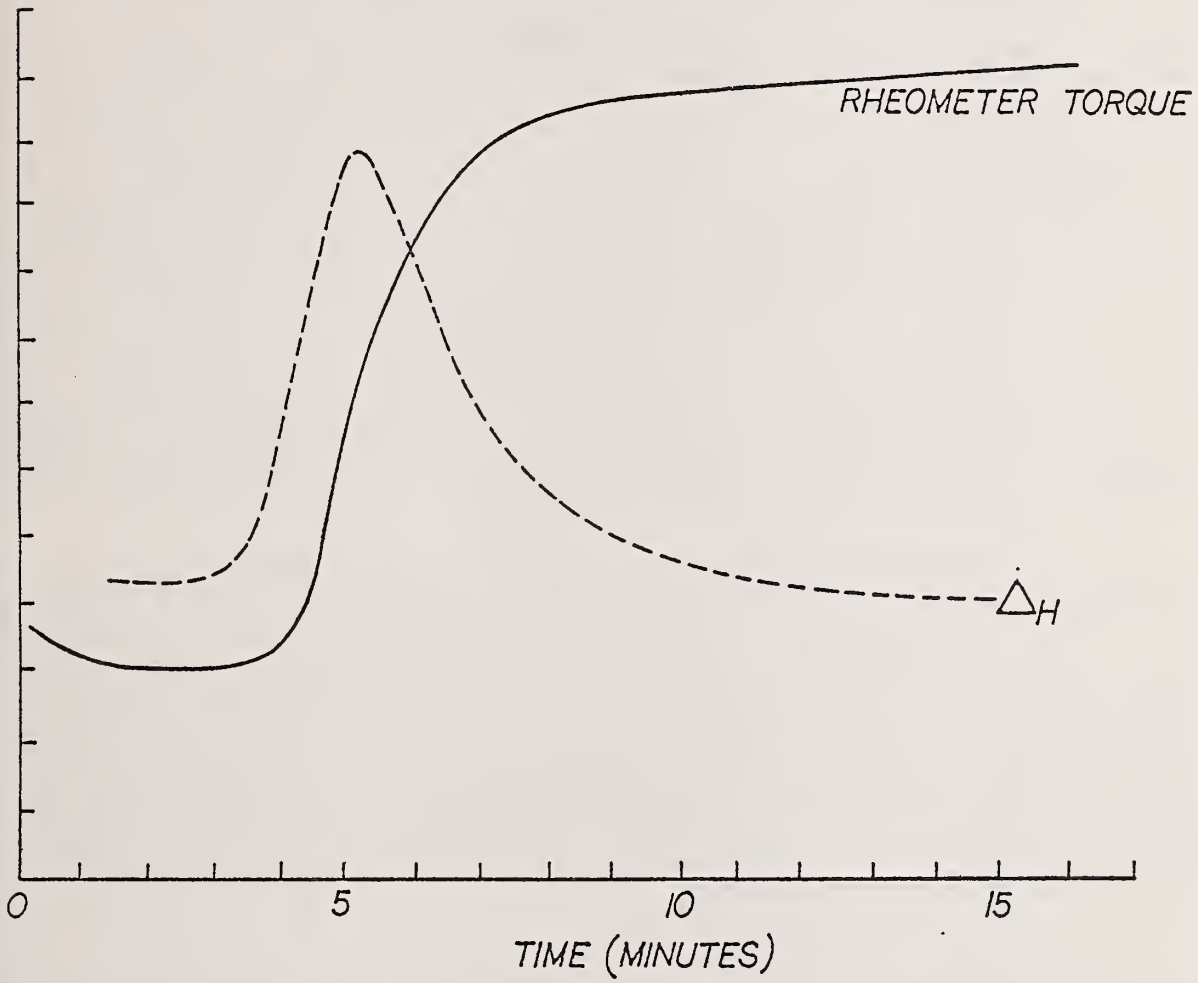

Figure 15. Comparison of isothermal vulcanization as observed in rheometry and calorimetry. Sulphur/tetramethyl thiuram cure system @ 150 °C. Unpublished Data.

In 1973 Markov et al. [38], published data indicating that the heat of vulcanization depended upon the allotropic form of sulphur used. Starting with polymeric sulphur (S_μ), the observed heat of vulcanization of polyisoprene and polybutadiene was less than that observed when rhombic sulphur (S_α) was used. Data was obtained by an isothermal thermographical method. This observation supports the view that interpretation of the DSC data is a formidable task as, in addition to the complex chemistry, the reactivity of different allotropic forms of sulphur must be considered at different phases of the overall reactions.

C. Thermomechanical Analysis (TMA)

1) General Applications:

The use of TMA in the study of elastomer systems is the least developed (or published) area involving thermoanalytical procedures. An excellent review was recently published by Maurer [39] and, as the experimental procedures were covered in some detail, comments will be restricted here. Basically, in TMA dimensional changes are monitored by some form of probe as a sample is heated (or cooled) at a known rate. The nature of the probe plays an important role in the observed TMA curve, particularly in the case of elastomers, which are subject to deformation under applied load. Four probe types are generally recognized – an expansion probe which in theory has zero mass when applied to the sample, a penetration (or indentation) probe in which probe geometry and load are specifically designed to allow penetration into the sample, a tension probe in which a ring sample (or fibre length) is studied under load, and finally, a dilatomer probe used primarily for powdered samples. As discussed by Maurer, transition and relaxation processes in high molecular weight polymers are temperature and time dependent. Thus, in TMA, where a scanning temperature regime is used, i.e. not isothermal, the temperature at which transitions such as the glass transition are observed is often quite different from that observed by isothermal methods. In general, the shape of a TMA curve will reflect the same features as a stress relaxation curve. Starting from low temperatures below the glass transition, the thermal expansion of the glassy state is determined, followed by the leathery region at temperatures in the glass transition range, and then into the so-called rubbery plateau corresponding to the normal use temperature range of elastomeric products. At higher temperatures, a flow region will be observed; however, this will depend upon the type of elastomer, the degree of cross-linking, and the nature of fillers present in the system.

Although predominantly used in the temperature scanning mode, the TMA can also provide very valuable information when operated in an isothermal condition. Maure [39] pointed out the possibility of using TMA to monitor elasticity and creep recovery using TMA as a parallel plate plastometer. We have undertaken similar experiments in our laboratory and the technique is very useful for qualitative studies; however, considerably more work is needed to reduce this to a quantitative procedure. Isothermal TMA has also been found very useful for rapidly estimating the solvent/environment resistance of thermoplastic and elastomeric materials. The TMA furnace is replaced with a holder containing the solvent or effluent in which the material is to perform. The use of TMA to determine rates of polymer swelling and dissolution (methacrylates, neoprene, polyethylene) was investigated by Mackin and Rogers [40,41]. Diffusion coefficients of the solvent in the polymers were derived from the swelling curves. Similar work on crosslinked elastomeric compounds does not appear to have been published to date.

2) Low Temperature Properties:

A large potential application area of TMA involves the determination of the low temperature properties of elastomer systems. Numerous standard procedures have been developed (ASTM Procedures - D746 Brittle Temperature by Impact, D-797 Youngs Modulus in Flexure, D-1053 Torsional Modulus, and D-1329 Temperature-Refraction Properties). However, all require the determination of a property at a series of isothermal temperatures. TMA has been evaluated [42] in relation to the Rigidity Modulus Test D-1053. Figure 16 illustrates TMA and DTMA curves in the temperature range -80 °C to +20 °C obtained on a practical neoprene vulcanizate (hose compound). In practice, the free expansion (zero mass probe) curve is very difficult to reproduce as the sample expands against the probe. More reproducible results are obtained using expansion with load – curve (b) – and two temperatures are defined, Tg_o the extrapolated temperature, and Tg_d the peak temperature as observed in the simultaneously recorded DTMA curve. The final curve was obtained using the tension probe with a ring sample and although not shown, Tg_o and Tg_d temperatures can be similarly defined. Once above the glass transition range, the behaviour of the sample depends upon the phyiscal properties of the vulcanizate in the rubbery region. Soft compounds continue to indent in the expansion with load mode; however, this is in competition with the thermal expansion of the sample. Events other than expansion or indentation are often observed; in neoprene, for example, three events are observed in the 40 to 60 °C range, temperatures often encountered by neoprene products in the field. DSC over the same temperature range

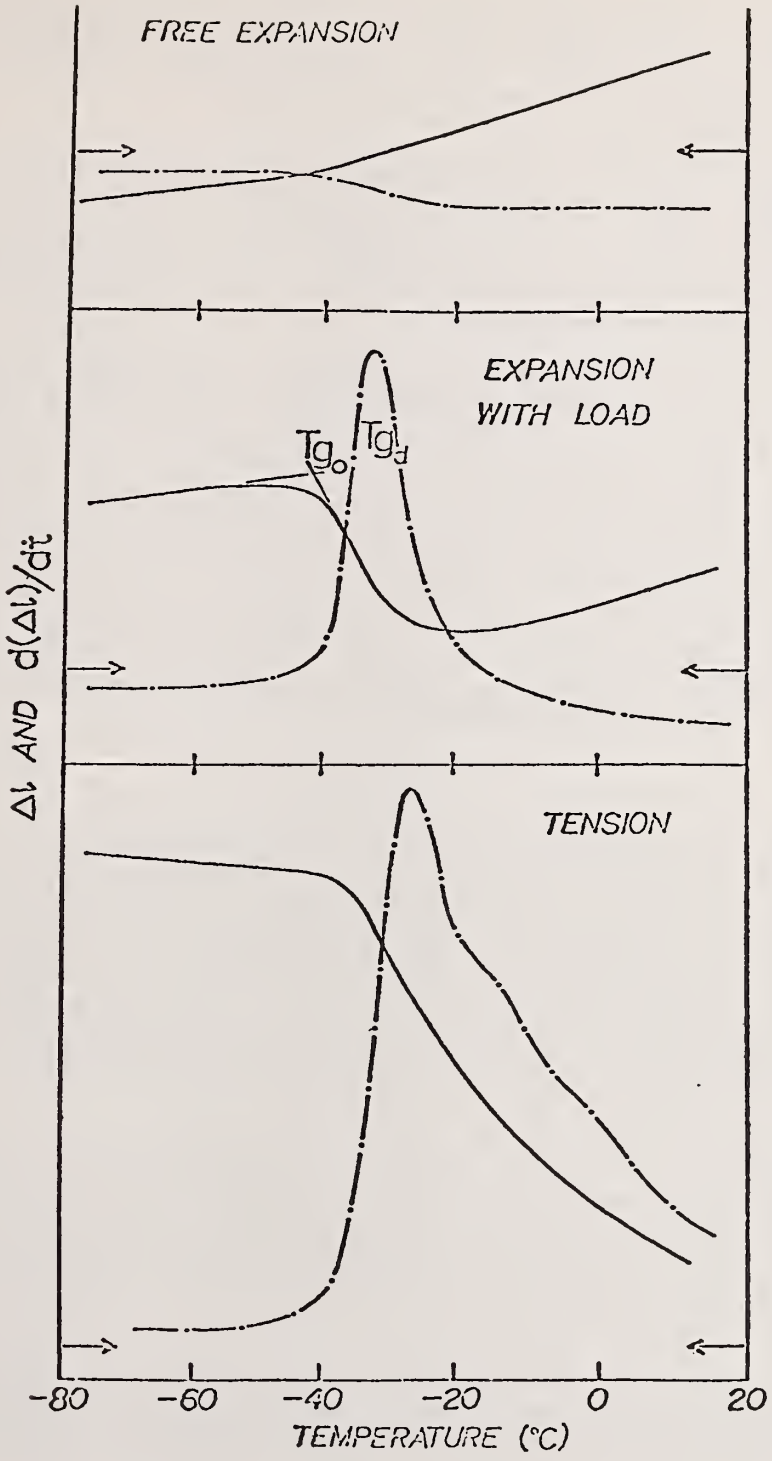

Figure 16. TMA/DTMA curves obtained in expansion, indentation and tension for typical glass transition in elastomer system [42]. ——— TMA, —·—·— DTMA. Tg_o and Tg_d defined in text.

indicates a single endotherm typical of that observed in crystallinity melt at +40 °C. Even with TMA, differences are often observed for the same sample depending upon the operation mode. Natural rubber-styrene butadiene rubber blends exhibit only a single glass transition at -60 °C when scanned in the indentation mode. Scanning in the tension mode reveals three events at -60, -27, and -5 °C. TMA and DTMA deserve to receive more attention in the future for fundamental studies of elastomer blends.

Table 8 compares the TMA and DTMA temperatures, as defined in figure 16 for the indentation and tension modes for a series of vulcanizates with the Gehman temperature as determined in ASTM D-1053. The Gehman temperature, G_T, is defined as the temperature at which the rigidity modulus is 1000 kg/cm^2/radian. The thermal coefficient of expansion below and above the glass transition temperature for each vulcanizate is also given (calculated from expansion probe curves).

Comparison of the data in Table 8 indicates a good agreement between the Gehman temperature and Tg_o as determined in the tension mode. Such agreement is fortuitous and in fact, with the exception of the BR/SBR/NR and BR/SBR blends, a good linear relationship exists between G_T and all temperatures determined by TMA and DTMA. Considering the differences in the experimental techniques, exact correlation is not anticipated. In the interests of rapid testing, high scan rates are desirable and little variation in Tg_o and Tgd determined by expansion with load was found over the scan rate range of 2 to 20 °C/min. At higher scan rates, instrumental temperature gradient effects resulted in significant differences in Tg_o and Tg_d. In addition to assessing low temperature properties, the TMA method can be used to evaluate the performance of plasticizers and their ability to depress the observed glass transition.

Conclusions

In 1969, Maurer [1] concluded his review on the thermal analysis of elastomer systems predicting a very bright future for thermal methods. Now, some ten years later, there is no doubt that this is being fulfilled at the industrial research laboratory level. To the author's knowledge to date, no rubber industry plant laboratory has introduced thermal analysis for large scale routine quality control applications. Industrial scientists are beginning to realize the potential of thermal analytical methods which have been used and developed by our academic colleagues for many years. Hope for acceptance at the plant level has increased with the recent introduction of robust quality control type instruments by several manufacturers. It is my belief that external factors such as increased product liability and environmental concerns will further increase interest in rapid testing procedures.

A major drawback to the rubber technologist considering thermal analysis is the lack of a comprehensive data base. In our own laboratory, hundreds of materials and products have been characterized (elastomers, plastics, thermoplastics, resins, textiles, etc.) and this provides valuable information in trouble-shooting processing and product problems. We have found very few areas where thermal methods failed to provide some clue as to the problem. The challenge – as always – is to interpret in a meaningful manner, the data that is obtained.

In conclusion, time has permitted only a few of the uses to be examined in a general manner. An attempt has been made to cover both a wide variety of research and application areas in the hope that the versatility of the techniques can be fully appreciated.

Table 8. Thermomechanical Analysis of Vulcanizates [28].

Vulcanizate	$a(°C^{-1}) \times 10^4$ ±0.03 below T_g ±0.1 above T_g	Expansion (°C)		Tension (°C)		Gehman (G_T)
		T_{gd}	T_{go}	T_{gd}	T_{go}	
Polyacrylate 1.	0.54(-120 to -40), 2.3(+80)	-8	-16	0	-11	-11
2.	0.53(-120 to -60), 1.8(+60)	-11,22	-21,16	-4	-15.5	-15.5
Medium nitrile NBR 1.	0.45(-80), 1.8(+40)	-18	-24	-15	-21	-21
2.	0.51(-80), 1.8(+40)	-22	-30	-18	-26	-26
Neoprene WRT	0.49(-60), 1.69(+40)	-33	-40	-27.5	-36	-34.5
Low nitrile NBR	0.45(-120 to -60), 1.47(+40)	-32	-40	-28	-36	-39.5
BR/SBR/NR	0.46(-110), 1.57(+20)	-74	-89	-58, -38, -5	-70	-65
BR/SBR	0.60(-110), 1.53(+40)	-78	-70±5	-57, -27, -6	-70	-75

References

[1] Maurer, J. J., Rubber Chem. Technol. 42, 110 (1969).

[2] Chakraborty, K. K., Rubber India 26(2), 14 (1974) and 26(3), 14 (1974).

[3] Brazier D. W., and Nickel, G. H., Rubber Chem. Technol. 48, 661 (1975).

[4] Dudley, N. A., and Smith, D. A., Rubber Chem Technol. 40, 445 (1967).

[5] Smith, D. A., Rubber Chem. Technol. 37, 937 (1964).

[6] Smith, D. A., Analytical Chem. 35, 1306 (1963).

[7] Smith, D. A., Rubber Chem. Technol. 37, 934 (1964).

[8] Smith, D. A., Kautschuk und Gummi, 19, 477 (1966) and J. Poly. Sci. Pt. B4, 215 (1966).

[9] Maurer, J. J., American Chemical Society Polymer Preprints, 14, 518 (1973).

[10] Maurer, J. J., J. Macrmol. Sci.-Chem. A8(1), 73 (1974).

[11] Sircar, A. K., and Lamond, T. G., Rubber Chem. Technol. 48, 301 (1975).

[12] Sircar, A. K., and Lamond, T. G., Rubber Chem. Technol. 45, 329 (1972).

[13] Sircar, A. K., and Lamond, T. G., Thermochimica Acta 7, 287 (1973).

[14] Sircar, A. K., and Lamond, T. G., Rubber Chem. Technol. 48 631 (1975).

[15] Sircar, A. K., and Lamond, T. G., Rubber Chem. Technol. 48, 640 (1975).

[16] Sircar, A. K., and Lamond, T. G., Rubber Chem. Technol. 48, 653 (1975).

[17] Brazier, D. W., and Schwartz, N. V., Rubber Chem. Technol. 51, 1060 (1978).

[18] Sircar, A. K., Rubber Chem. Technol. 50, 71 (1977).

[19] Chiu, J., Analytical Chem. 40, 1516 (1968).

[20] Chiu, J., Thermochimica Acta 1, 231 (1970).

[21] Brazier, D. W., and Schwartz, N. V., J. Appl. Poly. Sci. 22, 113 (1978).

[22] Maurer, J. J., Thermal Analysis, Schrenker, R. F., and Garn, P. D. (eds.), Academic Press, Vol. 1 (1969).

[23] Pautrat, P., Metavier, B., and Markeau, M., Rev. Gen. Caoutch Plast. 52, 273 (1975) and Rubber Chem. Technol. 49, 1060 (1976).

[24] Harris, J., Synthetic 8, 20 (1977).

[25] Jarosynska, D., Kleps, T., and Tulak, D., International Polym. Sci. & Tech. 4, T20 (1977).

[26] Jarosynska, D., and Kleps, T., Polimery 22(18), 292 (1977).

[27] Maurer, J. J., Rubber Age 10, 47 (1970).

[28] Schwartz, N. V., and Brazier, D. W., Thermochimica Acta 26, 349 (1978).

[29] Swarin, S. J., and Wims, A. M., Rubber Chem. Technol. 47, 1193 (1974).

[30] Smith, R. G., and Stephens, H. L., American Chemical Society Rubber Division Meeting, Toronto (1974).

[31] Ponce-Velez, M. A., and Campos-Lopez, E., J. Appl. Polym. Sci. 22, 2485 (1978).

[32] Coran, A. Y., Science & Technology of Rubber, Chapt. 7, Eirich, F. R. (ed.), Academic Press, New York (1978), and references therein.

[33] Bekkedahl, N., and Weeks, J. T., J. Res. Nat. Bur. Stand. 73A, 221 (1969) and Rubber Chem. Technol. 43, 1275 (1970).

[34] Bhaumik, M. L., Banerjee, D., and Sircar, A. K., J. Appl. Polym. Sci. 6, 674 (1962) and 9, 1367 (1965).

[35] Brazier, D. W., and Nickel, G. H., Rubber Chem. Technol. 48, 26 (1975).

[36] Brazier, D. W., Thermochimica Acta 18, 147 (1977).

[37] Bruce, D. L., Lyle, R., and Blake, J. T., Rubber Chem. Technol. 17, 404 (1944).

[38] Markov, V. V., Privalikhina, N. P., and Zanemonets, N. A., J. Polym. Sci. Polymer Symposiums 42, 633 (1973).

[39] Maurer, J. J., Thermal Methods in Polymer Analysis, Shalaby, S. W. (ed.), Franklin Institute Press, Philadelphia (1978).

[40] Machin, D., and Rogers, C. E., Polymer Eng. & Sci. 10, 300 (1970).

[41] Machin, D., and Rogers, C. E., Polymer Eng. & Sci. 10, 305 (1970).

[42] Brazier, D. W., and Nickel, G. H., Thermochimica Acta 26, 399 (1978).

THERMAL ANALYSIS IN THE RUBBER INDUSTRY

RAPPORTEUR'S COMMENTS BY

John J. Maurer
Exxon Research and Engineering Company
Technology Feasibility Center
P.O. Box 45, Linden, N.J. 07036

Practical elastomer systems are generally complex mixtures of process oils, multi-component cure systems, polymer(s), filler(s) and a variety of miscellaneous components (stabilizers, processing aids, etc.). Analysis of the composition, cure characteristics and properties of these formulations is, therefore, an inherently complex and challenging task. Classical methods for analyzing rubber formulations are generally lengthy and require large samples. For these and other reasons they are often of limited value for process trouble-shooting, routine diagnostic work, and/or certain Quality Assurance programs. The application of thermal analytical techniques has enabled the development of practical procedures for use in programs of this type. For example, it is now a relatively straightforward task, for many systems, to determine the basic composition of the formulation (i.e., process oil, plasticizer, total polymer, total filler and ash), using a very small sample and in a reasonably short time. In some cases, it is also possible to monitor polymer blend composition, and in still others, to obtain at least semi-quantitative analysis of carbon black blend composition. Thermal analysis has made it possible to undertake analyses of these complex systems, on a routine basis, which are not possible by other techniques.

In his lecture on "Thermal Analysis in the Rubber Industry," Dr. Brazier, who has made important contributions in this area, very capably described applications of several thermal analytical techniques which illustrate the basic types of information which these techniques can provide regarding the composition, cure system/characteristics and properties of compounds and vulcanizates. These procedures and others described in the references in his paper have proven their value in elastomer research, development, manufacturing, and quality assurance programs.

The discussion which followed this paper covered a broad range of topics including proven applications of thermal analysis in elastomer systems, methods for improving applicability in other systems and, finally, the outlook for broader utilization of these techniques in the rubber industry. In the first category, it was noted that for some cure systems a good correlation can be obtained between cure characteristics as measured by Differential Scanning Calorimetry (DSC) and by cureometer analysis, a technique which monitors cure development via torque/modulus development. It was reported that DSC also enables detection of certain reactions which occur prior to cross-linking and thus are not detected by cureometer analysis. In the second category, Dr. David Dollimore (University of Salford) proposed a possible reason for the poor correlations observed between oxidation kinetics of some carbon blacks and BET surface area measurements of these blacks. He suggested that improved correlations could be obtained by also taking into account the type of adsorption isotherm exhibited by the black. In the final category, Dr. Brazier commented on factors influencing the relatively slow rate of acceptance and utilization of thermal methods in the rubber industry. He expressed the opinion that increased acceptance of these methods will depend in part on the development of more rugged equipment which is better suited to the factory environment. In addition, he believes that more general acceptance of these methods will require in some cases a lengthy incubation period during which the industry becomes familiar with the techniques and they slowly displace some of the traditional methods of analysis.

The full potential of thermal analysis for the resolution of complex elastomer formulations has probably not yet been achieved. It is envisioned that major advances may be possible via computer analysis of, e.g., TG data for such systems. As one approach, computer techniques may enable improved analysis of blend composition (for known formulations) by comparing TG data of the sample with those of known compositions. Alternatively, for some systems it may be possible to synthesize, via computer techniques based on stored data for individual, simple systems, the blend composition whose decomposition characteristics are the best fit to the experimental TG curve. It is also conceivable that computer analyses may in some cases enable monitoring of cure system uniformity via its effect on filler decomposition characteristics. Additional insights should be forthcoming in other cases via combining thermal analysis with complementary techniques such as gas chromatography and mass spectroscopy.

The appearance of product specifications involving thermal analytical techniques indicates that these procedures are gaining increased acceptance in the rubber industry. This acceptance should broaden and be strengthened as these techniques become more commonly known and practiced, and as new advances are made.

National Bureau of Standards Special Publication 580. Proceedings of the Workshop on the State-of-the-Art of Thermal Analysis held at NBS, Gaithersburg, MD, May 21-22, 1979. (Issued May 1980)

THERMOGRAVIMETRY AT HIGH HEATING RATES: STUDIES ON POLYMER IGNITION

B. Miller and J. R. Martin

Textile Research Institute
Princeton, New Jersey 08540

Abstract

A commercial thermogravimetric analyzer has been used to monitor the behavior of polymeric solids brought to ignition by exposure to preheated air. Samples were inserted into the TG oven and weight loss and sample temperature monitored simultaneously as a function of time. By using a series of oven temperatures and measuring times to ignition, it was possible to establish the minimum heating rate required for ignition and the initial decomposition temperature at that rate. Critical rates for 14 polymers ranged from 380 to 3380 °C/min and the decomposition temperatures were considerably higher than what is observed at lower heating rates. The two measured parameters have been combined to give a single value which seems to be a good indicator of a material's ignitability hazard potential.

Introduction

Since polymer thermal decomposition is one of the pre-ignition steps leading to flaming combustion, it is often studied for the purpose of obtaining a better understanding of the flammability of fibrous and other polymeric materials. Such studies usually have been carried out at low heating rates (<100 °C/min) using dynamic thermogravimetry (TG), differential thermal analysis (DTA), or evolved gas analysis (EGA). However, in actual flame-producing ignition situations, heating rates are known to be much greater than those attainable with conventional thermal analysis techniques. Since polymer decomposition can involve sequential and competitive reactions, it is not unreasonable to expect heating rates to have a significant influence on the net decomposition process both in terms of overall kinetics and yield of pyrolysis products. Therefore, it may not be valid to apply results obtained by conventional thermal analysis to processes which occur at much higher heating rates.

About thirty years ago the idea was introduced that, in the presence of air, a polymer would ignite if its surface temperature was raised to a certain critical value [1][1]. This was defined as the "ignition temperature" of the material, and a plethora of published reports are available in which ignition temperature data for polymers are presented. Unfortunately, the methods used to obtain these temperatures were often grossly dissimilar and, in consequence, the published values for any given polymer vary over a wide range.

Conceivably, the establishment of a standard procedure for such a determination would not be difficult to accomplish; however, there is a more fundamental objection to the idea of a polymer having any such thing as a characteristic ignition temperature. It can be demonstrated, and has been in many thermal analysis laboratories, that one can heat a polymer in the presence of air to quite high temperatures without producing what is generally understood as ignition (i.e., the generation of self-sustaining flaming combustion for an observable time). Thermal decomposition without ignition will occur if the material is heated up at a slow enough rate – comparable to the rates used in conventional thermal analysis procedures. Such observations have led to the hypothesis that a critical factor determining whether or not a polymer will ignite is related to its rate of heat uptake

[1]Figures in brackets indicate the literature references at the end of this paper.

[2]. This idea is supported by the work of Durbetaki showing that the ignitability of the gases produced by polymer pyrolysis is dependent on the rate of heating [3]. What follows is a report of an experimental procedure for obtaining data to test the validity of this hypothesis and application of the results to produce a relative ranking for ignition hazard. The work has been done using fabric samples which have such a high surface-to-volume ratio and porosity that they can be heated uniformly, particularly by hot gases.

Experimental Details

With certain modifications in operating procedure, the DuPont 951 Thermogravimetric Analyzer was used to investigate polymer ignition. One major difference was that the oven atmosphere (i.e., air) was preset at a fixed temperature before the sample was inserted into it. The readout controls of the apparatus were set so that the two "Y" channels monitored sample weight and themocouple response, respectively, both as a function of time. The thermocouple output was used to follow the rapid changes of sample temperature (the validity of this will be demonstrated) as well as to time the interval between the moment of insertion into the heated air and the moment of ignition. Previous auto-ignition studies [2,4] used thermocouples near the sample only as a device to determine ignition times, since the response times of these thermocouples were too slow to give an accurate trace of sample temperature.

Single and multilayered fabric samples 4 mm x 8 mm, were placed in the sample pan of the thermogravimetric (TG) apparatus. With the isothermal heating mode set at the desired temperature level, the oven heater was activated. After the short time required for the oven to come up to temperature, the sample-holding assembly was manually pushed into the oven. (This could be done in a reproducible manner within approximately one second.)

With such experiments it was possible to determine ignition times as a function of oven temperature; these results were then used to establish the limiting conditions required for ignition. Average ignition times were mean values obtained for at least six replicate experiments with less than ±0.5s variance. In addition, it was possible to simultaneously determine the loss of weight up to the moment of ignition, as well as detect the start of sample volatilization.

The salient features of the responses used in this experiment are shown in figure 1. The break in the temperature-time curve indicates the moment of ignition, t_i, while t_d is the time at which pre-ignition decomposition begins. From this figure it is obvious how one can also ascertain exactly how much of a polymer is volatilized during the pre-ignition decomposition process.

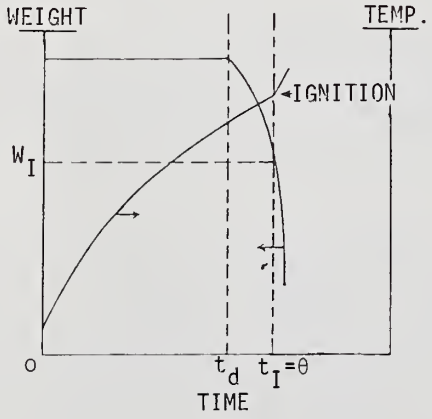

Figure 1. Typical responses in auto-ignition studies using the DuPont Thermogravimetric Analyzer to monitor sample weight and temperature.

Results and Discussion

Relationship Between Sample Temperature and Thermocouple Output

Auto-ignition studies with other devices have used the thermocouple output only as a timing device. However, since the DuPont TG thermocouple is reputed to give a fairly close approximation of the temperature of a sample, an investigation was carried out to see if this is true at the high heating rates required for auto-ignition. Temperature-indicating paints[2] were used on glass fabrics which had about the same mass and specific heat as the other materials to compare the response of the thermocouple with the actual surface temperature of the material. Figure 2 shows a typical comparison of the continuous response of the thermocouple with the responses of five paints. The points represent the minimum heating times required for each paint to undergo an irreversible observable thermal transition at a known temperature. The results show that the thermocouple response follows quite closely the heating rate of the fabric for at least the first 15 seconds of heating. In figure 3 the same data are plotted in the form to fit the general equation for nonequilibrium convective heating:

$$\log (T_\infty - T) = \log (T_\infty - T_o) - (hA/mC_p)t$$

where

T_∞ = final (air) temperature,

T_o = initial (ambient) temperature,

h = overall heat transfer coefficient,

A = sample area,

m = sample mass,

C_p = heat capacity of sample, and

t = time.

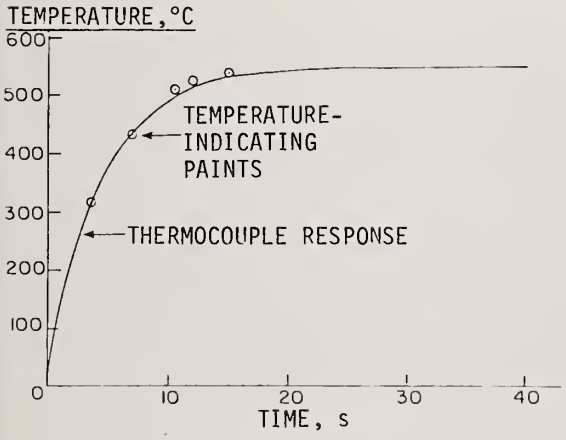

Figure 2. Agreement between TG thermocouple response and temperatures measured via irreversible color changes of temperature-indicating paints.

[2]Tempilag®; Tempil Corp., New York, NY.

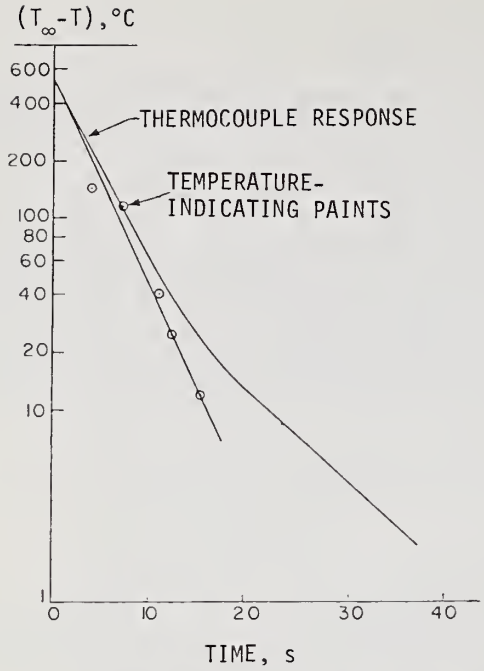

Figure 3. Semilog plot of time-temperature data.

It can be seen that the points seem to follow the expected heating rate while the thermocouple response falls behind as heating time increases. However, even after fifteen seconds the difference is only about 12 °C. Since the critical events during pre-ignition occur well before the thermocouple starts to lag significantly, it does seem possible to make a direct estimate of sample temperature and, in particular, its rate of change at any instant during the rapid heating.

Pre-ignition Weight Loss

Pre-ignition weight loss data were obtained for both polyester and cotton fabrics at a number of oven temperatures and initial sample weights (varied by using layered samples). Tables 1 and 2 show, for polyester and cotton samples respectively, a tabulation of weight loss up to the moment of ignition, expressed as both absolute weight loss and percent of original sample weight. For polyester, percentage weight loss goes down systematically as sample weight increases, but the absolute weight loss remains about the same, except for the 8-layer specimens. As air temperature is increased, weight loss decreases. (At 600 °C, the one-layer sample did not ignite; that is, no noticeable excursion of the thermocouple detector was observed. Most likely, ignition did occur but was not detected, since this material does ignite when tested in larger amounts.) The results for cotton show essentially the same behavior with the absolute weight loss for cotton consistently larger for the double layer. The most obvious conclusion to be drawn from the data in Tables 1 and 2 is that ignition does not depend on a specific fractional or absolute weight loss.

Table 1. Pre-Ignition Weight Loss of Polyester Fabric.

Air Temperature °C	Original Sample Weight mg	Weight Loss at Ignition %	Weight Loss at Ignition mg
600	1.91 (1 layer)	----[a]	----[a]
	3.82 (2 layers)	34.3	1.31
	7.65 (4 layers)	18.7	1.43
	15.29 (8 layers)	10.7	1.63
625	1.91 (1 layers)	38.7	0.74
	3.82 (2 layers)	16.0	0.61
	7.65 (4 layers)	11.0	0.84
	15.29 (8 layers)	6.7	1.02
650	1.91 (1 layers)	18.3	0.35
	3.82 (2 layers)	11.7	0.45
	7.65 (4 layers)	6.7	0.51
	15.29 (8 layers)	5.3	0.81
675	1.91 (1 layers)	13.0	0.25
	3.82 (2 layers)	7.0	0.27
	7.65 (4 layers)	4.0	0.30
	15.29 (8 layers)	3.0	0.45

[a]Ignition not detected.

Table 2. Pre-Ignition Weight Loss of Cotton Fabric.

Air Temperature °C	Original Sample Weight mg	Weight Loss at Ignition %	Weight Loss at Ignition mg
525°	3.39 (1 layer)	23.0	0.78
	6.78 (2 layers)	16.7	1.13
550°	3.39 (1 layer)	24.3	0.82
	6.78 (2 layers)	19.3	1.31
575°	3.39 (1 layer)	20.7	0.70
	6.78 (2 layers)	14.0	0.95
600°	3.39 (1 layer)	17.7	0.60
	6.78 (2 layers)	11.3	0.76

Critical Heating Rates for Polymer Ignition

As a possible criterion for polymer ignition, the idea of a critical rate of energy input or necessary minimum heating rate appears to be quite logical. The method of determining critical heating rates for a polymer first requires establishing the lowest oven temperature $(T_\infty)_c$ which can bring about ignition. This is done by extrapolating a plot of the reciprocal of ignition time ($1/\theta$) versus oven temperature to infinite ignition time ($1/\theta = 0$), which represents the limiting condition where there is zero probability of ignition. Figure 4 shows this extrapolation for polyester and demonstrates that the resulting temperature $(T_\infty)_c$ is independent of the original sample weight. This has been found to be the case for all materials and, therefore, in most instances, limiting temperatures were determined from data from one- and two-layer sample configurations.

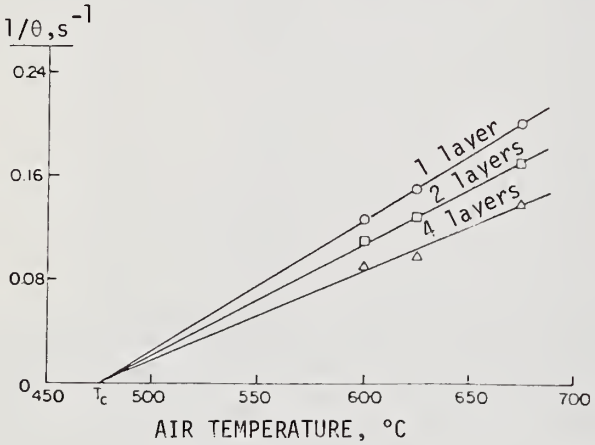

Figure 4. Representative extrapolation of reciprocal of ignition time vs. air temperature to obtain the minimum air temperature required for ignition, $(T_\infty)_c$. Polyester fabric; sample weight varied by layering.

Once $(T_\infty)_c$ has been ascertained, a fresh sample of polymer is then inserted as before into the TG oven preheated to this temperature, and sample temperature and weight are continuously monitored. The heating rate experienced by the sample as it starts to decompose is considered to be the minimum heating rate required for ignition (i.e., the critical heating rate). This is shown schematically in figure 5.

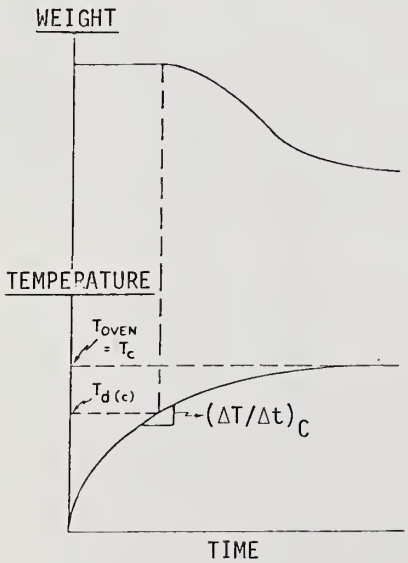

Figure 5. Determination of critical ignition conditions from TG curves obtained with oven at $(T_\infty)_c$: (1) Td(c) = temperature when sample weight begins to drop. (2) Minimum heating rate for ignition = slope of temperature-time curve at $T_{d(c)}$.

Table 3 summarizes the ignition data for a variety of single-component materials arranged in order of decreasing critical heating rates. The decomposition temperature at the critical heating rate $(T_d)_c$ is determined as shown in figure 5. Also included in Table 3 are the decomposition temperatures obtained when heating rates were programmed at 20 and 100 °C/ min.

Table 3. Ignition Data for Single-Component Materials.

	$(\Delta T/\Delta T)_c$, °C/min	$(T_\infty)_c$ °C	$(T_d)_c$ °C	(T_d)100 °C/min °C	(T_d)20 °c/min °C
Wool	3379	590	357	245	220
Kynol®	2087	575	455	450	400
Kermel®	1709	625	525	460	425
Arnel®	1478	463	340	320	300
Acrylic	1284	520	408	355	315
Polypropylene	933	494	410	405	375
Rayon	806	403	320	280	260
Nylon 66	802	507	430	405	370
Cotton	780	425	338	305	285
Nomex®	734	600	545	445	405
PBI	522	700	644	645	600
Polyester	419	480	427	395	385
Acetate	412	379	331	280	260
Vinylon	383	465	400	345	325

Evaluating Ignition Hazard

It is reasonable to consider that the potential ignition hazard of a polymer must be related to its initial decomposition temperature as well as to the critical heating rate for ignition. (No matter how fast a polymer is heated, it will not ignite unless it decomposes.) However, the data in Table 3 show that polymers exhibiting high critical heating rates are not necessarily those that have high decomposition temperatures.

Figure 6 shows critical heating rates plotted against decomposition temperatures at the critical heating rate and clearly demonstrates that there is no general correlation between these two quantities. However, from this plot one can see subgroupings in which there is a definite inverse relationship. Each of these groups could be classified according to its distance from some common "origin" located on the x-axis. When considered in this manner, those polymers which are known to be easily ignited (e.g., rayon and cotton) are seen to be close to the origin while fabrics known for ignition resistance (e.g., wool, Nomex®, PBI) are relatively far from it. Following from this observation a simple function has been derived, based on this "distance from the origin" concept. A material's probability of ignition is taken to be proportional to the reciprocal of the distance of its plotted value (as in figure 6) from an origin defined as [0,25 °C]. To obtain this value, the data plotted in figure 6 are first made dimensionless by dividing each result by the corresponding highest value obtained, i.e., 3379 for the critical heating rate and [644-25] for $(T_d)_c$. The assumption is then made that both factors have equal significance, and therefore the ignition hazard function can be expressed (by simple triangulation) as:

$$[I] = 100 \; / \; \{ \; [(\Delta T/\Delta t)_c/3379]^2 + [(T_{d(c)} - 25)/619]^2 \}^{\frac{1}{2}} .$$

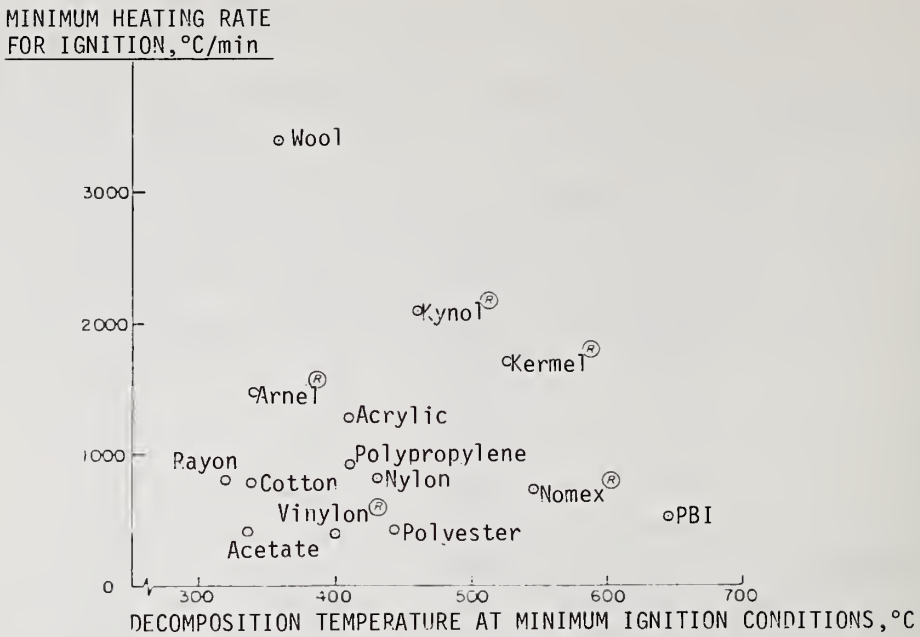

Figure 6. Minimum heating rate for ignition plotted against decomposition temperature at this heating rate for a group of single-component fabrics.

The calculated values of [I], listed in Table 4 in order of decreasing ignition hazard, fall into three groups corresponding to the levels of ignitability mentioned in connection with figure 5. Although the ranking of wool as less hazardous than materials developed for high temperature resistance is somewhat unexpected, the rest of the ranking conforms quite well with general experience, whereas rankings according to $(\Delta T/\Delta t)_c$ or $T_{d(c)}$ alone do not (see Table 3).

Table 4. Values of [I] for the Materials in Table 3.

Acetate	196
Rayon	188
Cotton	180
Vinylon (polyvinyl alcohol)	162
Polyester	151
Arnel® (cellulose triacetate)	149
Polypropylene	147
Nylon 66	144
Acrylic	138
Nomex®	115
Kynol®	108
Kermel®	105
PBI	99
Wool	88

The data in Table 3 also show conclusively that the decomposition temperature is significantly increased as the heating rate is increased. The decomposition temperatures at the critical heating rates range from 35 to 140° higher than those obtained at 20 °C/min. This can be taken as additional evidence that polymers do not have a characteristic ignition temperature.

Summary and Conclusions

The above results have demonstrated how an ignition criteria can be established in terms of a minimum critical heating rate applied while a polymer undergoes thermal decomposition. This quantity is specific for each polymer and represents one factor which determines the ignition hazard of a material. However, in ranking materials in terms of ignitability, the decomposition temperature must also be considered since the critical heating rate must be applied while the material is volatilizing. Since there is no general relationship between these two quantities, both must be considered in ranking materials in terms of ignition hazard.

References

[1] Setchkin, N. P., A Method and Apparatus for Determining the Ignition Characteristics of Plastics, J. Res. Nat. Bur. Stand., 43, 591-600 (1949).

[2] Miller, B. and Martin, J. R., Ignition of Polymers, in Flame-Retardant Polymeric Materials, Vol. 2, Lewin, M., Atlas, S. M. and Pearce, E. M., (eds.), Plenum Press (1978).

[3] Durbetaki, P., Effects of Ignition Sources and Fire Retardants on Material Ignition, Report to Center for Fire Research, National Bureau of Standards, March (1978).

[4] Miller, B. ,Martin, J. R., and Meiser, Jr., C. H., The Auto-ignition of Polymers, J. Applied Polymer Sci., 17, 629-642 (1973).

THERMOGRAVIMETRY AT HIGH HEATING RATES: STUDIES ON POLYMER IGNITION

RAPPORTEUR'S COMMENTS BY

Jen Chiu
E. I. DuPont De Nemours & Company, Inc.
Wilmington, Delaware 19898

Thermogravimetry (TG) has been widely applied to the study of thermal stability of polymers. However, the versatility of TG to measure sample weight change as a function of temperature or time offers many other unique applications limited only by the imagination of the user. In this paper, the authors showed a novel TG procedure to classify the ignition behavior of polymers using a commercial instrument. The talk was very stimulating, and a long and enthusiastic discussion followed. Dr. Miller clarified further many details raised during the question period. The following is a summary of the resulting discussion.

(1) Ignition is primarily associated with the diffusion rate of the fuel away from the specimen. Ignition occurs only when the rate is rapid enough to build up a localized concentration. In the presence of an external ignition source, the decomposition rate may be different. But the fundamental requirement of the sample to decompose at a sufficiently rapid rate still applies.

(2) The experiment is performed in static air. No gas flow is used.

(3) In the present study, convected heat transfer predominates. Any radiation heat component should be minor.

(4) The present study implies a correlation between chemical structure and ignition properties as shown by the three groups of polymers: cellulosics, polyolefins and vinyls, and polyamides and polybenzimides. It will be interesting to include other types of polymers. Also of importance will be the effect of additives such as flame retardants.

(5) The effect of processing of textiles on ignition is not noticeable. Although some differences in ignition behavior were observed for fresh textile items never laundered before, these may be due to finishing oils, etc.

(6) The same shape of specimen, a rectangular piece, 4 mm x 8 mm, is always used to maintain a constant surface area. The sample shape seems to be more important than the sample mass. Different masses can be obtained by using multiple layers. Filaments and yarns are wound on inert heat sink for measurement.

(7) Some earlier work on auto-ignition has shown the same activation energy value of ca. 10 Kcal/mole for all types of polymers. This is consistent with a common rate-controlling factor – the diffusion of fuel away from the material.

(8) It is suggested that the furnace of the DuPont TG apparatus should be allowed to move towards the sample instead of the other way around. High heating rates for TG is potentially useful for many other studies such as ablation, etc. Recent work reported the use of IR imaging furnace to obtain heating rates as high as 1000 °C per second for TG work.

(9) In order to understand the ignition mechanism it is of importance to identify the decomposition products, particularly during the initial stages of the ignition. Other techniques should be employed besides TG.

National Bureau of Standards Special Publication 580. Proceedings of the Workshop on the State-of-the-Art of Thermal Analysis held at NBS, Gaithersburg, MD, May 21-22, 1979. (Issued May 1980)

CERAMIC PROCESSES AND ENERGY CONSERVATION

W. Richard Ott

Department of Ceramics
College of Engineering
Rutgers - The State University
New Brunswick, New Jersey 08903

Abstract

Ceramics, including glass and cements, are reviewed for their use of thermal analysis. Processing is considered to include the mining of the raw materials, batch preparation, forming, drying, and firing. Energy conservation considerations include methods used to lower process temperatures or shortening process time as well as reducing energy consumption through greater process efficiency.

Examples include the use of DTA/TG/TMA/EGA in studies of solid state reactions, sintering, drying, etc. The use of the data as applied to pollution control and energy conservation in ceramics is discussed.

Thermal analysis is shown to be a critical tool in ceramics for material and process improvement. Substantial energy reductions have been relaized through effective use of thermal analysis on a wide variety of materials.

Ceramics (inorganic, non-metallic materials) comprise one-third of the material's field, with metals and polymers being the other components. Ceramics, because of the high processing temperatures, are significant energy consumers. Makhigani [1][1] estimates the energy consumption in processing ceramic materials at approximately 2.5 percent of the total U.S. energy consumption. With processing temperatures routinely approaching 1600 °C and higher, thermal analysis offers an ideal tool to investigate these processes. In fact, thermal analysis has a unique advantage in this regard.

Energy conservation can take several forms, including:

1. Less energy intensive raw materials
2. Shorter processing times or lower processing temperatures
3. Greater process efficiency

The energy required per unit of product can be reduced if the processing temperature can be lowered. Specificially, if a product can be fired at 1500 °C instead of 1600 °C for the same length of time, then less energy will be expended. Shorter processing times have the similar advantage of using less energy per unit of product. When process recoveries are increased, then the energy per unit of product will also decrease. For example, if a process for chrome-magnesite steel refractories expends 10 energy units per brick and 75 percent of the bricks are useable, then the energy utilization per suitable brick is 13.3 units. If the process efficiency is increased to a 90 percent recovery, then the net energy per good brick drops to 11.1 units – a savings of about 20 percent.

[1]Figures in brackets indicate the literature references at the end of this paper.

Throughout this entire discussion it should be noted that trade-offs develop which make the optimum energy efficient process difficult to identify. For instance, the processing temperature for most ceramics can be lowered by reducing the particle size of the initial raw materials. However, in addition to requiring energy to reduce the particle size, this step will increase the shrinkage during firing and lower the rate of recovery.

The processing of fine grained ceramics follows the general format:

Batch Preparation

Forming

Drying

Firing

Finishing

While much of the energy expenditure is in the drying and firing steps, many of the process parameters critical to that expenditure occur earlier.

The first area to be examined where energy can be conserved is that of the raw materials. The use of less refined raw materials offers an area of lower cost as well as lower energy consumption through elimination of the energy expended to further process these raw materials. A specific example is the substitution of ammonium paratungstate (APT) as a source of tungsten for the more costly tungsten trioxide or tungstic acid in tungsten carbides [2]. In this case, substitution of APT for one of the above resulted in particle sizes of tungsten which when carburized were too small for use in tools. The desired size range of the crystallites is approximately two microns. The goal of this study then was to increase the size of the tungsten particles derived from APT [3]. Variables which are readily adjustable during the reduction phase (with H_2) are: APT bed depth, hydrogen flow rate and the rate at which the APT is brought to the reduction temperature. An APT source from G.T.E. Sylvania with 25 ppm Na and 10 ppm Si was chosen for the study. Figure 1 shows the TG/DTG data for a sample with the decomposition sequence, as determined, using x-ray diffraction. The effect of heating rate on the tungsten crystallite size is shown in figure 2. All samples were held for thirty minutes isothermally at 950 °C and then cooled rapidly. This figure shows that the tungsten particle size increases from 0.026 microns at 2 °C/min to approximately 0.15 microns at 10 °C/min. The more rapid the heating rate the larger the crystallite size. The effect of sample size was explored using 300, 975, 1650, and 3000 mg sized samples. These four sizes were heated at 10 °C/min. Figure 3 shows that the crystallite size increases with increasing sample size. The size of the tungsten crystals reaches almost one micron. The effect of hydrogen flow rate was also investigated as a process variable. A sample size of 3000 mg was heated at 10 °C/min to the reaction completion temperature with a hydrogen flow rate of 10 l/hr and 300 l/hr. As can be seen in figure 4, the higher hydrogen flow rate reduced the tungsten crystallite size. The decrease in tungsten size is not large and suggests that the rate of 10 l/hr is reasonably effective in sweeping the reaction products away from the reaction site. Consequently, a stagnant hydrogen atmosphere should have a substantial effect in increasing the crystallite size. To test this hypothesis, the crucible holding the sample was capped. The cap had a small hole to allow the pressure to be maintained at one atmosphere.

The results of this experiment are also shown in figure 4 and are quite dramatic. The crystallite size increases from 1 micron to 1.9 microns.

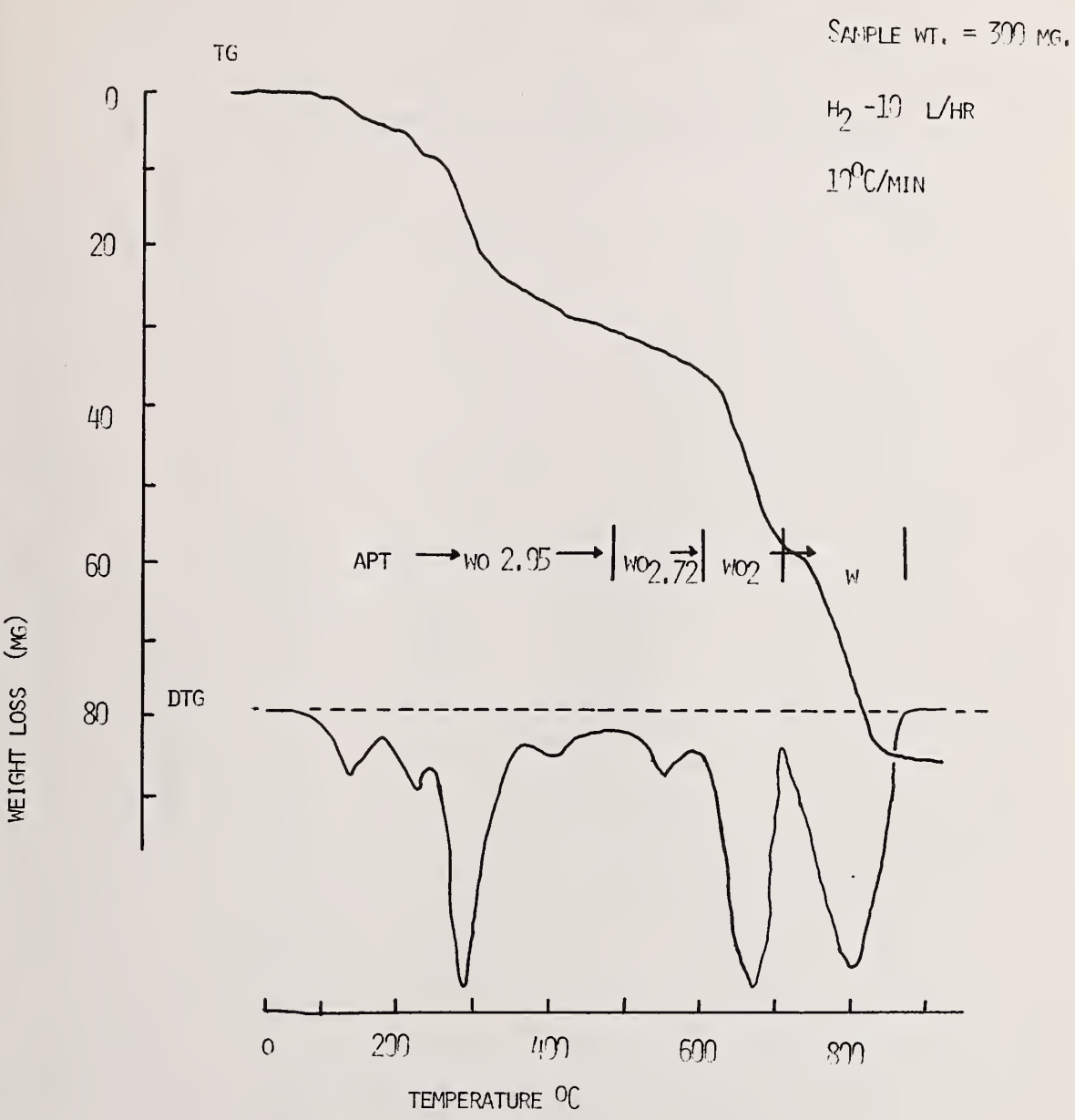

Figure 1. Thermal analysis data for the reduction of APT in hydrogen.

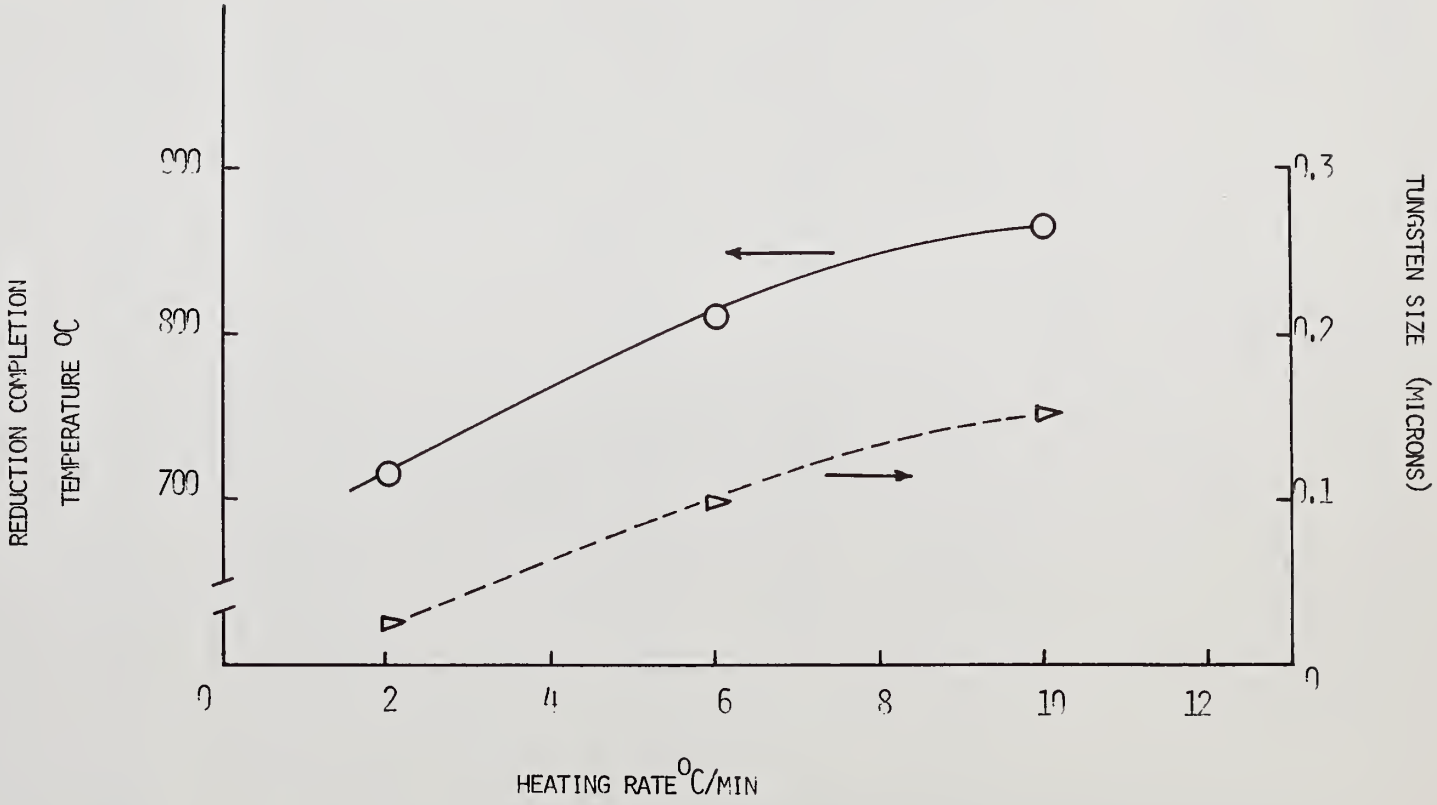

Figure 2. The effect of heating rate on the tungsten crystallite size.

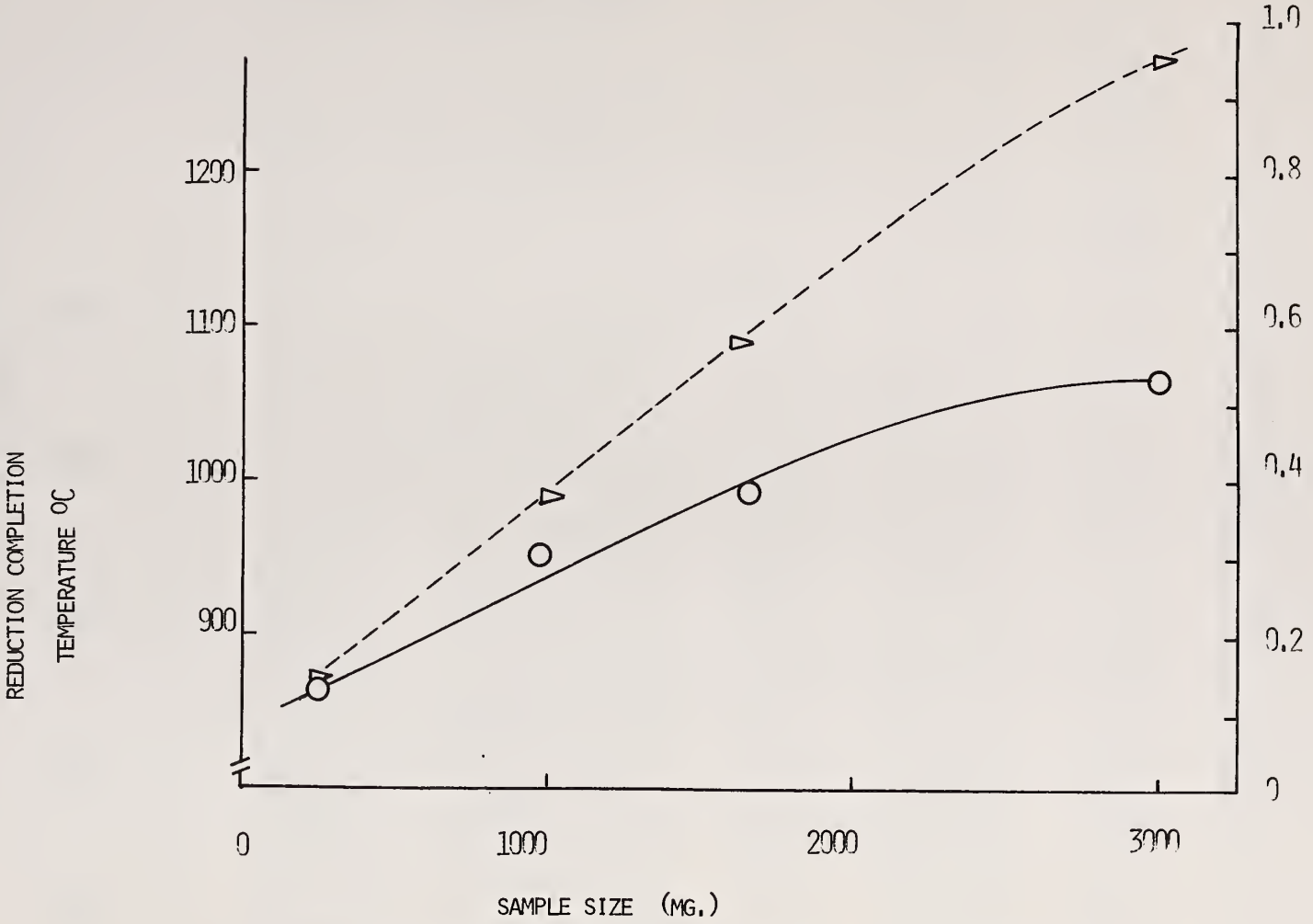

Figure 3. The effect of sample size on tungsten crystallite size.

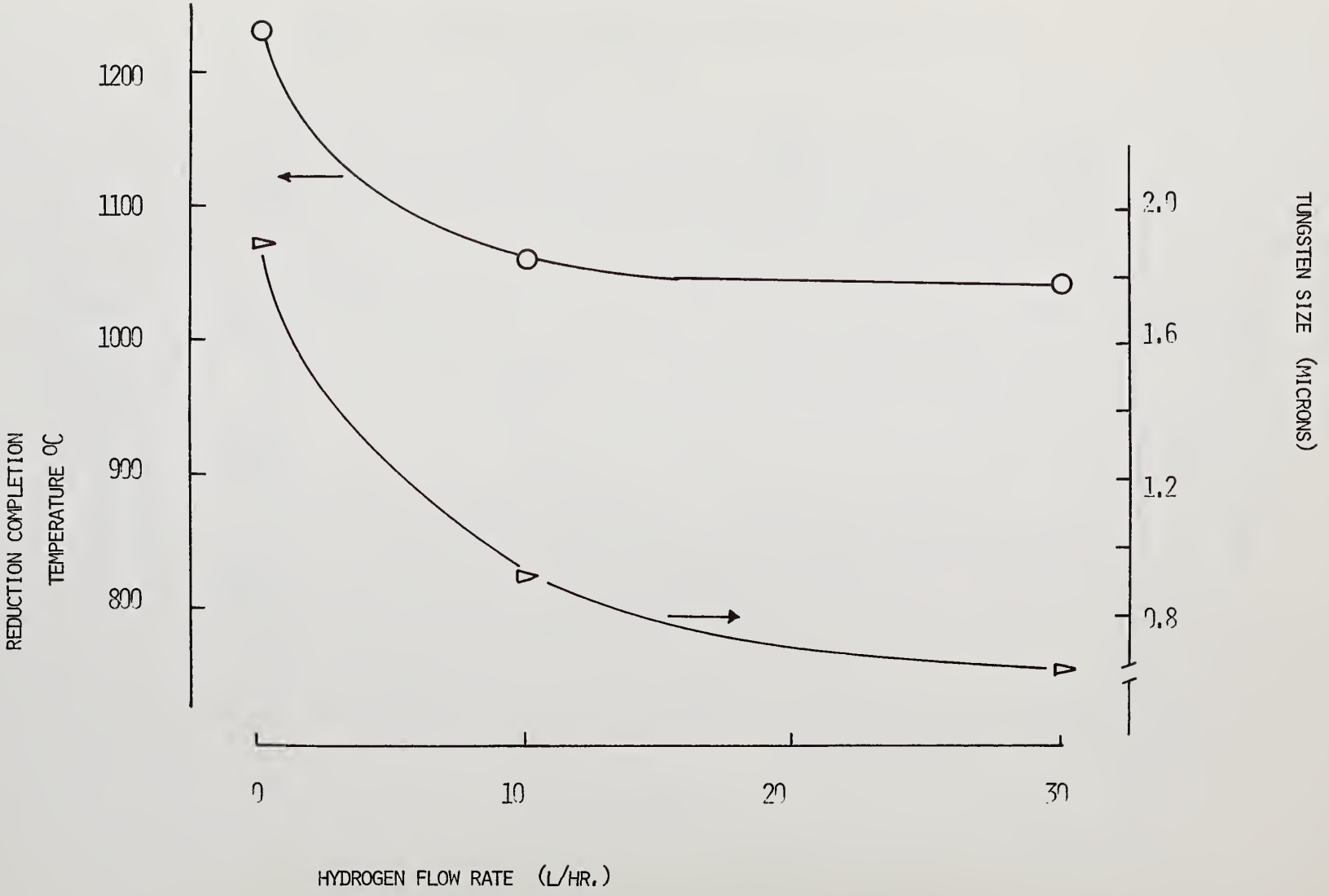

Figure 4. The effect of hydrogen flow on the tungsten crystallite size.

Increasing the sample size, reducing the hydrogen flow, and increasing the heating rate all increased the size of the tungsten crystals and increased the temperature at which the reduction reaction occurred. All of these steps had the effect of keeping the reaction products in the vicinity of the reaction site, or put more positively increasing the water/hydrogen ratio (i.e., the oxygen partial pressure) over the sample. These steps effected the solidstate reactions which require nucleation of the desired phase and subsequent crystal growth. The nucleation process occurs at a lower temperature than the temperature of maximum crystal growth. The partial pressure of oxygen over the sample controls the rate of reduction of WO_2. By retarding the reaction rate there is only limited opportunity for nuclei to form at low temperatures, and consequently these nuclei grow to a larger size as the available tungsten oxide is reduced. Conversely, when the reaction proceeds rapidly at low temperatures, large numbers of nuclei form and resultant crystal size is relatively small.

Since the nucleation step appeared to be critical and Na_2O has been cited as promoting nucleation, several APT sources with lower sodium were examined. APT with only 3 ppm sodium yielded a crystal size increase of 10 percent or 2.1 microns under optimum conditions. Based on the thermoanalytical study, APT is now used as a tungsten source in cobalt bonded tungsten carbides.

In drying ceramics, the energy expenditure is controlled by the amount of water present. Thermal analysis can assist in controlling drying by preventing cracking and thereby increasing the process efficiency. Beyond that, little is possible. Water levels are determined in accordance with the needs of the forming process. Dry pressing uses very little water but a process like extrusion requires water to obtain the plasticity necessary to permit extrusion. Drying energy consumption can most assuredly be a significant fraction of energy costs but it is difficult to reduce its level.

During heat treatment, two processes can occur: 1) Solid-state Reactions, and 2) Sintering. In each case the process occurs through diffusion. While, occasionally, nucleation of the new phase or the actual chemical reactions during solid-state reactions can be the limiting step, the preponderance of data indicates that the transport of materials by diffusion is generally the controlling step.

By way of demonstrating this fact, examine the reaction between sodium carbonate and silica [4]. Figure 5 shows the effect of temperature on a function (Ginstling-Brounshtein Model for a Diffusion Controlled Reaction) of the degree of completion of the reaction. As anticipated, the greater the temperature the greater the rate of reaction. These experiments were performed using isothermal thermogravimetric analysis in air. Beyond temperature, the second most significant variable in ceramic processing is particle size. As noted, the smaller the particle size the more rapid the solid-state reaction. This is the result of shorter diffusion paths. The particle size relationship is shown in figure 6 with the smaller particle sizes having larger rate constants. In sintering the process occurs more rapidly because the driving force is surface area and smaller particles provide greater driving force and hence more rapid sintering.

If water vapor is added at the reaction site, the result is quite dramatic. In figure 7 it can be seen that the diffusion model is no longer valid. The rate has increased to the point where the reactions occurring at the interface control the reaction rate (figure 8). This increase in reaction rate can be seen in figure 9. The effect of water vapor as an aid in accelerating ceramic reactions has been adequately described in the book of Koenig and Green [5].

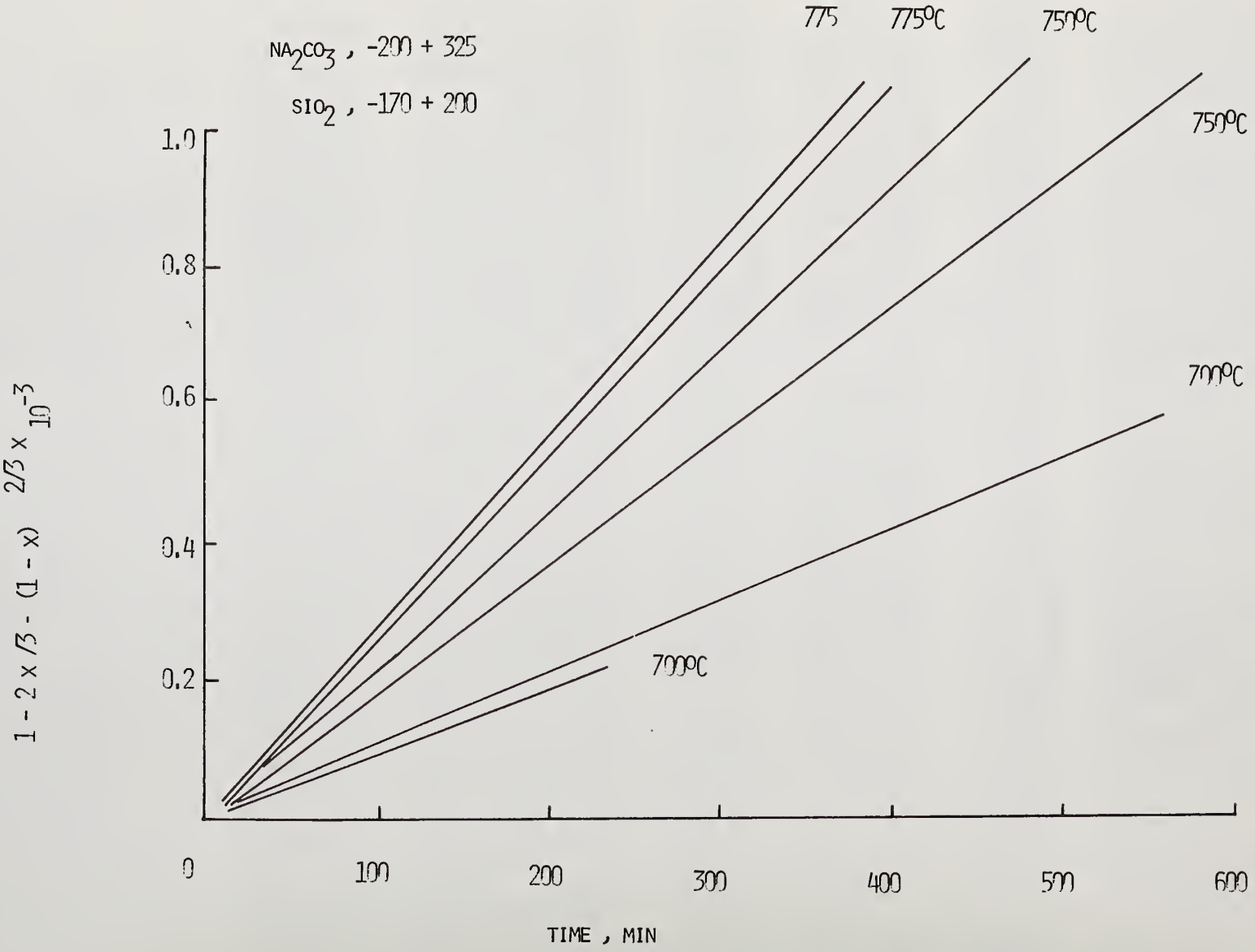

Figure 5. The Ginstling Brounshtein Model $Na_2CO_3 + SiO_2$.

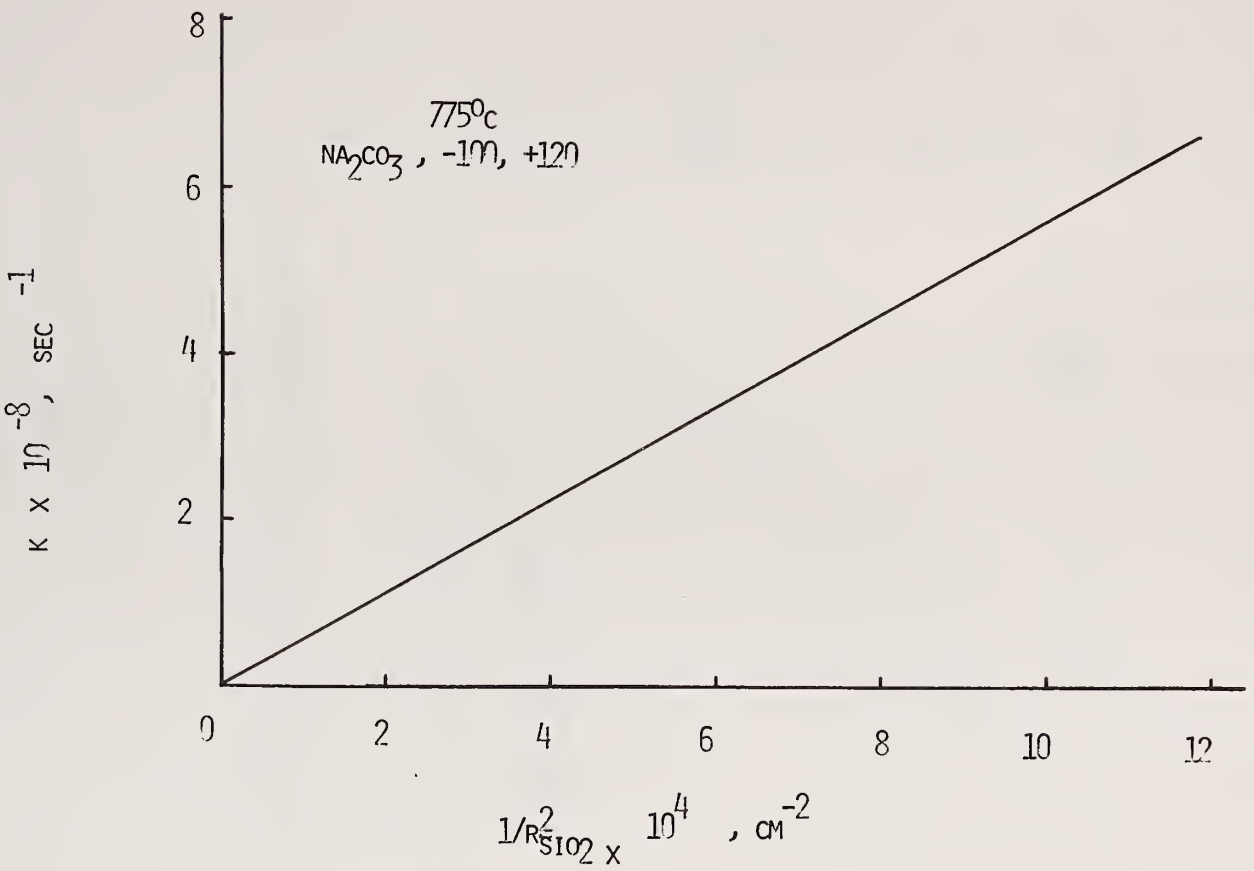

Figure 6. The effect of silica particle size on the rate constant.

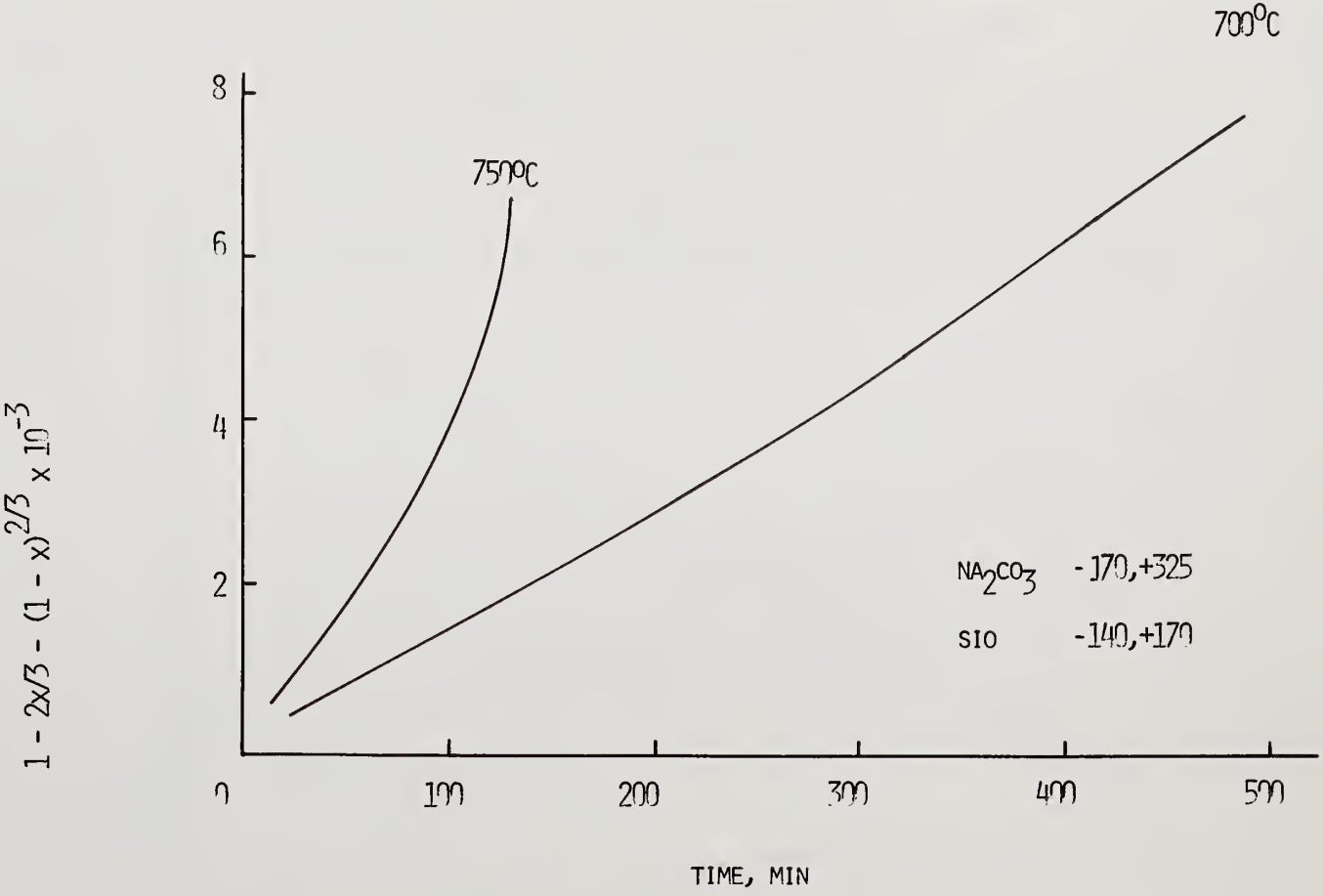

Figure 7. The Ginstling Brounshtein Model (sodium carbonate partially hydrated)

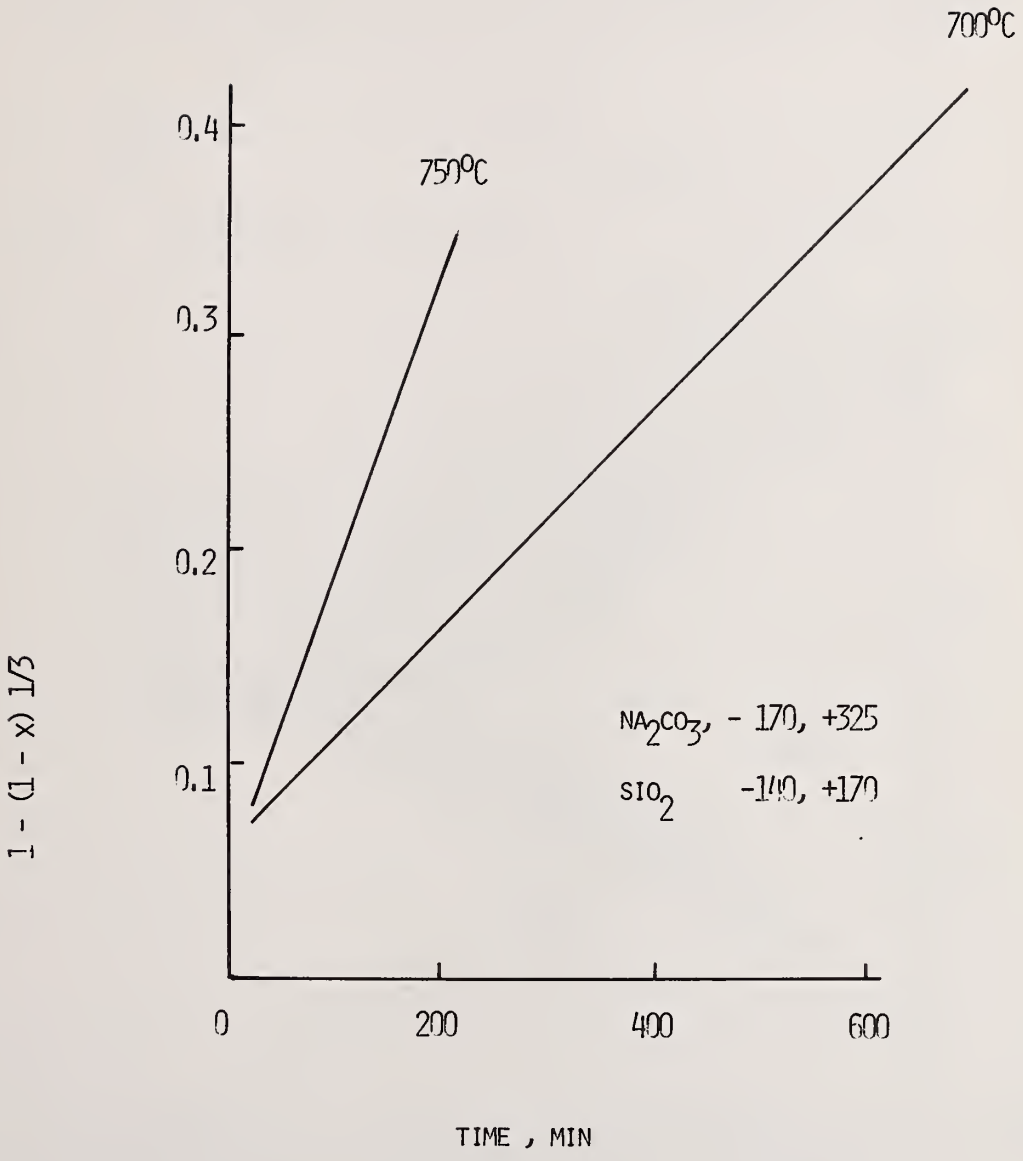

Figure 8. The Phase Boundary Model (sodium carbonate partially hydrated).

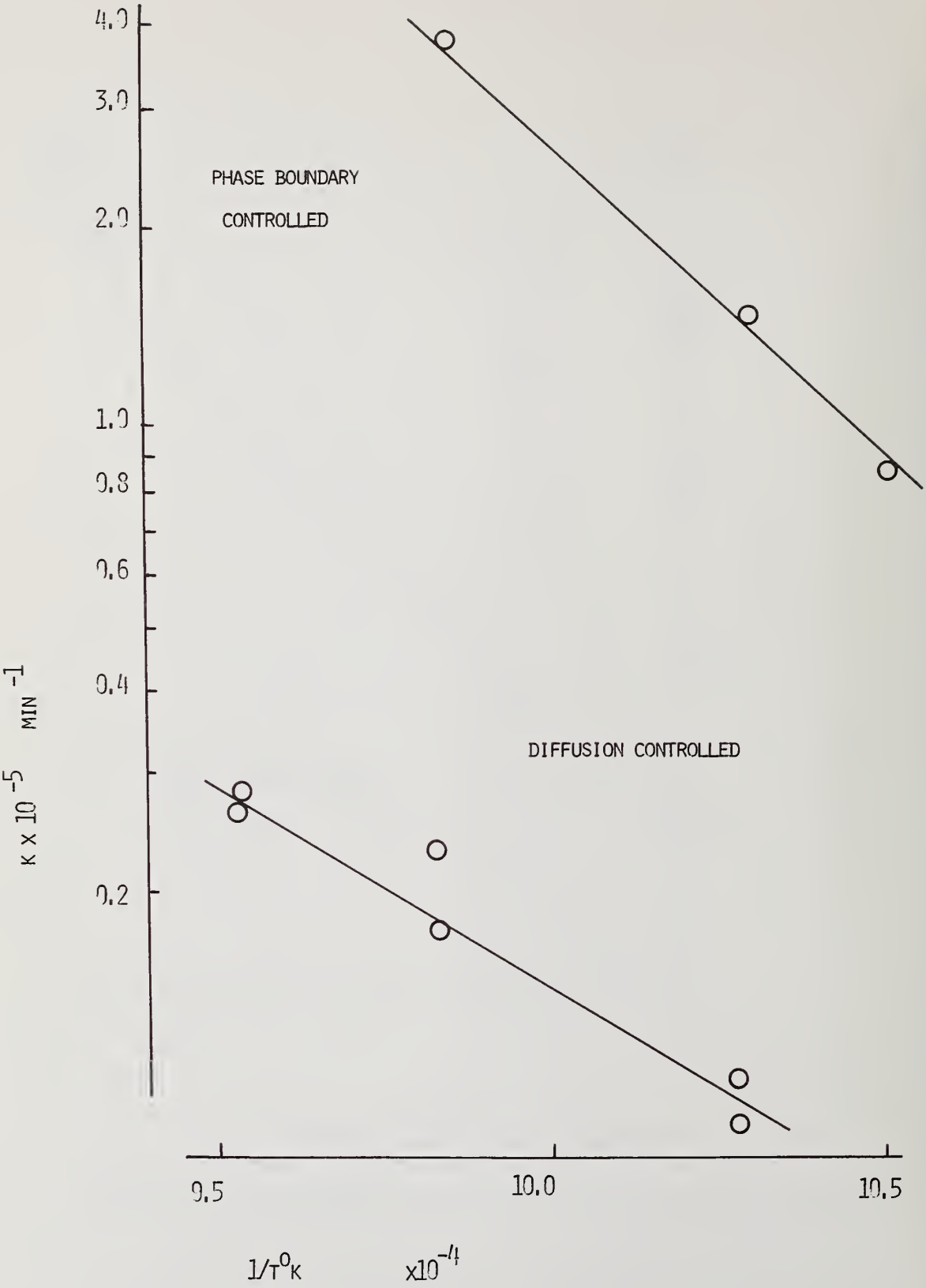

Figure 9. The effect of moisture on the reaction rate constant.

In sintering, both DTA and TMA are useful and vital tools. The principal process bonding ceramics into solid pieces is sintering and this results in shrinkage. Using TMA with either constant rate of heating (CRH) or isothermally, provides a method of analyzing this process. It is in the firing cycle that most ceramic defects occur. This is frequently the result of too rapid heating resulting in stresses. During the early stages of firing, the piece has little or no strength and hence cracks. Using TMA to determine the temperature of rapid sintering allows the firing schedule to be adjusted to extend the period of sintering and thus minimize stresses. Conversely, when no sintering is taking place the temperature increases can be quite rapid. The stress pattern for a square cross-section rod during a shrinkage period is shown in figure 10. This theoretically computed curve by Park [6] indicates the complexity of the task in minimizing firing stresses.

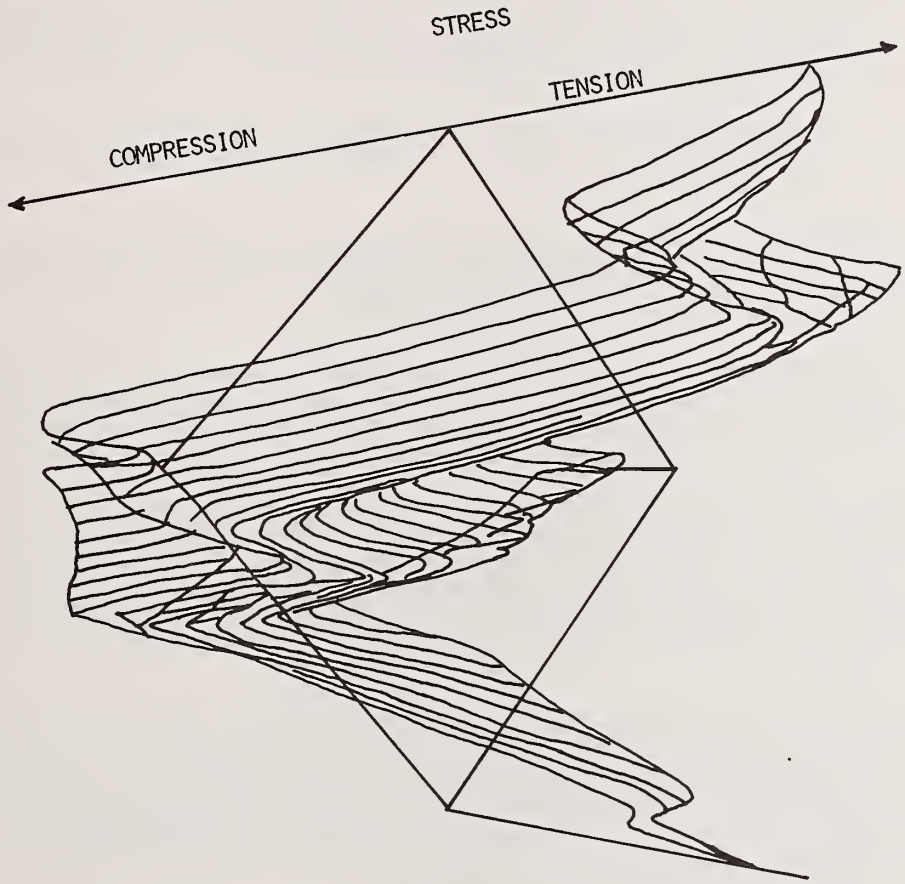

Figure 10. Three dimensional plot for the stress distribution.

It should also be noted that any gaseous phases generated during firing can cause difficulty. Failure to remove water required in processing frequently results in cracks from the expanding steam. Additionally, carbonates, organics, etc. evolved at higher temperatures likewise cause difficulty. TG is the ideal tool to identify these phenomena.

An example of the use of TMA in attacking sintering problems is illustrated by the recent study of Garvey and Ott. During the firing of six-inch diameter manganese-zinc-ferrites, severe cracking was experienced. Ferrites are processed by taking very fine particle size raw materials, blending them, and then calcining the blend to about 1000 °C. The calcine is ball milled in a steel mill with steel mill balls, pressed and fired. A variety of furnace atmospheres are used to control the oxidation state of the ferrite. In this case the material is heated in air to 1300 °C and then cooled in nitrogen.

Figure 11 shows the TMA data for a sample which has been pressed and was ready for firing. Using the combination of TMA and DTA, it was determined that the manganese was changing oxidation state. During the oxidation region oxygen was being taken up, and during the reduction region released. However, the rapid release of oxygen resulted in the body cracking. To confirm this a sample was held at 350 °C after pressing for 24 hours in air. Figure 12 shows the change of slope for oxidation has been eliminated. If the sample is quenched after the 550 °C reduction process, then no further oxidation should occur. Figure 13 shows the quenched sample which expands normally up to the start of sintering at 750 °C. The absence of any oxidation of the sample during testing suggests that oxygen diffusion into the pressed sample is slow and the phenomena may not be easily reversed. Based on these data it was determined to fully reduce the material at the calcine stage. A sample was held 24 hours at 500 °C after calcining and quenched. The sample was then milled and pressed. Figure 14 shows that the destructive oxidation-reduction process again occurs. Either the ferrite picks up oxygen during the milling process or a case and core effect exists and the milling process exposes fresh surface area. The latter seems the most likely possibility. The current solution requires that the material be milled, dried, and then heat treated to 550 °C and quenched. Alternatives are continuing to be investigated.

Once the process problem was overcome, all pieces could be fired more rapidly by using the TMA data to minimize firing stresses. The result was that the firing time was reduced 100 percent.

A similar study on large refractory blocks used for glass tanks has yielded even greater savings. These blocks ranging to six inches in thickness were fired to 1600 °C with a total cycle of over 30 days. Extensive study has cut this to only 11 days and data indicates cycles as short as five days may be possible.

In the area of glass, the use of thermal analysis has been a critical tool in studying glass batch reactions. This data has then been utilized to develop processing alternatives with the potential to save substantial amounts of energy as well as to addressing environmental needs. A specific example can be seen by examining the area of lead glasses.

The choice of raw materials in the commercial glass making process has largely been on the basis of short-run economic considerations. The effect of this has been a variety of production difficulties. These difficulties become acute when a glass batch containing a significant portion of lead oxide is melted and include dusting of raw materials, severe batch segregation, and volatilization from the batch during melting [7]. The result is excess emission of lead oxide in the effluent gasses of the furnace and an increased firing time.

It appears that much of the lead oxide emission is not inherent in the melting of a lead glass, but it the result of either segregation during melting or dusting of fine raw materials. Segregation during melting leaves the lead oxide chemically uncombined or poorly combined and therefore more easily volatilized. This was verified by Lakatos [8], who has shown a significant reduction in the loss of PbO from a red lead glass batch by the use of pelletizing. However, while pelletizing reduces dusting, it does not deal with segregation when commercially sized raw materials are employed.

The development of new batching technology is dependent on a thorough knowledge of the reactions which occur during the melting process. This knowledge is difficult or impossible to obtain by direct experimentation in a glass tank and is most readily obtained using the techniques of thermal analysis. These techniques provide a relatively rapid method of studying the reactions which occur under dynamic heating conditions.

The thermal analysis data indicated that low temperature reactions occurred which created stable lead compounds. These compounds, if generated prior to introduction into the glass tank and below the temperature where lead volatilization is significant, should ease the environmental problems associated with melting lead glass batch by reducing lead emissions. Additional benefits are anticipated from the increased pull rate which results from greater initial homogeneity.

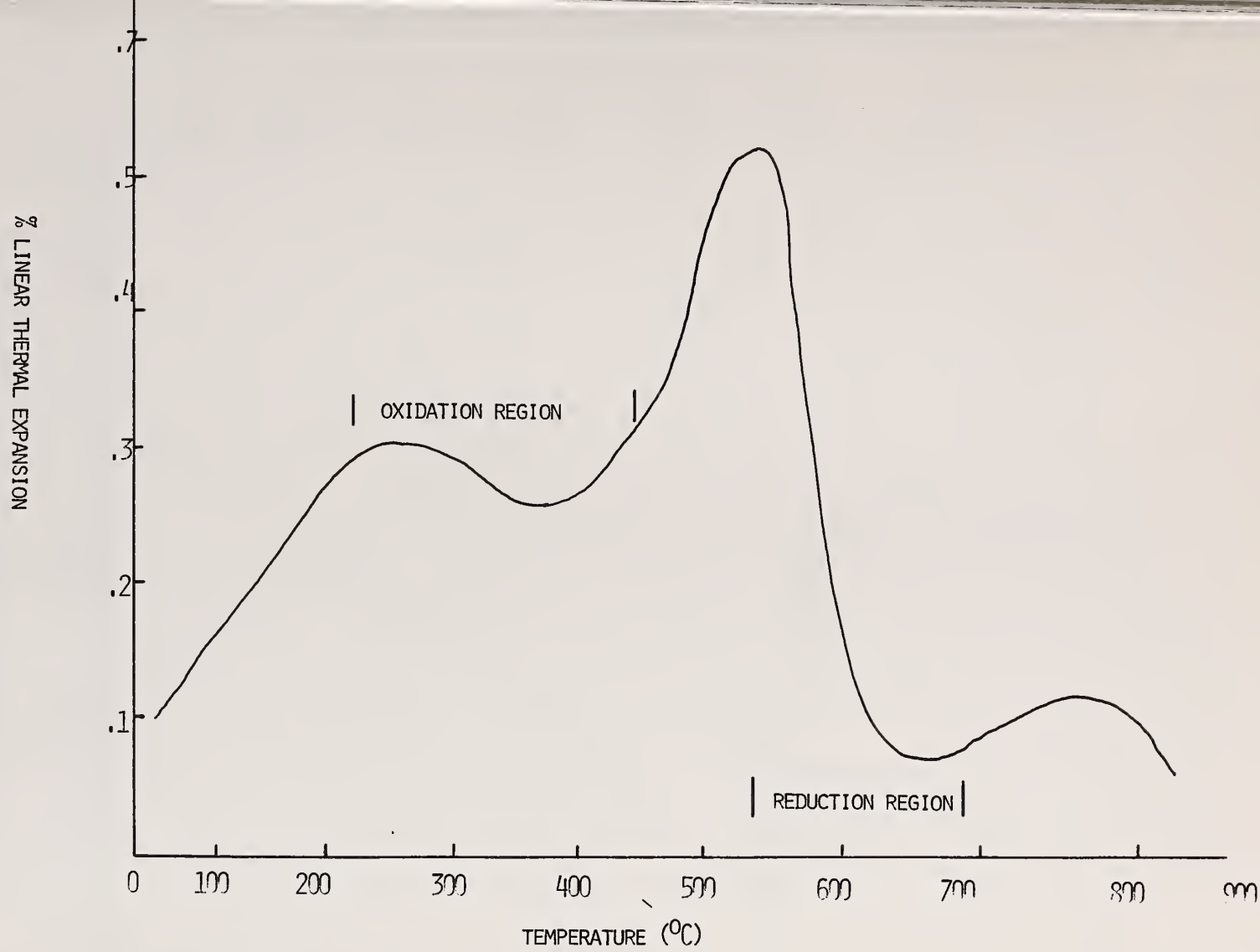

Figure 11. TMA of nickel-zinc-ferrite sample 4 °C/min.

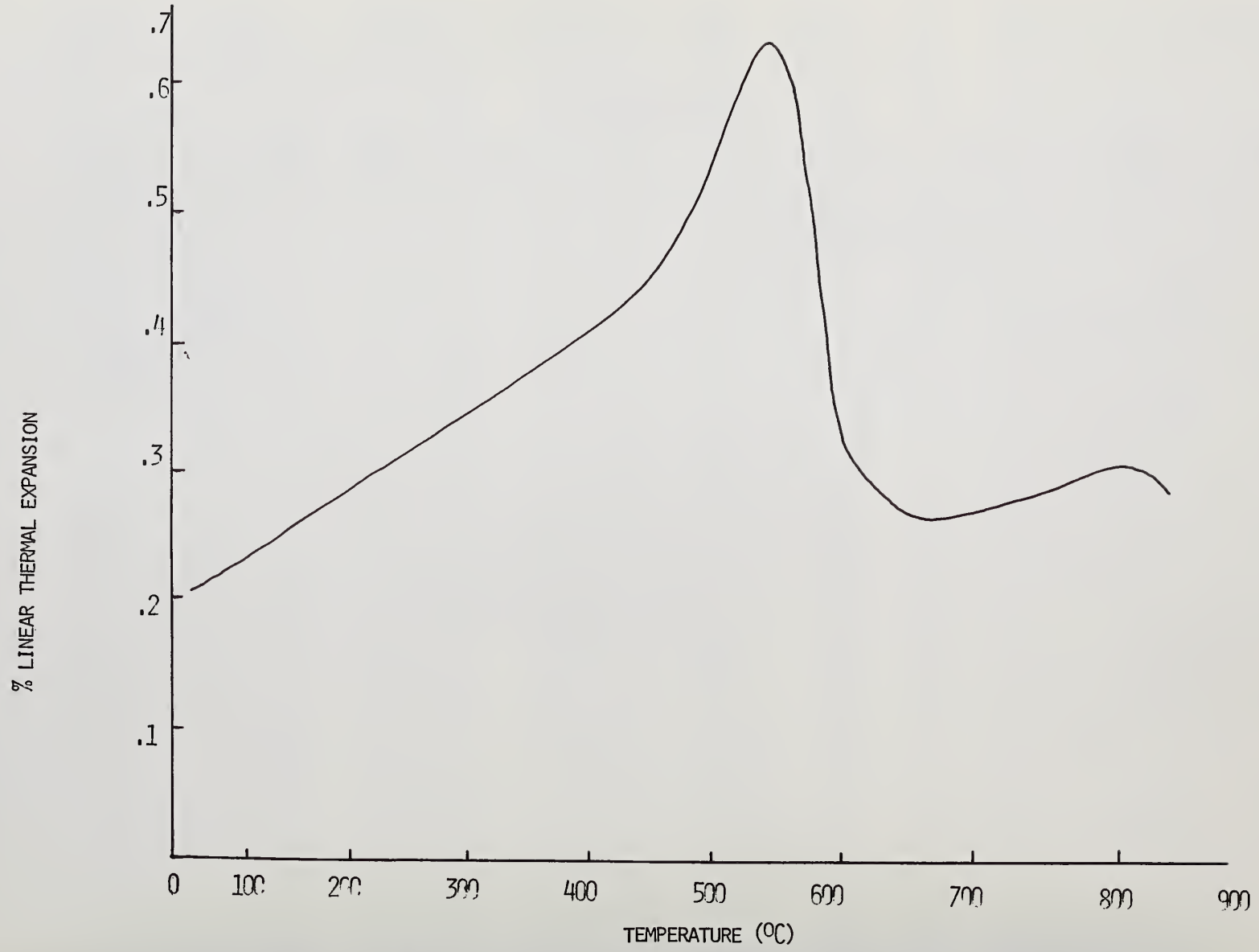

Figure 12. TMA of a nickel-zinc-ferrite held 24 hrs. at 350 °C in air.

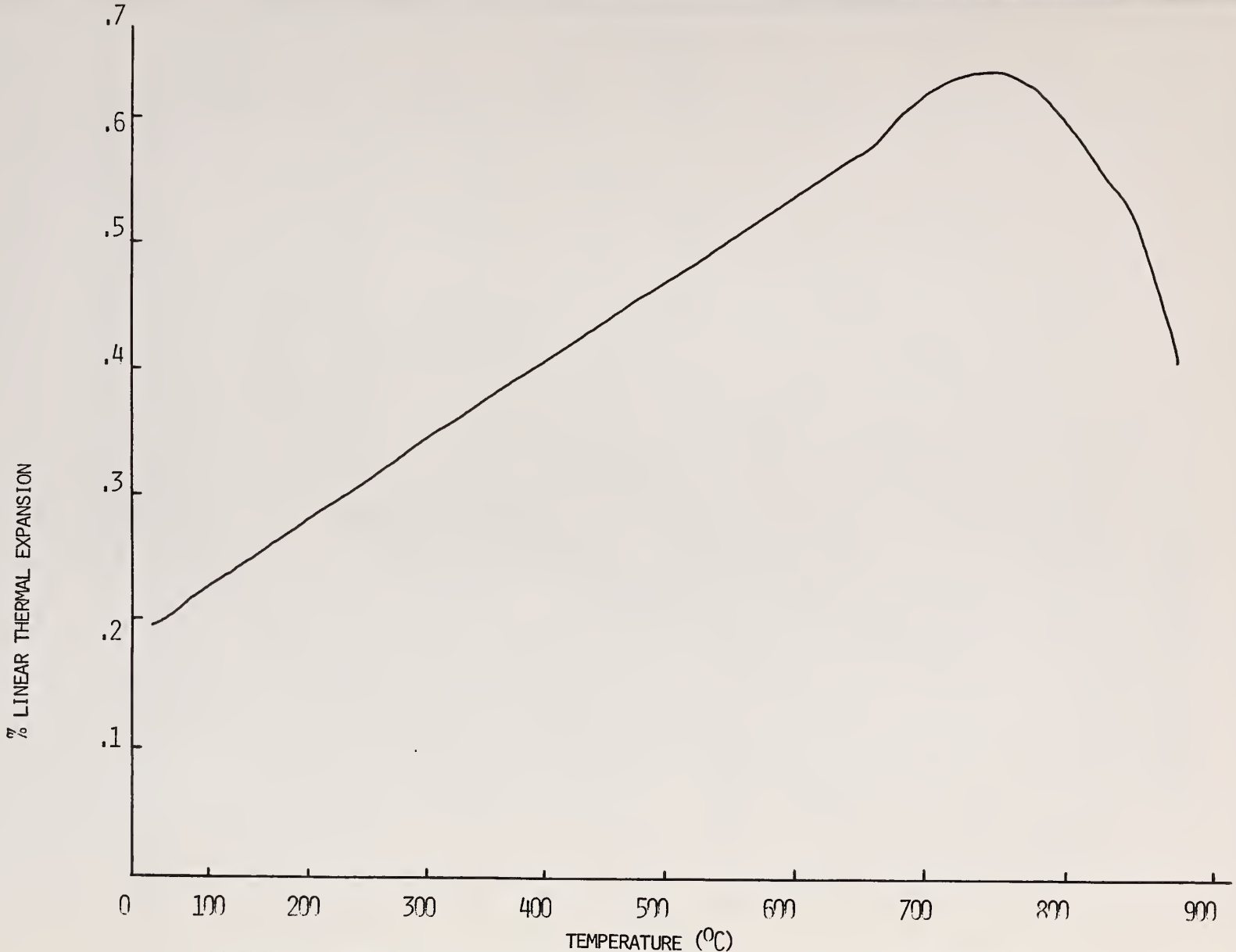

Figure 13. TMA of a nickel-zinc-ferrite held 24 hrs. at 550 °C and quenched.

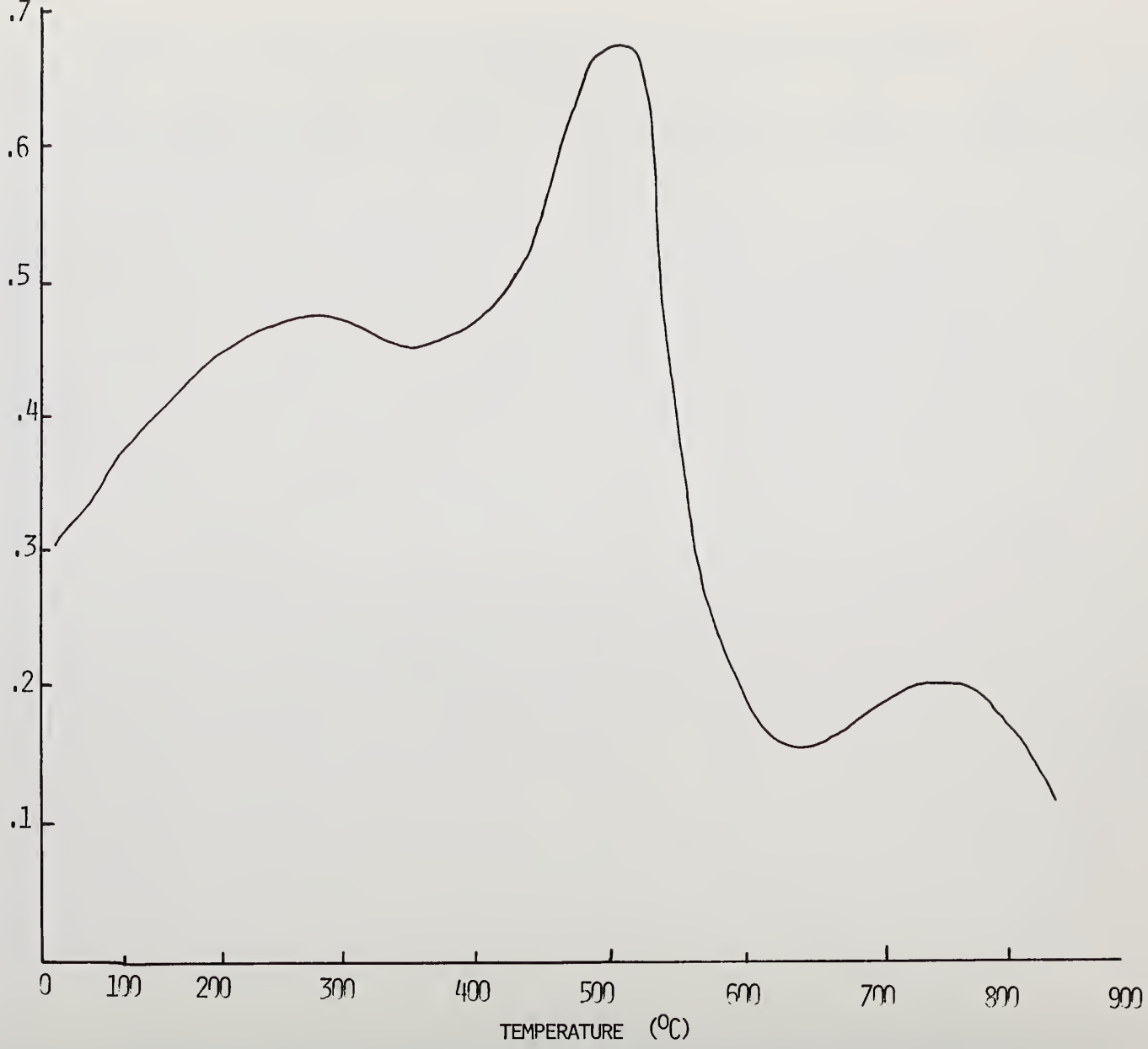

Figure 14. TMA of 550 °C quenched calcine nickel-zinc-ferrite.

A model continuous glass tank (figure 15) was used to examine the thermoanalytical conclusions in a manner compatible with current glass engineering practice. This model tank compared prereacted batch and commercial glass batch.

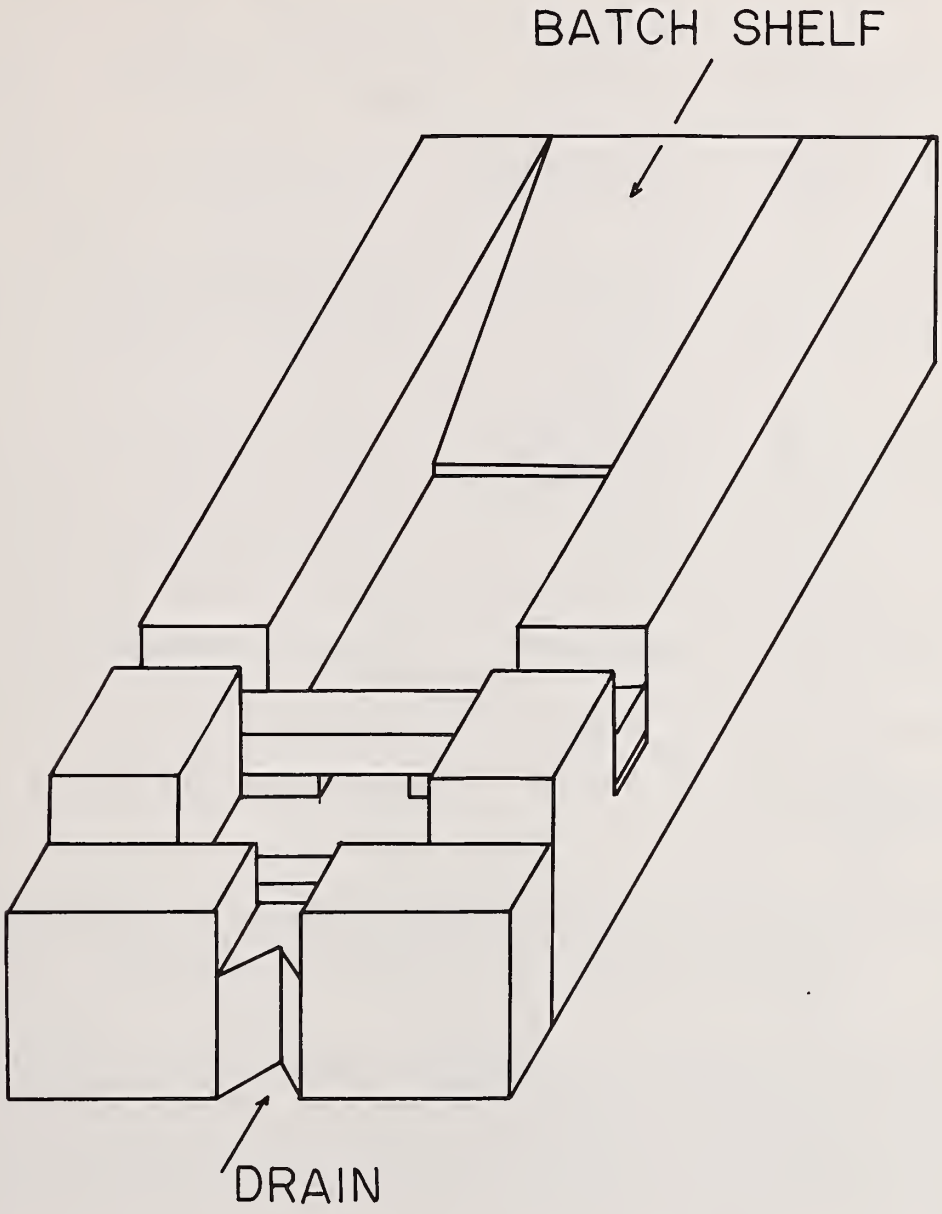

Figure 15. The model continuous glass tank.

The glass batch examined in Table 1 is a commercial tubing glass batch. The raw materials are specified by particle size and manufacturer.

Table 1. Glass Batch Composition and Raw Materials.

Materials	Grade	Supplier	Wt. %
Silica	Newport No. 1 flint glass	Pennsylvania Glass Sand Sand Corp.	49.47
Granular Tribasic	10 mesh	Hammond Lead Products, Inc.	30.99
Calcined potash	Potassium CO_3 calcined 99-100% K_2CO_3	Hooker Chemical Corp.	11.85
Soda ash	AC intermediate soda ash	Industrial Chem. Div. Allied Chemical Corp.	5.56
Calcined alumina	Calcined Al_2O_3 A-2 grade	Aluminum Co. of America	1.20
Sodium nitrate	Champion Brand nitrate of soda	Chilean Nitrate Sales Corp.	0.47
Antimony oxide	Antimony oxide KR grade	Harshaw Chemical Co., Div. of Kewanee Oil Co.	0.47
Powdered flint	No. 290 Sil-Co-Sil	Ottawa Silica Co.	
Ground Tribasic lead silicate	99%-325 mesh	Hammond Lead Products, Inc.	
Ground Silica	F-140 grade	Ottawa Silica Co.	
Intermediate size tribasic lead silicate	-60 +140 mesh	Hammond Lead Products, Inc.	

Note: The first seven materials listed are those used in the commercial glass batch. As explained in this study, the last materials were substituted for their respective commercial counterparts.

Phase transitions and chemical reactions give characteristic DTA and DTG peaks. By studying the one, two, three, and four component systems, the reactions and transitions which occur in the complete glass batch can be identified. The study used this procedure to examine the raw materials, combinations of two and three raw materials and the four component glass batch (silica, tribasic lead silicate, sodium carbonate, and potassium carbonate). The raw materials of the two and three component systems were mixed in the same ratio as used in the final glass batch.

The reactions typical of the individual, two component, and three component systems have been previously reviewed [9,10]. The three component systems with the alkali carbonates isolated in a continuous matrix of silica and tribasic lead silicate resulting from coarse carbonates in the fine silica and tribasic lead silicate are of most interest. Examination of the geometry of the system has shown that only these systems contribute effectively to the final reactions. The data for these batch reactions are shown below.

A. Sodium Carbonate-Silica-Ground Tribasic Lead Silicate

The DTA/DTG traces for this mixture are shown in figure 16. The DTA peak at 573 °C was due to the quartz inversion. There was a large weight loss with a DTG peak at 600 °C and a corresponding small DTA peak. This has previously been identified [9] as the result of the

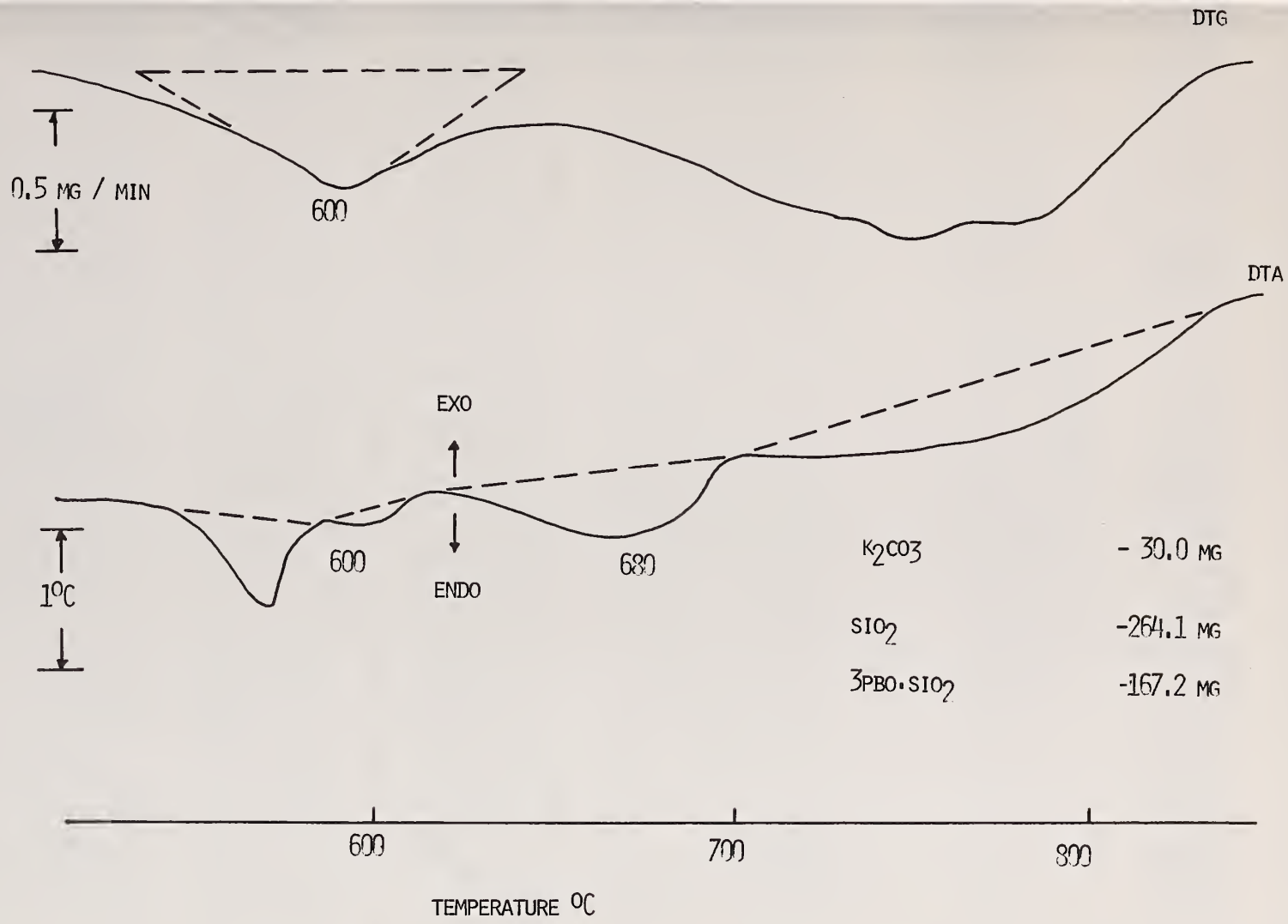

Figure 16. DTA and DTG data for the reaction between sodium carbonate, silica and ground tribasic lead silicate.

formation of a sodium-lead-silicate compound. The broad endothermic peak at 680 °C, over the range 650-715 °C, was the result of the reaction between tribasic lead silicate and silica [10].

As the temperature increased, eutectic melting occurred and the quantity of liquid phase increased until the reaction was completed by 840 °C. X-ray diffraction analysis of a sample quenched immediately following the completion of the reaction showed that the only crystalline phase present was silica. The remaining silica dissolved as the temperature increased.

B. Potassium Carbonate-Silica-Ground Tribasic Lead Silicate

Figure 17 shows the DTA and DTG traces for this mixture of raw materials. The DTA curve to 600 °C shows only the peaks characteristic of the raw materials. The broad DTA endotherm over the range 650-720 °C was the result of a reaction between silica and ground tribasic lead silicate. This reaction precluded the reaction between potassium carbonate and ground tribasic lead silicate. The main portion of the decomposition reaction was at 855 °C.

C. Sodium Carbonate-Potassium Carbonate-Silica-Ground Tribasic Lead Silicate

The DTA/DTG traces for the major components of the glass batch are shown in figure 18. The peak at 573 °C was due to the low-to-high quartz inversion. At 600 °C there was a DTG peak accompanied by a small endothermic effect. This was shown, in figure 16, to be due to the formation of a sodium-lead-silicate compound. The DTA endotherm over the range of 650-715 °C was produced by the reaction between ground tribasic lead silicate and silica. Up to this point the reactions occurred as expected from geometric considerations. The alkali carbonates each reacted independently in the silica-tribasic lead silicate matrix. Figure 19 shows the composite TG curve compared with that for the four component system. Up to 740 °C the two systems acted independently to give similar TG curves. Above this temperature the entire glass batch reaction proceeded more rapidly, most likely accelerated by the greater quantity of liquid phase present.

The major decomposition reaction occurred at 770 °C (DTA and DTG peaks) and was completed by 831 °C. The DTA trace continued to rise from 831 to 920 °C as a result of improved thermal contact of the sample with the crucible as the bubbles were eliminated from the melt. X-ray diffraction analysis of the sample quenched from 840 °C showed that the only crystalline phase present was silica. The remainder of the batch was a liquid phase containing all Na_2O, K_2O, PbO, and some SiO_2. This reactive liquid phase then dissolved the remaining silica as the temperature increased. By 1450 °C all the silica was dissolved.

D. Sodium Carbonate-Potassium Carbonate-Silica-Granular Tribasic Lead Silicate

The DTA/DTG curves for the major components of the glass batch using granular tribasic lead silicate are shown in figure 20. The alkali carbonate and the tribasic lead silicate particles were essentially isolated by a continuous matrix of silica. The first major DTA peak was produced by the melting of the tribasic lead silicate at 727 °C. The DTG peak at 735 °C resulted from the reaction of the liquid lead silicate with alkali carbonate particles. A second DTA peak associated with a DTG peak was observed at 820 °C. This peak was due to a reaction between the alkali carbonates and silica.

The use of granular tribasic lead silicate resulted in the formation of two different reactive liquid phases. One phase was an alkali lead silicate glass and the second was a lower density alkali silicate melt. The heat treatment of 8 °C/min was not adequate to produce a homogeneous melt, and it appeared that the lighter alkali silicate melt remained on top of the denser alkali lead silicate liquid. This was caused by the surface diffusion of the sodium component through the continuous matrix of silica allowing interaction with the potassium metasilicate reaction product. This conclusion is confirmed using the TG curves from 1000 to 1450 °C (figure 21) of the two glass batches made with ground and granular tribasic lead silicate. The volatilization loss from the batch using ground tribasic lead silicate was about twice that of the batch using granular tribasic lead silicate. The difference resulted from the lighter alkali silicate composition floating

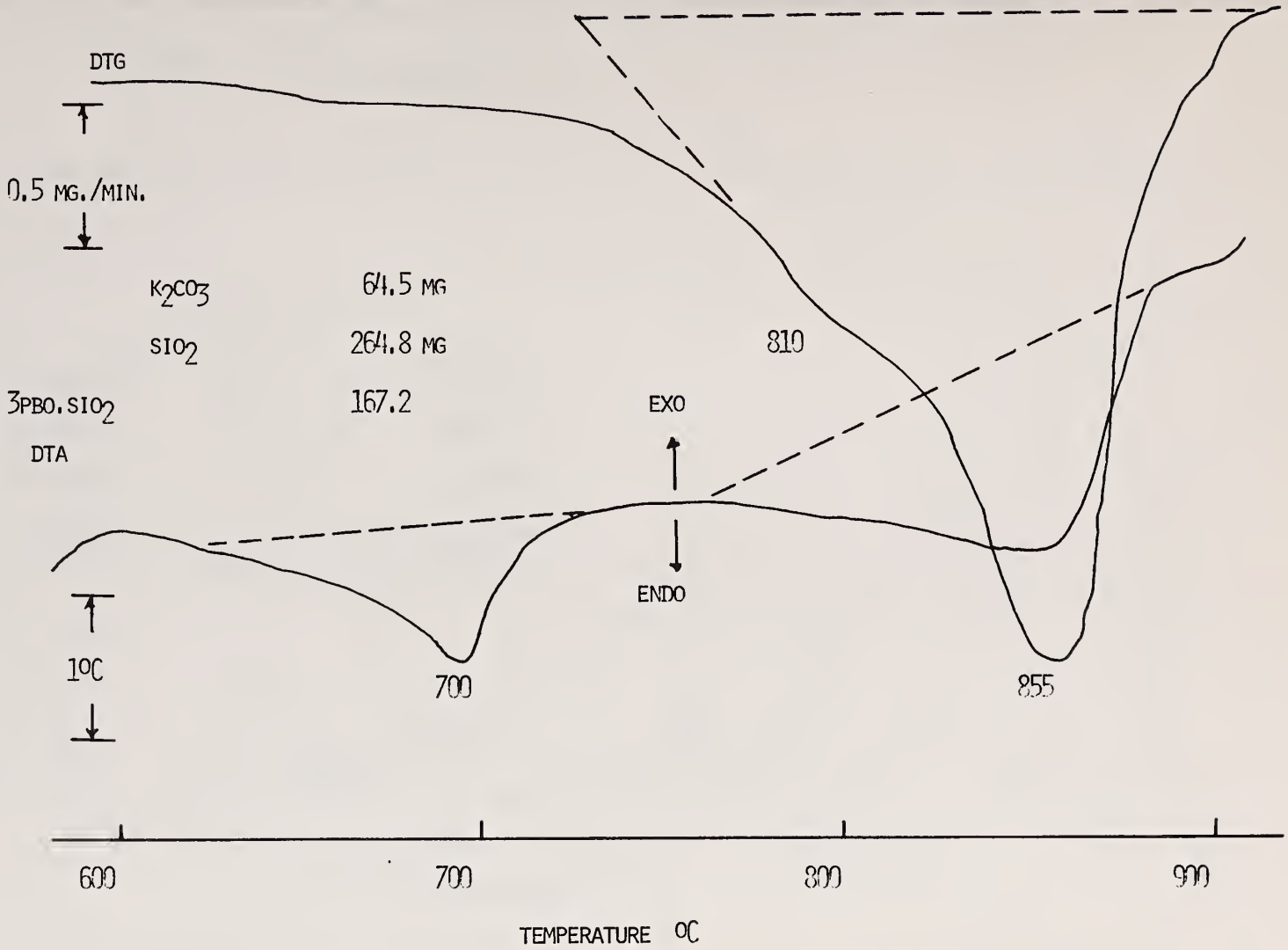

Figure 17. DTA and DTG data for the reaction between potassium carbonate, silica and ground tribasic lead silicate.

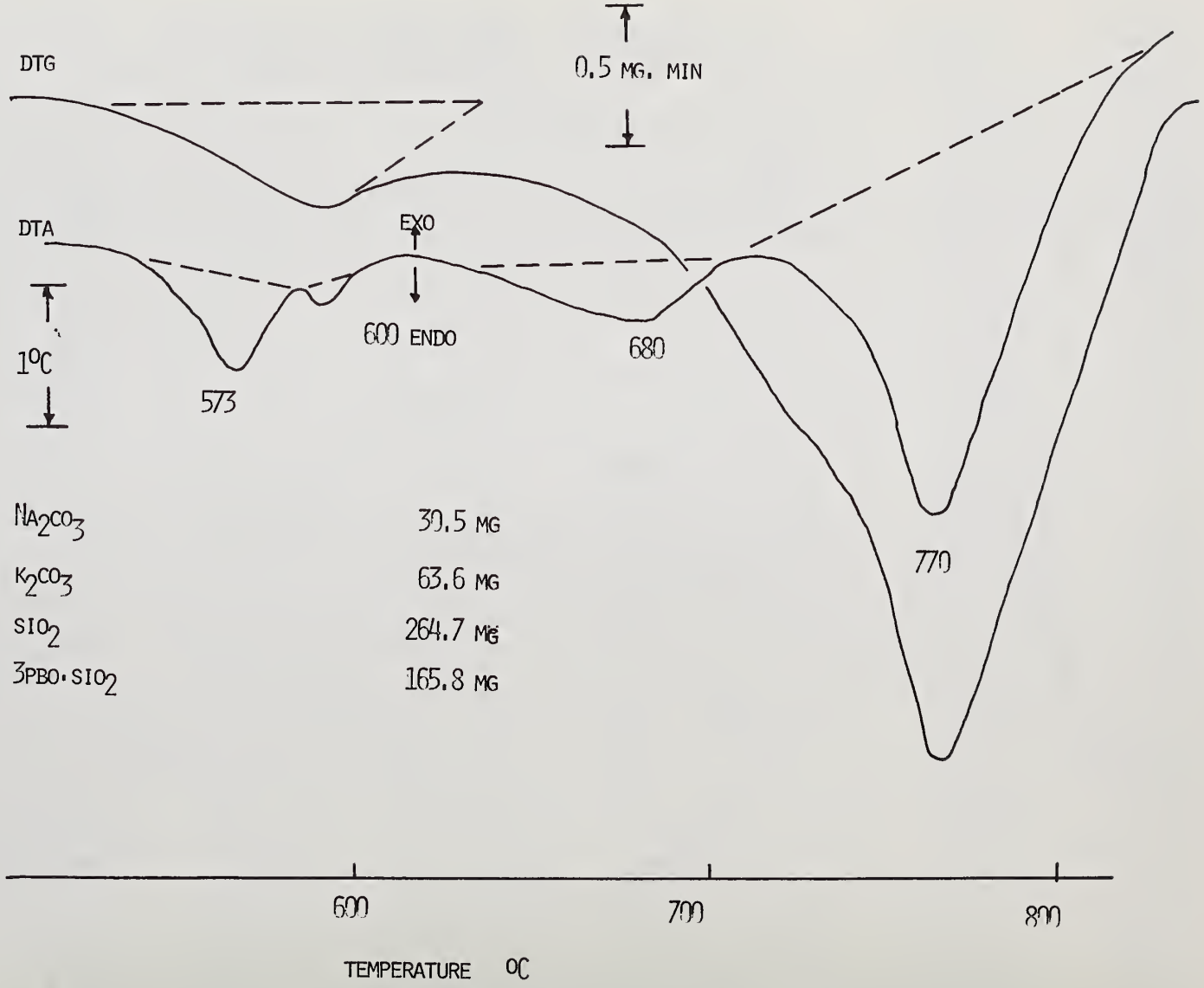

Figure 18. DTA and DTG data for the reaction between sodium carbonate, potassium carbonate, silica and ground tribasic lead silicate.

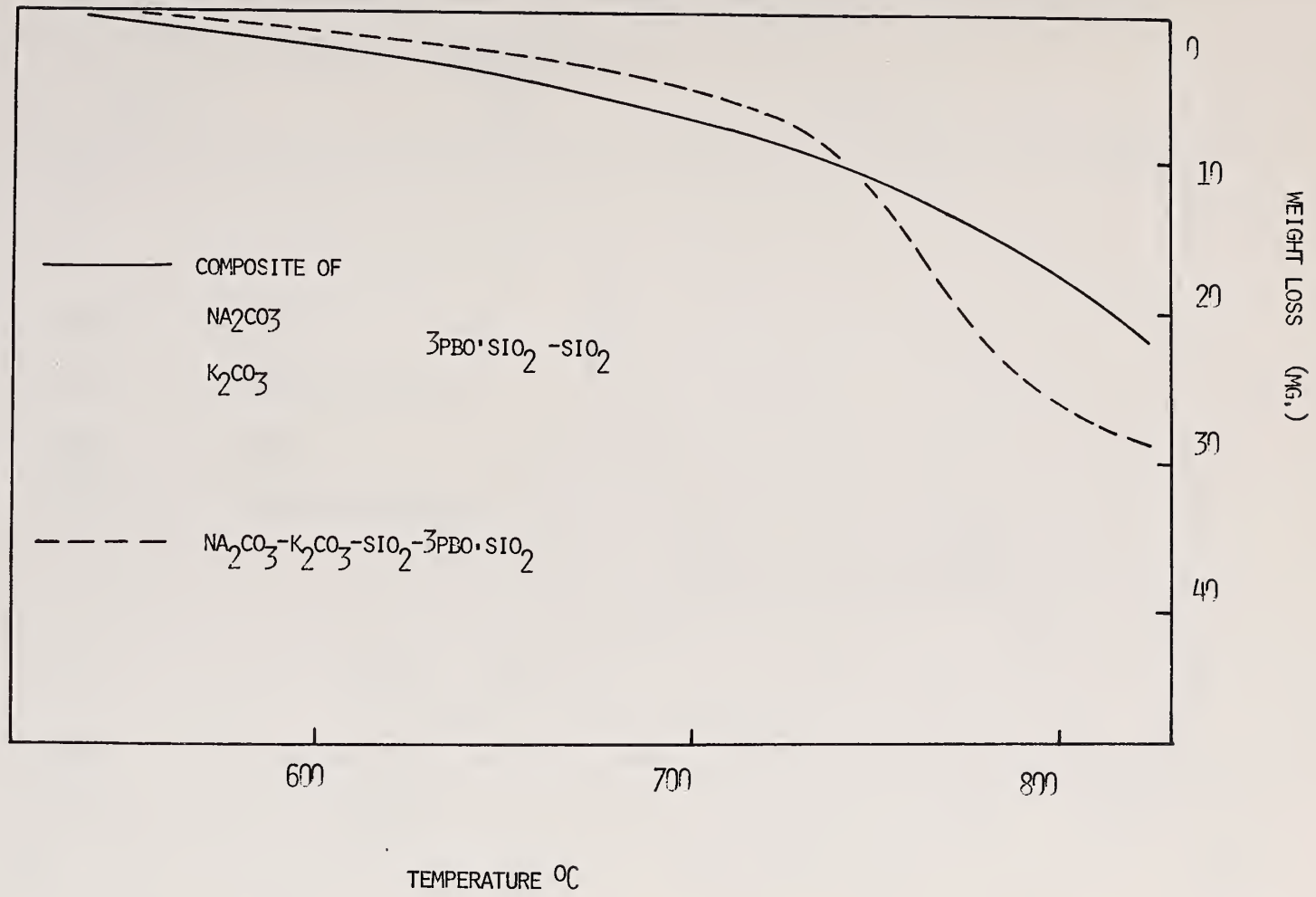

Figure 19. Composite of the TG data for the reaction between the alkali carbonates, silica and ground tribasic lead silicate compared with those of the reactions within the equivalent four-component mixture.

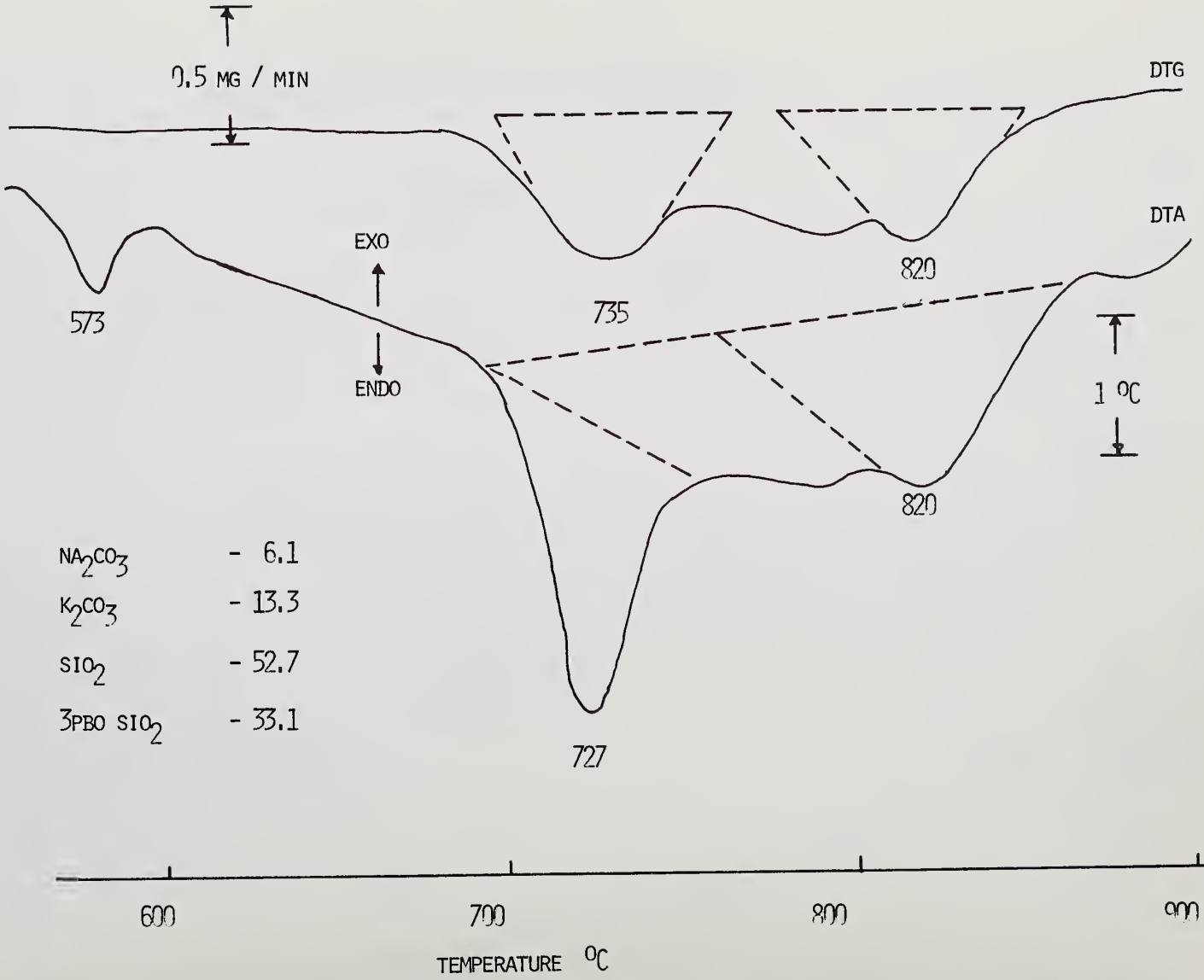

Figure 20. DTA and DTG data for the reaction between sodium carbonate, potassium carbonate, silica and granular tribasic lead silicate.

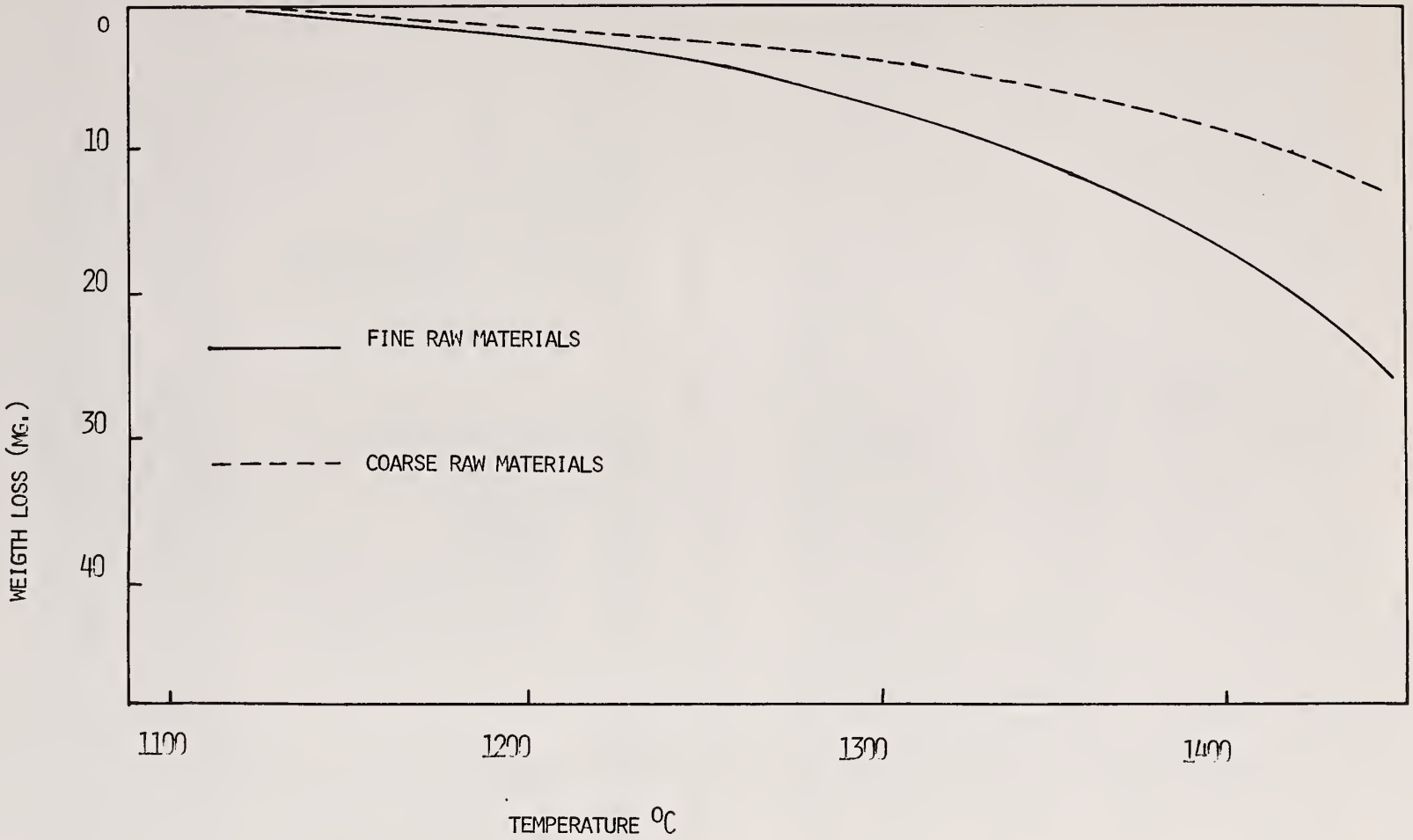

Figure 21. Volatilization from glass batch using ground (lower curve) and granular (upper curve) tribasic lead silicate.

on the denser alkali lead silicate melt forming a barrier through which the volatile materials first had to diffuse before escaping to the furnace atmosphere.

E. Role of Minor Batch Composition

The role of the minor batch components (Al_2O_3, Sh_2O_3, $NaNO_3$) is shown in figure 22, which depicts the TG curves of the glass batch with the four basic components compared with the TG data for the batch with alumina added (i.e., five components). The data are the same within the limits of the experiment and the alumina does not appear to substantially affect the sequence of reactions, although, of course, it plays an important role later in the process. The addition of the two dining agents (Sb_2O_3, $NaNO_3$) does produce a definite effect, causing the reactions to proceed more rapidly as defined by the TG data. This is consistent with the findings of Thomasson and Wilburn [11] in their study of the sodium carbonate-silica reactions. The basic sequence of reactions observed in unaltered.

From these data it appears that prereacted batch can be prepared at relatively low temperatures and will reduce both folatility and segregation.

This conclusion was verified with experimental work which would examine lead volatility in a manner comparable to current commercial practice. This was accomplished using a model continuous glass tank [12].

To determine the effect of using optimized batch on tank performance, three batches were melted: (1) prereacted batch, (2) the raw commercial batch, and (3) the optimized batch. These experiments were conducted under identical conditions using the model continuous glass tank. The temperature of the glass surface at the bridgewall, remained constant at 1315 °C. These batches were of identical composition, although the particle size and thermal history were varied (Table 2). Samples were collected from the tank twice each day, and the true density and seed count of each sample measured.

Table 2. Three Batches Melted in the Model Continuous Glass Tank.

Commercial Batch	Prereacted to 750 °C	Optimized Prereacted Batch Prereacted to 750 °C
$3PbO \cdot SiO_2$ (Granular)	$3PbO \cdot SiO_2$ (Ground)	$3PbO \cdot SiO_2$ (-60 +140 mesh)
SiO_2 (Sand)	SiO_2 (Powdered)	SiO_2 (-100 mesh)
K_2CO_3	K_2CO_3	K_2CO_3
Na_2CO_3	Na_2CO_3	Na_2CO_3
Al_2O_3	Al_2O_3	Al_2O_3
$NaNO_3$	$NaNO_3$	$NaNO_3$
Sb_2O_3	Sb_2O_3	Sb_2O_3

The true density, which allows calculation of the level of lead volatility occurring during the melting process, was measured according to ASTM C-329-56, with the higher true density indicating the lower level of lead volatility. Steel counts were used to compare the quality of the glass which was produced by each batch.

The first batch which was melted continuously in the model tank (the prereacted batch) was composed primarily of finely divided components. The feed rate was adjusted to 32 grams per hour in order to produce a good quality glass. The average lead loss for this batch was nine percent.

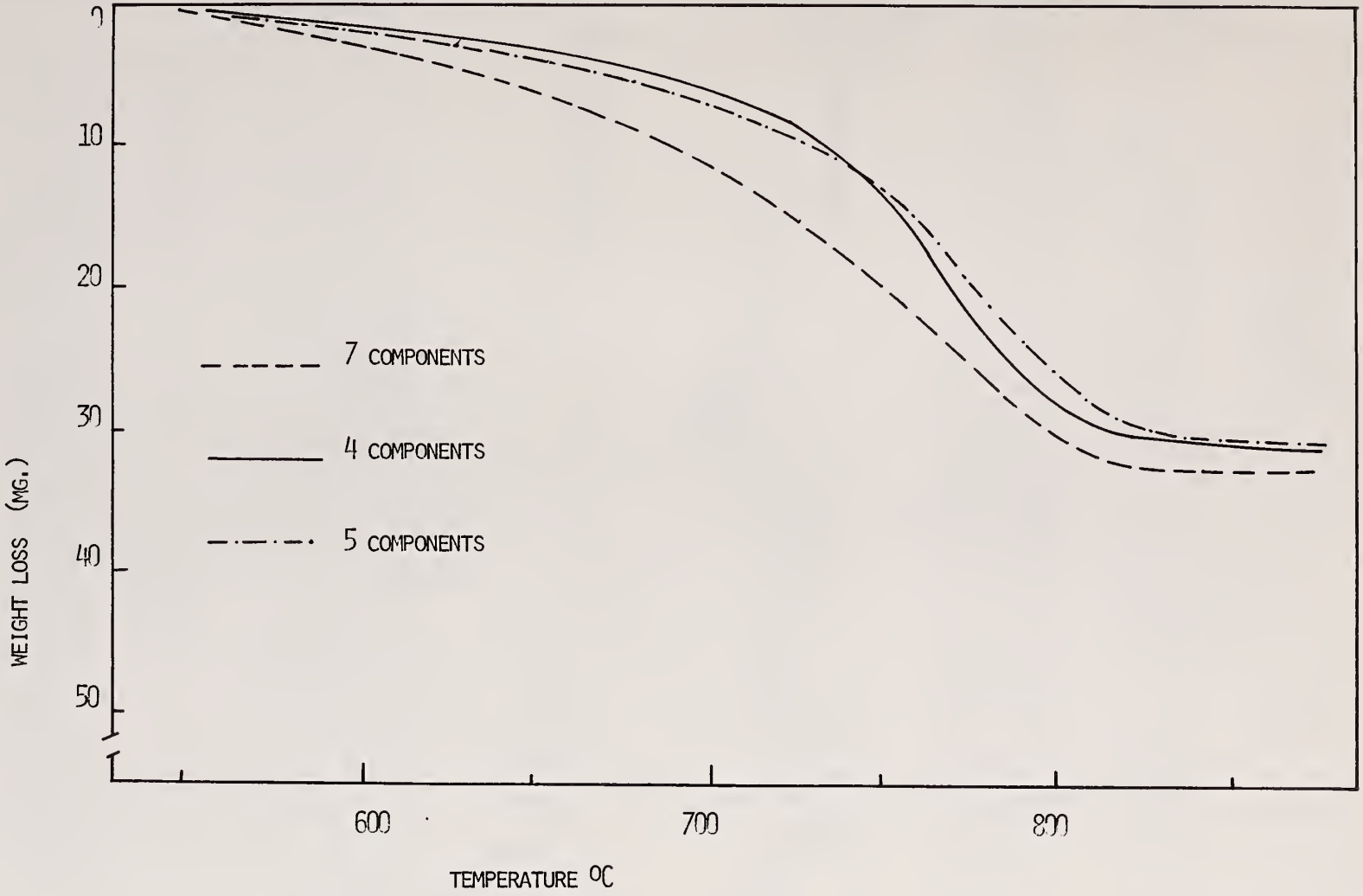

Figure 22. The effect of alumina and fining agents on the rate of reaction.

Under identical melting conditions, a raw commercial batch composed of commonly used raw materials was melted continuously in the model tank at the same rate of 32 grams per hour. The glass quality as determined by seed count was poor, and the lead loss was calculated to be 15 percent. The feed rate was reduced to 24 grams per hour in order to produce glass of equal quality to that produced by the original prereacted batch. The lead loss for the commercial batch melted at this slower rate was 16 percent.

The third batch to be melted continuously under these conditions was an optimized batch which was developed. The feed rate was adjusted to 34 grams per hour, and the glass produced was of equal quality to that produced by the prereacted batch at a lower feed rate. The lead loss for the optimized batch was 6 percent, a figure that represents a significant decrease in lead loss for the optimized glass batch.

In review, the lead loss from a medium lead content glass batch was reduced from 16 percent for a raw commercial batch and 9 percent for a finely divided prereacted batch, to 6 percent for a prereacted batch of optimum particle size. The true density of each batch, which is inversely related to the level of lead volatility, is shown in figure 23. The batch of optimum particle size could be melted 42 percent faster than the raw commercial batch, still maintaining the same good quality (figures 23, 24).

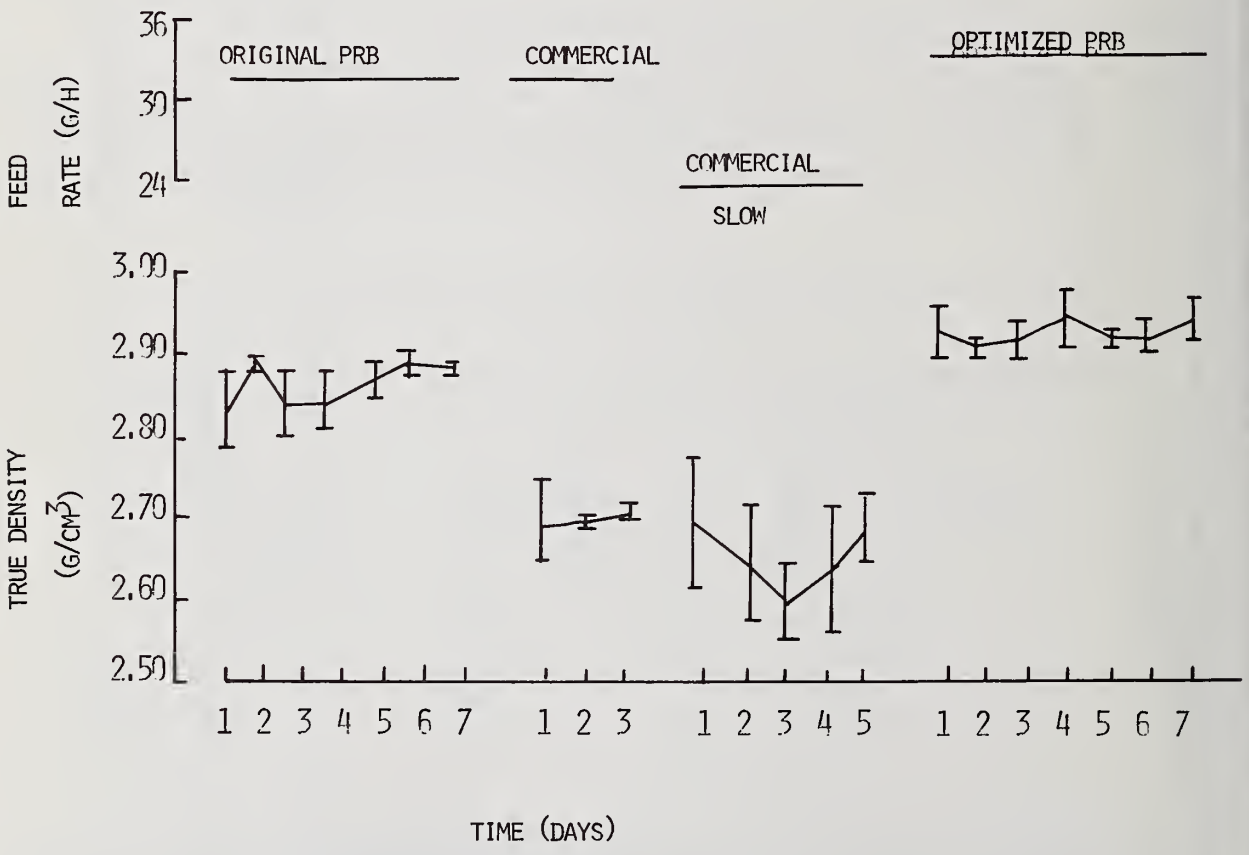

Figure 23. True density data with 95 percent least significant intervals for batch means.

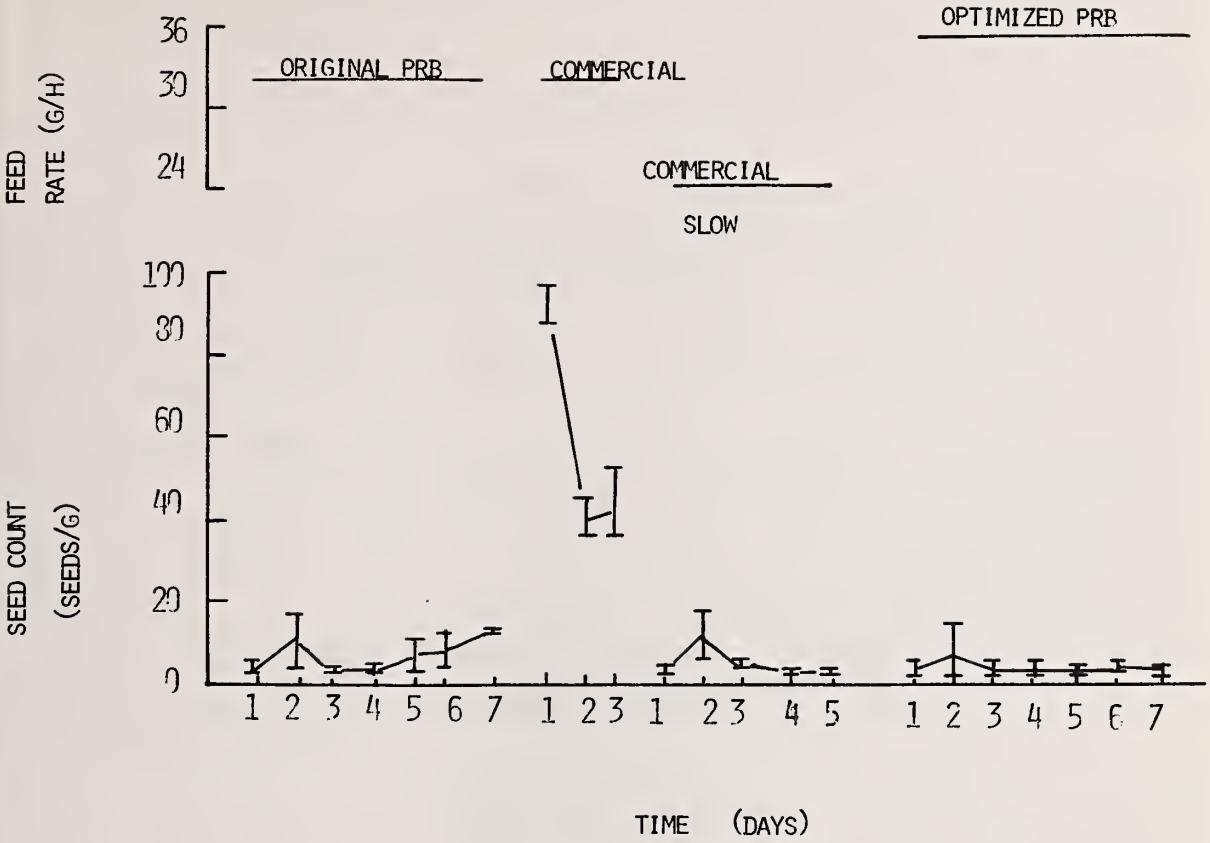

Figure 24. Percent PbO loss data with 95 percent least significant intervals for batch means.

Summary

Thermal analysis is a valuable tool in the study of ceramic processes. The high temperature processing inherent in the production of ceramics can be duplicated using thermoanalytical techniques. The resulting knowledge has and can lead to substantial improvements in energy efficiency. Several case histories of problems in polycrystalline ceramics and glass have been included which demonstrate ways in which this can be done.

References

[1] Makhijani, A. B. and Lichtenberg, A. J., Energy and Well-Being, Environment 14, (5), 10-18 (June 1972).

[2] Hara, A. and Migake, M., Formation of Process of (Tungsten-Titanium) Carbide Powder, Panseeker Pulvermetall. 18, 2 (1970).

[3] Lake, J. and Ott, W. R., Maximization of Tungsten Crystallites from Directly Reduced Ammonium Paratungstate, accepted for publication in Thermochimica Acta.

[4] Ott, W. R., Kinetics and Mechanism of the Reaction Between Sodium Carbonate and Silica, accepted for publication in Ceramurgia International.

[5] Koenig, C. J. and Green, R. L., Water Vapor in High Temperature Ceramic Processes, Bulletin 202, Ohio State University Experiment Station (1968).

[6] Park, C. I., Stress Distribution in Zircon and Chrome Oxide Bodies During Firing, PhD Thesis, Rutgers University, New Brunswick.

[7] Tooley, F. V., Handbook of Glass Manufacturers I, p. 63, Ogden Publishing Company, New York, (1960).

[8] Lakatos, T., Glastek, Tidskr, 25 (4), 83 (1970).

[9] Ott, W. R. and McLaren, M. G., Thermal Analysis, Schwenker, R. F. S., and Garn, P. D. G. (eds.), 2, 1329-1345, Academic Press, New York, (1969).

[10] Ott, W. R., McLaren, M. G., and Harsell, W. B., Glass Tech. 13 (6) 154-160 (1972).

[11] Thomasson, C. V. and Wilburn, F. W., Physic. Chem. Glasses 1, (2), 52 (1960).

[12] Ganzala, G. W. and Ott, W. R., Bulletin of the American Ceramic Society 6, 9-17 (1974).

CERAMIC PROCESSING AND ENERGY CONSERVATION

RAPPORTEUR'S COMMENTS BY

Paul D. Garn
The University of Akron
Department of Chemistry
Akron, Ohio 44325

Ceramic processing requires both time and temperature; within some limits they are reciprocal, a higher processing temperature enabling completion in a lesser time. The greater rate of energy supply needed to maintain the higher temperature may compensate for the shorter time but great economies are not available. Other approaches are needed.

Another prima facie method for conserving energy is by increasing reactivity by diminution of particle size. Here, too, the energy saved may be totally consumed by the preliminary grinding. Less-thorough chemical preparation, i.e., the use of less-pure reactants, may lead to saving of costs in that part of the processing, but if the reject rate is increased, the savings may disappear. Processing of a reject consumes as much energy as processing a usable item.

The problem of conservation of energy by one of our major energy consumers, the glass/ ceramic industry, is clearly very complex. The obvious engineering parameters appear not to offer major savings. One important avenue remains -- careful examination of the chemical process itself. Many of the extant glass/ ceramic processes were developed quite empirically at a time when energy was plentiful, when time and material costs were the most important considerations.

Ott speaks to the energy conservation problem in his description of experiments using a continuous reactor for glass forming. Thermal analysis was used to establish effective conditions for each reaction. The materials fed into the reactor yielded higher quality glass more rapidly than did the current processes. Costing-out on >100 tons/day will ascertain the potential saving of energy.

In response to queries, Ott pointed out to J. Jordan that the ammonium paratungstate was an intermediate in making the tungsten trioxide or tungstic acid so that the costs of the further steps are saved -- although partly offset by the cost of shipping ammonia and water with the tungsten oxide.

Whether the reactivity of the commercial WO_3 was substantially less than that of freshly-decomposed APT (P. D. Garn) was not known. The excess weight could be eliminated if there was no change in the APT reactivity.

Concerning the stability of finely-divided tungsten carbidi (O. Menis), Ott responded that it was cobalt bonded -- a liquid phase bonding process. To Menis's further inquiry about the sintering processes in these materials, Ott pointed out that the driving force is the surface energy -- the particles tend to diminish the total surface area by forming necks at point contacts, movement of material is by diffusion which may be along the surface or along grain boundaries. Diffusion may be facilitated by impurities, especially if they lead to liquid formation. Sintering can also be hastened by hot pressing, which increases the initial contact area.

D. Dollimore commented that another important parameter in sintering was the atmosphere over the material. In particular, water vapor enhances the sintering in almost all cases. He then raised the question of the method of heating, specifically a gas flame directed over the surface of the glass as compared to electric heating. There are various atmospheres above the surface, and the presence of either reducing and oxidizing atmospheres may have an effect on the process. Ott explained that the glass furnace was heated by a gas flame across the batch of materials as the batch was being loaded. This heating can be supplemented by electric heat. As the material enters, it experiences a very high temperature (1600 °C). The porous material forms liquid phases on the outside; carbon dioxide is being generated so that the reactions are almost certainly occurring under a high partial pressure of CO_2; and if a lead glass is being made there is reduction -- lead metal is found in the bottom of the tank.

National Bureau of Standards Special Publication 580. Proceedings of the Workshop on the State-of-the-Art of Thermal Analysis held at NBS, Gaithersburg, MD, May 21-22, 1979. (Issued May 1980)

CURRENT CONTRIBUTIONS OF THERMAL ANALYSIS TO THE STUDY OF TECHNOLOGICAL ADSORBENTS

J. Rouquerol

Centre de Thermodynamique et de Microcalorimétrie du C. N. R. S.
26 rue du 141ème R.I.A.
Marseille 13003, France

Abstract

The adsorbents considered here are mainly those used in gas adsorption (either physical or chemical) and in heterogeneous catalysis. A number of specific features of this class of material and the corresponding problems raised in thermal analysis are examined (problems of atmosphere control, temperature and pressure gradients, spurting out under vacuum, sampling, re-adsorption from air, high sensitivity for the detection of desorption).

The use of thermal analysis is considered throughout the life of an adsorbent:

a) Production of porous adsorbents by thermolysis and achieving of a reproducible standard state of the surface.

b) Characterization of the adsorption properties (through a study of gas adsorption, gas desorption, and gas exchange).

c) Thermal destruction of adsorbents (sintering and also destructive characterization).

Among the thermal analysis techniques examined here are TG, DTA, DTG, EGD, EGA, and also Temperature Programmed Desorption and Controlled Decomposition Rate Thermal Analysis (including Quasi-Isothermal Thermogravimetry).

Introduction

We may say that, from the famous paper of Le Châtelier entitled "Action of Heat on Clays" and published in 1887 [1][1], up to now, the various methods of thermal analysis were continuously applied to the study of "technological adsorbents." By this term we mainly understand solids with a high specific surface area (ranging between 10 and 1000 m^2g^{-1}), which may be either porous solids ("mesoporous" for 2 <d <30 nm and "micropouous" for d <2 nm, following IUPAC recommendations [2]) or finely divided powders. It happens indeed that all the "life" of an adsorbent may be followed by thermal analysis: its thermal activation (i.e., development and/or outgassing of the available surface); its use as an adsorbent (provided the adsorption takes place from the gas phase – if it is from the liquid phase, thermal analysis is of minor help); and finally its "destruction" (which means mainly the loss of its surface area, i.e., its sintering). These three steps (which are schematically represented in figure 1) will be followed in the foregoing presentation.

[1]Figures in brackets represent the literature references at the end of this paper.

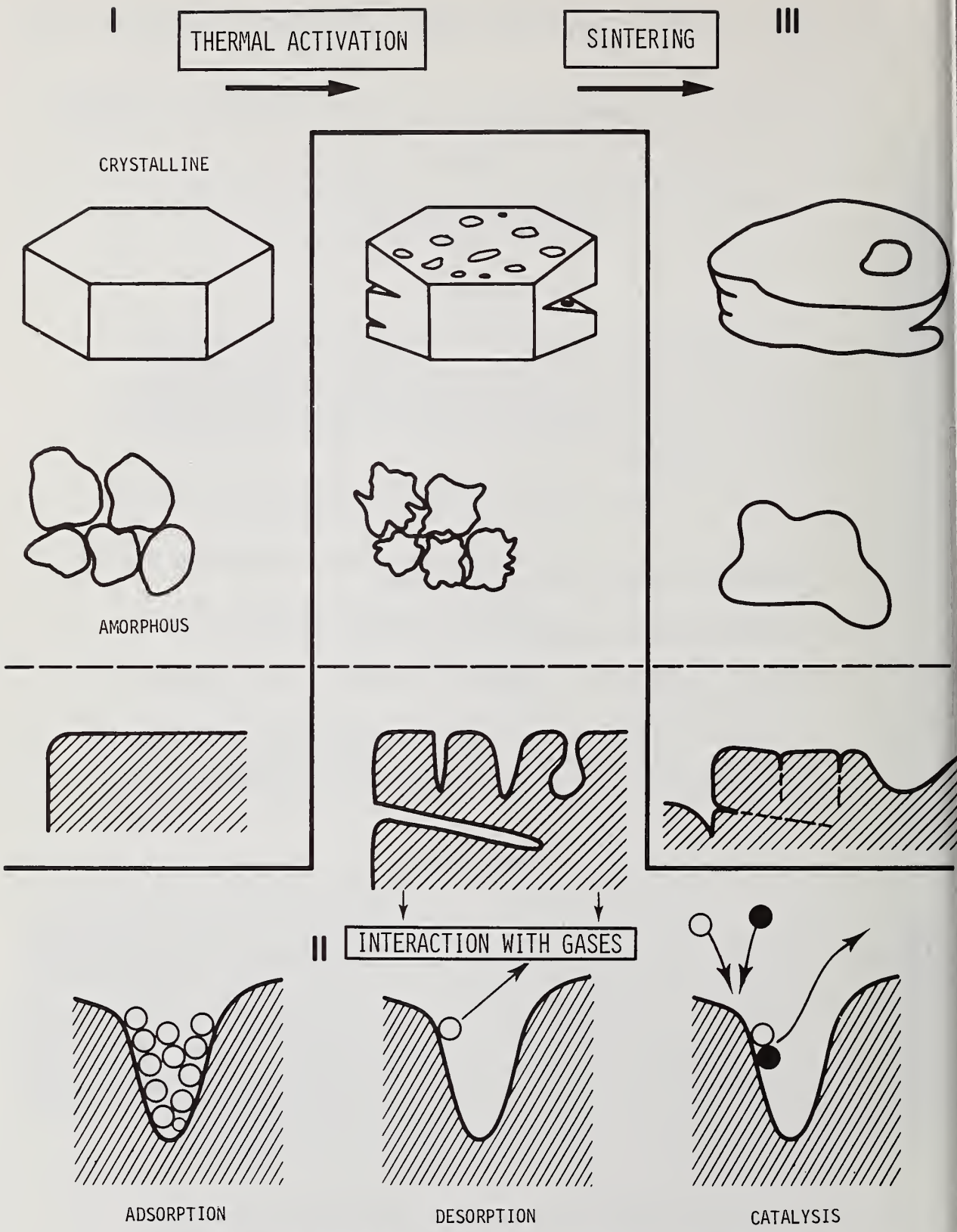

Figure 1. The main events which may be followed by thermal analysis in the "life" of an adsorbent.

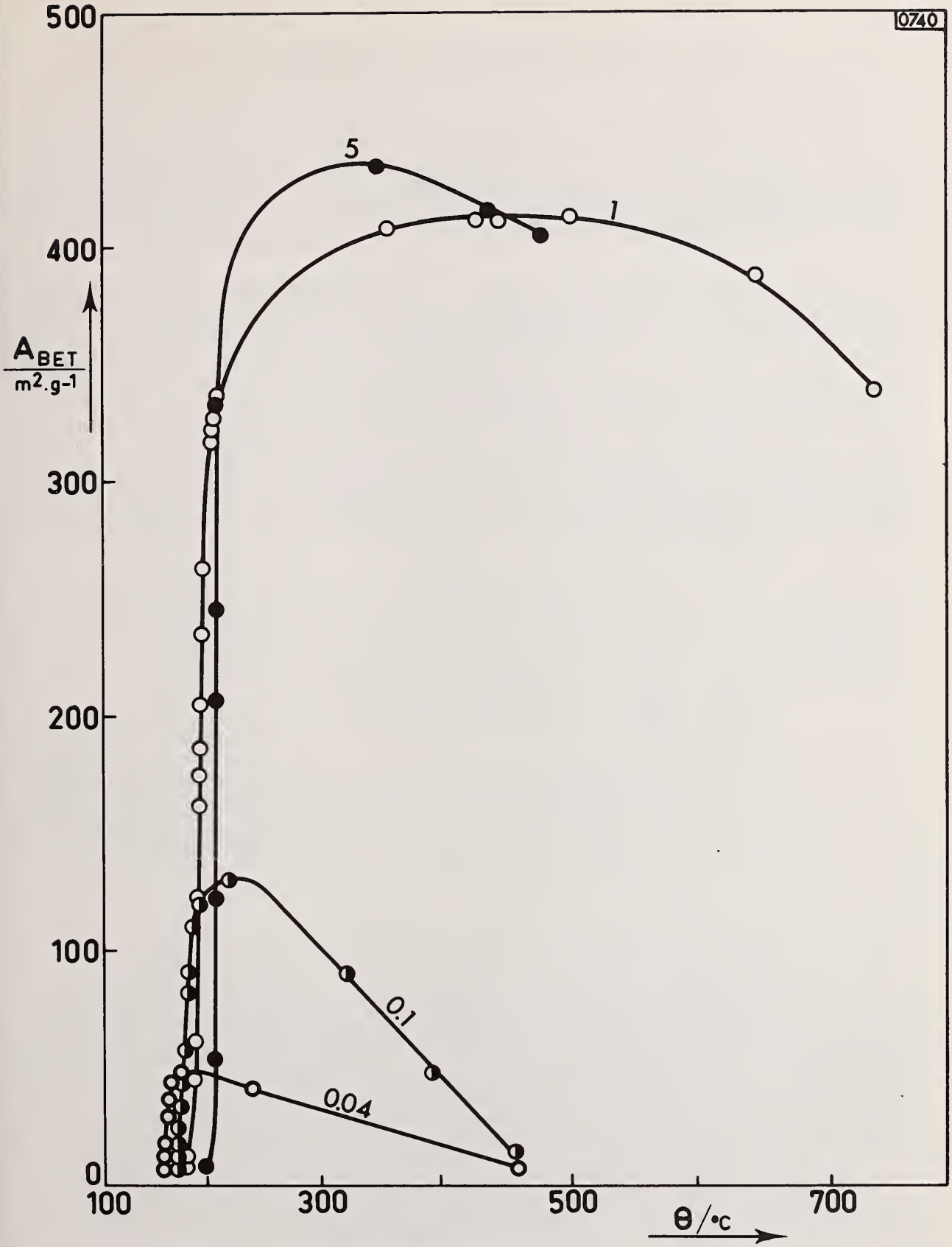

Figure 2. Development of the specific surface area of a gibbsite sample (grain size: 1 μm) during its thermal decomposition under various water vapor pressures (indicated in torrs) (from [3]).

A. Production of Porosity

This is likely to be – from the thermal analysis point of view – the most interesting step, all at once because of the variety of problems to solve, because of the need to understand the mechanism of pore formation and because of its practical application to the processing of adsorbents. The aim of most studies is here to understand and to obtain the formation of a homogeneous and, if possible, "precalibrated" porosity through the thermal decomposition of a parent material (hydroxyde, carbonate, oxalate, polymer, etc...).

A first difficulty stems from the need of a controlled atmosphere. This is strikingly illustrated, in figure 2, by the dependency of the specific surface area of an alumina (obtained by thermolysis of a gibbsite sample $Al(OH)_3$) on the residual water vapour pressure (ranging here from 0.04 to 5 torrs) during the thermolysis. Depending on that pressure, the maximum specific surface area available to nitrogen (and determined by the B.E.T. method) ranges from less than 40 to more than 400 m^2g^{-1}; this suggests that, for such a system, it is not worth trying to understand the mechanism of pore formation if one is unable to closely control the residual water vapour pressure. Similar influence of the water vapour pressure on the surface area of MgO was shown to occur during the thermolysis of brucite $Mg(OH)_2$ [4]. A clear proof (even if the actual CO_2 pressure is unknown) of the influence of the atmosphere on the course of the thermolysis of calcium oxalate monohydrate was brought by Paulik and Paulik [5] and is shown in figure 3; we may guess (although the checking was not made) that the thermal paths are different enough to influence the pore structure of the product.

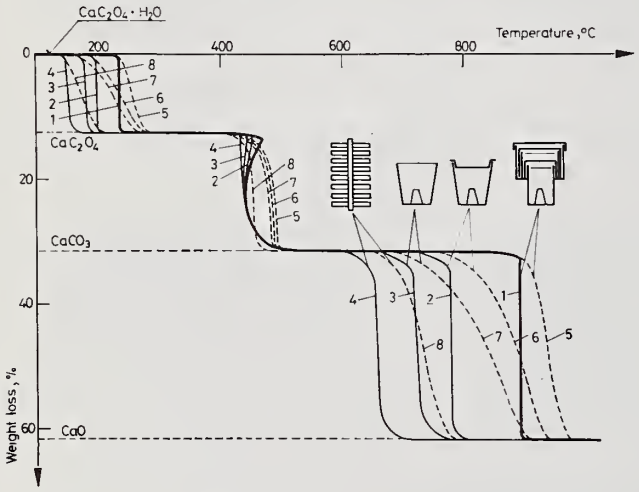

Figure 3. Decomposition of calcium oxalate monohydrate with various types of crucibles (represented) and with two heating programs: quasi-isothermal (curves 1 to 4) or dynamic (10 $K.mn^{-1}$, to 8) (from [5]).

It follows from figure 2 that the pressure throughout the sample must be known and, if possible, kept constant. In other words, pressure gradients must be avoided. Moreover, if kinetical parameters must be drawn from the thermal analysis experiments, then the temperature gradients in the sample (which is often a poor thermal conductor) must be kept to a minimum. This is specially difficult to achieve when the thermolysis is carried out under vacuum, as suggested by many authors (to avoid any re-combination of the gas with the solid and therefore any complication of the mechanism); at the same time, it is difficult to get a satisfactory vacuum (since the gas evolved tends to "break" the vacuum) and, above all, to avoid any spurting of the sample (especially when it is in the form of a fine powder). A final problem is brought by sampling: a technological adsorbent suffers from heterogeneity and a representative sample is necessary (in this respect, we experienced that, even for a ground and mixed sample, it was usually unwise to operate on samples weighing less than 20 mg). The above problems are schematically reminded in figure 4 (A to E).

Various answers were suggested. For instance, the atmosphere control is achieved in two major ways. The simplest is the one using the principle of "self-generated atmosphere" suggested by Garn both for TG [6] and for DTA [7] (cf. figure 5 A-1). We must forget the air-tight aluminum pans (A-3) often used in DTA or DSC; they do apply the above principle but without any control of the actual pressure (always changing) in the pan. Another possibility is to send over the sample (A-4, A-5) or, better, through the sample (A-6) a pure or mixed atmosphere (with known partial pressures) [8]. On the other hand, it fortunately happens that the problems of temperature gradients, pressure gradients, and spurting out under vacuum may usually be solved all at the same time. The solutions (which all exclude the use of DTA since this is based, by principle, on the existence of detectable temperature gradients) are the following:

a) Use of very thin samples (B-1, like for instance down to 80 nm thick, as it was the case in a study of alkaline-earth carbonates [9]). This needs a very high sensitivity of the thermal analysis equipment and may not allow to prepare enough sample for subsequent adsorption experiments.

b) Use of an ultra-slow heating program (B-2), as was initially suggested by Eyraud et al. [10] for the thermolysis of gibbsite. Of course, this procedure is extremely time-consuming and therefore rarely used.

c) Use of controlled decomposition rate thermal analysis. In this rather general technique [11] the heating of the furnace is monitored by any parameter directly related to the rate of decomposition. The controlling parameter may be a flow of gas [12] or a DTG signal [11 and 13]. The decomposition rate is set at a satisfactorily low value. In the gas-flow version (B-3) which is related to EGD, the technique may be used at any pressure ranging from 10^{-5} up to 20 torrs, at any decomposition rate ranging from 10^{-5} up to a few grams per hour and with weights of sample ranging from 50 mg up to more than 100 g (specially interesting for preparative purposes). Burch [18] experiences that such a control is necessary to ensure a "medium vacuum" not worst than 35 mtorrs during the thermal decomposition of a molybdenum oxalate. The DTG version (B-4) uses to be called by Paulik and Paulik the "quasi-isothermal thermogravimetry" [13].

Among the recent trends of thermal analysis in these studies of pore formation we would like to quote:

a) Experiments in a wide range of constant pressure (from 5.10^{-5} torr of self-generated atmosphere [14] up to 8 bars of water vapour [15], 10 bars of O_2, SO_2, N_2, or CO_2 [18], 30 bars of H_2S or CO_2 [28], or even 150 bars of various gases, with the flow-metric thermal analysis of Martre et al. [17]). At the same time, a variety of atmospheres is used to detect the way of modifying the porous structure of the surface.

b) Advance in the understanding and kinetical use of controlled decomposition rate experiments with recent works of Criado [19] and of Sorensen [20]. The latter takes advantage of an unsatisfactory control of the DTG signal (cf. figure 6, central trace on the diagram) to detect changes of the material being decomposed from the corresponding overshoots of the semi-periodical DTG trace. For an accurate and nearly "assumptionless" determination of the apparent activation energy, we suggest [23,24] a method derived from the cyclic heating method of Flynn [25], but adapted to the case of constant decomposition rate analysis; instead of choosing two temperatures (top and bottom of each cycle) we choose two decomposition rates (figure 7). This method does not suffer from the theoretical limitations (due to the necessary assumptions) of the usual dynamic methods, nor from the practical limitations (at the beginning and at the end of the thermolysis) of the isothermal methods.

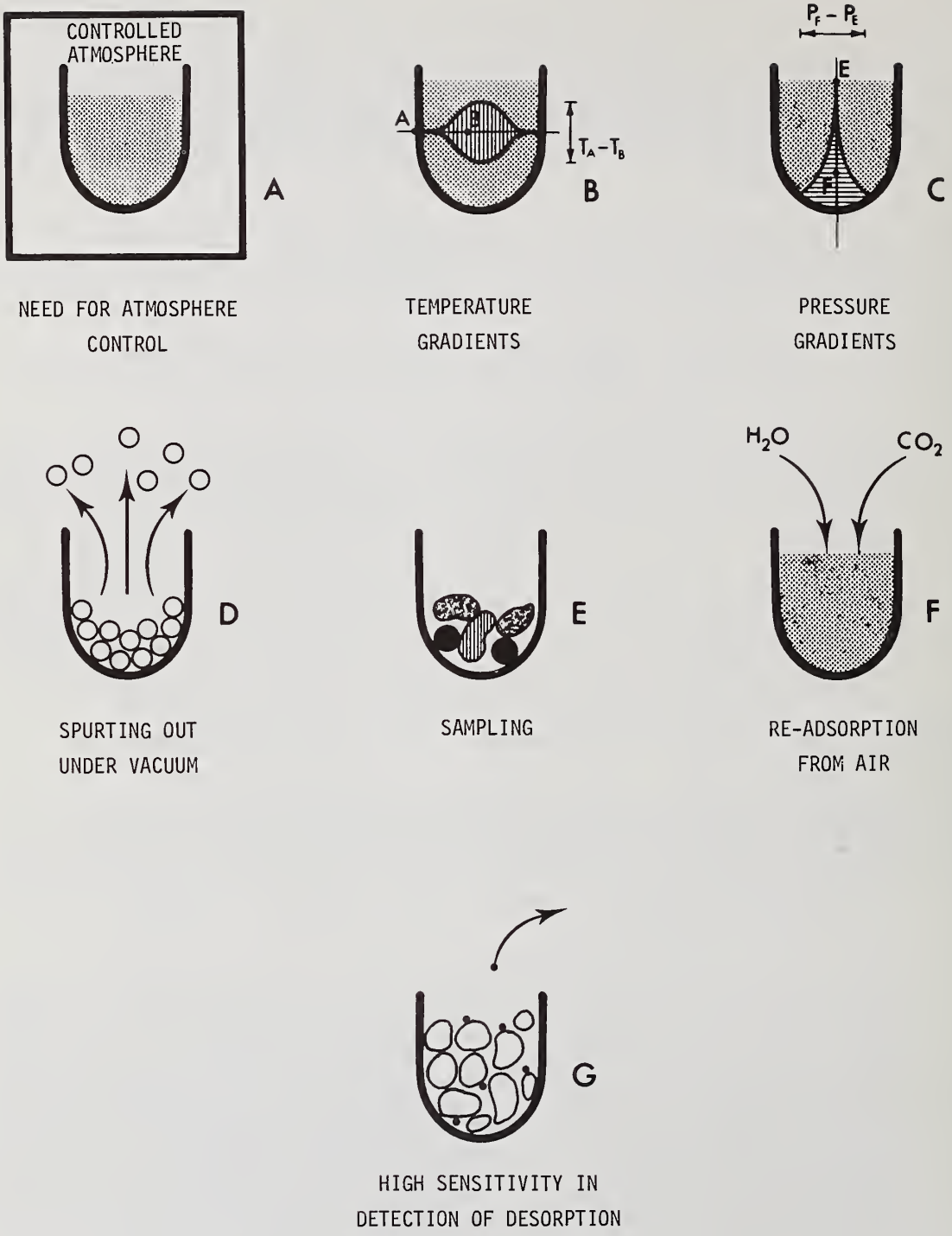

Figure 4. A few problems specially found in the thermal analysis of adsorbents.

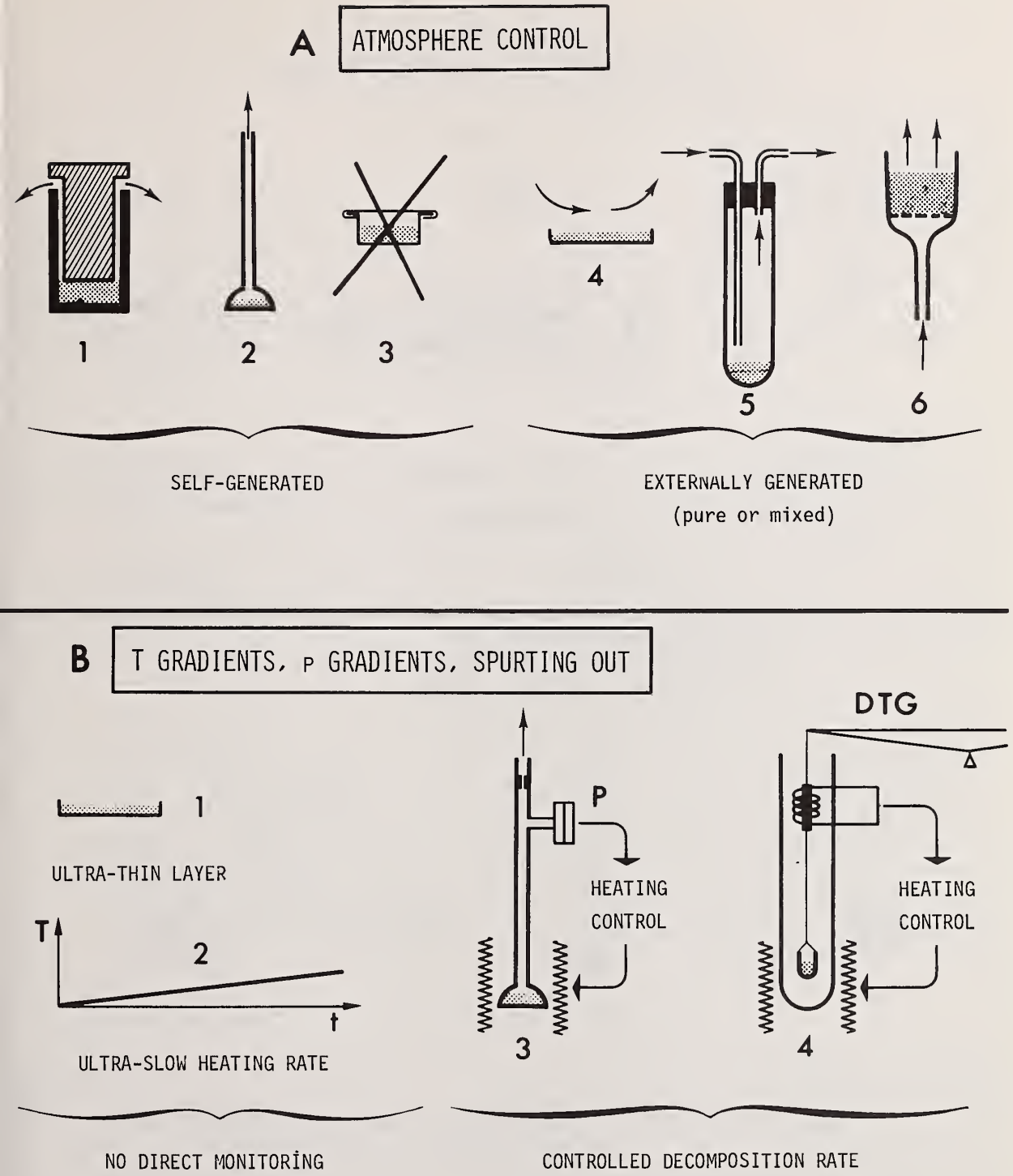

Figure 5. Various answers brought to the problems found in the thermal analysis of adsorbents.

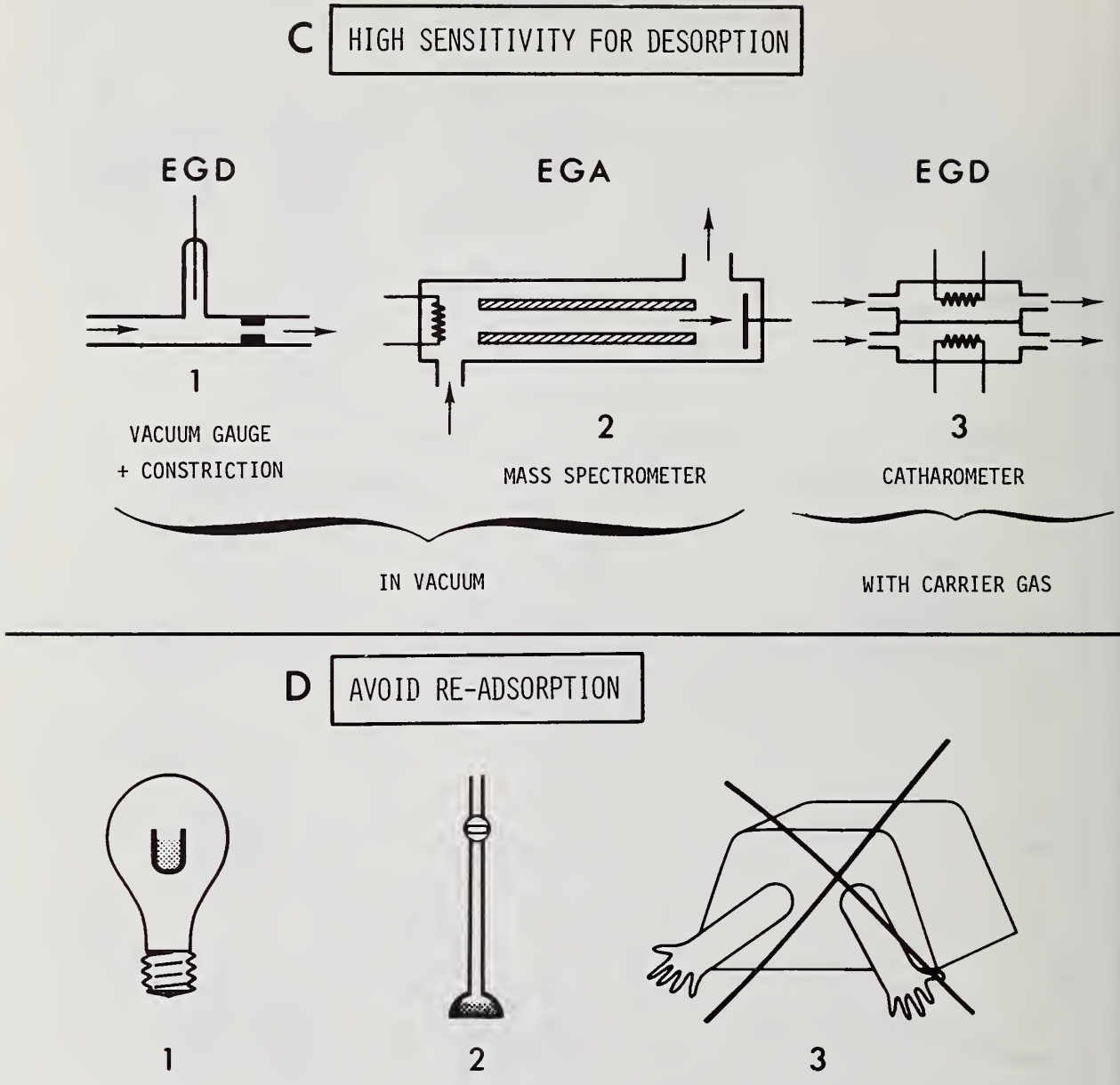

Figure 5 (Continued). Various answers brought to the problems found in the thermal analysis of adsorbents.

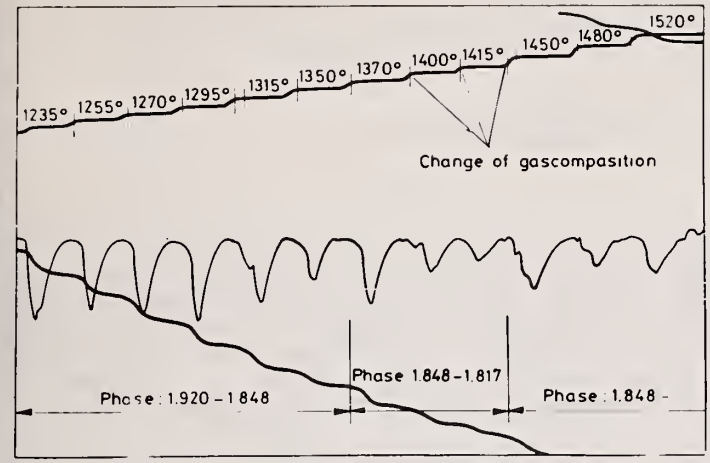

Figure 6. Constant decomposition rate thermal analysis (DTG version) of non-stoechiometric CaO_2 in CO_2/CO atmospheres (from [20]). From top to bottom (all curves being recorded as a function of time); temperature, controlled DTG signal, TG trace.

c) Association of numerous techniques (like TG + DTA + EGA + X-ray diffraction + adsorption techniques for the thermolysis of hydrous chromium oxides [21], or like TG + DTA + mass spectrometry under various pressures of CO_2 for the thermolysis of various calcite-type carbonates [22]). A special difficulty in these studies is the characterization of the porous structure of the adsorbents during the course of the thermal analysis. The only method lending itself to a continuous evaluation of the specific surface area during heating is the "emanation method" of Hahn (emanation of a radioactive gas from the surface of the solid; this gas is swept away by a carrier gas and detected later by a Geiger counter [26,27]). Nevertheless, because this method is difficult to handle (problems of preparation of the labelled sample and limited accuracy) it was never used extensively. Instead of that, the thermolysis of the samples is usually carried out step by step, leaving the possibility of intermediate non-destructive experiments. One difficulty (cf. figure 4F) is to avoid any intermediate readsorption. Since a microporous solid is able to adsorb water, at room temperature, from partial pressures as low as a few mtorrs, the use of a glove box for the transfer of the sample from a crucible to an adsorption bulb is usually not recommended. On the other hand, two satisfactory procedures are either to perform the adsorption experiments "in situ" (easy to achieve in a thermobalance, by use of adsorption gravimetry, and also in a EGD apparatus, by use of a mixed gas flow adsorption technique) or to perform the thermal analysis and the adsorption experiment in the same glass bulb (figure 5 D-2) which can be quickly tranferred from one place to the other (easy to do when the thermal analysis technique is EGD or EGA).

B. Choice and Achievement of a Reproducible State of the Surface

Prior to any gas adsorption determination, the adsorbent must be brought to a standard state i.e. at which its mass and also the nature and the extent of its surface are reproducible. It has often been considered that the outgassing of physically adsorbed vapours (especially water) could theoretically occur at room temperature, but that, in order to save time, it was usually possible to outgas the sample at temperatures ranging from 100 to 150 °C. Actually, the best outgassing temperature not only prevents any irreversible transformation of the adsorbent but it must also give the most reproducible state of the adsorbent. In the very frequent case when the TG curve of an adsorbent shows an inflexion point in the 50 – 200 °C temperature range, this is the optimum one since it usually corresponds to the end of the departure of the physically bound water and since the mass change vs temperature is minimum there, ensuring the best reproducibility of the water content, and therefore of the mass, of the standard state (any error on the mass is of course also found in the specific surface area). These remarks show the interest, to increase the meaning and the value of the adsorption measurements, of preliminary vacuum TG or vacuum EGD

experiments to determine the best "standard" outgassing temperature, even if this is not yet of common practice. These lines are now being followed by the group which is now, in the scope of the Bureau Communautaire de Reference (BCR) in Brussels, choosing and characterizing a set of reference adsorbents under the chairmanship of Professor D. H. Everett.

Characterization of Adsorbing Properties

A. Study of Adsorption

For the sake of a better understanding of the phenomenon, it happens that adsorption tends to be studied mainly in isothermal experiments which are not, strictly speaking, in the scope of thermal analysis although they may use thermoanalytical equipment (mainly thermobalances but also calorimeters and even, sometimes, DTA equipment). The fight against air pollution by factories (especially when burning coal with high S content) recently inspired several high-temperature adsorption experiments, at pressures up to 30 bars, of H_2S on half-calcined dolomite [28], and of SO_2 on calcined limestone [18] or dolomite [29].

There is nevertheless one type of experiment in which a typical thermal analysis technique (DSC) seems to have a growing interest, namely the study of porosity by the significant lowering of the melting temperature of the adsorbate condensed within the porous structure (in pores 4 nm wide, ice already melts at -60 °C [32]). This technique, which has the interest of detecting the internal diameter of the cavities (even when they are of the ink-bottle type), is being improved and developed now especially for the study of catalysts [30] and of soils [31]; it is also extremely well suited to the study of the frost resistance of porous building material (stones, bricks, concrete [32]).

B. Study of Desorption

An increasing popular technique is now known among the catalysis people as the "Temperature Programmed Desorption" or "TPD" [33]. It actually studies the desorption from a surface either by TG (see for instance [34] for the desorption of H_2O from Mn O_2 and [42] for the desorption of H_2 from Al_2O_3-supported catalysts) or, much more frequently, by EGD or EGA. As may be seen from figure 8, this is a very efficient and sensitive technique for detecting various states of a given species on the surface. The strength of the corresponding bondings may be derived from the calculation of the apparent energy of activation. Nevertheless, in such a case, (and especially with the "Flash desorption" technique, where the sample, in the form of a metallic wire, is heated by direct Joule effect at a rate higher than 100 $K.mn^{-1}$ [36,37]) we quite agree with Garn's proposal of speaking of a "temperature coefficient of reaction" rather than of an energy of activation [38], since the actual nature of the parameter "caught" in such a way is unknown. The TPD technique may be used either with a carrier gas or in a vacuum; in the latter case it lends itself to a mass spectrometric analysis (for instance, desorption of SO_2, H_2O, and CO_2 from an asbestos sample [39]). Typical TPD experiments were reported concerning the desorption of ethylene from alumina [33], H_2O from anatase [40], O_2 from NiO [41], H_2 from Ni [43]. A special mention must be made of the technique used by Dollimore [44,45] with an "incremental isothermal heating program", in which the rate of desorption is measured (and compared, to determine activation energies) at the beginning and end of each temperature step. Another feature of the technique (cf. figure 9) is a reservoir allowing to store (with the help of a diffusion pump with high critical backing pressure) all the gases evolved, prior to a mass spectrometric analysis.

$$\frac{d\alpha}{dt} = A \exp(-E/RT).f(\alpha).g(P_0-P)$$

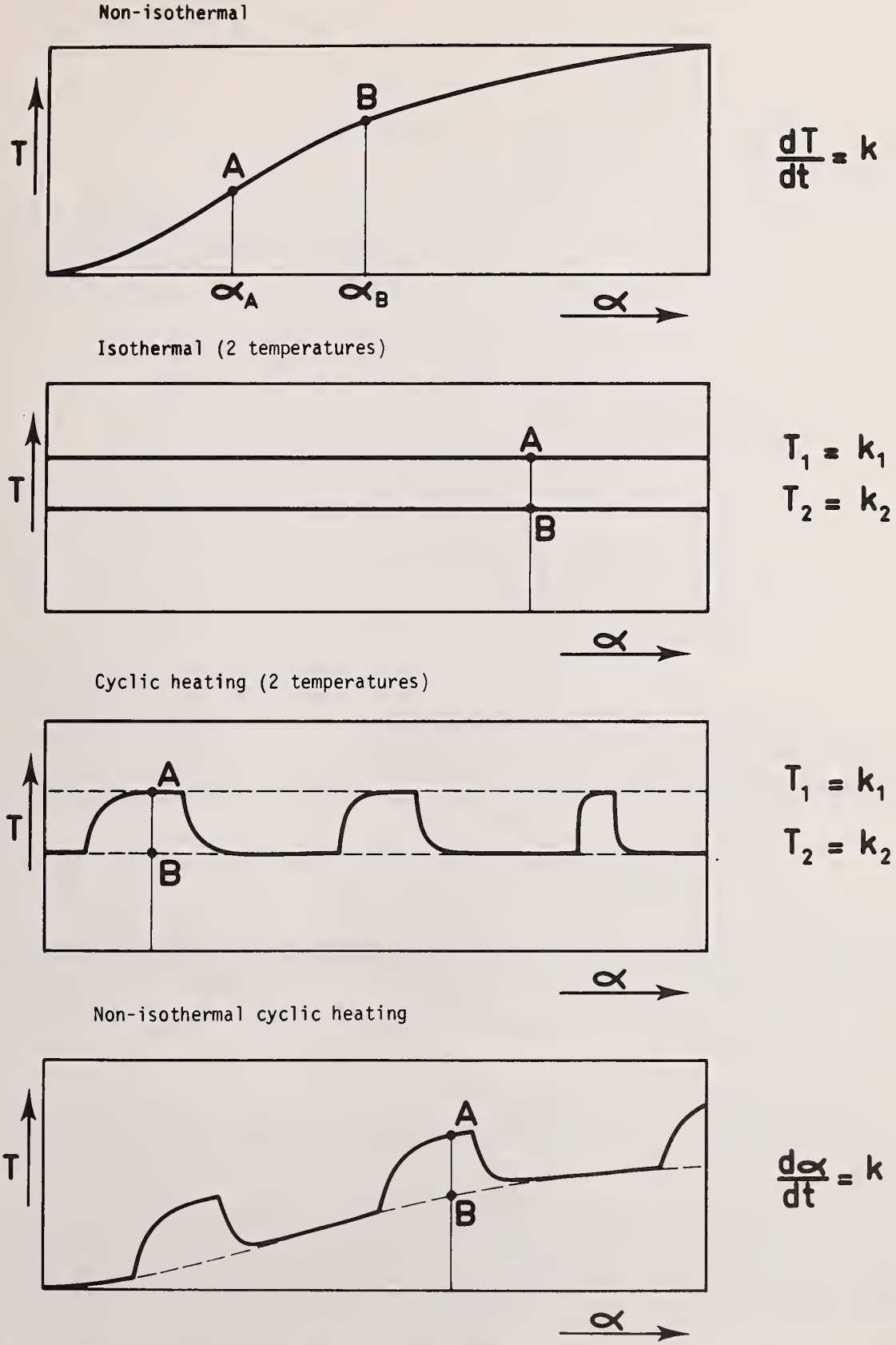

Figure 7. Different ways of determining the apparent activation energy for a thermal decomposition: "dynamic" (top), isothermal (center), and controlled decomposition rate (bottom) approaches.

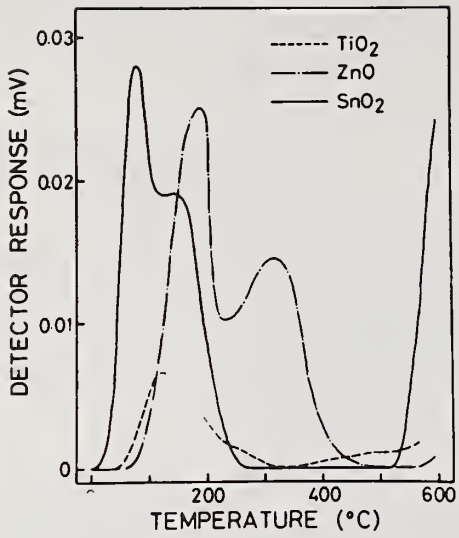

Figure 8. "TPD" (here, with helium flow and thermal conductivity detector) trace for the desorption of oxygen from TiO_2, ZnO, and SnO_2 samples with specific surface areas of 10.3, 5.5, and 16.1 m^2g^{-1} (from [35]).

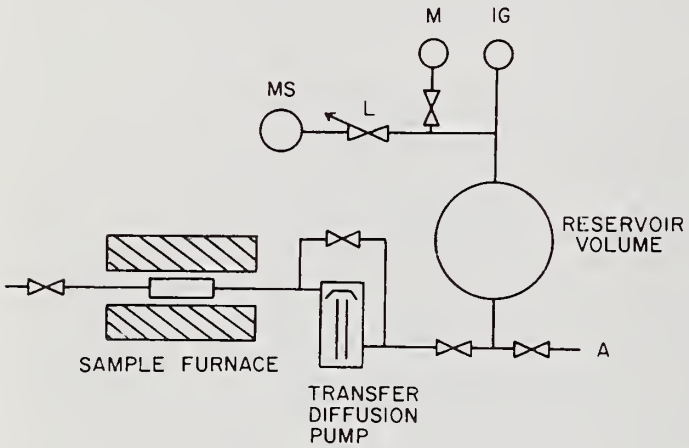

Figure 9. Thermal desorption apparatus with evolved gas reservoir for quantitative determinations (from [44]).

It may be worthwhile to point out the extremely high sensitivity of these EGA and EGD techniques (figure 5 C); for instance, with the controlled decomposition rate EGD technique (which we use either with a vacuum gauge (C-1) or with a quadrupole mass spectrometer (C-2)) it happened that we worked at controlled rates of less than 1 $\mu g.mn^{-1}$ (the 1 g gibbsite or calcite samples used would have needed more than 2 years to lose all their water or carbon dioxide...).

C. Study of Both Adsorption and Desorption

An interesting approach for studying adsorption and desorption at high temperatures was devised by Mizutani and Kate [48]. The principle is to heat or cool the adsorbent at constant rate in a flow of at least two mixed gases such as $He-O_2$, $Ar-H_2$, etc.... The changes in the composition of the gas passing through the reactor are detected by a thermal conductivity detector. One gas is a carrier inert gas and the other is the reacting gas. Figure 10 gives a typical example of recorded curves (in a flow of $He + CO_2$) with heating and cooling rates of 10 $K.mn^{-1}$ and with a sample weight of only 10 mg. The carbonation of CaO is reversible above 700 °C but not at 520 °C. The composition of the gas mixture may be changed at will.

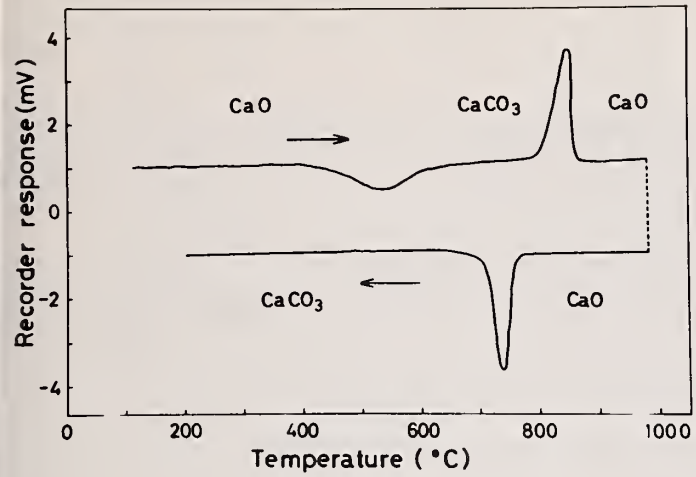

Figure 10. Evolved (or adsorbed) gas analysis under a He-CO_2 flow (ratio 10/1) (from [48]).

Thermal Destruction of Adsorbents

A. Destructive Characterization

Accepting now the destruction of the adsorbent, we may perform more conventional thermal analysis experiments. Among recent applications we may quote the detection of the degree of conversion of high alumina cements [47], the study of kerogens pyrolysis done with the help of chromatographic EGA [48] or of mass spectrometric EGA [49], and a comprehensive study of dolomite pyrolysis in order to allow its quantitative detection by DTA [50].

B. Sintering (Loss of Surface Area)

A practical trouble with the sintering of usual adsorbents is the wide temperature range (often 500 K wide) in which the phenomenon takes place, without the possibility, in the meantime when operating by DTA, to record any baseline....Moreover, very high temperature techniques are normally necessary in this field. The density (or length) [51] and the electrical conductivity [52] are among the easiest parameters to follow during the thermal analysis.

Sometimes, sintering begins at rather low temperatures. Most frequently the loss in surface area is due to the "absorption" of micropores by larger ones. But the reverse situation may also occur; for a TiO_2 gel, sintering takes place through a constriction of the pores, itself followed by a sudden recrystallization of TiO_2, easily detected by constant decomposition rate EGD. This constriction of pores gives rise to an enhanced enthalpy of adsorption which may be shown by adsorption microcalorimetry of argon or nitrogen [53].

Conclusion

We could see that because adsorbents are often prepared by heating (thermal activation), used during heating (chemisorption, catalysis), regenerated by heating (outgassing) and destroyed by heating (sintering), thermal analysis may be closely associated with the main steps of their life.

Nevertheless, their extended surface area makes them especially sensitive to their immediate environment during heating and this was a reason for the development of specially refined thermal analysis procedures. But this is not the end, since it is likely that these techniques, initially designed to help in the understanding of the thermal behaviour of adsorbents, will be progressively used for preparative purposes, thermal analysis being then a convenient way (especially EGD and EGA) to monitor the process in a continuous way and under controlled conditions.

References

[1] le Chatelier, H., Bull. Soc. Fr. Mineral., 10, 204 (1887); J. Phys. Chem. 1, 396 (1887).

[2] International Union of Pure and Applied Chemistry. Manual of symbols and terminology for physicochemical quantities and units. Appendix. Definitions, terminology and symbols in colloid and surface chemistry, part I., ed. by D. H. Everett. London, Butterworths, 1972.

[3] Rouquerol, J. and Ganteaume, M., J. Thermal Analys. 11, 201 (1977).

[4] Horlock, R. F., Morgan, P. L., and Anderson, P. J., Trans. Faraday Soc. 59, 721 (1963).

[5] Paulik, F. and Paulik, J., J. Thermal Analys., 5, 253-70 (1973).

[6] Garn, P. D. and Kessler, J. E., Analyt. Chem., 32, n° 12, 1563 (1960).

[7] Garn, P. D., Analyt. Chem., 37, 77 (1965).

[8] Stone, R. L., J. Amer. Ceram. Soc., 35, 76 (1952).

[9] Pokol, G., Gal., S., Domokos, K., and Pungor, E., in, Proc. 1st Europ. Symp. Thermal Analys., D. Dollimore Ed. (London, Heyden, 1976) p. 7.

[10] Blanchin, L., Imelik, B., and Prettre, M., C.R. Acad. Sco., 1029 (1951).

[11] Rouquerol, J., J. Thermal Analys. 2, 123 (1970).

[12] Rouquerol, J., in, Thermal Analysis, vol. 1 (Academic Press, 1968) p. 281.

[13] Paulik, J. and Paulik, F., Analyt. Chim. Acta, 56, 328 (1971); Paulik, F. and Paulik, J., Analyt. Chim. Acta, 60, 127 (1972).

[14] Rouquerol, F., Regnier, S., and Rouquerol, J., in, Thermal Analysis, Vol. 1, Proc. 4th ICTA, Budapest, 1974, ed. by I. Buzas (Budapest, Akademiai Kiado, 1975), p. 313.

[15] Garn, P. D., Rev. Sci. Instrum., 44, 231 (1973); Garn, P. G. and Freund, F., Trans. J. Brit. Ceram. soc., 14, 23 (1975).

[16] Ulerich, N. H., O'Neill, E. P., and Keairns, D. L., Thermochim. Acta, 26, 269 (1978).

[17] Martre, A. M., Pouillen, P., and Aumont, R., J. Therm. Analys. 6, 203 (1974).

[18] Burch, R., J. Chem. Soc., 14, 2991 (1978).

[19] Criado, J. M., Thermochim. Acta, 28, 307 (1979).

[20] Sørensen, D. T., J. Thermal Analys. 13, 429 (1978).

[21] Fenerty, J. and Sing, K. S. W., in, Proc. 1st Europ. Symp. Thermal Analys., D. Dollimore Ed. (London, Heyden, 1976), p. 304.

[22] Bayer, G. and Wiedemann, H. G., in, Proc. 1st Europ. Symp. Thermal Analys., D. Dollimore Ed. (London, Heyden, 1976), p. 256.

[23] Rouquerol, F. and Rouquerol, J., in, Thermal Analysis, Vol. 1, Proc. 3rd ICTA, H. G. Wiedemann, Ed (Davos, 1971). (Basel, Birkhauser, 1972), p. 373.

[24] Rouquerol, J., J. Thermal Analys., 5, 203 (1973).

[25] J. H. Flynn, in, Thermal Analysis, Vol. 2, (New York, Academic Press, 1969), p. 1111.

[26] Hahn, M., quoted by D. Fouque et al., reference 27.

[27] Fouque, D., Fouilloux, P., Bussiere, P., Weigel, D., and Prettre, M., J. Chim. Phys., 62, 1088 (1965).

[28] Dobner, S., Kan, G., Graff, R. A., and Squires, A. M., Thermochim. Acta, 16, 251 (1976).

[29] O'Neill, E. P., Keairns, D. L., and Kittle, W. F., Thermochim. Acta, 14, 208 (1976).

[30] Quinson, J., Brun, M., Lallemand, A., and Eyraud, C., in, Proc. 1st Europ. Symp. Thermal Analys., D. Dollimore Ed. (London, Heyden, 1976), p. 59.

[31] Homshaw, L. G., in, Journees de calorimetrie et d'analyse thermique, Marseille, 10-11 mai 1979, Vol. 10, Marseille, Secret.; Univ. Provence, 1979, (Assoc. Fr. Calorim. Analys. Therm.); L. G. Homshaw and J. Chaussidon, Proc. 6th Internat. Clay Congress, 1978.

[32] Fagerlund, G., Mater. Construct. n° 33, 191 (1973).

[33] Cvetanovic, R. J. and Amenomiya, Y., Catalys. Rev., 6, 21 (1972).

[34] Lee, J. A., Newnham, C. E., Stone, F. S., and Tye, F. L., J. Colloid. Interf. Sci., 45, 289 (1973).

[35] Iwamoto, M., Yoda, Y., Yamazoe, N., and Seiyama, T., J. Phys. Chem., 82, 2564 (1978).

[36] Alnot, M., Fusy, J., and Cassuto, A., Surf. Sci., 12, 467 (1978).

[37] Yates Jr., J. T., Klein, R., and Madey, T. E., Surf. Sci., 58, 469 (1976).

[38] Garn, P. D., Thermochim. Acta, 28, 185 (1979).

[39] Murphy, W. J. and Ross, R. A., Canad. J. Chem., 56, 1847 (1978).

[40] Munuera, G., Moreno, F., and Prieto, J. A., Z. Phys. Chem. N.F., 78, 113 (1972).

[41] Iwamoto, M., Yoda, Y., Egashira, M., and Seiyama, T., J. Phys. Chem., 80, 1989 (1976).

[42] Bolivar, C., Charcosset, H., Frety, R., Leclercq, G., and Neff, B., in, Proc. 1st Europ. Symp. Thermal Analys., D. Dollimore Ed. (London, Heyden, 1976), p. 55.

[43] Bekassy, S., Petro, J., and Liptay, G., Thermochim. Acta, 11, 45 (1975).

[44] Dollimore, J. and Harrison, B. H., J. Catalys., 28, 275 (1973).

[45] Barton, S. S., Harrison, B. H., and Dollimore, J., J. Phys. Chem., 32, 290 (1978).

[46] Mizutani, N. and Kato, M., Analys. Chem., 47, 1389 (1975).

[47] Barnes, P. A. and Baxter, J. H., Thermochim. Acta, 24, 427 (1978).

[48] Martin, S. J., in, Adv. Org. Geochem., Proc. Int. Meet. 7th, 1975, Ed. by R. Campos and J. Goni. Madrid, Empresa Nac. Adaro Invest. Mineras, 1977.

[49] Souron, C., Boulet, R., and Espitalie, J., Rev. Inst. Fr. Petrol., 29, 661 (1974).

[50] Davies, P., Dollimore, D., and Heal, G. R., in, Proc. 1st Europ. Symp. Thermal, Analys., D. Dollimore, Ed. (London, Heyden, 1976), p. 348.

[51] Young, W. S. and Cutler, I. B., J. Amer. Ceram. Soc., 53, 859 (1970).

[52] Dequenne, J., Rev. Hautes Temper. Refract., 10, 141 (1973).

[53] Torralvo, M. J., Grillet, Y., Rouquerol, F., and Rouquerol, J., J. Chim. Phys. (under press).

CURRENT CONTRIBUTIONS OF THERMAL ANALYSIS TO THE STUDY OF TECHNOLOGICAL ADSORBENTS

RAPPORTEUR'S COMMENTS BY

H. G. McAdie
Ontario Research Foundation,
Sheridan Park Research Community,
Mississauga, Ontario, Canada L5K 1B3

The preparation and application of adsorbents of commercial interest, such as catalysts, subjects these materials to various temperature regimes and, therefore, these processes are amenable to study by thermal methods of analysis. In his oral presentation Dr. Rouquerol defined the major experimental problems and their solutions and provided somewhat more detail methodology than appears in manuscript. Through it he emphasized the particular need for control of temperature and partial water vapor pressure at the reaction site. To effect this control requires techniques and conditions which minimize the respective gradients within the sample, ideally to the point when readily measureable and controllable external values accurately reflect conditions at the reaction site.

A particular problem exists with practical materials of commerce, viz. homogeneity. While it is desirable to minimize thermal gradients within a DTA sample through reduction of sample size, it is difficult, if not impossible, to obtain truly representative samples of less than 20-100 mg. Few instruments at present are equipped to provide the desirable levels of atmosphere and temperature control required within such relatively large samples.

One approach to atmosphere control is that of a self-generated atmosphere. Dr. Rouquerol properly points out that the widely used "covered pan" does not produce a stable self-generated atmosphere but that both composition and pressure can change during the heating programme.

Dr. Rouquerol strongly advocated the use of the controlled decomposition rate approach to the study of these materials by thermal analysis. In this approach, the pressure of gas evolved from a decomposing solid is maintained constant through feed-back control of the heat flow to the decomposing solid. This permits the bulk of the decomposition to take place under a fixed partial pressure, as a result of which the majority of the reaction also occurs at essentially constant temperature.

Imposition of these conditions results in apparent zero order kinetics or an apparent order which is sample shape dependent. Thus, kinetics obtained by this approach may not represent the kinetics of bulk processes involving the same materials. However, the technique does provide better control of the reaction conditions during a decomposition than in many conventional thermogravimetric studies.

This excellent survey of the practical problems of technique and interpretation would have been enhanced by one or two examples drawn from industrial experience since many "problem-solving" industrial laboratories remain unconvinced regarding the applicability of thermal methods of analysis to their day-to-day problems. The work of Dr. Rouquerol and others clearly shows the practical value of these techniques.

National Bureau of Standards Special Publication 580. Proceedings of the Workshop on the State-of-the-Art of Thermal Analysis held at NBS, Gaithersburg, MD, May 21-22, 1979. (Issued May 1980)

ENTHALPIMETRIC ANALYSIS: THERMOCHEMICAL TITRATIONS AND RELATED METHODS

J. Jordan, J. D. Stutts, and W. J. Brattlie

Department of Chemistry, The Pennsylvania State University
152 Davey Laboratory
University Park, Pennsylvania 16802

Abstract

Conventional methods of thermal analysis involve generally the characterization of solid samples. In contradistinction, enthalpimetric analysis relies on measuring temperature changes in dilute solutions, under effectively adiabatic conditions. The basic principle of enthalpimetric analysis is a linear correlation between the heat evolved (or absorbed) in a chemical reaction and the amounts reacted. The relevant proportionality constant is ΔH°. However, experimental conditions must be judiciously adjusted to minimize extraneous caloric effects, heats of dilution and maintain invariant heat capacity. These crucial requirements mandate reliance on highly sensitive temperature transducers which have a fast response. Thermistor circuits and novel curie-point sensors will be discussed in this context, focussing on ultimate limitations in signal-to-noise ratios. The state of the art of thermometric enthalpy titrations (TET), direct injection enthalpimetry (DIE), and flow enthalpimetry will be outlined. Significant areas of applications will be reviewed, including quantitative analysis and determination of thermodynamic and kinetic parameters. The salient feature of enthalpimetric methods is their universal applicability, predicted by the fact that ΔH is the most general property of chemical processes. Paradoxically though, this – per se – imposes severe restrictions due to lack of specificity. The difficulty has been circumvented by reliance on chemical processes which are highly specific by their very nature, e.g., immunological and enzymatic reactions. Recent progress will be described. Capabilities and limitations of enthalpimetric analysis will be assessed, focussing on contemporary national needs, ranging from clinical chemistry to monitoring of contaminants in the new coal conversion technologies.

Introductory Overview

Conventional methods of thermal analysis involve primarily (though not exclusively) the characterization of solid samples. In contradistinction, enthalpimetric analysis relies on measuring temperature changes in dilute solutions, under effectively adiabatic conditions. The basic principle of enthalpimetric analysis is a linear correlation between the heat evolved (or absorbed) in a chemical reaction and the amounts reacted. The relevant proportionality constant is ΔH°. However, experimental conditions must be judiciously adjusted to minimize extraneous caloric effects (e.g., heats of dilution) and maintain invariant heat capacity. These crucial requirements mandate reliance on highly sensitive temperature transducers which have a fast response, such as thermistor circuits and novel curie-point sensors. The state of the art of TET, DIE, and flow enthalpimetry is outlined in this paper. Significant areas of applications are reviewed, including quantitative analysis and determination of thermodynamic and kinetic parameters. The salient feature of enthalpimetric methods is their universal applicability, predicated by the fact that ΔH is the most general property of chemical processes. Paradoxically though, this–per se–imposes severe restrictions due to lack of specificity. This difficulty can be most successfully circumvented in the case of chemical processes which are highly specific by their very nature, e.g., immunological and enzymatic reactions. The presentation which follows

emphasizes selected recent significant developments, rather than attempting an exhaustive coverage. In particular, this paper has been advisedly restricted to adiabatic techniques; thus, imaginative analytical and clinical applications [1][1] of heat flow (Tian-Calvet) microcalorimetry have been excluded for the sake of conciseness. Capabilities and limitations of enthalpimetric analysis are assessed, focussing on contemporary national needs, ranging from clinical chemistry to the monitoring of contaminants in the new coal conversion technologies.

The history of thermometric titrations dates back to the turn of the century [2]. Their modern instrumental implementation was facilitated by two developments in the fifties, viz., utilization of thermistor circuits and volumetric automation [3,4]. This was followed by DIE in the sixties [5] and by a variety of "flow" enthalpimetric methods in the sixties and seventies, including continuous flow [6-8] and so-called "flow-injection" techniques [9,10], as well as "segmented flow" instrumentation [11-14]. Enthalpimetric analysis has apparently "come of age" during the last 10 years, as is documented by several monographs [15-18] and authoritative reviews [19-25]. Research and development in fundamentals and significant applications of enthalpimetric analysis are continuously forthcoming from industrial, academic, and government laboratories in the U.S. and abroad, including France, Germany, Great Britain, Hungary, Italy, Japan, and Sweden. Commercial equipment for enthalpimetric analysis is currently offered by manufacturers in several countries including the U.S., Canada, Japan, Hungary, and Sweden.

Review of The State of The Art

Principles and Instrumentation

The common denominator of most enthalpimetric methods is reliance on the measurement of temperature change engendered by a chemical reaction. The use of relatively simple adiabatic calorimetry cells is an attractive feature.[2] Batch-methods include:

a) thermometric enthalpy titrations (TET) where a reagent is gradually added at a constant rate to a titrand solution;

b) direct injection enthalpimetry (DIE) where a sample is rapidly injected into an excess reagent solution.

In both instances the measured signal, viz., a temperature increment or decrement, ΔT, is related to the desired analytical information by Equation 1.

$$\Delta T = \frac{-n \cdot \Delta H}{\kappa} = -\frac{1}{\sigma} \cdot \Delta H \cdot \frac{n}{V} = -\frac{\Delta H}{\sigma} C \qquad (1)$$

where n denotes the number of moles reacted, V—volume, κ—heat capacity, σ—specific heat per unit volume, C—molar concentration, and ΔH is the effective heat of the relevant reaction. Equation 1 is the fundamental quantitative relationship on which capabilities and limitations of enthalpimetric analysis ultimately depend. It is apparent that linearity between ΔT and concentrations is contingent on the invariance of ΔH. This can conveniently be approximated in dilute solutions, where

$$\Delta H = \Delta H^{\circ} \qquad (2)$$

i.e., heats of dilution to C = 0 are negligible compared to the heat of the reaction. Thus, the preferred applications of enthalpimetric analysis are to samples of small concentrations

---

[1]The figures in brackets indicate the literature references at the end of this paper.

[2]Sophisticated isothermal techniques, relying on the thermoelectric compensation of reaction heats and isoperibolic calorimetry have also been employed, with the inevitable tradeoff of a loss in speed and convenience versus improvement in calorimetric accuracy. These developments transcend the scope of the coverage of the present review: the relevant journal literature [26,27] should be consulted for reference.

(0.0001 to 0.01 molar) which—in turn—require the accurate measurement of small temperature changes (0.001 to 0.1 degree). To attain a precision on the order of ±1 percent, a resolution capability of 10^{-5} degrees is required at the lower limit. Consequently, sensitive temperature sensors are essential for the feasibility of enthalpimetric analysis. In contemporary practice, resistance thermometer-type temperature transducers have been used throughout, mainly thermistors. Enhanced sensitivities might be attained in the future with the aid of Curie-point sensors, consisting, e.g., of appropriate barium titanate ceramics. Typical plots of the variation of the ohmic resistance of these devices, as functions of temperature, are illustrated in figure 1: corresponding information for a conventional platinum resistance thermometer has been included for comparison. When a thermistor is appropriately wired as an arm of a Wheatstone bridge (ac or dc), electrical variables (fixed resistors, bridge voltage and current, etc.) can be adjusted to yield an unbalance potential which is proportional to $\underline{\Delta T}$ over small temperature intervals. Absolute resolution limits are inherent in the nature of the pertinent solid state physics (Johnson noise) and amount to ±10 microdegrees [28,29]. Thus a $\underline{\Delta T}$ of 0.001 degree can be measured with a precision of ±1 percent. The corresponding concentration detection limits are listed in Table 1.

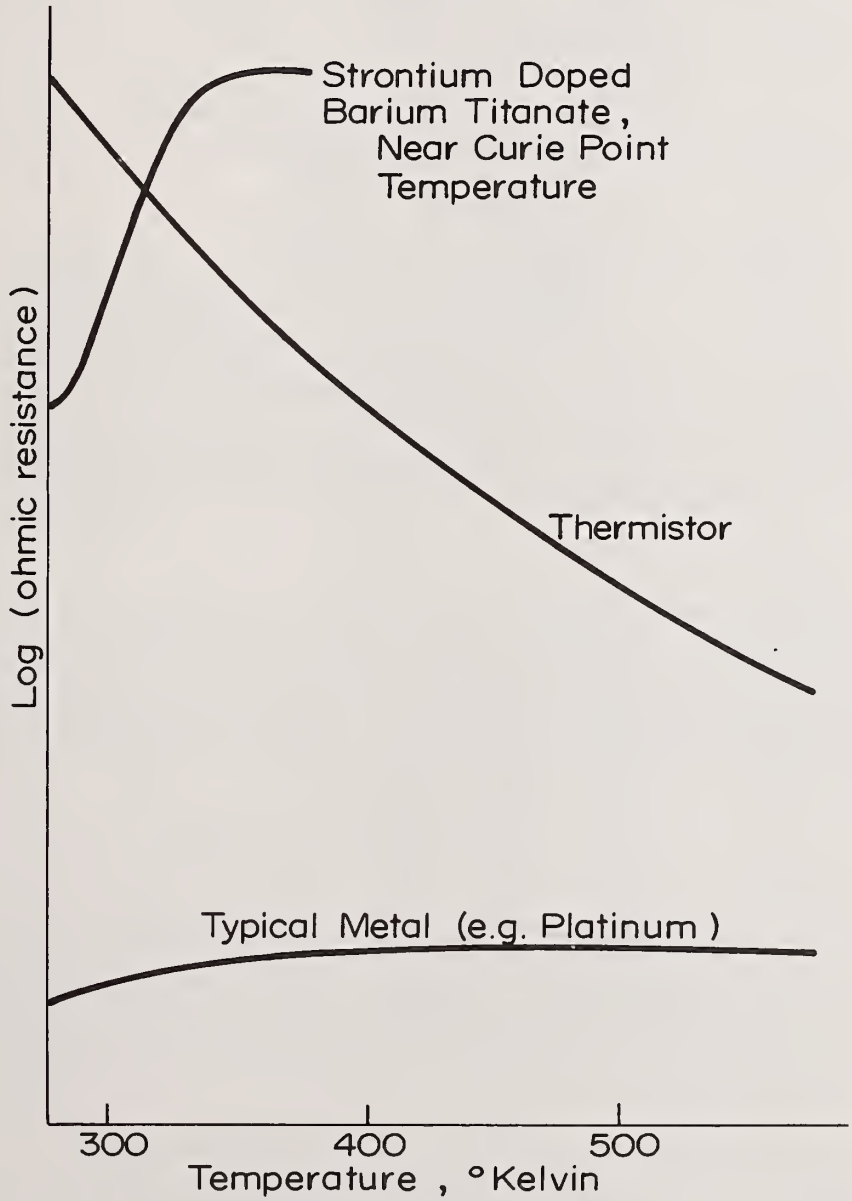

Figure 1. Comparison of temperature dependence of resistance thermometers.

Table 1. Concentrations Measurable in Aqueous Solution with One (1) Percent Relative Precision.

ΔH (kcal/mole)	Lower Concentration Limit[a] (Millimole per Liter)
100	0.01
50	0.02
10	0.1
5	0.2
1	1.0

[a]Estimated from Equation 1, using "state of the art" temperature sensing circuits (resolution $\pm 10^{-5}$ degrees).

In addition to the temperature sensor circuit, state-of-the-art batch-type enthalpimetric analyzers consist generally of the following components:

1. An adiabatic cell (e.g., a Dewar, of 2 to 50 mL capacity).
2. A constant temperature bath (controlled to 0.001 degree to provide an invariant heat sink).
3. A joule heating-calibration circuit.
4. A sample (or reagent) delivery system (motor-driven buret for TET; rapid injection system of fixed volumes for DIE).

A cross-sectional drawing of an enthalpimetric analyzer which has versatile capabilities for TET as well as DIE is shown in figure 2.

Thermometric Enthalpy Titrations

Thermometric enthalpy titration (TET) curves are fundamentally plots of temperature versus time. However, the titrant is usually delivered at a constant rate and consequently the same curves represent corresponding plots of temperature versus volume as illustrated in figure 3. The top curve (3a) is the experimental result of the oxidimetric titration of a four millimolar sodium thiosulfate solution with 0.2 molar potassium triiodide. The choice of relatively concentrated titrant was predicated by the consideration of minimizing changes in heat capacity (v.i.). The equilibrium

$$2\ S_2O_3^{--} + I_3^- = S_4O_6^{--} + 3I^- \ ;\ \Delta H^\circ = -10.96 \text{ kcal/mole} \qquad (3)$$

is entirely to the right, and was attained instantaneously throughout the entire titration. As shown in figure 3b, the titration curve consisted of several regions, viz., AB—pre-titration baseline, BC—titration region, CD—excess reagent region, and DE—post titration region. In Curve 3a, the temperature increment $(\Delta T)_{EP}$ has been back-extrapolated[3] from the equivalence point (EP) and corresponds to the quantity ΔT in Eq. 1.

[3]The significance of this extrapolation is discussed later in conjunction with Eq. 10 (v.i.).

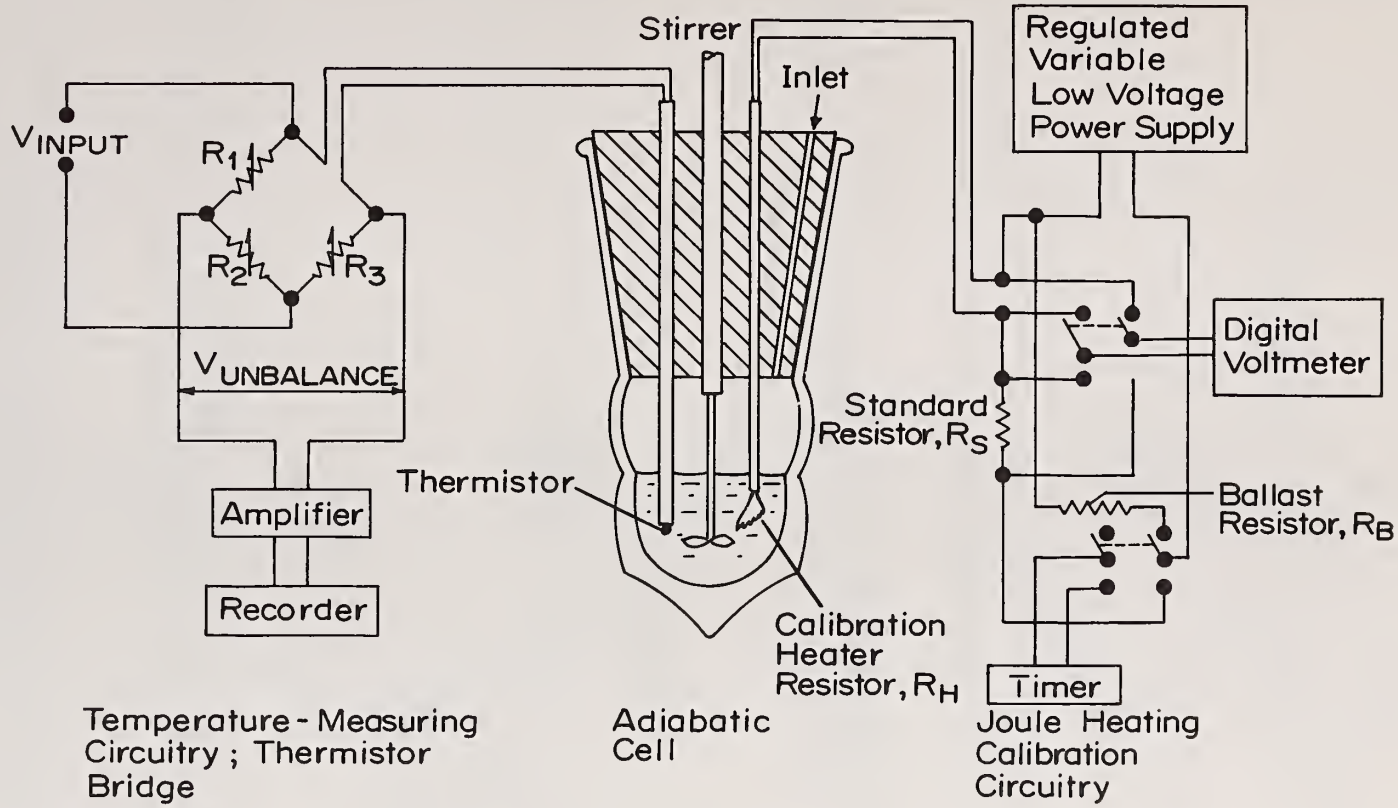

Figure 2. Versatile Enthalpimetric Analyzer for Thermometric Titrations and Direct Injection Enthalpimetry. INLET: Connected to delivery system (e.g., motor-driven buret or syringe injector). Based on Reference 24, viz., Anal. Chem., 48, 427A (1976). Reprinted with the permission of the copyright owner, the AMERICAN CHEMICAL SOCIETY.

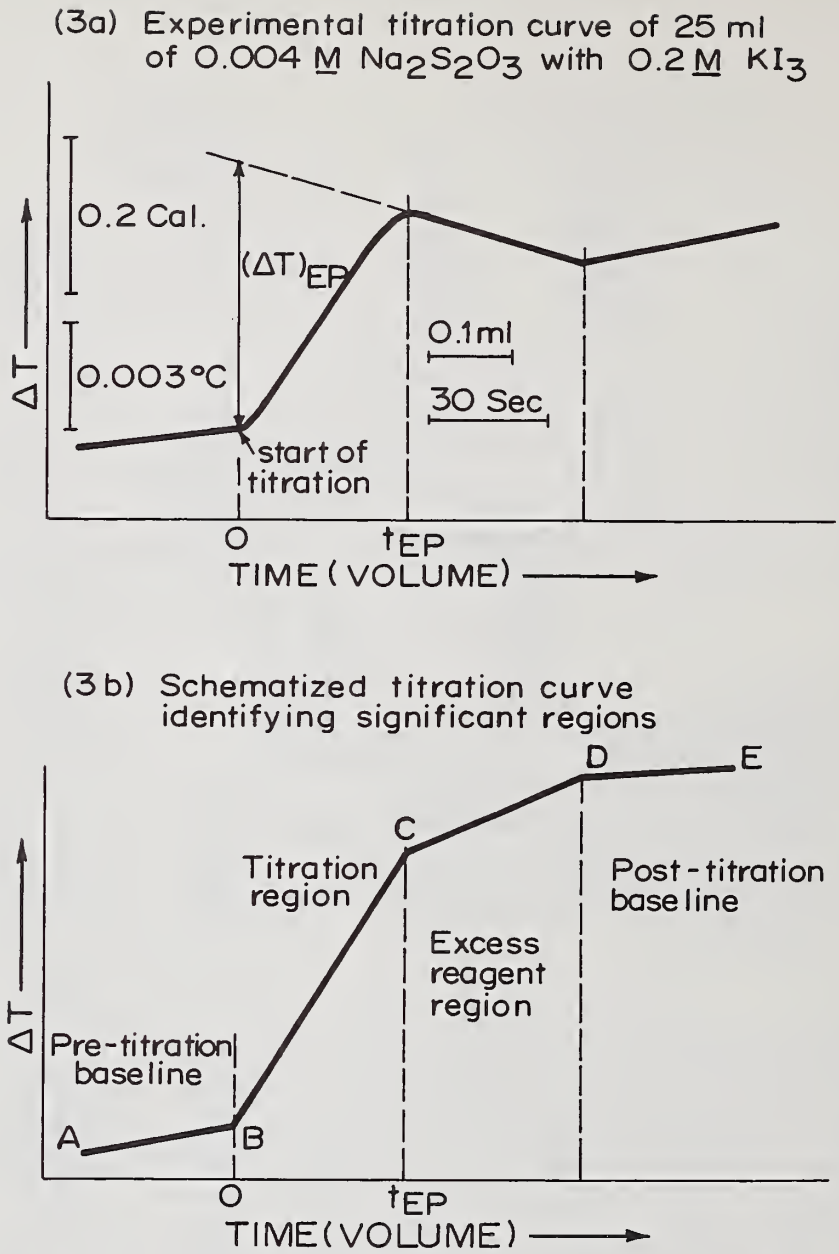

Figure 3. Thermometric enthalpy titration curves characteristic of reactions whose equilibrium constant $\to\infty$ and rates are rapid. Titrant delivered at constant rate. The excess reagent line, CD, can be endothermic as in 3a, or exothermic as in 3b. The subscript EP identifies the equivalence point. Curve 3a based on reference 36.

For convenience in developing a general mathematical expression to describe enthalpy titration curves, the folloiwng notations are used: the "total heat flux," $F = dQ/dt$; the time coordinate corresponding to the equivalence point, C in figure 3, t_{EP}. Q designates the heat evolved as a result of all thermal processes that may occur at a given point in time during the course of the titration. By way of summarizing the many effects considered in various derivations [18,30-33], the individual thermal processes that can contribute to the total heat flux are identified in Table 2 by their nature and during which portions of

Table 2. Thermal Effects Contributing to the Total Heat Flux, F, During the Course of a Thermometric Enthalpy Titration.

Flux Term	Identity	Region Effective see figure 3
F_{stir}	Exothermic; generated by mechanical stirring	All regions
F_{ther}	Exothermic; self-heating of the thermistor	All regions
F_{vap}	Endothermic; due to evaporation of solvent (most critical in volatile, non-aqueous solvents)	All regions
F_{loss}	Endo- or exothermic; heat exchange between calorimeter and environment	All regions
F_{match}	Endo- or exothermic; temperature mismatch between titrant and calorimeter's contents	Regions BC, CD
F_{dil}	Endo- or exothermic; heat of dilution of titrant	Regions BC, CD
F_{rxn}	Endo- or exothermic; heat of reaction of interest	Region BC

the titration curve they operate. Many of these heat effects remain essentially constant throughout all the regions of the curve which they affect, when state-of-the-art instrumentation is used, i.e.,

$$F = F_{rxn} + f \text{ (a constant)} \tag{4}$$

where

$$F_{rxn} = -\Delta H \cdot (dn/dt) \tag{5}$$

and dn/dt is the rate of products formed and is determined solely by the rate at which titrant is added. The following relationships hold under these circumstances.

For the titration region:

$$0 < t < t_{EP}; \quad Q = \int_0^t [-\Delta H \cdot (dn/dt) + f] \cdot dt \tag{6a}$$

$$= -n \cdot \Delta H + ft \tag{6b}$$

For the equivalence point:

$$t = t_{EP}; \quad Q_{EP} = \int_0^{t_{EP}} [-\Delta H(dn/dt) + f] \cdot dt \tag{7a}$$

$$= -n_{EP} \cdot \Delta H + ft_{EP} \tag{7b}$$

For the excess reagent region:

$$t > t_{EP}; \quad Q = Q_{EP} + \int_{t_{EP}}^t f dt \tag{8a}$$

$$= Q_{EP} + f(t-t_{EP}) \tag{8b}$$

Calculation of the complete thermometric titration curve then simply requires the application of Equation 9.

$$\int_0^t (dT/dt)dt = \Delta T = \int_0^t (1/\kappa) \cdot F dt \tag{9}$$

Under conditions of time invariant heat capacity (κ) (approximated when the titrant concentration is greater than 100 times that of the tirand), Equation 9 simplifies at the equivalence point to

$$(\Delta T)'_{EP} = (1/\kappa) \cdot [-n_{EP} \cdot \Delta H + f \cdot t_{EP}] = Q_{EP}/\kappa \tag{10}$$

This is equivalent to Equation 1 if the term, $f \cdot t_{EP}$, can be quantitated and corrected for. A simple "back-extrapolation" procedure, illustrated in figure 3a, may be used to correct for the thermal effects contained in F, e.g., heats of dilution, temperature differences between titrant and titrand, etc.[4] The reader is referred to the literature for a thorough examination of the effect of these data manipulation techniques on precision [34], and for a more detailed treatment when certain simplifications are not valid [18,35].

The analytical relationship explicited in Equation 1 reveals an important aspect about the direct enthalpimetric use of thermometric titration curves, viz., that the temperature increment $(\Delta T)_{EP}$, (identified in figure 3a) can be used as a measure of concentration. In contradistinction, the conventional equivalence point determinative procedure relies on measuring the time (hence the volume of titrant added) corresponding to a break in the titration curve. This point is the intersection of the temperature-time plots corresponding to the titration region and the excess reagent region (point C in figure 3). In the event that such an experimental endpoint coincides with the stoichiometric equivalence point, use of thermometric titration via this procedure results in a method for determining the absolute amount of unknown in a given sample. It is clear that such a procedure may be also used to evaluate reaction stoichiometries when the concentrations of both titrand and titrant are known.

It is apparent from Equation 1 that the response variable, ΔT, in a thermometric titration is a linear function of concentration. The necessary and sufficient conditions for resolving mixtures (e.g., of Bronsted acids by thermometric titration with a strong base) are:

$$K_i/K_{i \pm 1} > 25 \tag{11}$$

$$K_i C_i > 10^{-15} \tag{12}$$

$$\Delta H_i/\Delta H_{i \pm 1} > 1.2 \tag{13}$$

where K_i denotes the ionization constant of the i^{th} component. Requirements 11, 12, and 13 are less stringent than for potentiometric titrations, where the relevant response variable (electrode potential) is a logarithmic function of concentration. In that situation, the analogous requirements are:

$$K_i/K_{i \pm 1} > 10^4 \tag{14}$$

and

$$K_i C_i > 10^{-12} \tag{15}$$

---

[4]The relevant quantities in Eq. 1, Fig. 3, and Eq. 10 are correlated as follows:

$$\Delta T = (\Delta T)_{EP} = (\Delta T)'_{EP} - f \cdot t_{EP}$$

even higher concentration of substrate, the enzyme becomes "saturated," V_o attains a constant rate (V_{MAX} in figure 7) and zero order kinetics prevail. Under such conditions ([S] remaining effectively constant throughout the entire experiment), the slope of the DIE plot represents a measure of the so-called enzymatic activity, (EA), i.e.,

$$EA = \frac{dn_S}{dt} \tag{30}$$

where (dn_S/dt) denotes the number of moles of substrate converted per unit time. Obviously,

$$Q(t) = -n_S(t) \cdot \Delta H^\circ. \tag{31}$$

Comparison of Equations 30 and 31 yields

$$EA = - \left[\frac{1}{\Delta H^\circ}\right] \cdot \left[\frac{dQ}{dt}\right]. \tag{32}$$

Equation 32 has been successfully utilized as the basis for a novel enthalpimetric enzyme assay [44]. In this context, it should be noted that the ordinate of the TET and DIE plots can interchangeably be calibrated in terms of temperature (ΔT) and/or heat evolved (Q). The correspondence (which is apparent in the dual labelings of the ordinate scales in figures 3a and 6) is contingent on maintaining effectively invariant heat capacity. If the enzymatic activity (EA) is known, the heat of reaction can be determined from Equation 32. The heat of oxidation of ethanol by nicotinamide adenine dinucleotide (NAD), catalyzed by yeast alcohol dehydrogenase, has been determined in this manner [45]. Figure 8 shows a typical time-resolved DIE plot for this reaction carried out in a 0.2 M phosphate buffer of pH 8.8. The overall process is identified in Equation 33.

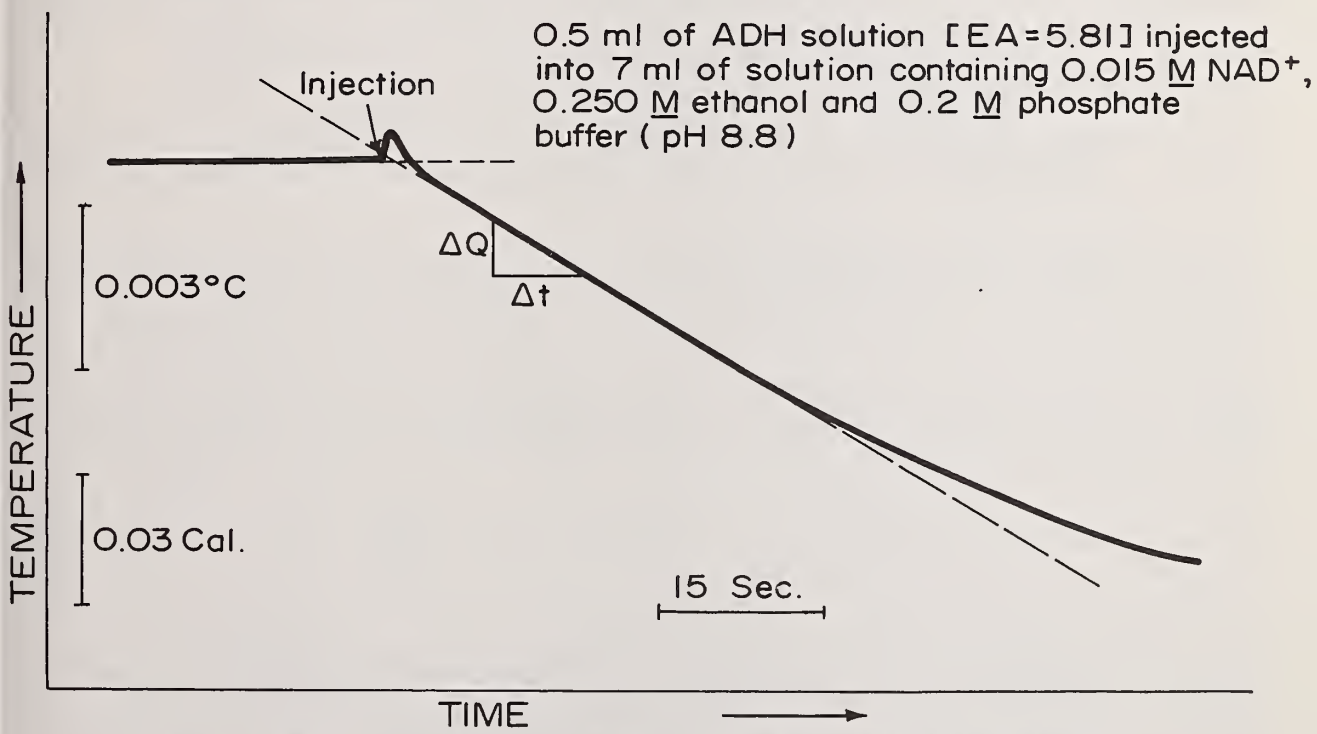

Figure 8. Time resolved DIE plot, monitoring the progress of the reaction:

$$CH_3CH_2OH + NAD^+ + HPO_4^+ = CH_3CHO + NADH + H_2PO_4^-$$

in the presence of the enzyme alcoholdehydrogenase. ΔH° = 17.6 kcal/mole was evaluated from the slope dQ/dt and Equation 32.

$$CH_3CH_2OH + NAD^+ + HPO_4^{=} = CH_3CHO + NADH + H_2PO_4^-$$

$$\Delta H^{o\prime} = 17.6 \text{ kcal/mole.} \tag{33}$$

DIE has also been applied to the determination of Michaelis constants (K_M, see figure 7) via measurements of V_o as a function of [S]. Systems recently characterized in this manner [47-49] include the hydrolysis of urea catalyzed by the enzyme urease; the conversion of pyruvate to lactate in the presence of lactate dehydrogenase; and the hydrolytic cleavage of the N-acetyl-L-tyrosine ethyl ester by the enzyme α-chymotripsin.

Thermokinetic Analysis (TKA) is a variant of the DIE method. TKA is applicable to non-separative analysis of mixtures [37-41], when several components (X_1, X_2, ... X_i) react with a given reagent at different rates (k_1, k_2, ... k_i). Differentiation can be accomplished with the aid of relationships of the form,

$$-(Q_\Sigma)_t = \sum \nu_i \cdot \Delta H_i \cdot [X_i]_o \cdot (1 - e^{-k_i t}) \tag{34}$$

$$-(Q_i)_\infty = \nu_i \cdot \Delta H_i \cdot [X_i]_o \tag{35}$$

where ν_i denotes stoichiometric coefficients and the subscript Σ identifies the cummulative effect of all the reactions occurring simultaneously. Well-known general principles and procedures of kinetic analysis [46] can be readily adapted to TKA. For instance, the determination by TKA of each and every component of a mixture containing nitromethane, nitroethane, and two isomers of nitropropane has been reported [41]. TKA can also be used as an alternate method for determining rate constants.

Continuous Flow, Flow Injection, and Segmented Flow Methods

For routine analytical use, flow methods offer a distinct advantage over batch methods. Compared to TET and DIE, flow methods require smaller samples and are faster because the long periods of thermal equilibration are obviated.

Continuous flow enthalpimetry [6-8] utilizes the principle of merging two discrete solution streams in a mixing cell where they react. The experimental setup is schematized in figure 9a. One stream contains the sample and the other the reagent. The latter is in stoichiometric excess to ensure virtually complete conversion to product. The temperature of the emerging "product stream" is monitored and provides a direct measure of sample concentration. The readout is a "step function" in whose height the desired analytical information is linearly encoded. A convenient "working equation" has been derived for continuous flow enthalpimetry from applicable heat balance considerations yielding:

$$\left[\frac{-\Delta H}{\kappa}\right] C_X = T_P \left[\frac{\Phi_R + \Phi_X}{\Phi_X}\right] - T_X - \left[\frac{\Phi_R}{\Phi_X}\right] T_R \tag{36}$$

where the subscripts X, R, and P have the same significance as in Equation 16 (X-sample moiety, R-reagent, P-product) and Φ denotes flow rates. It is apparent from Equation 36 that, if the temperatures of the sample and reagent streams (T_X and T_R) and the ratio of the flow rates are held constant, a change in sample stream concentration (C_X) will be detected as a change in the temperature (T_P) of the product stream.

(9a)

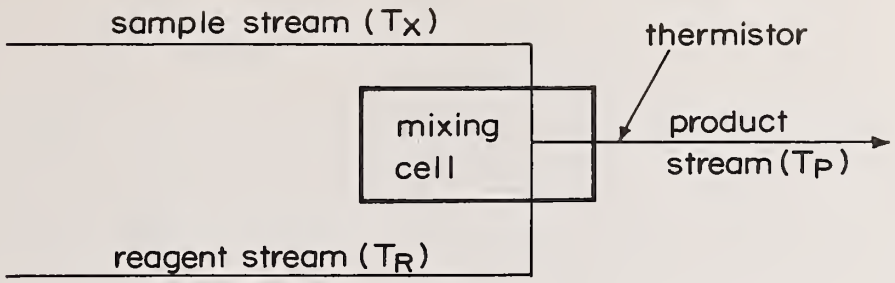

(9b)

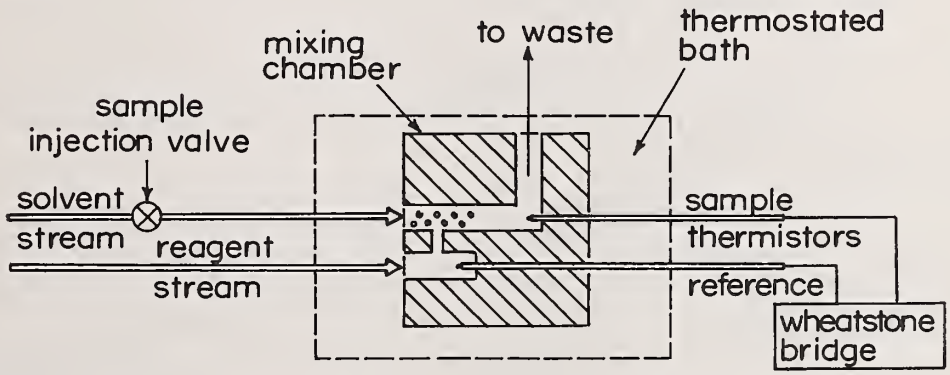

Figure 9. Flow systems for enthalpimetric analysis. Based on references [6-9]. (a) A continuous flow analyzer. (b) Block diagram of a peak enthalpimeter. The subscripts X, R, and P identify respectively the temperature (T) of the sample, reagent, and product streams.

Flow injection methods involve the injection of sample into a "carrier stream." Peak enthalpimetry utilizes two streams, viz., a "carrier" solvent and a reagent stream, which converge into a vibrating reaction chamber packed with glass beads, as shown in figure 9b. A valve joined to the solvent stream allows injection of a sample plug, approximately 100 microliters in volume. Because of diffusional spreading, the initially cylindrical plug has a Gaussian profile by the time it reaches the reaction chamber. When the two streams meet, mix, and react, the heat of the reaction is sensed as a temperature change by a differential thermistor bridge, which compares the temperature of the effluent stream to the invariant temperature of the entering reagent stream. The temperature readout is a reflection of the Gaussian concentration profile of the sample that entered the cell, i.e., the measured temperature change at any time is proportional to the instantaneous concentration of the reacting sample. The temperature profile is Gaussian in shape, reminiscent of chromatographic peaks. If the reaction proceeds to virtual completion (i.e., if the unreacted fraction of the sample is negligible), integration under the Gaussian temperature profile yields the amount of sample injected into the solvent carrier stream. The corresponding "working equation" for peak enthalpimetry is:

Equilibrium constants are an important consideration in the use of TET from another standpoint as well. Referring to figure 4, the titration of diazotized egg albumin (DEA) antibody by a haptenic agent evidences a shape characteristic of reactions whose equilibrium constant is relatively small [37]. As a result, an appreciable excess of titrant is required to drive the reaction to completion. The heat evolved during the course of the thermometric titration is proportional to the amount of product formed. Necessarily then the amount of heat, Q_{EP}, predicted by Equation 8 will not be evolved until sufficient titrant, in excess of a stoichiometric equivalent, has been added to result in virtually 100 percent conversion to products. Identifying the equivalence point under such conditions can prove difficult. It must be approximated by extrapolation from that portion of the excess reagent region of the curve where the reaction has been driven to virtual completion. It is a general property of "equilibrium curvatures" that, in principle, such extrapolations may be made. In practice, however, prohibitive limitations may arise if the relevant equilibrium constant is very unfavorable.

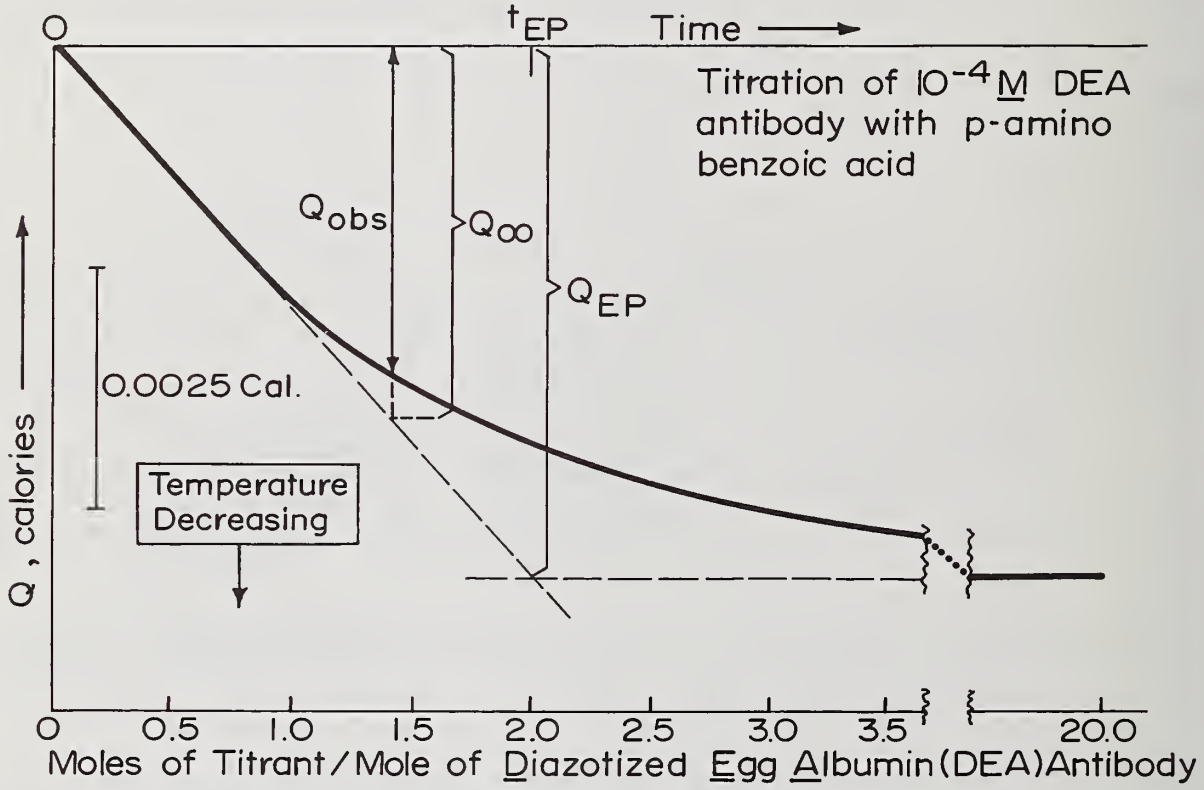

Figure 4. Thermometric enthalpy titration curve characteristic of a reaction with a relatively small equilibrium constant but a rapid rate. Intersection of dotted lines is stoichiometric equivalence point. The titrant, p-amino-benzoic acid, is a hapten which reacts specifically with the DEA-antibody titrand. Based on references 37 and 38.

Situations, where the extrapolations may be made to within specified tolerances of precision and accuracy, lend themselves to the determination of the equilibrium constant. In some instances the complete thermodynamics, i.e., ΔH°, ΔG°, and ΔS°, can be determined from a single titration curve as follows. For any reaction

$$X + R = P; \tag{16}$$

a conditional equilibrium constant is defined by the expression

$$K_{eq} = [P]/([X][R]). \tag{17}$$

Referring to figure 4, at a point ($0 < t < t_{EP}$) along the titration region, after n_R moles of titrant have been added, the equilibrium constant can be calculated by comparing the following quantities: Q_{obs} – measured on the ordinate of the actual experimental titration curve; Q_∞ – measured from the extrapolated titration curve (dotted lines in figure 4) which corresponds to the titration curve that would have been obtained were K_{eq} infinitely large. Q_{obs} is porportional to the number of moles of product, n_p, formed. Hence:

$$Q_{obs} = -\Delta H \cdot n_p = -\Delta H \cdot [P] \cdot V \tag{18}$$

where V denotes the volume of titrand. Were the equilibrium constant in fact exceedingly large, all of n_R added would yield P so long as X was available, i.e., up to the theoretical equivalence point. The heat that would have been evolved is

$$Q_\infty = -\Delta H \cdot n_R. \tag{19}$$

Denoting time by the subscript, t, the ration (Q_{obs}/Q_∞) can be expressed as

$$Q_{obs}/Q_\infty = [P]_t/n_R/V). \tag{20}$$

Equation 20 yields

$$[P]_t = (n_R/V) \cdot (Q_{obs}/Q_\infty) \tag{21}$$

The corresponding concentrations of unreacted titrant and titrand are

$$[R]_t = (n_R/V) - [P]_t = (n_R/V)[1 - (Q_{obs}/Q_\infty)] \tag{22}$$

$$[X]_t = [X]_0 - [P]_t = [X]_0 - (n_R/V)(Q_{obs}/Q_\infty) \tag{23}$$

where the initial concentration of titrand $[X]_0$ must be known. Evidently Equations 17 and 21-23 yield the equilibrium constant of Reaction 16 from the experimental titration curve, viz.,

$$K_{eq} = (Q_{obs}/Q_\infty)/[(1 - Q_{obs}/Q_\infty)([X]_0 - [n_R Q_{obs}/VQ_\infty])] \tag{24}$$

From K_{eq} the corresponding Gibbs Free Energy is readily obtained

$$\Delta G^\circ = -RT \ln K_{eq}. \tag{25}$$

Concomitantly, the TET curve also yields independently the heat of the reaction, viz.,:

$$-\Delta H^{\circ} = \frac{(Q_{\infty})_{EP}}{n_p} \tag{26}$$

and the corresponding entropy assignment

$$\Delta S^{\circ} = \frac{\Delta H^{\circ} - \Delta G^{\circ}}{T} \tag{27}$$

Analogous treatments are applicable to more complex reactions as well. The capabilities of TET for the rapid elucidation of thermodynamic parameters are documented in Table 3 for a series of immunological processes similar to the reaction illustrated in figure 4 [37,38].

Table 3. Thermodynamic Data from Enthalpy Titrations of Diazotized Egg Albumin (DEA) Antibody with Antigens (DEA and EA) and Haptens (PAB, OCB, MCD).

Titrant	Stoichiometry	ΔH° (kcal/bond)[a]	ΔG° (kcal/bond)[a]	ΔS° (eu/bond)[a]
Egg Albumin (EA)	5 antibody/EA	+ 6.9	-6.6	+45
Diazotized egg albumin (DEA)	6 antibody/DEA	+11.0	-6.6	+59
p-amino benzoic acid (PAB)	2.00 PAB/antibody	+ 8.9	-6.6	+52
o-chlorobenzoic acid (OCB)	2.01 OCB/antibody	+ 8.3	-6.6	+50
m-chlorobenzoic acid (MCB)	2.01 MCB/antibody	+ 8.4	-6.6	+50

[a]Heats, Gibbs free energies and entropies are given per "mole of immunological bonds."

A different situation prevails if the relevant reaction kinetics are slow. Simple linear extrapolations yield endpoints that have no stoichiometric significance. The rate of titrant addition becomes an artificially imposed competing rate process and, because attainment of equilibrium is not instantaneous, the temperature-time plot of a typical TET lags behind that predicted if the reaction rate were more rapid. This is apparent in figure 5. The spurious endpoints can be converted to stoichiometrically significant endpoints by solving the Ricatti Equation, which is applicable to the second order rate processes of the type [39-41]:

$$A + T' \rightarrow A' + T \tag{28}$$

Conversely, kinetically controlled TETs may be used for evaluating rate constants. The method has capabilities, in this context, comparable to stop-flow methods, but permits the utilization of simpler experimental techniques, i.e., the rate of titrant addition can be judiciously adjusted to compete with the relevant reaction.

I Idealized titration curve computed assuming reaction rate and equilibrium constant => ∞

II Experimental titration curve of 0.015 M nitromethane with NaOH $\Delta H^\circ = -7.4$ kcal/mole

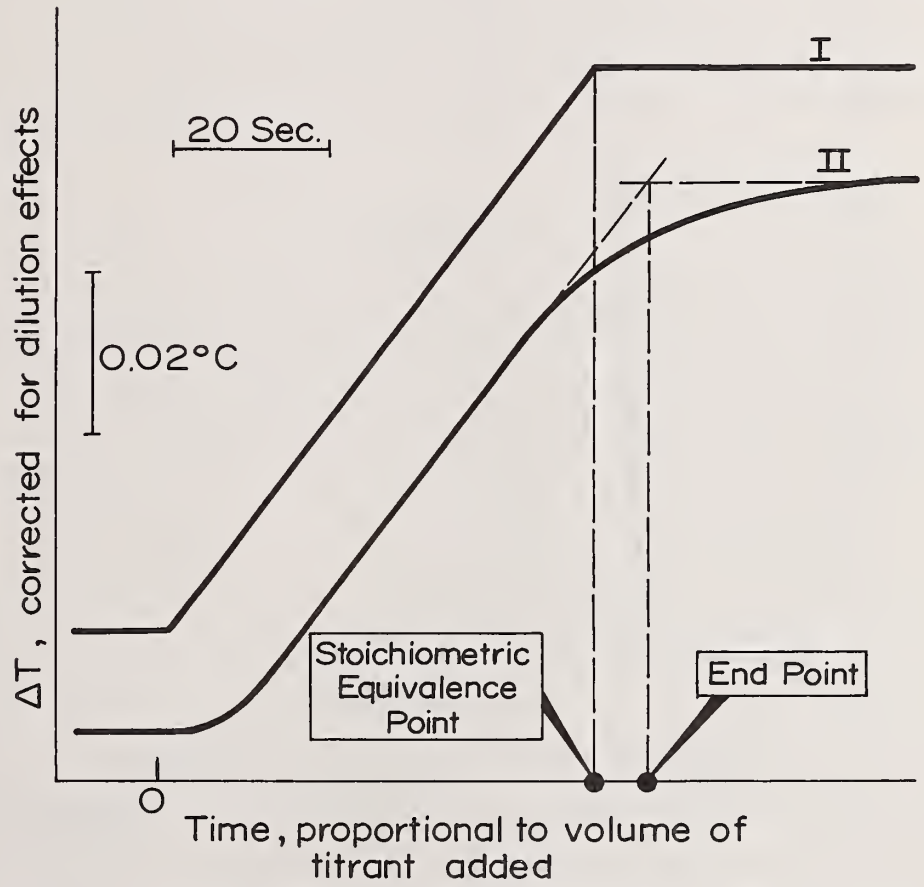

Figure 5. Effect of reaction rates on thermometric enthalpy titration curves. Curve I: Rate of titrant addition slow relative to reaction kinetics, equilibrium constant large. Curve II: Rate of titrant addition fast compared to rate of reaction, curve kinetically controlled. Based on Reference 40.

Direct Injection Enthalpimetry

Direct Injection Enthalpimetry (DIE) is a "quasi-instantaneous thermometric titration." It involves the addition of a reagent to an isothermal solution of a complementary reagent, rapid mixing and measurement of the temperature change engendered by the heat of the reaction. A typical direct injection enthalpogram is shown in figure 6. After establishment of a nearly isothermal baseline ($\overline{AB}$) excess barium chloride was injected (B) into a dilute solution of sodium sulfate, resulting in a rapid temperature rise. With the cessation of the reaction, an isothermal line ($\overline{CD}$) was re-established. Using a self-explanatory

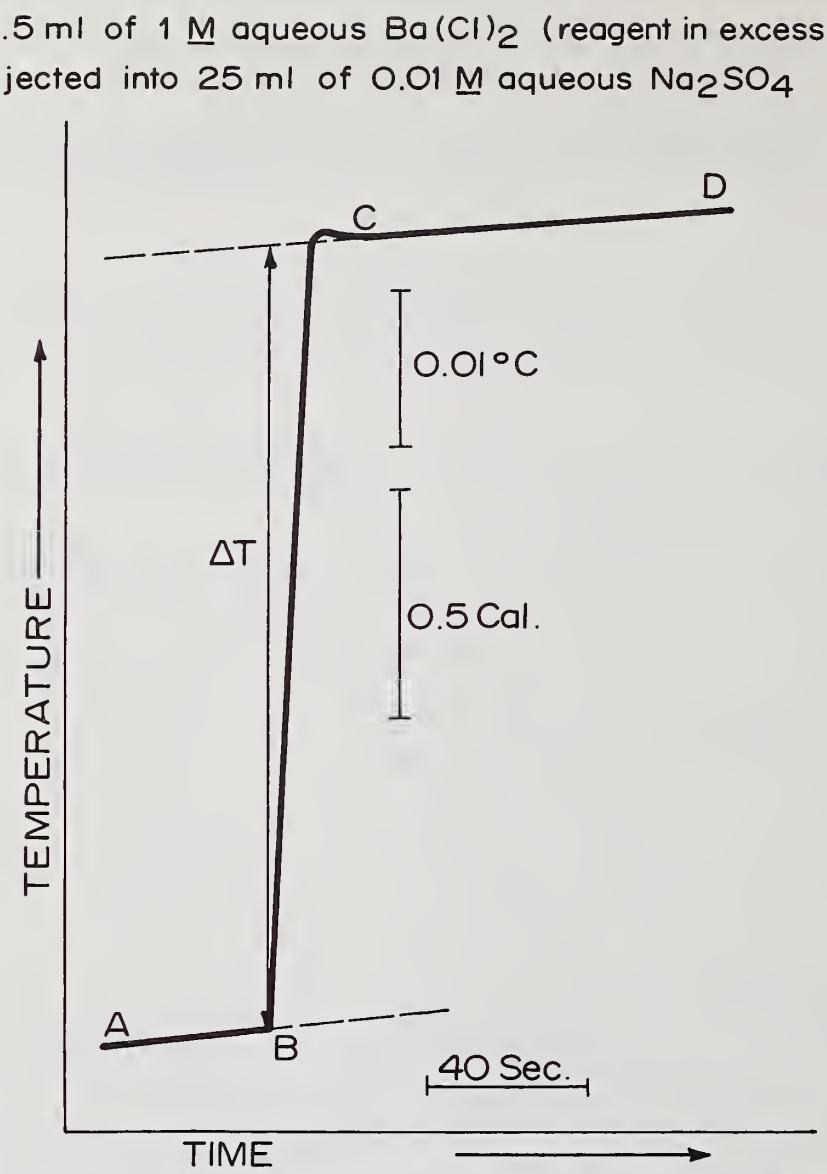

Figure 6. Direct injection enthalpogram, corresponding to the precipitation reaction:

$$SO_4^{=} + Ba^{++} = BaSO_4(s);\ \Delta H^\circ = -5.3 \text{ kcal/mole}$$

procedure, the temperature change due to the precipitation of barium sulfate (ΔT) can conveniently be measured. ΔT is directly proportional to the number of moles of reacted sample and, under conditions of effectively invariant heat capacity, to the heat of the reaction (ΔH) as well.

The "classic" mode for implementing DIE is the injection of a large excess of reagent into an isothermal sample solution, as illustrated in figure 6 and described in the previous paragraph. Alternatively, a small volume of sample may be added to a solution containing an excess reagent. The latter approach has the advantage that seriatim determinations can be carried out without refilling the adiabatic cell. An attractive feature of DIE (in either "mode") is that unstandardized reagents can be used; the exact concentration need not be known. However, the reagent must be added in sufficient excess to drive the reaction, both thermodynamically and kinetically, to virtual completion.

The concentration of a sample can be determined in two ways. The simplest approach is an empirical one. By measuring ΔT for a series of standards, concentrations may be obtained directly from a linear calibration curve. The response can be measured in any convenient units, such as calories (heat evolved or absorbed), degrees (temperature change), millivolts (unbalance potential of thermistor bridge), or recorder deflection. Of course, all determinations in a given series should be performed under identical experimental conditions (e.g., comparable volumes, etc.). As an alternative approach of quantitative analysis by DIE, the heat of the reaction can be used as the standard of reference if the heat capacity (κ) is independently determined by a calorimetric calibration procedure (e.g., joule heating, c.f., figure 2). This method is attractive since it relies directly on Equation 1, i.e., results are parametrized in terms of a fundamental thermodynamic quantity, ΔH°, in lieu of empirical standards. However, it entails a great deal of care because extraneous heat effects, such as temperature mismatch between reagents, heats of dilution, etc., must be judiciously minimized or corrected for.

Figure 6 illustrated a DIE experiment where the relevant reaction was virtually instantaneous. This accounts for the effectively vertical "temperature pulse." On the other hand, promising recent applications of DIE involved reactions which proceeded at measurable rates and took a few minutes to attain completion. Determination of glucose by the enzyme-catalyzed phosphorylation process [42,43]

$$\text{glucose} + \text{Mg(ATP)}^{2-} \xrightarrow{\text{hexokinase}} \text{glucose-6-phosphate}^{2-} + \text{Mg (ADP)}^{-} + \text{H}^{+} \qquad (29)$$

represents an example for this type of approach. Such "time-resolved DIE" can also yield thermodynamic or kinetic information. As shown in figure 7, the so-called "initial rate" (V_0) of enzymatic reactions has a hyperbolic relationship with substrate concentration, [S], viz., $[S] \cdot V_0 = \text{constant}$. At low substrate concentration, where the reaction is approximately first order, V_0 is proportional to concentration. As the substrate concentration is increased, mixed order kinetics prevail and the linearity between V_0 and [S] is "lost." At

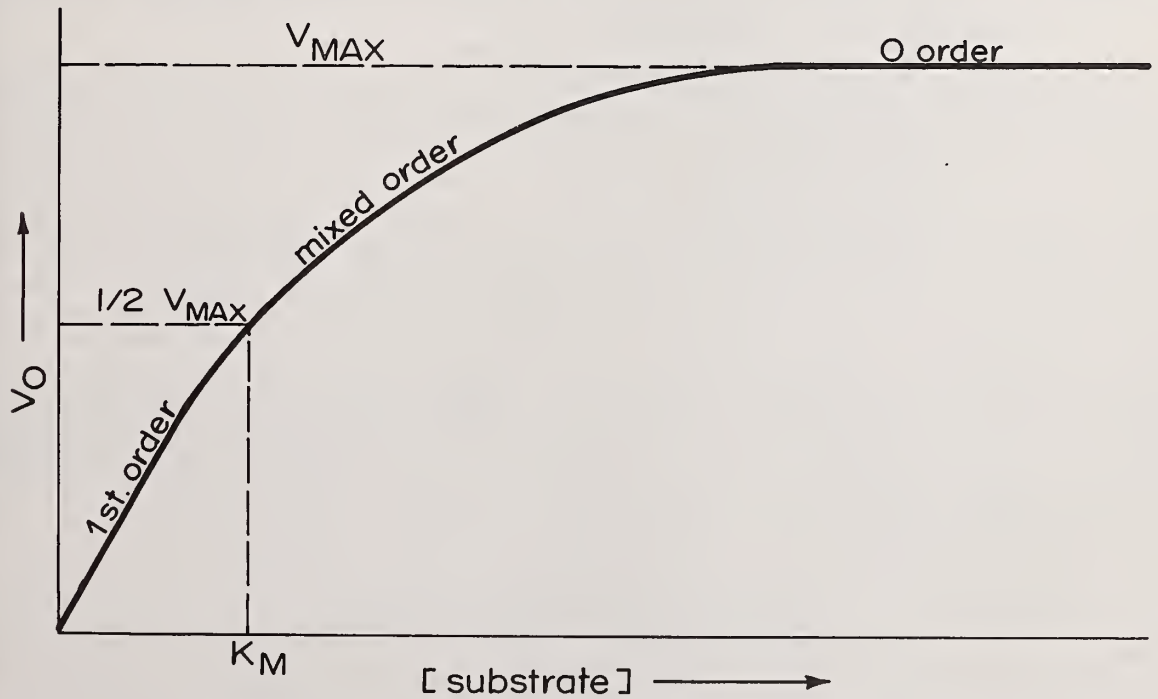

Figure 7. Plot of the initial reaction velocity (V_0) of an enzymatic reaction, as function of the initial substrate concentration. K_M–denotes the so-called Michaelis constant.

$$\int \Delta T(t)dt = \left[\frac{\Phi_X}{\Phi_X + \Phi_R}\right] \cdot \left[-\frac{\Delta H}{\kappa V}\right] \cdot n_X \qquad (37)$$

where t denotes time and V is the volume of the sample plug injected. As Equation 37 indicates, the integration of the temperature-time profile yields the analytically significant information, viz., the number of moles of sample (n_X), provided the other factors on the right side of Equation 37 are constant, viz.,

$$\left[\frac{\Phi_X}{\Phi_X + \Phi_R}\right] \cdot \left[\frac{\Delta H}{\kappa V}\right] = \text{constant}.$$

The analytical potential of peak enthalpimetry has been documented by the determination of chloride in human serum [9,50]. Advantage was taken of a classical clinical chemistry procedure, viz., titration of chloride with a standard mercuric nitrate solution yielding a salt ($HgCl_2$) which is exceptional in that it is a weak electrolyte, viz.,

$$2Cl^- + Hg^{2+} = HgCl_2; \quad \Delta H^\circ = -13.4 \text{ kcal/mole}. \qquad (38)$$

In the conventional determination the endpoint is detected by a color indicator which responds to excess Hg^{2+}. This is evidently slow and tedious. It is apparent from Equation 38 that the relevant reaction is appreciably exothermic. The peak enthalpimeter was utilized to convert the conventional procedure to a convenient and rapid method of instrumental analysis. Referring to figure 9b, a 1-molar aqueous solution of mercuric nitrate was employed as the reagent stream. The solvent stream was pure water. Chloride was successfully determined in this manner in a range of concentration between 50 and 180 milliequivalents per liter with a precision and accuracy of 1 percent. This compares with typical "high," "normal," and "low" serum chloride levels of 110, 103, and 95 milliequivalents per liter respectively. The pertinent reference [9] concludes that "by recycling a sufficiently concentrated mercuric nitrate reagent stream the seriatim performance of several hundred chloride analyses is evidently feasible. The technology for automatic injection and digital printout is readily available."

An alternate flow injection method [10] involves the use of an immobilized enzyme "reactor" column, as shown in figure 10a. This setup is particularly suited for reactions which are negligibly slow in the absence of a catalyst, but occur rapidly in the presence of a specific enzyme. Thus, reagent and sample can be premixed and transported to the enzyme column where all heat effects remain localized. The crux of this technique is to restrict the site of the reaction to the enzyme reactor. (A similar device, referred to as an "enzyme thermistor," has been described earlier by Mossbach and Danielsson [51].) A large amount of enzyme, at least a tenfold excess relative to what is required for the instantaneous conversion of the most concentrated anticipated sample, is immobilized on packed glass beads. Since the reaction does not occur until the enzyme is contacted, only one stream is needed in this type of system. A pump is used to force a carrier solution, which contains the necessary reagents, through the system under tight temperature control. At a point before the reaction column, the sample is introduced into the stream by means of a valve. A thermistor at the column exit senses, in the effluent, the temperature change which is a linear measure of sample concentration. Readouts were "peak" shaped and exhibited appreciable tailing. Peak heights, proportional to the temperature change, correlated linearly with sample concentration. The enzymatic reactor proved successful in the determination of urea via the reaction

$$NH_2CONH_2 + H_2O \xrightarrow{\text{urease}} CO_2 + 2NH_3: \qquad (39)$$

$$\Delta H^\circ = -13.17 \text{ kcal/mole}.$$

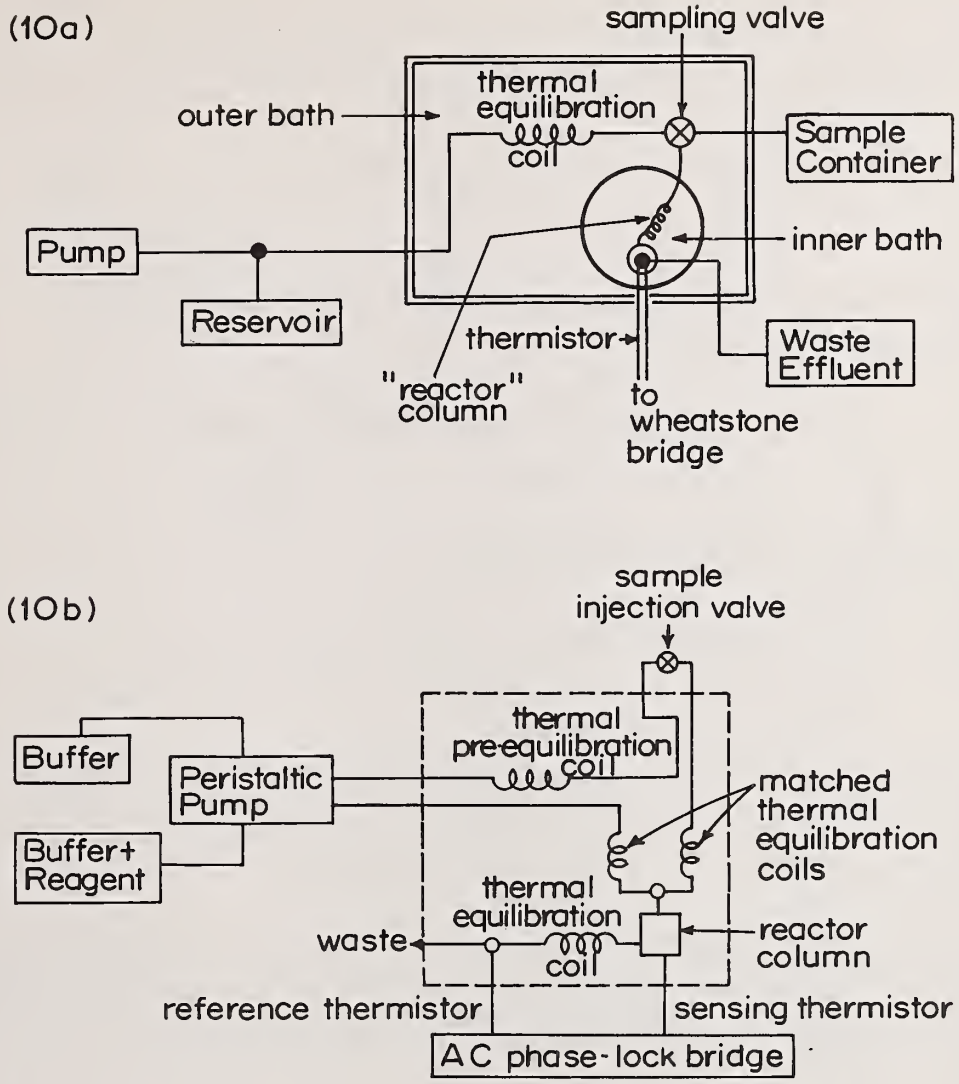

Figure 10. Flow injection analyzers. Based on references [10 and 53]. Reactor columns, thermistors, and ancillary devices are immersed in thermostated water baths. (a) For enzymatic reactions: enzyme immobilized in "reactor" column. (b) For uncatalyzed conventional chemical reactions.

By injecting 100 microliter samples of a simulated human blood serum into a stream of a 0.5 M aqueous phosphate buffer of pH 7.4, urea was determined in a range of concentration between 1 and 100 millimoles per liter at a rate of 30 analyses per hour. The precision was three percent or better.

A high sensitivity flow injection thermochemical analyzer has recently been developed [53]. The methodological approach is similar to peak enthalpimetry and the apparatus resembles the immobilized enzyme reactor (described previously in this paper) in that a packed stationary column was employed to provide mixing (however, no enzymes were used). A block diagram of the flow system is shown in figure 10b, which is self-explanatory. Sample and reagent streams are mixed just prior to entering the adiabatic reactor. Differential readouts are obtained (with the aid of an ac phase-lock Wheatstone bridge) between a "sensing thermistor" and a "reference thermistor." The sensing thermistor was positioned in the adiabatic reactor near the outlet and responded to the heat of the reaction. The reference thermistor was positioned in the effluent stream, which was thermally re-equilibrated

with the ambient constant temperature bath. Readouts (of ΔT on a time base) consisted of peaks, each corresponding to a discrete sample. The peaks were not symmetrical; tailing was apparent. Both the peak heights and the corresponding integrals were linearly related to concentration. The versatility of the high sensitivity thermochemical flow injection analyzer was documented by determinations involving acid-base, complexation and oxidation-reduction reactions, viz.,

(a) acidimetric determination of tris(hydroxymethl)amino methane (THAM)

$$H^+ + THAM \rightleftharpoons HTHAM^+; \quad \Delta H = -11.3 \text{ kcal/mole;} \tag{40}$$

(b) complexation of calcium with ethyleneglycol-bis(β-amino-ethylester) N,N'-tetraacetate (EGTA)

$$Ca^{++} + H_2EGTA^{2-} + 2THAM = CaEGTA^{2-} + 2HTHAM$$
$$\Delta H = -30.6 \text{ kcal/mole;} \tag{41}$$

(c) oxidation of sulfamic acid with nitrite

$$NH_2SO_3H + HNO_2 = N_2 + HSO_4^- + H_2O + H^+;$$
$$\Delta H = -95.6 \text{ kcal/mole.} \tag{42}$$

(In the present configuration, the use of precipitation reactions is not possible in this particular analyzer since it would clog the adiabatic column.) Using 120 microliter samples, a precision of 1-3 percent was attained. The analysis rate was 60 samples (120 microliters each) per hour, using an optimum flow rate of 2.5 mL/min. Sample carry-over was negligible.

Segmented flow methods [54] have had a major impact on the automation of applied analytical chemistry during the second half of the current century. They differ substantially from continuous flow and flow injection methods [55], which have been discussed earlier in this section. The salient distinctive feature of segmented flow procedures is that solutions containing sample are moved through the system as discrete plugs.

Peuschel and Hagedorn [11-14] have devleloped an automated thermometric analyzer which relies on the principles of segmented flow methodology. The modular instrumental system is outlined in figure 11. Precise amounts of sample are aspirated by a peristaltic pump. Successive samples are then "segmented" with air, i.e., each liquid sample segment is intercalated between two air pockets. The segmentation serves to restrict axial dispersion and preserve the integrity of the sample. If needed, the plug is diluted and made to flow through a helical coil to ensure complete mixing of the sample and diluent. The sample stream, and a separate unsegmented reagent stream, are then passed through the so-called "thermometric flow cell." Prior to entry into the thermometric cell, the two streams are de-bubbled and thermally equilibrated to a matching temperature within ±0.005°. This is important in this system since only one thermistor is used rather than a differential setup. In the thermometric cell, the two streams are vigorously mixed by means of a mechanical stirrer and the relevant reaction occurs. The temperature change engendered by the heat of the reaction is monitored by a thermistor which is embedded in the inner surface of the cell and incorporated into a Wheatstone bridge. The temperature change is recorded as the bridge unbalance potential in the usual manner. The readout consists of a series of "peaks" (each corresponding to a discrete sample), which, however, are not even qualitatively Gaussian in shape; they consist of an ascending convex trace abruptly terminated by a vertical dropoff. The analytic geometry of the rising portion is reminiscent of a bimolecular rate law plot which has been truncated before it levels off. The deflection height at its maximum (i.e., just prior to the dropoff of the signal) is empirically correlated to sample concentration by linear calibration plots which are contingent on strict control of

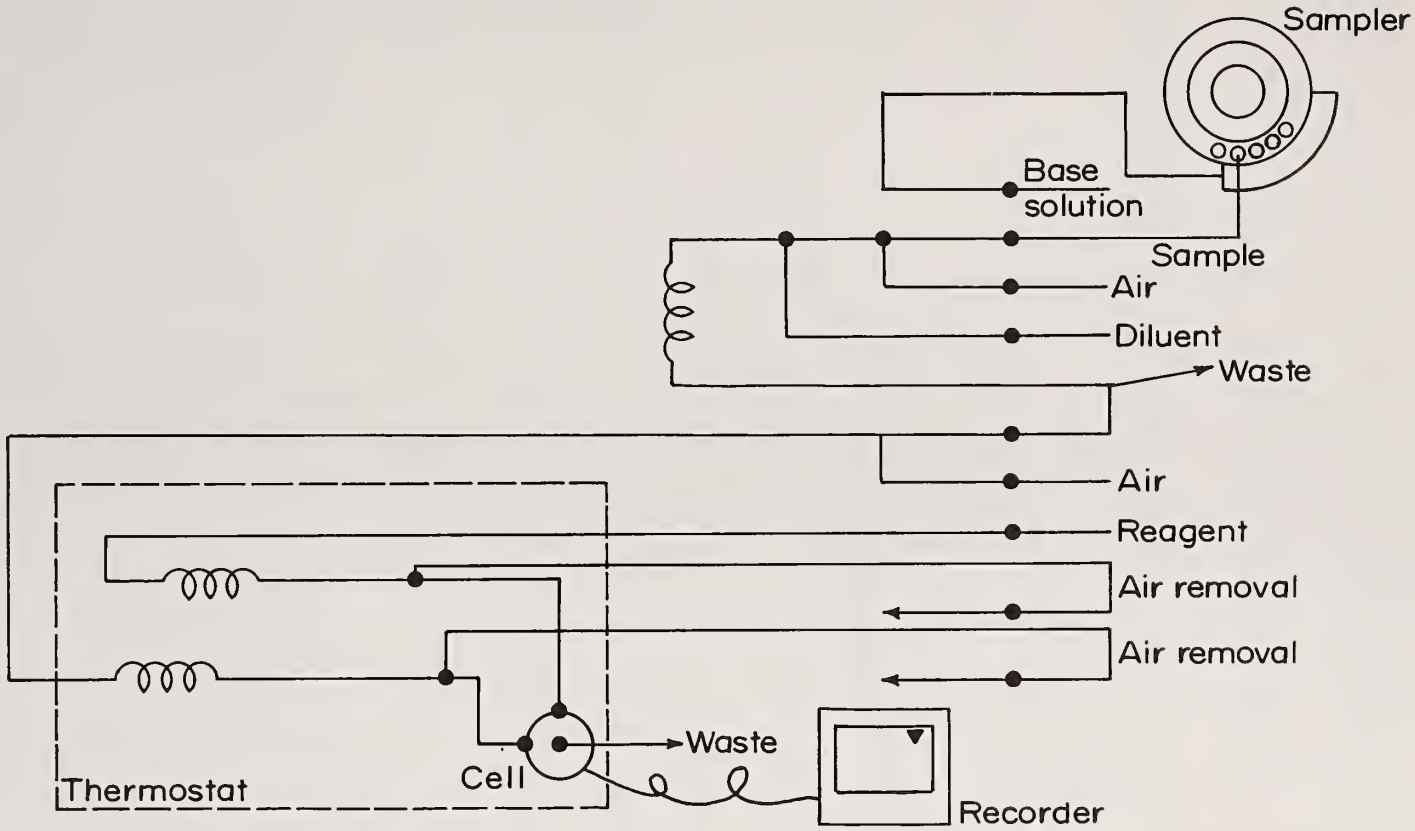

Figure 11. Schematic of a Segmented Flow Automatic Thermometric Analyzer. "Cell" denotes a thermometric flow cell equipped with a thermistor for monitoring heats of reaction. Based on References 11-14.

such experimental variables as sample size and flow rate. Each sample is allowed to react in the thermometric cell for a predetermined fixed time; the aim is to truncate the response curve when the reaction in the thermistor cell has attained a precisely reproducible fraction of completeness (which may be appreciably less than 100%). The design of the thermometric cell limits samples to a minimum size of a 1 mL and to relatively high concentrations. However, as many as 40 samples per hour can be processed. A synopsis of representative determinations, in a wide variety of materials, is presented in Table 4, which documents the versatility of the segmented flow thermometric analyzer. The chemical reactions utilized included acid-base, precipitation and oxidation-reduction processes.

Table 4. Selected Examples of Determinations with the Flow Injection Automatic Thermometric Analyzer.[a]

Determined Moiety	Reaction Employed	Reagent	Nature of Analyzed Material	Dynamic Range	Precision
Ammonia	Conversion to hexamethylenetetramine	Formaldehyde	Fertilizer	5%-7% N_2	0.02%
Magnesium	Precipitation of ammonium magnesium phosphate	$(NH_4)_3PO_4 + NH_4OH$	Fertilizer	0%-8%	0.04%
K_2O	Precipitation of potassium perchlorate	Perchloric acid	Fertilizer	46-63%	0.2%
Chloride	Precipitation of silver chloride	Silver nitrate	Kieserite ($MgSO_4 \cdot H_2O$) concentrates	0%-4%	0.03%
Sulfate	Precipitation of barium sulfate	Barium chloride	Fertilizer	0%-9%	0.1%
Hydrogen peroxide	Reduction of H_2O_2 to H_2O	Iodide	Aqueous solution	0.5-5%	0.02%
Sodium hydroxide	Neutralization with a strong acid	HCL	Aqueous solution	10-30 g/l	0.1 g/l

[a]Based on Reference 13.

Capabilities and Limitations

Preferred Applications

Mutually related with the heat of a reaction are a Gibbs free energy and an entropy change (Equation 27). Most conventional methods of chemical analysis depend on the prevailing equilibrium conditions and, therefore, basically on the Gibbs free energy change. In instances where ΔG° is relatively small, measurements dependent on the heat of the reaction can often yield more illuminating results because of contributions associated with the $T\,\Delta S$ term. Equations 11-15 related equilibrium constants to the capability of two techniques, TET and potentiometric titrations, to resolve a number of sequential endpoints in a mixture. The advantages of TET as a preferred method in this context have been strikingly documented [38,56] in the determination of the prototropic groups of an ovalbumin moiety (MW 43,800). That protein is a 72-valent Bronsted acid. The quantitative characterization of its prototropic groups is a formidable analytical undertaking. The difficulty is apparent from the potentiometric acid-base titration curve in figure 12. Upon addition of sodium hydroxide to the ovalbumin solution, the potentiometric titration yielded a single drawn-out inflection which did not correspond to any plausible stoichiometric equivalence

point. In contrast, the thermometric titration curve (also shown in figure 12 for comparison) exhibits three well-defined endpoints indicating the presence of 46 carboxyl, 7 imidazole, and 19 primary amine groups. The remarkable difference between the potentiometric and thermometric titration curves is accounted for by the relative values of the effective ionization constants, heats of ionization and heats of neutralization of the three different types of prototropic groups, which are listed in Table 5. The prototropic groups of hemoproteins have been characterized by an ingenious computerized combination of simultaneous thermometric and potentiometric titrations [70]. Enthalpimetric methods may be especially useful in situations where normally preferred methods fail due to the nature of the sample. For example, most types of absorption and luminescence spectroscopy are interferred with by turbidity, which has no significant effect on TET or DIE.

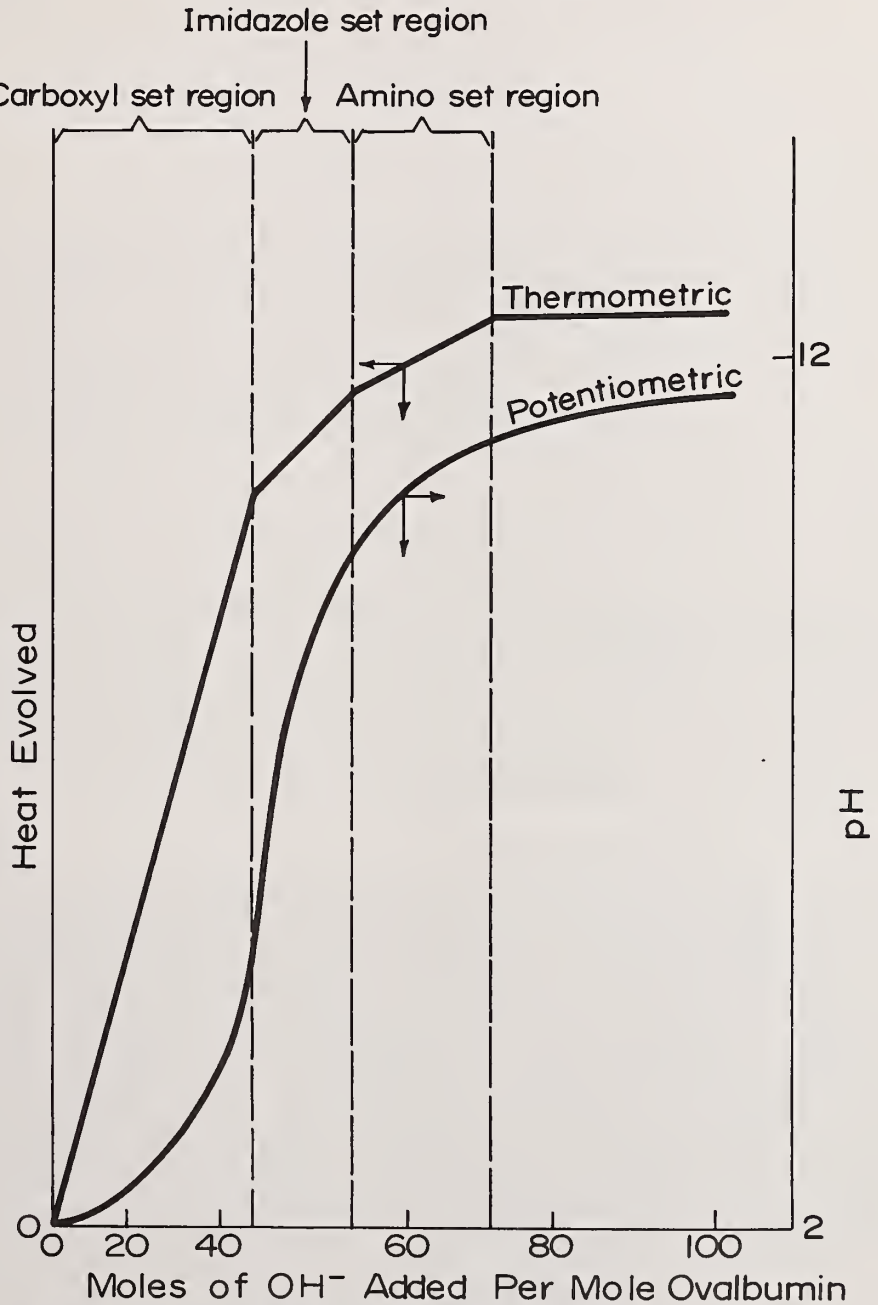

Figure 12. Comparison of thermometric and potentiometric titration curves of an ovalbumin moiety containing the following prototropic groups: 46 carboxyls, 7 imidazoles, 13 ε-amino acids. Based on reference 56.

Table 5. Ionization Constants and Thermochemical Parameters Associated with the Prototropic Groups of Ovalbumin.[a]

Prototropic Set	Ionization Constant (pK at 25°)	Heat of Ionization (kcal/mole)	Heat of Neutralization (kcal/mole)
-COOH	4.3	0	-13.4
Imidazole	7.5	7.5	- 5.9
$-NH_3^+$	10.4	12.5	- 0.9

[a]Based on Reference 56.

Enzymatic and Immunological Reactions

As previously mentioned, the main drawback of enthalpimetric methods is their lack of specificity, which must emanate from the chemistry involved. Consequently, the judicious selection of the types of reactions and reagents used is crucial. Immunological reactions represent a preferred choice, because high specificity is the most salient characteristic of their very nature. A more indirect, but very powerful, approach to enhance specificity is reliance on reactions which are slow *per se*, but can be catalyzed by enzymes. The degree of specificity depends on the chemical properties of the enzyme which determine the number and type of compounds it will bind and act upon. In order to minimize side reactions, great care must be taken in picking the correct enzyme-substrate system. Many recent reports have been published in the literature describing work implicating two mutually complementary objectives, viz.,

(a) the use of enzymes for developing new thermoanalytical techniques;

(b) utilization of thermochemical methods as a new approach for the investigation of enzyme-catalyzed mechanisms.

Selected aspects of immunological and enzymatic enthalpimetry have been described earlier in this write-up. Others are discussed below in the section on national needs. One particularly challenging prospect is to superimpose rapid enthalpimetric techniques (in lieu of radioactive tracers) on the numerous known methods of radioimmunoassay. This may add a genuinely novel dimension to clinical chemistry.

Indirect Analysis by Non-Selective Reagents

If sufficiently specific reagents are not available for each and every component of a mixture, their non-separative analysis by direct injection enthalpimetry may nevertheless be feasible. Means of implementation have been discussed in recent papers [25,57,58]. The principle is to measure heats engendered by z different reactions for quantitating z components. Each reaction may implicate some or all the components of the sample. As many as z different reagents may be used, which need not be selective and may react with some (or all) the components. However, each reagent must have a different heat of reaction with every component with which it reacts. In this context, it should be noted that it is *not necessary* that as many as z different reagents be used, but rather only that z different "thermochemically distinguishable" reactions occur. Changes in pH of the milieu in which a pH dependent reaction occurs can result in a sufficiently altered heat, as may simply changing the nature of the buffering medium used if substantial differences in the heats of ionization are involved. A set of z simultaneous equations of the form

$$(\Delta T)_z = \frac{1}{\kappa}\left[\sum_i -n_i \cdot \Delta H^\circ_{zi} + Q_{dil,j}\right] \qquad (43)$$

are obtained in this manner. In Equation 43, the various symbols have the following significance: the subscripts i, j, and z identify, respectively, components, reagents, and thermochemically distinguishable reactions; ΔT denotes the "temperature pulse" identified in figure 6; κ-heat capacity, Q_{dil}-heat of dilution of the reagent used. The set of measured temperature pulses (ΔT) can be related to the discrete amount of each component (n_i) if the individual reaction enthalpies (ΔH°_{zi}) and heats of dilution (Q_{dil}) are known.

Potentialities of the indirect DIE method based on Equation 43 have been documented [57], e.g., by the analysis of a ternary mixture of chloride, bromide, and iodide, using precipitation reactions of the halides with silver nitrate and their oxidation with Chloramin-T, viz.,

$$Cl^- + Ag^+ = AgCl(s) \text{ in } 0.01 \text{ M } HNO_3 \quad (44a)$$

$$Br^- + Ag^+ = AgBr(s) \text{ in } 0.01 \text{ M } HNO_3 \quad (44b)$$

$$I^- + Ag^+ = AgI(s) \text{ in } 0.01 \text{ M } HNO_3 \quad (44c)$$

$$2Br^- + HClO + H^+ = Br_2 + Cl^- + H_2O \text{ in } 0.001 \text{ M } HCl \quad (45b)$$

$$2I^- + HClO + H^+ = I_2 + Cl^- + H_2O \text{ in } 0.001 \text{ M } HCl \quad (45c)$$

$$2I^- + ClO^- + 2HCO_3^- = I_2 + Cl^- + H_2O + 2CO_3^{2-} \text{ in} \quad (46c)$$

carbonate-bicarbonate buffer of pH 8.9

Precision and accuracy of two percent were attained. The applicability of Equation 43 is evidently contingent on the additivity of the reaction heats ($-n \cdot \Delta H_{zi}$), i.e., a particular component must generate the same heat in a given reaction, irrespective of the other reactions occurring simultaneously. This requirement has been referred to by some authors [25] as the postulate of "partial system molar heats." Its validity is obvious in dilute solutions (see Equation 2) on elementary thermodynamic considerations, because ΔH° is a function of state.

Applications to National Needs

Clinical Chemistry

Requirements for a good clinical method of analysis include certain attributes, such as specificity, sensitivity, and imperviousness to interferences which are invariably present. Thermometric methods have been shown to possess the requisite capabilities. Discussed below are a few selected examples of recent work which foreshadow that enthalpimetric analysis may contribute materially towards reinforcing current trends of converting clinical chemistry from the status of yesteryear's art to a modern instrumental science. A promising recent advance is the development of enthalpimetric flow systems utilizing immobilized enzyme reactors of the type discussed in a preceding section of this paper. Representative performance capabilities include the determination of urea in serum via Reaction 39 utilizing a reactor column packed with immobilized urease and improved twin-thermistor instrumentation [59]. Human serum samples (120 microliter in size) were analyzed at a rate of 40 per hour. The dynamic range of the method extended to an upper limit of 75 mg of urea-nitrogen per liter. By replacing the urease column with a hexokinase packing, the same system was used to determine serum glucose levels [60]. The reaction involved was the hexokinase catalyzed phosphorylation of glucose (Equation 29). A linear calibration curve was found to hold up to glucose concentrations of 25 millimoles per liter using 100-150 microliter serum samples. It seems most probable that enthalpimetric analysis will make further inroads into clinical chemistry in future years. In particular, the automation of immunological testing (including blood typing) is long overdue. The inherent specificity

of antibody-antigen and antibody-hapten interactions earmark them as prime candidates for instrumental analysis by enthalpimetric methods.

Besides flow systems, immobilized enzymes have been used in other configurations [52,61,62]. Glucose has been determined on enzymes bound to the tip of a thermistor by cross-linked coating [52], as shown in figure 13a. Two thermistors, a so-called "measuring thermistor" and a "reference thermistor," were used. They were incorporated as two arms of a differential Wheatstone bridge. Both thermistors were coated with albumin. The "measuring thermistor" was also coated with an appropriate enzyme. The enzyme and albumin were cross-linked with a gluteraldehyde. A perforated glass jacket was placed around the thermistors to permit access of ambient solutions to the enzyme but minimize heat dissipation. The following general procedure was used. The "measuring thermistor" shown in figure 13a (referred to as an enzyme-bound thermistor, EBT) and the "reference thermistor"

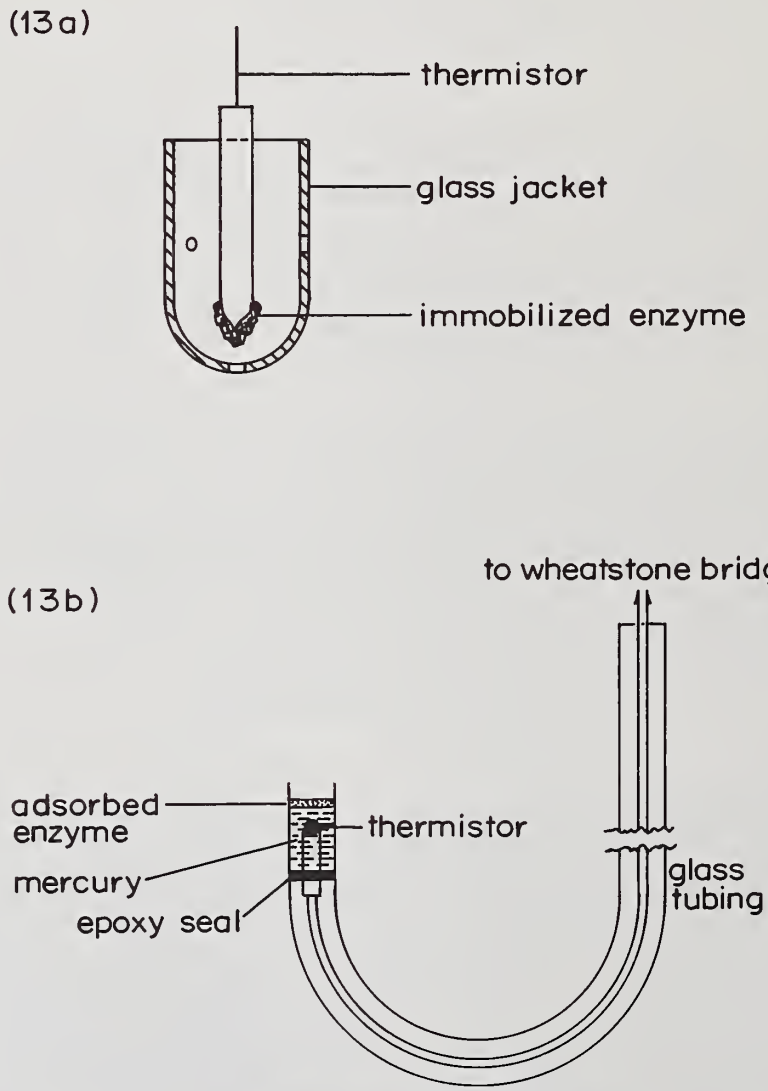

Figure 13. Design features of enzymes immobilized on thermistors. 13a: Enzyme bound thermistor (EBT) with enzyme immobilized by cross-linked coating. The glass jacket shown was perforated to permit access to ambient solutions. 13b: Thermistor enzyme probe (TEP) with enzyme immobilized by adsorption on mercury. Based on references 52 and 62. Redrawn with permission of the copyright owners. 13b courtesy of Analytical Chemistry and the American Chemical Society.

were placed into a solution (containing the appropriate reagents and buffer) which permeated the space between the perforated glass jacket and the immobilized enzyme. After a baseline was established, the sample (a substrate appropriate for the immobilized enzyme) was introduced into the stirred ambient solution. This engendered a temperature change at the EBT due to the heat evolved (or absorbed) by the chemical reaction occurring at the enzyme-coated surface. When concentrations were adjusted to yield first order kinetics, the temperature change (ΔT) at the EBT was proportional to sample concentration. ΔT was a valid linear measure of the initial reaction velocity, V_0 (see figure 7), under the prevailing experimental conditions. For the determination of glucose, two enzymes were immobilized on the EBT, viz., glucose oxidase (GOD) and catalase. Glucose served as the substrate for Reaction 47, for which the enzyme GOD is known to be a highly specific catalyst.

$$H_2O + \beta\text{-D-glucose} + O_2 \xrightarrow{GOD} H_2O_2 + \text{D-gluconic acid} \qquad (47)$$

The molecular oxygen required by Reaction 47 was generated *in situ* from hydrogen peroxide via Reaction 48.

$$H_2O_2 \xrightarrow{\text{catalase}} 1/2\ O_2 + H_2O. \qquad (48)$$

The prevalence of pseudo-first-order kinetics for Reaction 47 was obviously contingent on an invariant oxygen concentration. This was maintained by an ingenious technique, viz., addition *ab initio* of excess H_2O_2 to the solution which yielded a constant supply of O_2 via Reaction 48. In this manner the concentrations of glucose in plasma samples could be determined from ΔT (thermistor bridge response) with a precision of five percent for concentrations less than 0.003 mole/ℓ and two percent for concentrations greater than 0.005 mole per liter.

A novel and radically different thermistor enzyme probe (TEP) has recently been developed. It consists of an encapsulated thermistor sealed in a U-shaped piece of glass as shown in figure 13b. A thin layer of mercury covers the thermistor and serves as a site for enzyme immobilization and as a heat conductor. An enzyme can be adsorbed at the mercury surface by immersing the TEP into an appropriate solution or suspension. The TEP is subsequently washed, while the enzyme remains immobilized on the mercury. To carry out an analysis, the TEP is placed into a solution containing a buffer (and—if necessary—complementary reagents), along with a reference thermistor (same as the TEP, except *without* any enzyme adsorbed on the mercury). The two sensors are wired into a differential Wheatstone bridge, whose unbalance potential measures changes in the temperature of the TEP. When a sample is present which can function as a substrate of the immobilized enzyme, ΔT yields a linear measure of the relevant concentration. The readout signal of the thermistor bridge resembles a time resolved DIE-plot which levels off at a plateau: the latter corresponds to ΔT (see figure 6). The capabilities of TEP methods have been documented [62] by determining urea concentrations, while the hydrolytic enzyme urease was adsorbed on the mercury surface of the TEP.

Two further imaginative illustrations might suffice to delineate the scope and potential of enthalpimetric methods of analysis in the clinical field.

(a) "Prothrombin time," a critical blood chemistry parameter, has been determined with the aid of an entirely novel calorimetric approach [63,64]. Onset of coagulation was detected by an abrupt surge in the temperature of a thermistor probe which was immersed in a human blood sample. The probe was wired in a conventional Wheatstone bridge circuit, with a current (i = 2 milliampere) passing through the thermistor whose resistance (ρ) was 2000 ohm. The probe temperature reflected the difference between the joule heating energy ($= i^2/\rho$) supplied to the thermistor and the heat conducted away into the ambient blood. Following the addition of thrombin and calcium, an abrupt increase in the probe temperature was observed. The time-lapse corresponded accurately to the prothrombin time. The enhanced self-heating effect is accounted for by a diminution in the heat transferred at the thermistor/liquid interface.

(b) A method has very recently been reported [65] for determining serum cholinesterase activity (which serves as a means of monitoring liver function) by DIE, using the hydrolysis Reaction 49.

$$C_3H_7COO(CH_2)_2\overset{+}{N}(CH_3)_3I^- + H_2 \xrightarrow{\text{cholinesterase}} C_3H_7COOH + HO(CH_2)_2\overset{+}{N}(CH_3)_3I^-; \quad (49)$$

$$-0.3 < \Delta H^\circ_{49} < \text{zero kcal/mole.}$$

The heat of this reaction is too small for reliable quantitation. An ingenious stratagem was employed to circumvent this difficulty, by coupling Reaction 49 to a proton transfer process between butanoic acid (which is one of the two products of the hydrolysis) and the Bronsted conjugate base form of the THAM [tris(hydroxymethyl)amino methane, R-NH_2] buffer which was used for pH control, viz.,

$$R\text{-}NH_2 + HOOC\text{-}C_3H_7 = R\text{-}\overset{+}{N}H_3 + \bar{O}OC\text{-}C_3H_7: \quad (50)$$

$$\Delta H^\circ_{50} = -11.3 \text{ kcal/mole}$$

Thus, the heat of the effectively athermic Reaction 49 was "amplified" forty-fold. Substituting ΔH°_{50} into Equation 32, the serum enzyme cholinesterase was successfully assayed at physiological concentration levels. Precision and accuracy of two percent were attained.

Coal Conversion Technologies

Enthalpimetric methods of analysis are playing a major role in an effort in progress in our laboratories to lay the foundations for a new comprehensive approach for monitoring sulfur contaminants in the new coal-based energy technologies [66]. A broad program has been initiated encompassing the analytical requirements of diverse processes, ranging from removal of sulfur from flue gases and coal liquefaction, to coal gasification and magneto-hydrodynamic (MHD) power generation. The overall aim of the project is to provide a comprehensive capability for the quantitative analysis of all compounds involved in the "sulfur balance" of coal-based process streams. The crux of this effort is the concomitant use of several different methodologies. If the same quantitative assignment can be substantiated by independent measurements, which are not prone to similar sources of error, the result is expected to be virtually fail-safe. On these considerations, it is obviously desirable to rely on methods whose conceptual foundations are as diverse as possible. Enthalpimetric analysis possesses genuinely unique features in this context, including the significant involvement of entropies (Equation 27). Thus, it provides an ideal methodological balance in conjunction with other instrumental techniques, e.g., mass spectrometry and electroanalysis [66]. Work is in progress [36] on the enthalpimetric determination of sulfur in the +4 and -2 oxidation states (viz., SO_2, HSO_3^-, SO_3^{2-}, and H_2S, HS^-, S^{2-}) using reagents which are highly specific, viz., formaldehyde for S(+IV) moieties and the organometallic compound o-hydroxy mercury benzoate (HMB) for S(-II) species. The relevant thermochemistry transpires from Equations 51-53.

$$HSO_3^- + H_2CO = HOCH_2 \cdot SO_3^-; \Delta H^\circ = -13.0 \text{ kcal/mole} \quad (51)$$

$$HS^- + 2HMB = S(MB)_2 + H_2O + OH^-; \Delta H^\circ = -32.7 \text{ kcal/mole} \quad (52)$$

$$H_2S(g) + 2HMB = S(MB)_2 + 2H_2O; \Delta H^\circ = -44 \text{ kcal/mole} \quad (53)$$

Typical results of corresponding DIE determinations are shown in figures 14 and 15. The latter provides an illustration of "gas enthalpimetry" [68,69]. Enthalpimetric analysis is readily amenable to the use of gaseous samples and/or gaseous reagents. In fact, gases are preferable to liquids in this context, because the smaller the specific heats, the less the interfering heat capacity effects. Quite generally, enthalpimetric analysis is remarkably catholic in its applicabilities. Its future potential is inherent in the prospect of utilizing the heats of all major categories of reactions, encompassing Bronsted and Lewis acid-base chemistry, precipitation and oxidation-reduction processes, and ranging from simple inorganic materials to complex organic and biological moieties.

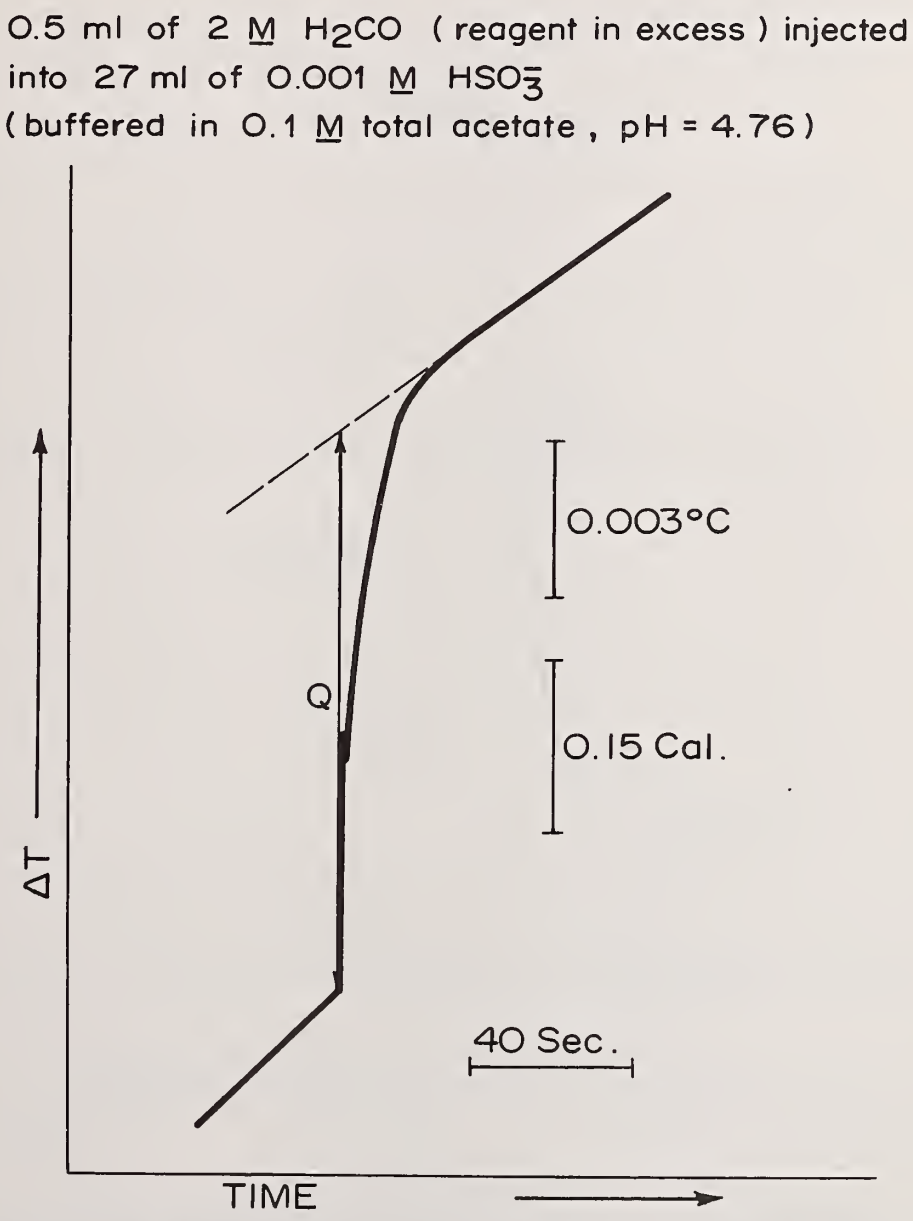

Figure 14. Determination of bisulfite by direct injection enthalpimetry via the reaction:

$$HSO_3^- + H_2CO = HOCH_2 \cdot SO_3^-;\ \Delta H^\circ = -13.0 \text{ kcal/mole.}$$

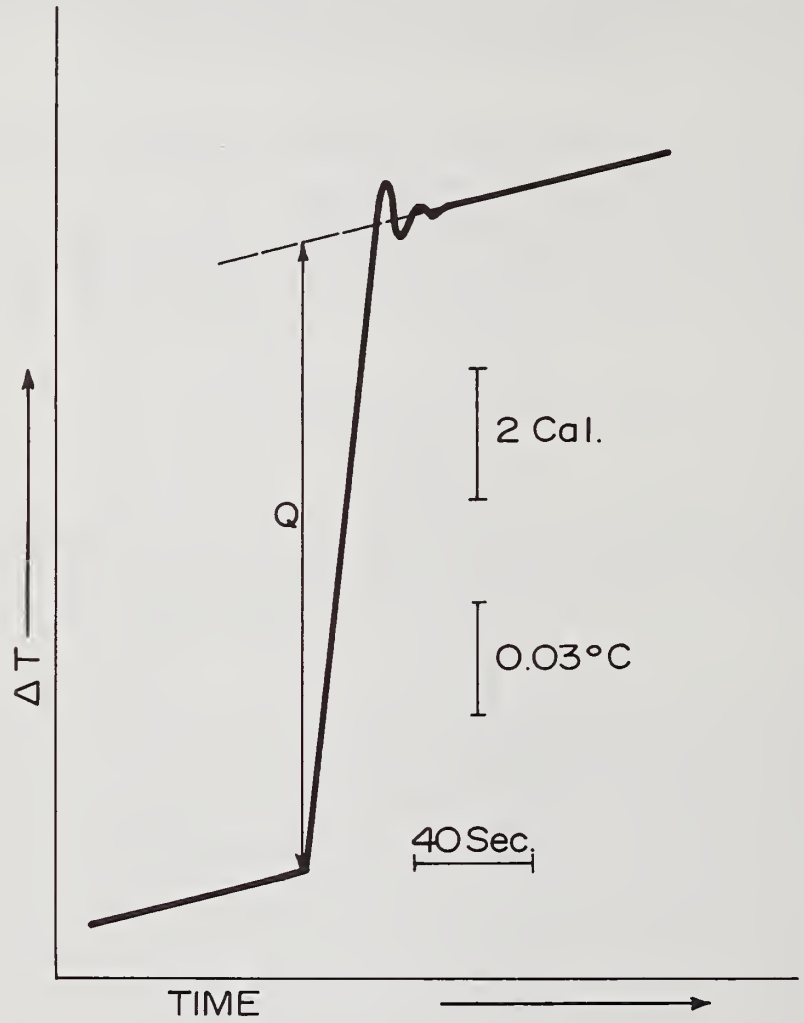

Figure 15. Determination of hydrogen sulfide by direct injection enthalpimetry via the reaction:

$$H_2S(g) + 2HMB = S(MB)_2 + 2H_2O;\ \Delta H^\circ = -44\ \text{kcal/mole}.$$

The work described in this paper was supported in part by the U.S. Department of Energy under Contract No. EF-77-S-01-2710 with The Pennsylvania State University and by Research Grant CHE 76-21666 from the National Science Foundation. The use of computer facilities whose acquisition was supported by an instrument grant from the National Science Foundation is also gratefully acknowledged.

References

[1] Goldberg, R. N. and Armstrong, G. T., Medical Instrumentation, 8, 30 (1974); Goldberg, R. N., Prosen, E. J., Staples, B. R., Boyd, R. N., Armstrong, G. T., Berger, R. L., and Young, D. S., Anal. Biochem., 64, 68 (1975); Goldberg, R. N., Biophys. Chem., 3, 192 (1975); Goldberg, R. N., Prosen, E. J., Staples, B. R., Boyd, R. N., and Armstrong, G. T., in Thermoanalytical Investigations by New Techniques, H. Kambe and P. D. Garn, Eds., Wiley, New York, 1975; Evans, W. J., "The Conduction-Type Microcalorimeter," in Biochemical Microcalorimetry," H. D. Brown, Ed., Academic Press, New York, 1969, p. 257.

[2] Bell, J. M. and Cowell, C. F., J. Am. Chem. Soc., 35, 49 (1913).

[3] Linde, H. W., Rogers, L. B., and Hume, D. N., Anal. Chem., 25, 404 (1953).

[4] Jordan, J. and Alleman, T. G., Anal. Chem., 29, 9 (1957).

[5] Wasilewski, J. C., Pei, P. T., and Jordan, J., Anal. Chem., 36, 2131 (1964).

[6] Priestley, P. T., Sebborn, W. S., and Selman, R. E. W., Analyst, 90, 589 (1965).

[7] McLean, W. and Penketh, G. E., Talanta, 15, 1185 (1968); Grompton, T. R. and Cope, B., Anal. Chem., 40, 274 (1968).

[8] Yoshida, H., Taga, M., and Hikime, S., Japan Analyst, 20, 361 (1971).

[9] Censullo, A. C., Lynch, J. A., Waugh, D. H., and Jordan, J., "Biochemical and Clinical Applications of Titration Calorimetry and Enthalpimetric Analysis," in Analytical Calorimetry, R. S. Porter and J. F. Johnson, Eds., Plenum Press, New York, 1974.

[10] Canning, Jr., L. M. and Carr, P. W., Analytical Letters, 8, 359 (1975).

[11] Peuchel, G. and Hagedorn, F., Kali Steinsalz, 6, 4 (1972).

[12] Peuchel, G. and Hagedorn, F., Z. Anal. Chem., 277, 177 (1975).

[13] Hagedorn, F., Peuchel, G., and Weber, R., Analyst, 100, 810 (1975).

[14] Weber, R., Blanc, G., Peuchel, G., and Hagedorn, F., Analytical Chimica Acta, 86, 79 (1976).

[15] Tyrrell, H. J. V. and Beezer, A. E., Thermometric Titrimetry, Chapman and Hall Ltd., London, 1968.

[16] Bark, L. S. and Bark, S. M., Thermometric Titrimetry, Pergamon Press, Oxford, 1969.

[17] Vaughan, G. A., Thermometric and Enthalpimetric Titrimetry, Van Nostrand Reinhold, London, 1973.

[18] Barthel, J., Thermometric Titrations, Wiley, New York, 1975.

[19] Jordan, J., "Thermometric Enthalpy Titrations," in Treatise on Analytical Chemistry, I. M. Kolthoff and P. J. Elving, Eds., Part I, Vol. 8, p. 5175, Interscience, New York, 1968.

[20] Bark, L. S., Bate, P., and Grime, J. K., "Thermometric and Enthalpimetric Titrimetry," in Selected Annual Reviews of the Analytical Sciences, Vol. II. L. S. Bark, Ed., Society for Analytical Chemistry, London, 1972.

[21] Christensen, J. J. and Izatt, R. M., "Thermochemistry in Inorganic Solution Chemistry," in Physical Methods in Advanced Inorganic Chemistry, H. A. O. Hill and P. Day, Eds., Interscience, New York, 1968, p. 538; Hansen, L. D., Izatt, R. M., and Christensen, J. J., "Applications of Thermometric Titrimetry to Analytical Chemistry," in New Developments in Titrimetry, J. Jordan, Ed., Marcel Dekker, New York, 1974, p. 1.

[22] Carr, P. W., "Analytical and Measurement Aspects of Thermometric Titrimetry," in CRC Critical Reviews in Analytical Chemistry, Vol. 2, p. 491, Chemical Rubber Co., Cleveland, 1972.

[23] Spink C. H. and Wadso, I., "Calorimetry as an Analytical Tool in Biochemistry and Biology," in Methods of Biochemical Analysis, Vol. 23, p. 1, D. Glick, Ed., Wiley, New York, 1976.

[24] Jordan, J., Grime, J. K., Waugh, D. H., Miller, C. D., Cullis, H. M., and Lohr, D., Anal. Chem., 48, 427A (1976).

[25] Bark, L. S., J. Thermal Anal., 12, 265 (1977).

[26] Barthel, J., Becker, F., and Schmahl, N. G., Z. Phys. Chem. (Frankfurt), 29, 57 (1961).

[27] Christensen, J. J., Gardner, J. W., Eatough, D. J., Izatt, R. M., and Hart, R. M., Rev. Sci. Instrum., 44, 481 (1973).

[28] Bowers, L. D. and Carr, P. W., Thermochim. Acta, 10, 129 (1974).

[29] Van Til, A. E. and Johnson, D. C., Thermochim. Acta, 23, 1 (1978).

[30] Keily, H. J. and Hume, D. N., Anal. Chem., 28, 1294 (1956).

[31] Christensen, J. J., Izatt, R. M., Hansen, L. D., and Partridge, J. A., J. Phys. Chem., 70, 2003 (1966).

[32] Barthel, J., Becker, F., and Schmahl, N. G., Z. Phys. Chem. (Frankfurt), 35, 3 (1963).

[33] Barthel, J., Becker, F., and Schmahl, N. G., Z. Phys. Chem. (Frankfurt), 37, 52 (1963).

[34] Bowers, L. D. and Carr, P. W., Thermochim. Acta. 3, 427 (1972).

[35] Piloyan, G. E. and Dalinina, U. V., Talanta, 21, 975 (1974).

[36] Stutts, J. D., Thesis in Progress, Pennsylvania State University (1980).

[37] Jordan, J. and Jespersen, N. D., Coll. Int. Cent. Nat. Rech. Sci., 20, 59 (1972).

[38] Jespersen, N. D., Thesis, Pennsylvania State University, 1971.

[39] Jordan, J. and Carr, P. W., "Enthalpimetric Analysis," in Analytical Calorimetry, R. S. Porter and J. F. Johnson, Eds., Plenum Press, New York, 1968, p. 203.

[40] Carr, P. W. and Jordan, J., Anal. Chem., 45, 634 (1973).

[41] Jordan, J., Henry, R. A., and Wasilewski, J. C., Microchem. Journ., 10, 260 (1966).

[42] McGlothlin, C. D. and Jordan, J., Anal. Chem., 47, 786 (1975).

[43] McGlothlin, C. D. and Jordan, J., Clinical Chem., 21, 741 (1975).

[44] McGlothlin, C. D. and Jordan, J., Anal. Chem., 47, 1479 (1975).

[45] Brattlie, W. J., Thesis in Progress, Pennsylvania State University (1980).

[46] Mark, Jr., H. B. and Rechnitz, G. A., Kinetics in Analytical Chemistry, Wiley Interscience, New York, 1968.

[47] Beezer, A. E., Thermochim. Acta, 7, 241 (1973).

[48] Barclay, K. and Jespersen, N. D., Analytical Letters, 8, 33 (1975).

[49] Grime, J. K., Lockhart, K., and Tan, B., Analytica Chimica Acta., 91, 243 (1977).

[50] Waugh, D. H., Thesis, Pennsylvania State University, 1978.

[51] Mosbach, K. and Danielsson, B., Biochemica Biophys. Acta, 364, 140 (1974); Mattiasson, B., Danielsson, B., and Mosbach, K., Analytical Letters, 9, 217 (1976).

[52] Tran-Minh, C. and Vallin, D., Anal. Chem., 50, 1874 (1978).

[53] Schifreen, R. S., Miller, C. S., and Carr, P. W., Anal. Chem., 51, 278 (1979).

[54] Snyder, L., Levine, J., Stoy, R., and Conetta, A., Anal. Chem., 48, 942A (1976).

[55] Betteridge, D., Anal. Chem., 50, 832A (1978).

[56] Jespersen, N. D. and Jordan, J., Analytical Letters, 3, 323 (1970); Lynch, J. A., Thesis, Pennsylvania State Unviversity, 1976.

[57] Bark, L. S. and Nya, A. E., Analytica Chimica Acta., 87, 473 (1976).

[58] Marik-Korda, P., Buzási, L., and Cserfalvi, T., Talanta, 20, 569 (1973).

[59] Bowers, L. D., Canning, Jr., L. M., Sayers, C. N., and Carr, P. W., Clinical Chem., 22, 1314 (1976).

[60] Bowers, L. D. and Carr, P. W., Clinical Chem., 22, 1427 (1976).

[61] Weaver, J. C., Cooney, C. L., Fulton, S. P., Schuler, P., and Tannenbaum, S. R., Biochim. Biophys. Acta. 452, 285 (1976).

[62] Rich, S., Ianniello, R. M., and Jespersen, N. D., Anal. Chem., 51, 204 (1979).

[63] Bostick, W. D. and Carr, P. W., Amer. J. Clin. Pathol., 60, 330 (1973).

[64] Bostick, W. D. and Carr, P. W., Anal. Chem., 46, 1095 (1974).

[65] Grime, J. K., Tan, B., and Jordan, J., Analytica Chimica Acta, In Press (1979).

[66] Jordan, J., "New Program at Penn State for Developing a Comprehensive and 'Fail-Safe' Capability for the Instrumental Analysis of Sulfur Compounds in Coal Process Streams," Research Accomplishments, 5th Annual DOE/Fossil Energy Conference on University Coal Research, University of Kentucky, 1978, CS-11, p. 223.

[67] Bark, L. S. and Nya, A. E., Thermochim. Acta, 23, 321 (1978).

[68] Duffield, B. J. and Hume, D. N., Analytical Letters, 7, 681 (1974).

[69] Zambonin, P. G. and Jordan, J., Anal. Chem., 41, 437 (1969).

[70] Marini, M. A. and Martin, C. J., Meth. Enzymol., 27, 590 (1973); Marini, M., Aminco Lab. News, 25, 8 (1969).

ENTHALPIMETRIC ANALYSIS: THERMOCHEMICAL TITRATIONS AND RELATED TOPICS

RAPPORTEUR'S COMMENTS BY

J. H. Flynn
National Bureau of Standards
Polymer Science and Standards Division
Washington, D.C. 20234

Enthalpimetric analysis is not a technique of thermal analysis. According to the ICTA Nomenclature Committee, Thermal Analysis covers techniques in which a physical property of a substance is measured as a function of temperature while the substance is subjected to a controlled temperature program. In enthalpimetric analysis changes are measured under adiabatic conditions where heat flow, an essential factor in thermal analytical techniques, is suppressed. In both enthalpimetric analysis and differential thermal analysis (DTA), enthalpic events are determined from the changes in a temperature difference between the material and its surroundings, but these surroundings remain essentially isothermal in enthalpimetric analysis whereas, in DTA, the surrounding temperature is programmed so that the enthalpic events are measured from their effects on the temperature difference set up by restricted heat flow.

In spite of these terminological antitheses, I feel that we are indeed fortunate to have Professor Jordan's informative review included in the proceedings of The State-of-the-Art of Thermal Analysis Symposium. Enthalpimetric Analysis is a powerful analytical tool and a promising method for investigation of the thermodynamics and kinetics of condensed phase systems. More importantly, and in a more direct relation to the purpose of this symposium, Professor Jordan stresses many lessons to be learned from enthalpimetric analysis on precise experimental measurement and novel programming techniques. From these, thermal analysts should find new ideas for the improvement of their own instruments and methods.

For example, thermal analytical equipment has lagged far behind the state-of-the-art in precise measurements of sample temperature. The use of thermistors and Curie-point sensors, as described in this paper, should be of particular interest. Also, it is only in the past decade that DSC and DTA techniques have been extended appreciably to low-temperature, non-solid state systems such as aqueous enzyme reactions. The handling of solid-liquid, solid-gas and liquid-gas phase reactions by stopped flow, flow injection, segmented flow and other techniques and, in general, the programmed mixing of fluid reactants should find parallel application in many of the conventional techniques of thermal analysis.

The reader will find this paper an excellent review of its field. It will be a source of inspiration for those interested in extending the frontiers of thermal analytical methods toward new and relevant applications, better instrumentation and innovative programming techniques.

National Bureau of Standards Special Publication 580. Proceedings of the Workshop on the State-of-the-Art of Thermal Analysis held at NBS, Gaithersburg, MD, May 21-22, 1979. (Issued May 1980)

CHEMICAL COMPLEXES

Paul D. Garn

The University of Akron
Akron, OH 44325

Up to a few years ago my own work on thermal decompositions of chemical complexes was rather sparse; then partly in response to an invitation to speak on the subject, I prepared a survey and commentary. Because of some of the questions which arose, I have become active myself.

The literature on inorganic complexes can be overwhelming, so I confined my survey efforts to those articles which offered something more than a collection of curves, using examples of experimentation, good and bad, which would be illustrative; interpretations of data on equilibrium, on mechanism or on kinetics, which could be reinforced or criticized.

It became clear very quickly that a substantial majority of workers were treating the thermal decompositions as irreversible processes without offering evidence. Hence, I shall deal in part with the atmosphere effect, showing evidence of its importance for some complexes without claiming that it is important for every case – except for the secondary effects, such as heat or mass transfer.

Rates of thermal decomposition have been measured by a number of authors. Measurements have been made both isothermally and non-isothermally. The usual kinetic parameters have been calculated using models which were apparently selected for ease of computation rather than accuracy of description. We shall need to examine the validity of the treatments and attempt to deduce some meanings of the derived data.

Here and there in the discussion some useful experiments will be suggested. The variation in decomposition temperatures with pressure of the product gas is of special importance, but other studies are frequently needed to answer specific questions.

Finally, I shall discuss my own current efforts to obtain clearly interpretable data.

A simple form of thermal analysis of complexes has been in use for quite a while. Duval [1][1] and co-workers used complexing agents to obtain precipitates which undergo clearly resolved reactions, so that the weight gave a good measure of the amount of metal. They sought precipitating agents whose thermogravimetric curves displayed some region of constant weight wide enough to enable simple heating to a selected temperature followed by ordinary weighing. The thermobalance was a convenience because the weight losses could be identified with good assurance.

It is well known that there are groups of complexes whose decomposition temperatures are only slightly dependent upon the nature of the central atom and others whose decomposition temperatures are very much dependent upon the nature of the central atom. The deformability of the central atom may also change the sequential decomposition steps. For example, Liptay et al. [2] show that pyridine complexes containing the metal, four pyridine, and two halides, may decompose in three or four steps. For the chloride (figure 1a), nickel and cobalt go to an intermediate with two-thirds mole of pyridine. Manganese does not show that intermediate. But if the halide is bromide (figure 1b) instead of iodide, the reverse is observed, the manganese showing the additional intermediate state.

Obviously in these cases, the metal-nitrogen bond is the most easily broken. But in other compounds, some part of the ligand is the first to decompose, and the identity of the central ion has only a secondary effect upon the temperature of the first decomposition

[1]Figures in brackets indicate the literature references at the end of this paper.

Figure 1a.

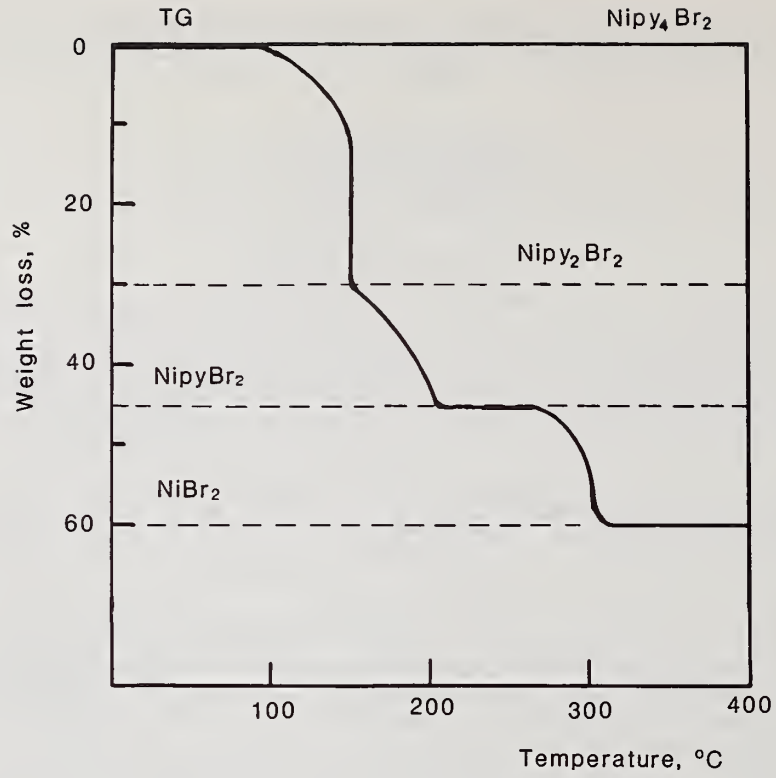

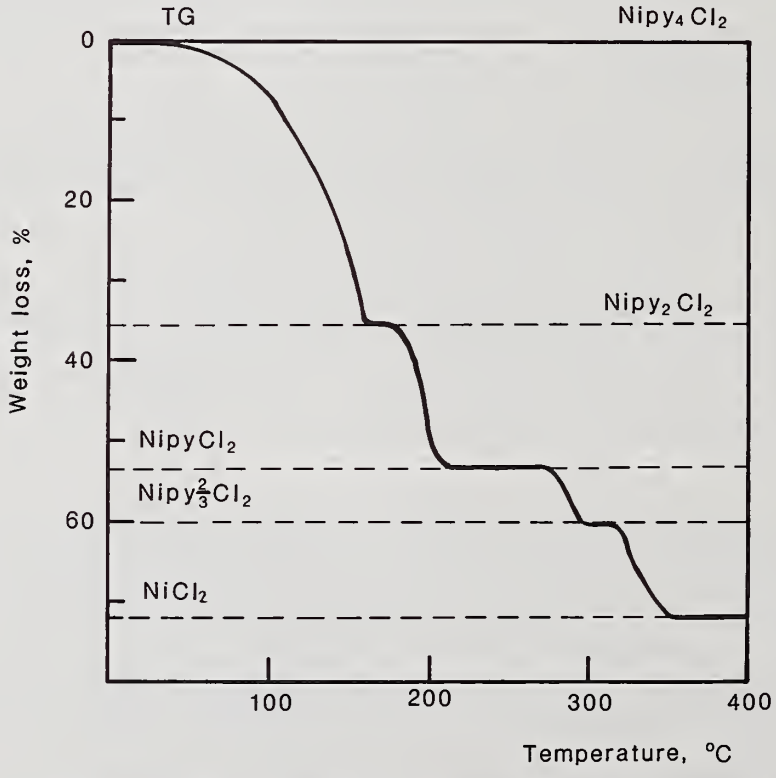

Figures 1a and 1b. Thermogravimetric curves of pyridine complexes of nickel and manganese with chloride and bromide anions. (From Liptay et al. [2].)

Figure 1b.

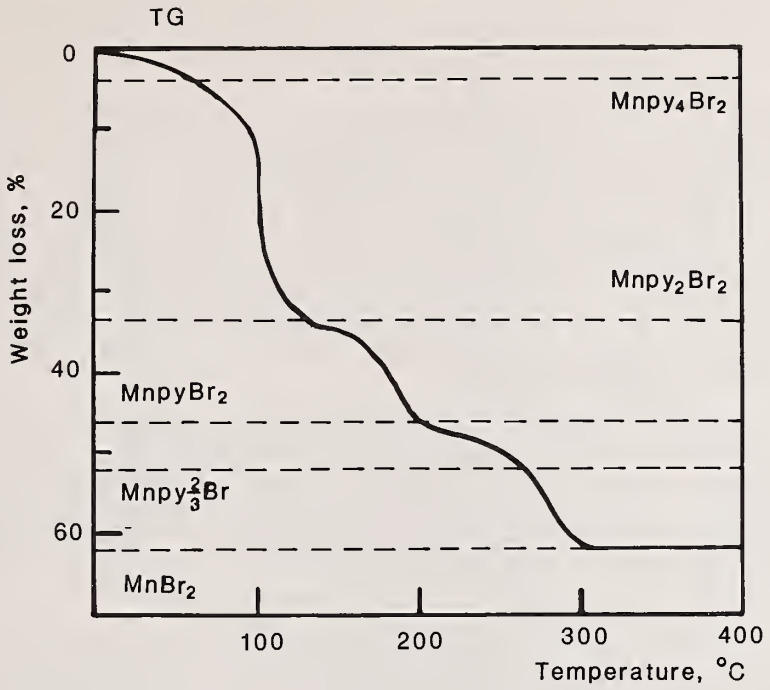
TG
0
20
40
60
Weight loss, %
$Mnpy_4Br_2$
$Mnpy_2Br_2$
$MnpyBr_2$
$Mnpy_{\frac{2}{3}}Br$
$MnBr_2$
100
200
300
400
Temperature, °C

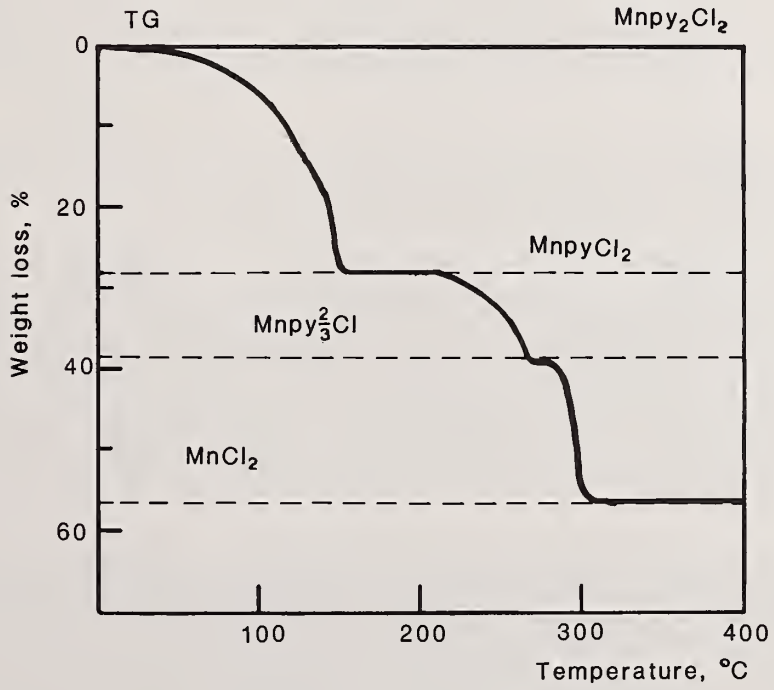
TG
$Mnpy_2Cl_2$
0
20
40
60
Weight loss, %
$MnpyCl_2$
$Mnpy_{\frac{2}{3}}Cl$
$MnCl_2$
100
200
300
400
Temperature, °C

step. That is, some part of the ligand will degrade within some rather limited temperature range, and within that range the polarity of the bond to the metal or the deformation of the ligand can stabilize or de-stabilize the complex with one metal compared to another.

As an example, Bottei and Schneggenburger [3] have attempted to relate the thermal stabilities of a number of amino acid chelate systems to their stabilities in aqueous solution and with the metal to nitrogen bond stretching force constant, finding, of course, little correlation. They reported the thermal stability orders for a number of metals with each amino acid, finding typically that metals such as zinc, nickel, cadmium, and cobalt, with octahedral or tetrahedral coordination tend to form complexes of higher thermal stability than the square-planar complexes of platinum, palladium, and copper. There are, of course, many exceptions, but their curves for the bis-glycino chelates suggest a rather clear separation of curves for zinc and nickel, platinum, copper, and palladium falling in a group with about 100 degrees separation from the first. The same kind of separation can be seen for the bis-dl-α alanino chelates.

No close relationship should be anticipated between thermal and aqueous stabilities. The thermal stability reflects substantially different influences. The amino acid has no place to go as an entity and it is not volatile. In water, the complex is competing against the hydration energy of both the metal and the amino acid. Bottei and Schneggenburger [3] suggest the probability of redox reactions in the thermal process providing catalysis for the decomposition; for example, cobalt typically forms rather easily decomposed complexes compared to other metals.

However, for ligands which decompose internally before the metal-ligand bond, the deformation by a strong bond will tend to weaken the ligand. Liptay et al. [2] showed that some ligands showed inverse relationships between the stability constants and the start of decomposition for limited series of metal ions.

An example of the effect of cation size and bond polarizability is given by Nikolaev, Logvinenko, and Myachina [4], who studied a series of binuclear complexes, among them magnesium EDTA which crystallizes with nine waters (figure 2). In the homonuclear material, all the waters are evolved in a single step, with no evidence of stepwise process in the 100-180 degree peak. Nor is the EDTA decomposition split. Substitution of lead for one magnesium does not change the crystal structure but changes the decomposition behavior markedly. Not only are three waters held more strongly than the other six, as we can see from the splitting of the dehydration peaks, but the loss of the first six begins about 20 degrees lower.

The EDTA degradation is also split, the break in the TG curve appearing about 50 degrees lower than in the dimagnesium compound, but the second peak being at nearly the same temperature as the single peak in the dimagnesium compound.

Based in part on data in this same publication, and in part on data by Bhat and Iyer [5], Nikolaev et al. [4] suggested a strong relationship between the temperature at which water is lost from EDTA complexes and the nature of its bonding – water lost at temperatures in excess of 200 °C being attributed to coordinated water, whereas water lost below 150 °C was presumed to be lattice water. Similar proposals have been made for more general cases. Nuttall and Stalker [6] examined a number of EDTA complexes and concluded that there were enough cases of weak coordination or strong hydrogen bonding to reduce the validity of the hypothesis. Nuttall and Stalker [6] concluded that – in isolation from other data – the temperature of water elimination does not delineate the type of water present.

There is, of course, a classic case of coordination water being lost before lattice water, viz. copper sulfate pentahydrate. The coordinated waters are lost at temperatures below 100 °C in air or vacuum and below 150 °C even in water vapor, whereas the lattice water between the sulfate and the cation remains until ca. 250 °C.

Some of the evidences which support the atmosphere effect are a bit subtle, but we have reached a state of instrumental sophistication which enables us – or rather, should impel us – to assume that any reproducable deviation from a regular peak shape is due to a real physical or chemical process. Beech and Kaufmann [7] provide us examples in their

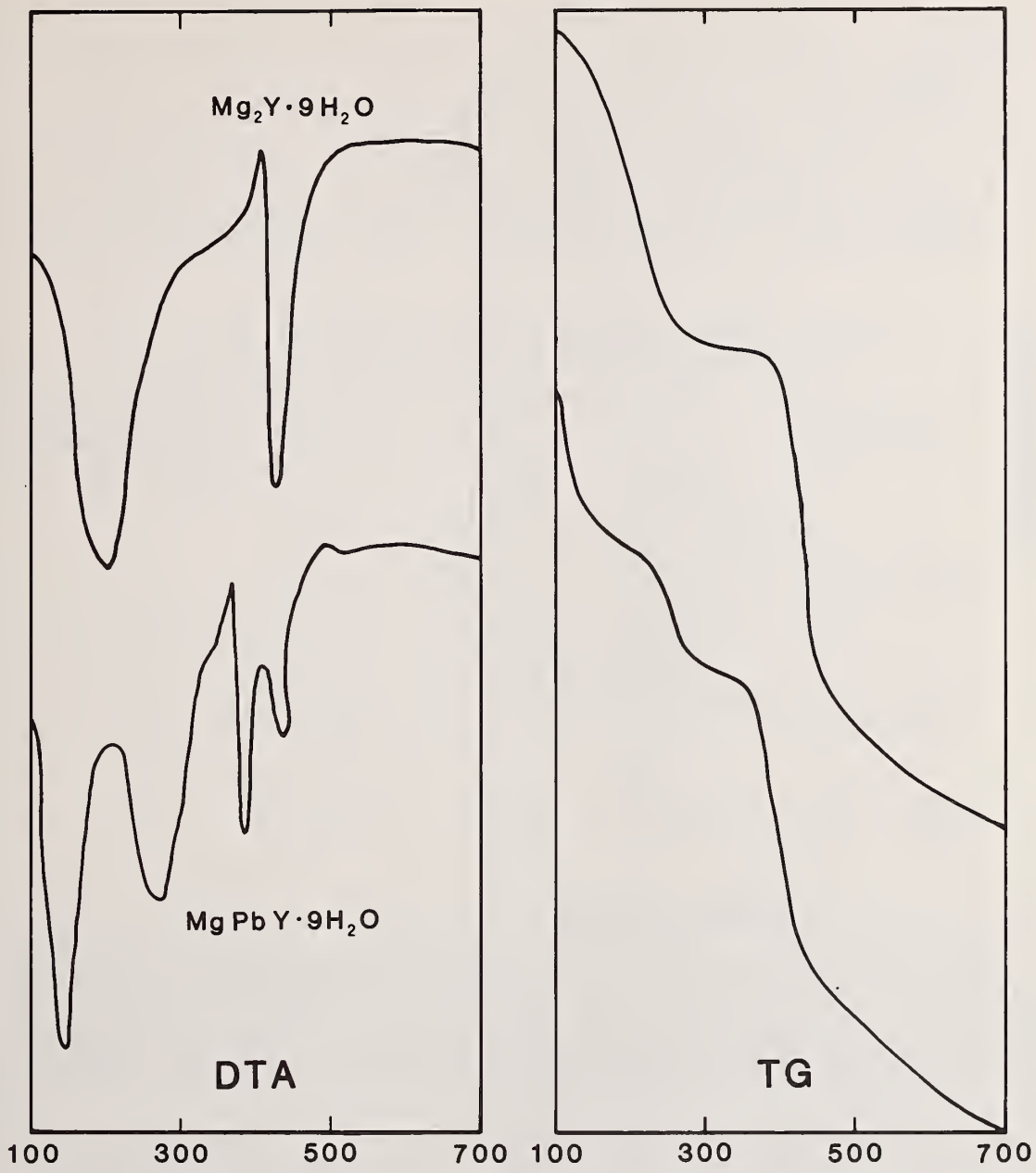

Figure 2. DTA and TG curves of ethylenediaminetetraacetic acid salts $Mg_2Y \cdot 9H_2$) and MgPbY · $9H_2$). From Nikolaev et al. [2].)

work on 150 thiocyanate complexes. They concluded that the first major peak in figure 3 was due to loss of two pyridines. This was in agreement with Erdey and Liptay [8] and with Wendlandt and Ali [9], but not with Duval [1], who had reported that the tripyridine complex was the first product. Here we must look at the conditions of the experiment. Beech and Kaufmann [7] used a few milligrams of sample on a flat pan at a high heating rate. Erdey and Liptay [8] used a larger sample at a fairly high heating rate, as did Wendlandt and Ali [9]. Duval [1], on the other hand, used a much larger sample but a much lower heating rate, nearly half a gram in a crucible at less than two degrees a minute. Both have an effect on resolving the peaks.

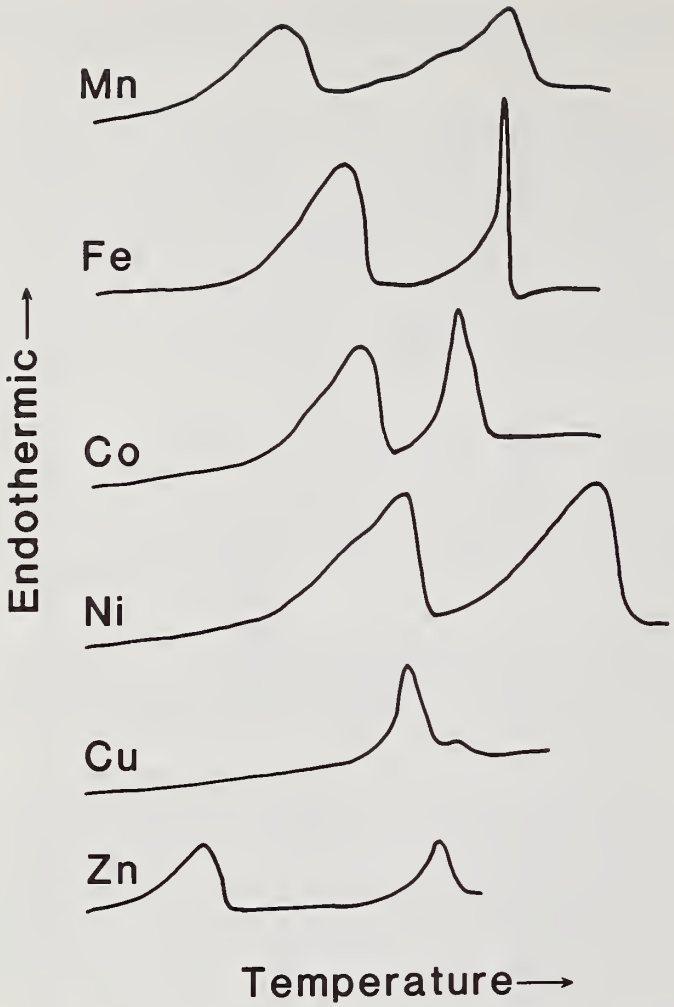

Figure 3. DSC curves of some metal complexes with pyridine and thiocyanate. (From Beech and Kaufmann [7].)

The larger sample size, even in an atmosphere of nitrogen or air, will enable a concentration of pyridine to be built up which would repress a second-stage loss – so that it can be seen separately – if, of course, there is a reversible step in the process. Further, the lesser heating rate, even with the greater sample, can enable the first product to form throughout the sample. At high heating rates, the second reaction follows the first too rapidly to allow resolution of the first.

Now we can note that there are decided deviations from smoothly progressing peaks. As Beech and Kaufmann [7] point out, there is an inflection in the nickel curve; this suggests that the tripyridine complex is formed. They report other supporting evidence.

If the atmosphere surrounding the sample were actually pyridine, it is probable that even at moderate heating rates the tripyridine peak would be resolvable both for large and small samples.

In an accompanying paper, Kaufmann and Beech [32] calculated the various parameters from the order-of-reaction and Arrhenius equation combination (Table 1). They noted that both the calculated activation energy and the calculated order or reaction change depending upon the fraction of the whole process examined, especially, of course, in the case of nickel. What we can conclude from this is that the equation does not hold over the whole range. Kaufmann and Beech [32] considered the possibility that a tripyridine complex was formed in most cases. Two overlapping reactions could hardly be expected to obey a single equation. But now let us note the variation of A, which should apparently be log A, with the apparent activation energy. This behavior has been observed by several authors; it is called the kinetic compensation effect. It arises from the use of the Arrhenius equation where it is not appropriate [10,11,12].

Table 1. Kinetic parameters for $MPy_4(NCS)_2$ calculated by Kaufmann and Beech [33]. Largest and smallest ranges of α are cited.

M	Range of α	n	E	A(log A)
Mn	0.03-0.88	0.52	16.9	7.0
	0.03-0.22	1.5	20.6	9.2
Fe	0.03-0.84	0.32	18.2	7.2
	0.03-0.17	0.77	17.7	6.9
Co	0.02-0.91	0.47	20.9	8.6
	0.02-0.21	1.26	25.5	11.1
Ni	0.01-0.87	0.43	18.4	7.1
	0.04-0.35	1.8	24.2	10.2
Zn	0.02-0.86	0.38	19.5	9.9
	0.02-0.31	0.62	20.2	10.3

Briefly, it arises from the practice of assuming for solids the same kind of continuous distribution of energies that is well established for gases in the face of the equally well established knowledge that the perfect crystal has the lowest possible energy [12].

In uncontrolled atmospheres, the heating rate, the sample size, and the sample geometry all have effects both upon the rate and upon the observed temperatures of reversible and many irreversible reactions. This is easily demonstrated by using Simon's [13] curves (figure 4) for calcium oxalate hydrate. The dehydration is reversible so any effect which allows the build-up of water vapor will repress the reaction, requiring a higher temperature for the reaction to continue. The more rapid heating rate obviously supplies a larger water vapor so in either holder – at either sample size – the fastest heating rate gives the highest temperatures. The displacement to higher temperatures on the right is due partly to sample size, which simply yields more water which must escape, and partly to the degree of confinement, a gram of sample at the bottom of the crucible. We can compare similar samples, though. Simon [13] showed that equal samples in different vessels reacted differently in temperature or, as here plotted, time. We can compare the one-degree rate in the multiplate or free-diffusion sample holder and in the labyrinth crucible or self-generated atmosphere sample holder. The confinement of the water vapor in the crucible delays the reaction compared to the free escape of vapor from the multiplate holder.

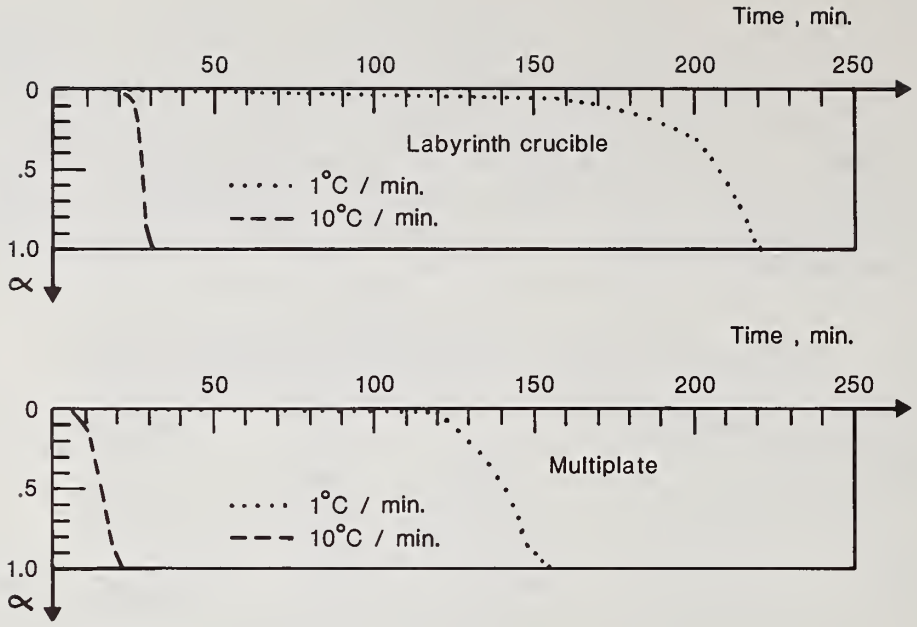

Crystallized $Ca(COO)_2 \cdot H_2O$. Comparative diagram for the effect of atmosphere

Sample size : 200 mg

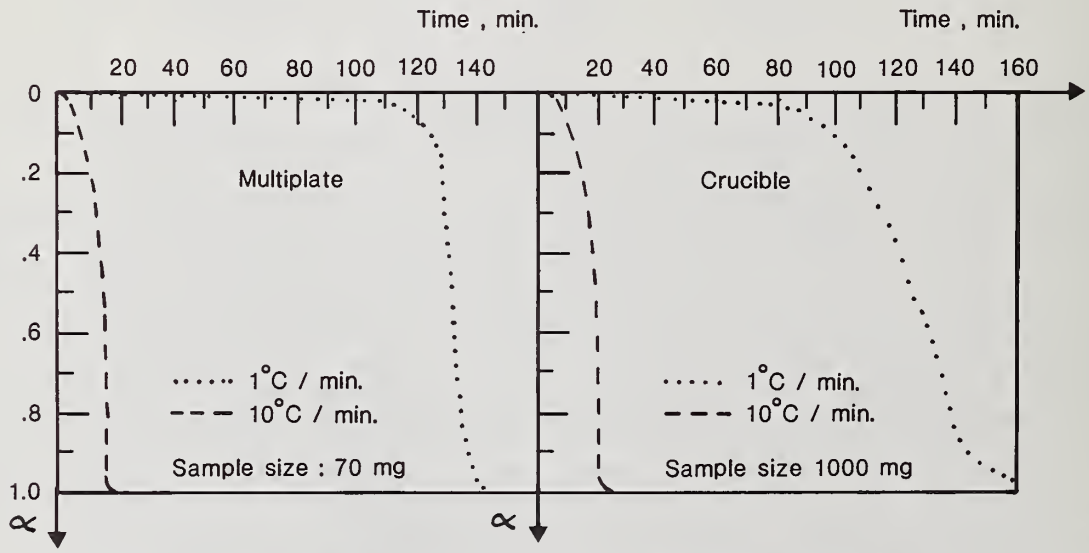

Crystallized $Ca(COO)_2 \cdot H_2O$. Effect of heating rate

Figure 4. Dehydration of calcium oxalate hydrate. (From Simon [13].)

Coordination compounds can also decompose reversibly and reversibility should be expected until tests show otherwise. For example, the curves for copper tetrammine sulfate hydrate in the Atlas edited by Liptay [8] differ apparently as a function of the sample holder but actually by reason of the confinement of ammonia to different degrees in the crucible and the shallow sample holder.

Similarly, tris-ethylenediaminechromium chloride shows a distinct atmosphere dependence, Sithole [14], from self-generated atmosphere experiments. We will actually use an ethylenediamine atmosphere, Garn [15], as soon as we get organized after a recent move to a new building.

Thermal decompositions may also proceed to different products at different ligand pressures. This is well known and in many cases an intermediate step is assumed. Copper sulfate pentahydrate, for example, can go to the monohydrate in vacuo or to the trihydrate at moderate pressures of water vapor. The trihydrate is often postulated as an intermediate even in the vacuum dehydration. Zagray, et al. [16] have performed x-ray diffraction studies on partially dehydrated species and found that, whereas the trihydrate is formed via elliptical nuclei and is oriented with respect to the parent crystal, the vacuum dehydration proceeds via star-(or X-)shaped nuclei directly to the monohydrate. Ng, et al. [17] have examined the comparative stabilities of the freshlyformed trihydrate and material that had been prepared by solvent dehydration, finding a much greater thermal stability for the latter.

The variation of reaction rate with controlled pressure of the product gas applied externally has been demonstrated for isothiocyanatopentammine cobalt (III) perchlorate by Chou and Olson [18] (figure 5). They used different pressures of ammonia in a constant total pressure. The presence of ammonia not only inhibits the early process in which it is a lesser product. Chou and Olson [18] attributed the slowing of the ammonium perchlorate degradation step to chemisorption of the ammonia on the solid product, but Stone [19] had demonstrated in 1960 that the presence of ammonia inhibits a low temperature exotherm which Bohon [20] described as a pre-ignition decomposition.

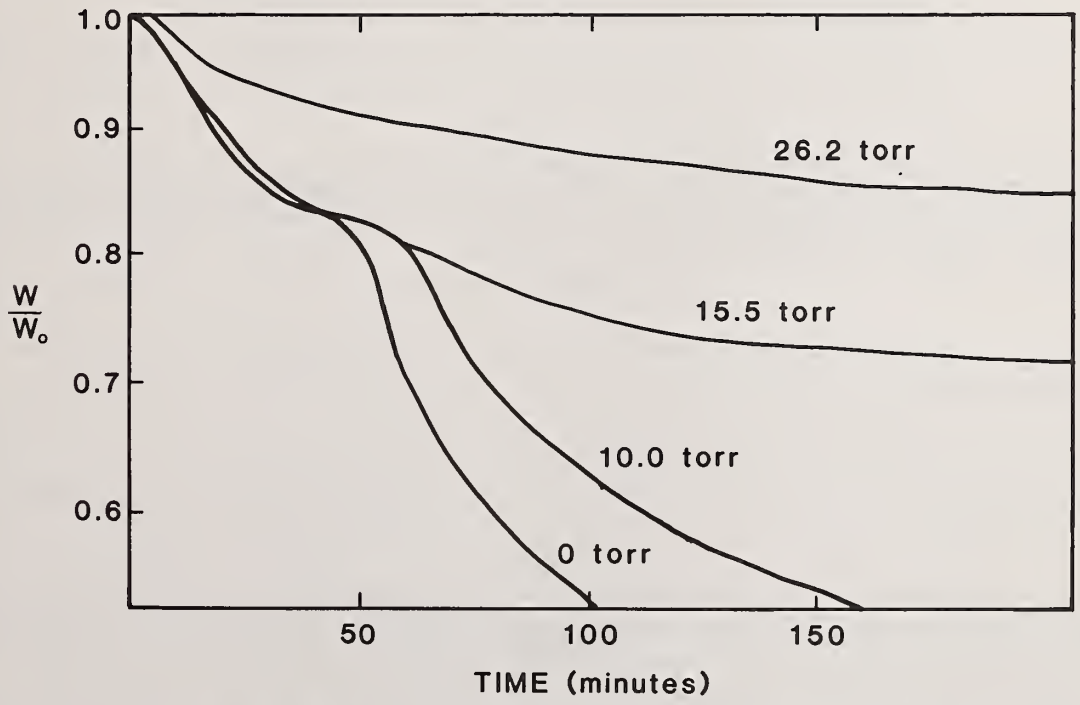

Figure 5. Thermal decomposition of isothiocyanatopentamminecobalt perchlorate under various partial pressures of ammonia.

Looking at the temperature dependence under static air we can see that the processes would be hard to separate at the higher temperatures. Presumably, even with very small samples the first process is not resolved in the uncontrolled atmosphere.

The presence of a major fraction of helium beclouds the issue somewhat, because even helium inhibits diffusion of other gases outward. Two approaches are indicated.

Substitution of a much heavier gas, argon or a fluorocarbon, for example, would show – by comparison – the effect of diffusion within the particle. On the other hand, use of pure ammonia at the given partial pressures would enable verification of equilibrium temperatures for any steps that are truly reversible.

The report by LeMay [21] and others on the dehydration of tetrammine dichlorocobalt-(III)-iodate dihydrate has special interest because it includes studies of pressure effects on the dehydration. Trans-cis rearrangement occurs during the dehydration and is proportional to the degree of dehydration. The authors varied the pressure of water vapor, finding that above fifty torr the reaction was impeded by the water vapor pressure (Table 2). The temperature dependence, expressed as an activation energy, shows an increase which is quite closely proportional to pressure.

Table 2. Energy of activation for decomposition of isothiocyanatocobalt chloride as a funcation of pressure of ammonia in a total pressure of 650 torr as calculated by Chou and Olsen [18].

Pressure (torr)	E, kcal/mole
0 (flowing nitrogen)	13.7 ± 1.0
0.1	14.0 ± 0.8
0.4	14.3 ± 0.2
50	14.2 ± 0.6
300	21.7 ± 0.4
500	25.2 ± 0.1
650	28.0 ± 1.4

Most accurately, there appears to be some minimum value for this apparent activation energy. This temperature dependence at low pressures is presumably related to the process itself, but at pressures high enough, the decomposition is repressed. Calculations show that the more-complete Arrhenius expression would be

$$k = Z \exp[E_o + 15P)/RT],$$

where (E_o) is the zero-pressure apparent activation energy and ($\underline{P}$) is in atmospheres. We can, of course, separate this to read

$$k = Z \exp(-14/RT)\exp(-15P/RT)$$

if we choose to express the rate constant in a more descriptive form as a function of several variables.

At this point we would note also that LeMay [21] and others performed another important examination; they watched as the sample decomposed on a hot stage. The reaction usually began near the centers of the prominent faces of the thin crystals and spread gradually toward the edges. That is, the contracting envelope model is not applicable.

More interesting is the location of nucleation. One might expect and would usually find, nucleation at a high energy point, or at an edge defect. We might postulate strain arising during the heating which raises the energy of a mid-face site of the phombohedral crystal above the (strain) energy of a defect or corner. Admittedly, we could postulate

true random nucleation, which would occur most frequently on the largest faces simply because there are more such sites. Actual observation of a number of crystals would be needed to answer the question and this could easily be done in a thermobalance. An experiment is suggested. For materials which yield well-formed crystals large enough that the dehydration of one crystal can be measured on the balance, a hanger could be devised to suspend the single particle. If a quartz or Pyrex furnace tube is used and the heater does not obstruct the view, the initiation and the general progress of the decomposition can be observed with a controlled atmosphere and pressure. This observation should give valuable aid in establishing the kinetic model for the process. At the very least, hot-stage microscopy ought to be used on typical samples.

LeMay [21] had shown earlier that trans-dichloro-bis-1,2-diaminopropanecobalt(III)-diaquohydrogenchloride isomerized with deaquation, but the extent of dehydration was greater both at lower temperatures and in deeper samples, that is, under conditions which favor retention of water vapor. On the other hand, the initial rate of isomerization was greater at higher temperatures and thinner samples. The reaction was initiated on the outside of the sample and was obviously topotactic. Still, it was apparently diffusion limited. The rate constants calculated from

$$-\log(1-\alpha) - kt^2$$

showed no systematic variation with temperature.

But now we encounter a problem. LeMay [21] and others pointed out that the best fit for the kinetic data was by use of the diffusion equation,

$$-\log(1-\alpha) = kt^{1/2} + c$$

for thin layers of sample. These rate constants were used in calculating the apparent activation energy. LeMay [21] and others took care to check the effect of a deeper sample and found that the expression fitting best was now

$$-\log(1-\alpha) = kt + c.$$

The sample size effect is more likely a sample geometry effect, arising from a greater accumulation of water vapor within the sample. This kind of test should be routine in kinetic examinations. Obviously, if the rate constant or form of the rate equation changes with sample size, the correct rate equation has not yet been found. Parenthetically, I might add that there is very seldom any effort to find the correct rate equation.

Other techniques for study include some which make use of specific properties of the metal ions. One such is the detection of changes of oxidation state by magnetic measurements. For example, Wendlandt [9] and co-workers have hung samples between the pole pieces of a large magnet and observed the reduction of chromium three to chromium two as the complex decomposed. Here, of course, one must eliminate the effect of changes in mass, so they sealed their samples into tubes.

The constant total volume has a side effect – the increase in pressure of the product gas. For reversible decompositions this will spread out the process, while for irreversible or non-gas-forming processes the reaction would be unaffected by the sealing. This suggests a simple modification which would discriminate between atmosphere-dependent and independent processes. If the experiment is run in each of two vessels of identical geometries within the magnetic and thermal environments, but one having a four or perhaps tenfold greater total volume, any reversible process would be disclosed by the lower temperature or smaller temperature range in the larger volume compared to the lesser.

One of the ways of following changes and determining what is happening is by optical spectrometry. In the visible and UV region, reflectance spectrometry has been used by Wendlandt [22] and others; but as a dynamic technique it suffers from either the need to scan quickly over a limited range or, if a narrow band is monitored, a lack of opportunity to observe all the processes. Obtaining good isothermal spectra at selected temperatures is not easy because one must take into account the probable temperature gradients, atmosphere effects, etc. Still, information may be obtained by using standard techniques at room temperature on samples heated to the desired temperatures.

Gallaher and Schrey [23] have used Mossbauer spectra in a similar manner. Their data on europium hexacyanoferrate hydrate show the progress through a very finely divided state to well crystallized orthoferrite. I am not aware of any technical reason why Mossbauer spectra could not be obtained at elevated temperatures.

Evolved gas analysis by several techniques is highly informative, but the ways of doing it may change the progress of the reaction. That is, one must either transport the evolved gas to the analyzer with a stream of gas, or pump it, as in the mass spectrometer. In either case, some control of the experimental conditions is lost unless special designs are used.

We will look at some evolved gas analysis noting first another form of the atmosphere effect, the probability of oxidation processes in air or oxygen. Gallagher [23] and coworkers, have studied the hexacyanoferrates as starting materials for catalyst preparations. Figure 6 shows their decompositions in oxygen and helium. Both curves in oxygen are quite simple because of rapid oxidation. In helium, however, the complex decomposition is complex indeed. There is a general weight loss in the 200-700 degree range with occasional peaks. Evolved gas analysis is clearly prescribed.

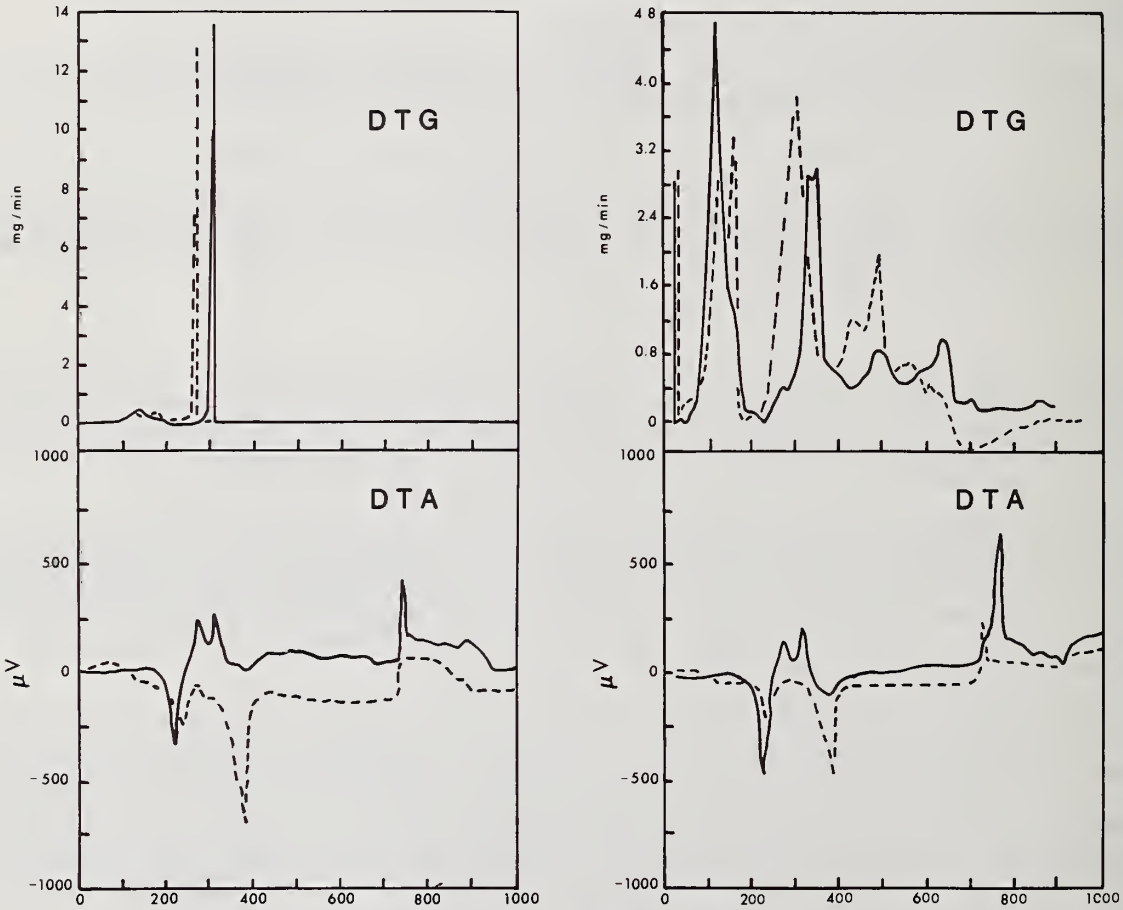

Figure 6. Thermal decompositions of europium hexacyanatoferrate hydrate and ammonium europium hexacyanatoferrate tetrahydrate. (From Gallagher and Schrey [23].)

Taking the gases into a mass spectrometer and monitoring the principal products, Gallagher [24] was able to relate the various thermal and mass effects to the species coming off. For the europium hexacyanoferrate pentahydrate, the water comes off early in two poorly defined steps, then some europium hydroxide releases a little more water later.

Hydrogen cyanide is evolved, also in ill-defined steps, while cyanogen appears in a single peak near 400 degrees on. Looking at ammonium europium hexacyanoferrate tetrahydrate and monitoring ammonia rather than cyanogen, Gallagher [24] found that the early dehydration was better resolved, that the ammonia came off in a single peak near 300 degrees, and the hydrogen cyanide evolution was broader. The mass 28 evolution again started about 400 degrees and continued.

If it is necessary to simulate the atmosphere during the actual processing, the gas stream would have to be sampled and directed into a mass spectrometer or through a gas chromatograph. For the mass spectrometer alone, stream splitting would be adequate, but for chromatographic separation and measurement, repetitive sampling is needed [25]. The system cited used the chromatographic technology of twenty years ago and involved three columns. The present range of columns should enable many real problems to be done on one column [26].

Frequently, better resolution of reactions is available using self-generated atmospheres. In this case, the sample chamber feeds into the sample loop through a long, narrow diffusion path so that the atmosphere within the sample holder is the evolved gas at whatever pressure is applied to the sample loop. We have used this to study mineral decompositions over an eight-fold range of pressures [27] and a similar arrangement with a mass spectrometer to study the degradation products of cellulose treated with flame retardants [28,29,30].

In using gas streams in the apparatus, one must choose carefully if any detailed quantitative conclusions are to be reached, particularly concerning kinetic parameters. Even apparently inert gases have an effect for several reasons, principally different diffusion characteristics. Heat transfer is also affected by the diffusion.

Though I am using some other kinds of reactions to illustrate, the concern is quite general. Table 3 shows some rate data by Fremont-Lamouranne [31] and others showing the relative effects of stationary and flowing gas on the calcite decomposition. The rate is affected seriously by the nature and the flow of gas. Obviously the observed rate is a function of the heat and mass transfer, so it is not reasonable to calculate rate constants or kinetic parameters without including the limit due to the heat path.

Table 3. Effect of static and flowing inert gases on the decomposition of calcium carbonate (Fremont-Lamouranne [31]).

	Rate in percent per hour		
Gas	Helium	Nitrogen	Argon
Flow condition			
Static	12.8	7.5	6.9
Flowing	11.7	6	6.3

My own preference in experimentation is to strive toward clearly-known thermodynamic conditions at the sample. In DTA we inevitably have a non-uniform temperature but at least a constant atmosphere can be provided. In thermogravimetry we can interrupt any dynamic temperature program at will, as well as change the atmosphere or its pressure.

A few years ago I designed a DTA furnace assembly for study of some arene-$(CO)_3Cr(O)$ complexes wherein the arene was benzene or a substituted benzene. They typically melt in the 90-120 degree range and decompose at temperatures not much higher.

Some of the processes are reversible. Also, heating benzene$(CO)_3Cr(O)$ in carbon monoxide yields $Cr(CO)_6$, whereas heating in benzene vapor yields bis-benzenechromium. The task of providing known atmospheres of benzene was handled by using a variation of my water vapor furnace [32]. Using a quartz tube with internal heaters in a block surrounding the sample (figure 6) I was able to control the liquid level during the initial heating

– avoiding dissolving the sample – and maintain a pressure – typically one to four atmospheres – of benzene vapor within the furnace cavity (figure 7).

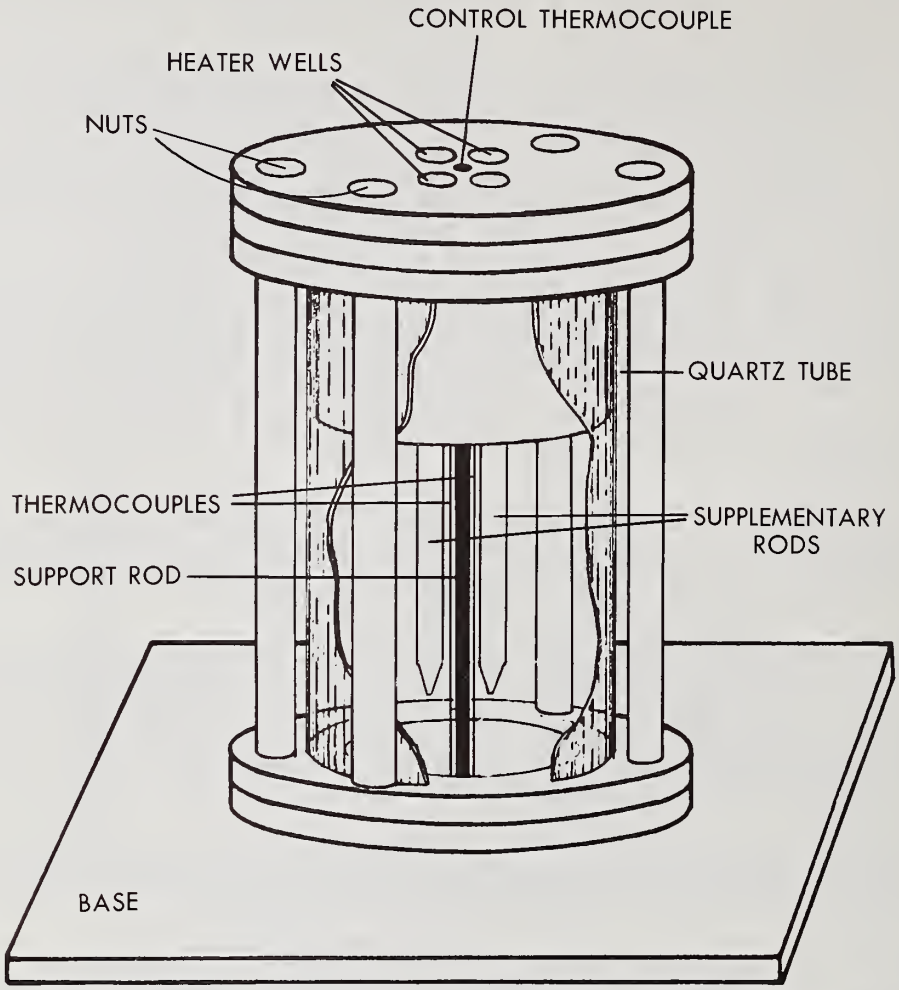

Figure 7. Internally-generated-atmosphere furnace for study of complexes.

I have used this furnace assembly for water vapor atmospheres too. Barium chloride dihydrate and copper sulfate pentahydrate both decompose to lower hydrates, barium chloride dihydrate to a non-stoichiometric compound having ca. 1.08 H_2O, then to another lower hydrate, prior to complete dehydration.

At the price of several sets of O-rings, we have also used ethanolamine. The study was interrupted by graduation of the student, but I may be able to take it up again. Naturally, ordinary gases such as ammonia and carbon monoxide can be – and have been – used. For these, the outlet was directed nearly a meter into a flexible exhaust.

My most recent efforts though, are going into a controlled-atmosphere, controlled-pressure thermobalance. I have been unwilling to invest money or time in a thermobalance that would not enable studies under quite rigorous conditions. Just recently, I have obtained — with the assistance of Cahn Instruments – an electrobalance, the Cahn 1000, that has sufficient capacity to permit special sample holders when needed, and what I believe to be a satisfactory resistance to vapors to enable thermogravimetry in known and controlled atmospheres. By keeping the balance mechanism at a high enough temperature to prevent condensation even at several atmospheres pressure, I will be able to introduce the

liquid ligand at the bottom of the furnace tubes in the same manner as in the DTA furnace and carry out equilibrium studies as well as decomposition studies.

Using this thermobalance I expect to be able not only to ascertain the reversibility and the specific pressure dependence of complex decompositions but also to find and identify any intermediates that may exist. In addition, isothermal weight measurements at known pressures of gaseous products will yield kinetic data that can be interpreted with assurance. Still further, exact formulae of non-stoichiometric complexes and hydrates can be determined.

The author is grateful to the U. S. National Science Foundation for the support that enabled many of the studies cited herein and the several co-authors whose efforts are described in the cited publications.

References

[1] Duval, C., Inorganic Thermogravimetric Analysis, Elsevier, Amsterdam (1953).

[2] Liptay, G., Burger, K., Mocsari-Fülöpand, E., and Porubszky, I., J. Thermal Anal. 2, 25 (1970).

[3] Bottei, R. S., and Schneggenburger, R. G., J. Thermal Anal. 2, 11 (1970).

[4] Nikolaev, A. V., Logvinenko, V. A., and Myachina, L. I., Thermal Analysis, Proc. of 2nd Intl. Conf. 1968, Schwenker, Jr., R. F. and Garn, P. D. (eds.) Academic Press, New York, 779-791 (1969).

[5] Bhat, T. R., and Iyer, R. K., J. Inorg. Nucl. Chem., 179-182 (1967).

[6] Nuttall, R. H., and Stalker, D. M., J. Inorg. Nucl. Chem. 40, 39-41 (1978).

[7] Beech, G., and Kaufmann, G. B., Thermochim. Acta 1 (1), 93 (1970).

[8] Atlas of Thermoanal. Curves 1, Liptay, G. (ed.) Budapest (1971).

[9] Wendlandt, W. W., and Ali. S. I., Z. Anorg. Allgem. Chem. 337, 6-13 (1965).

[10] Garn, P. D., J. Thermal Anal. 7, 475-478 (1975).

[11] Garn, P. D., Thermal Anal. 1, Budapest, 25-32 (1975).

[12] Garn, P. D., J. Thermal Anal. 13, 581-593 (1978).

[13] Simon, J., J. Thermal Anal. 5, 271 (1973).

[14] Sithole, S. D., Unpublished Measurements, The University of Akron (1979).

[15] Garn, P. D., Am. Chem. Soc. Symp. Series 96, 253-261 (1979).

[16] Zagray, A. I., Zyryanov, V. V., Lyakhov, N. Z., Chupakhin, A. P., and Boldyrev, V. V., Thermochima. Acta 29, 115-119 (1979).

[17] Ng, W. L., Ho, C-C., and Ng, S-K., J. Inorg. Nucl. Chem. 34, 459-462 (1970).

[18] Chou, C. J., and Olson, F. A., Anal. Chem. 44 (11), 1841 (1972).

[19] Stone, R. L., Anal. Chem. 32, 1582-1588 (1960).

[20] Bohon, R. L., Anal. Chem. 33, 1451-1453 (1961).

[21] LeMay, Jr., H. E., Sheen, J. R., and Babich, M. W., J. Inorg. Nucl. Chem. 34, 149 (1972).

[22] Wendlandt, W. W., and Hecht, H. G., Reflectance Spectroscopy, Interscience, New York (1966).

[23] Gallagher, P. K., and Schrey, F., Thermal. Anal. 1, Schwenker, Jr., R. F., and Garn, P. D. (eds.) Academic Press, New York 623 (1969).

[24] Gallagher, P. K., Thermal Anal., Kambe, H., and Garn, P. D. (eds.) Kodansha Ltd., Tokyo, 90-116 (1974).

[25] Garn, P. D., and Kessler, J. E., Anal. Chem. 33, 952 (1961).

[26] Garn, P. D., and Anthony, G. D., Proc. Inst. of Environmental Sciences, 308 (1970).

[27] Anthony, G. D., and Garn, P. D., J. Amer. Ceram. Soc. 57, 132-135 (1974).

[28] Garn, P. D., and Denson, C. M., Text. Resch. Journal 47, 485-491 (1977).

[29] Garn, P. D., and Denson, C. M., Text. Resch. Journal 47, 535-542 (1977).

[30] Garn, P. D., and Denson, C. M., Text. Resch. Journal 47, 591-597 (1977).

[31] Fremont-Lamouranne, R., Bretey, E., and Guerin, H., J. Thermal Anal. 5, 625 (1973).

[32] Garn, P. D., Rev. of Sci. Instru. 44, 231-233 (1973).

[33] Kaufmann, G. B., Beech, G., Thermochima. Acta 1 (1), 99 (1970).

CHEMICAL COMPLEXES

RAPPORTEUR'S COMMENTS BY

C. B. Murphy
Xerox Corporation
Xerox Square, W139
Rochester, N.Y. 14644

The materials covered by Professor Garn were the chemical complexes. The factors that influence the decomposition were discussed with examples showing where correlations clearly existed, as well as other instances where correlations did not exist. Cation size, bond polarizability, heating rate, influence of gaseous decomposition products, atmosphere control, and controlled pressure were discussed. Illustrations were drawn from differential thermal analysis and thermogravimetry.

However, it appears that a distinction should have been made between chelates and Werner complexes and between chelates formed through coordinate covalent bonding and those formed, at least in part, by ionic bonds. At the outset, it was stated that the thermal stability of chemical complexes had little relationship to their aqueous stability. Amino acids were not volatile and had no place to go on decomposition of amino acid chelates. While the amino acid chelate will undergo decomposition rather than reversal of reaction, the tris-ethylenediamine chromium chloride chelate was shown to have a self-generated atmosphere dependence. As no ionic bonds are involved in the latter, this would be expected. The reaction is reversible.

In aqueous media, chromium chloride can react with ethylenediamine to give the solution of the hydrated chelate. The anhydrous chelate on dilution in water should give the same final product. Thus, one would expect that the heat of reaction, measured in aqueous solution, should differ from thermal analysis data only by the heat of solution and hydration for those complexes where the thermal analysis decomposition involves reversible processes.

Further work planned by Professor Garn with ethylenediamine and ethanolamine atmospheres should provide further insight into this situation. The work with ethanolamine may be significantly more complicated. Under certain circumstances, the proton from the alcoholic group may be lost in complex formation. Then, the reaction would not be reversible, and, as in the amino acid case, the ionic radical would decompose.

National Bureau of Standards Special Publication 580. Proceedings of the Workshop on the State-of-the-Art of Thermal Analysis held at NBS, Gaithersburg, MD, May 21-22, 1979. (Issued May 1980)

PAPER TECHNOLOGY FROM EGYPTIAN, CHINESE, AND MAYAN CULTURES

Hans G. Wiedemann[1]

Oriental Seminar of the University of Zurich
Zurich, Switzerland

1. Introduction

The development of paper-like materials played an important role in the intellectual evolution of various high cultures of the world in the Mediterranean Countries, in Asia, and in Central America. The today's word "paper" is taken from "papyrus," the paper of ancient Egypt. Papyrus was also one of the important construction materials for boats, mats, sandals, etc., the main use, however, was as writing material.

As its name implies, the material was produced from a reed-like plant – the papyrus – by means of special processing techniques. Many consider this historic writing medium to be the ancestor of paper as we know it today. That may partly be true as far as the basic raw materials are concerned, but it applies to the production and properties of the material only to a much lesser degree.

In China, Ts'ai Lun from Kuei-Yang (todays Hunan) has been cited in authenticated history not as the man who invented paper but as one who opened the door to its production. He started with disintegrated fibers of the mulberry tree. This paper is a tissue-like material, the individual fibers of which are separated before by mechanical action and deposited on a mold suspended in water. After maceration, the fibers are picked up by a sieve-like device which allows the water to drain. The interwoven fibers form a felt-like mass which, after drying and pressing, becomes paper.

Fray Toribio Benavente was one of the Franciscans sent to New Spain to assist in the spiritual education of the Aztecs. He writes: A good paper is made from "metl" (Agave), the sheet is as large as two sheets of ours, and they make much of this in TLAXCALA and throughout a great part of New Spain. There are other trees from which it is made in the hot-lands. One of these trees is called "amatl" (fig-tree), which is the reason why they call letters, books, and paper "amatl."

The paper "metl" was made from the leaves of the "maguey." The leaves of this plant were first soaked in water in order to putrefy them. Then the fibers were washed, smoothed, and extended for manufacture of their coarse paper which was then polished for the purpose of painting and writing on it.

Several samples from these different cultures and ages are investigated at present by thermoanalytical methods and other techniques. The results obtained from these investigations lead to:

- new insights of the assumed ancient production,
- some new ideas about the materials used,
- and a knowledge of effects by fungi.

---

[1]Present address: Mettler Instruments AG, CH-8606 Greifensee/Zurich, Switzerland.

2. Egyptian Papyrus

2.1. Historical

Egypt was not only the well-known land of the Pyramids, Temples, Tombs, and Mummies with a multiform world of gods, but also the land of officials and scribes. The outstanding importance of the written word on papyrus parchment, limestone, and clayware has been preserved in abundance in form of texts and inscriptions. This is the written heritage of a culture which has maintained its splendor over thousands of years in spite of foreign influences and changes. The discovery of papyrus as an important material for writing goes back to the early times of the Egyptian history. The oldest, undescribed papyrus ever found originates from the first Dynasty (3000 B.C.). The earliest inscribed papyri can be assigned to the fifth Dynasty (2400 B.C.).

During the nineteenth century, the first papyrus writings were added to the Egyptian collections of the Museums in Paris, London, Turin, Leiden, and Berlin by purchases of private collections. Many of the valuable texts and papyri, however, were destroyed by improper excavation techniques. At the beginning of the twentieth century, scientific excavation campaigns of archaeologists and egyptologists in middle and upper Egypt brought about an unexpected, rich discovery of papyrus writings. These texts referred to various fields of the public and private life in ancient Egypt, e.g., to the administration, economy, jurisprudence, and religion. The frequently observed excellent preservation of the papyri is due to the favorable climatic conditions, that means to the dryness and to the overlaying desert sand.

2.2. Papyrus

The writing material papyrus is made from pressed stems of the plant, which are arranged cross-wise in layers (figure 1).

Figure 1. Cross-wise layers

Looking through literature and pictures today available of the "Ancient Egypt," we will find descriptions of technical processes and recipes of many of the products then manufactured. Although Papyrus was manufactured for their own use and for exportation, the description of the manufacturing process is missing. Papyrus was rather expensive, therefore we suppose that this was kept secret in order to maintain the monopoly for exportation.

Only the production of Papyrus mats (figure 2) is documented with pictures. These mats were used as seats and for protection against sun and sand and probably as lifesaver vests. The mats – after weaving – had to be beaten in order to get a certain flexibility to be worn around the shoulders. The papyrus Anastasi IV (1500 B.C.) [1][2] from the British Museum, which describes the hardship of the Egyptian soldier's life, gives presumably a further information on the beating process of papyrus. It says that "the soldiers were beaten like papyrus."

[2]The figures in brackets indicate the literature references at the end of this paper.

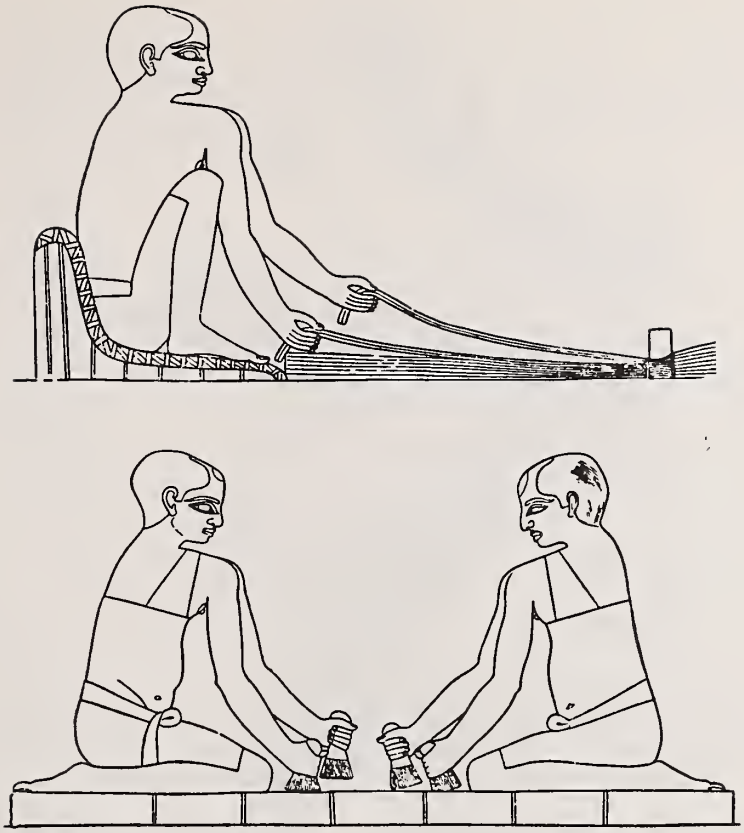

Figure 2. Production of papyrus mats.

Pictures of the transport of the gathered stems after harvesting papyrus (figure 3) are sometimes seen as wall paintings in tombs.

A summary on the production of "papyrus-paper" is for the first time found in Pliny's "Natural History," where he spoke of the method of making papyrus used in ancient Egypt.

The stems of the disbarked papyrus were cut into fine stripes, which were spread out parallel to each other; a second layer was put across on top of the first one. The double sheets were placed between two cloths, beaten with a wooden hand-hammer and pressed for a longer period. This resulted in a coherent papyrus sheet, which was bonded together by the muddy water of the river Nile.

The surface was smoothed with wooden instruments in order to avoid any running of the ink during the writing process. Papyrus rolls of several meters in length could be produced by joining individual sheets. Pliny's statement [2] about the gluing action of the muddy Nile water has been reinvestigated by several papyrologists. The most practical and conclusive proof about the falacy of this theory was given by the papyrus institute of Cairo, which used filtered Nile water and found that the papyrus strips stick together just the same. Therefore, the mud of the Nile water does not play any adhesive role. A new theory about the adhesion of papyrus strips based on physical factors was recently brought forward by the President of the papyrus institute, Hassan Ragab [3], who was successful in making a papyrus-like material according to his theory. Another study on this problem was made by Corado Basile [4] of Sicily, who tried to make papyrus by the methods of the ancient Egyptians. He claims that chemical factors, pretreatment with aluminum sulfate solutions, are responsible for the bonding of the papyrus fibers.

Figure 3. Transport of the gathered stems.

Both materials showed distinctly different behavior during our own studies with thermoanalytical methods (figure 4). Corresponding DTA curves give the peaks, which are due to the oxidative decomposition of cellulose (200–300 °C) and of lignin (350–430 °C). The Sicilian papyrus of today behaves rather similar to the majority of the post-Christian Egyptian papyri. On the other hand, the freshly made Egyptian papyrus shows a close relationship of its DTA-peaks to those of some of the pre-Christian papyri.

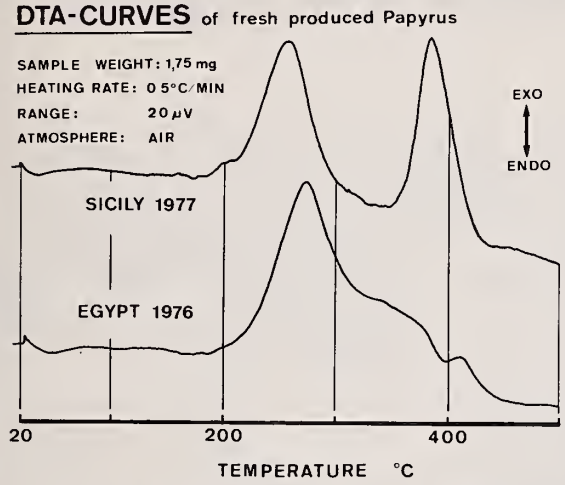

Figure 4. DTA curves of fresh produced papyrus.

Cuts of both products with a microtome clearly showed the two layers, in length and lateral (figure 5). Tests with iodine/potassium iodide proved the non-existence of a starch adhesive. Only isolated grains of starch, grown in the papyrus plant, are clearly visible (figure 6). For comparison, we also examined the famous ancient Papyrus EBERS

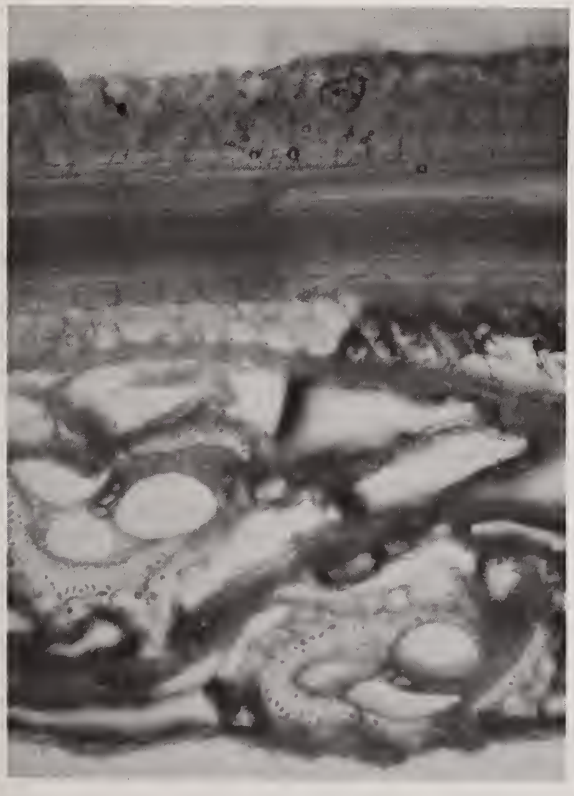

Figure 5. Microtome cut shows the layers in length and lateral — 250X.

Figure 6. Grains of starch, grown in the papyrus plant — 1000X.

[6] (middle of 16th century, B.C.) from the Library of the University of Leipzig. This cut again shows the two layers, but this time very clearly, the layer of starch adhesive, dark blue colored, is visible (figure 7). This surprising result at first led to the assumption that this was one of the joints where the sheets had been glued together to a scroll. There should be, however, four layers present. Over 50 cuts on various parts of the papyrus – where it was certain that there were no joining points of the roll – still showed the layer of starch adhesive between the papyrus layers. Therefore, these results are the first definitive proof that starch was used as a gluing agent for ancient Egyptian papyri.

Figure 7. Microtome cut of Papyrus EBERS, shows between the two layers of papyrus the layer of starch adhesive – 120X.

2.3. Experimental Investigations

Measurements on ancient materials are always linked with various difficulties. Whenever possible, non-destructive methods are preferred. However, there are certain limitations due to the nature of the materials. Definitive and conclusive results are only obtainable from dated original papyri. Under certain circumstances, certain destructive methods are allowed if they are very sensitive, and require only very small amounts of materials.

In the case of papyrus, thermoanalytical investigations with a Mettler TA 2000 proved to be very effective, the amount of the sample required was only 1 - 2 milligrams. Reproducibility of the DTA curves which were usually recorded with a heating rate of 0.5 °C/min was excellent (figure 8). In this connection it is very important to carry out the experimental runs in oxidizing atmosphere because the thermal effects are much larger than in an inert atmosphere. These measurements were supported by several other experimental techniques, e.g., scanning electron microscopy, infrared absorption spectroscopy, thermomicroscopy and histological studies. As mentioned already, no directions have ever been found describing methods how the writing material papyrus was made in ancient Egypt, especially how the adhesion between the individual layers of papyrus was achieved. A compilation of DTA curves of some very famous ancient papyri is shown in figure 9. Principally, all the curves show two main peaks: the first, lower-temperature peak corresponds to the oxidation of cellulose; the second one to the oxidation of lignin. A very small endothermic peak at about 150 °C is always present in papyri which were treated mechanically, e.g., by beating. The very broad exothermic peak at 325–375 °C is due to growth of fungi in the papyrus, which contains chitine as one of the main components.

DTA curves of the relatively well-preserved papyrus EBERS [6] showed that the rather dark parts differ in their behaviour from the bright parts. With identical sample weights, the first big peak corresponding to cellulose is the same in both curves; the second one, however, the lignin peak is bigger for the dark material. This means a stronger dimerization respectively cross-linking of the lignin and therefore a higher energy being necessary to break up and oxidize the lignin.

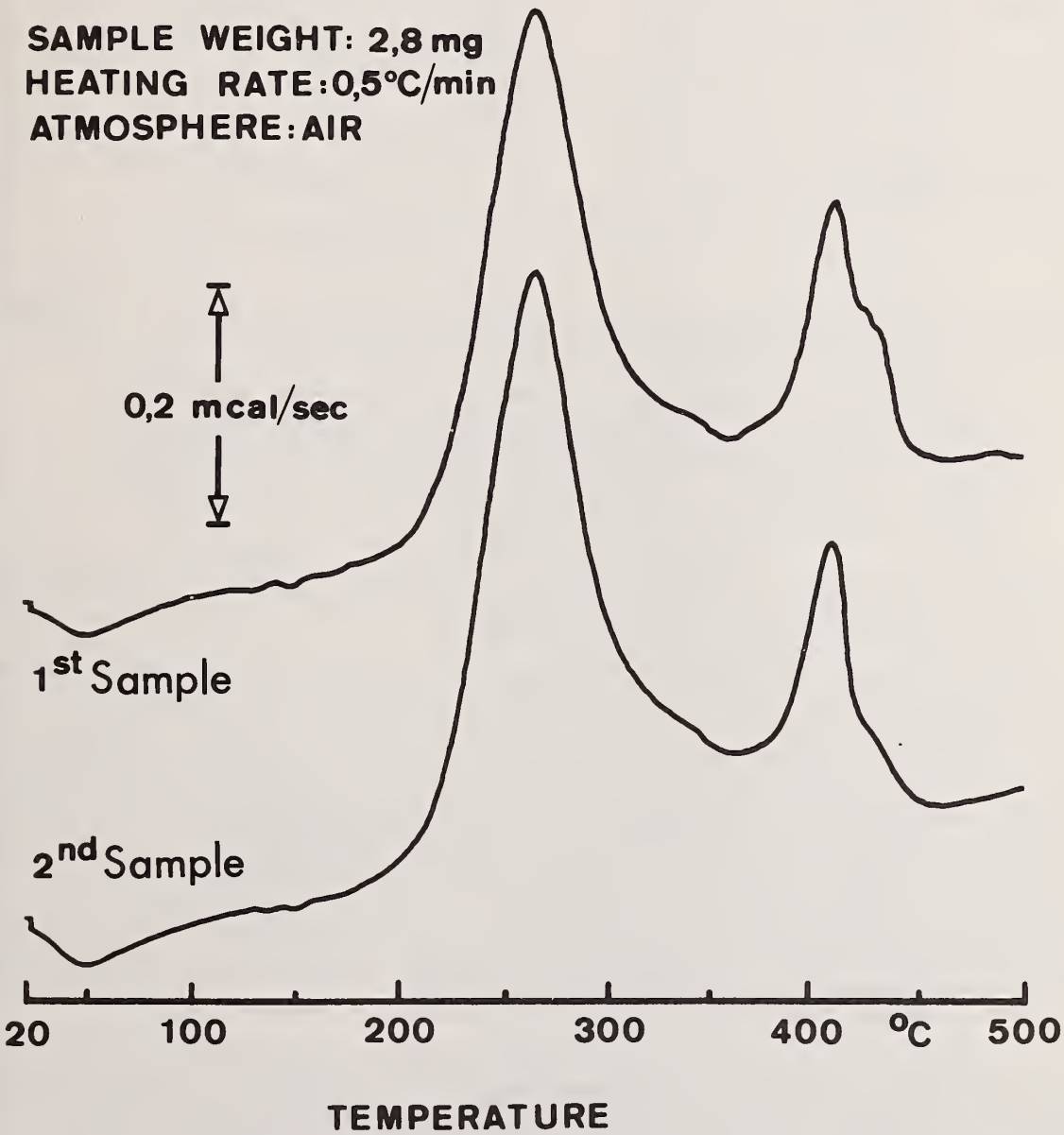

Figure 8. Reproducibility of DTA curves.

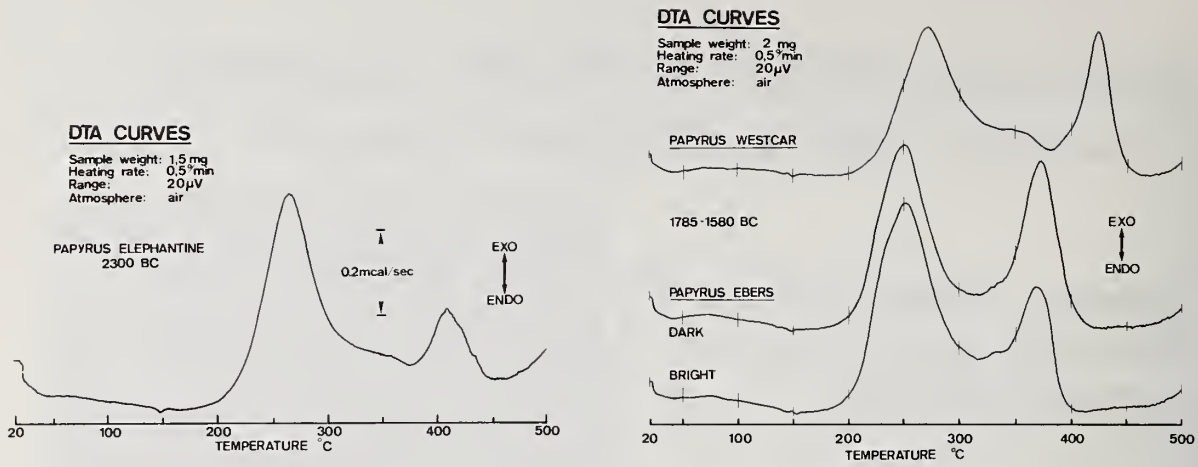

Figure 9. DTA curves of several ancient papyri.

Further DTA investigations on the papyrus Westcar [7] (1700 B.C.), which is attributed to the same era, gave curves completely different from the papyrus EBERS.

> The explanation for this disagreement may be the following: The papyrus Westcar was in fact written in the above-mentioned time, however, the papyrus material used was probably one of the reconditioned older papyri types, that means the original old inscription was erased by washing before it was rewritten. The final confirmation of this assumption requires further experimental investigations.

Microtome sections of a papyrus fragment from Elephantine, 2300 B.C. (Old Empire), showed again the two layers in length and lateral as the thousand years younger papyrus EBERS and also contained the layer of starch in between.

In order to clarify the manufacturing process of papyrus in the era towards the end of ancient Egypt and at the time of Pliny, we asked the Egyptian Museum in Berlin for dated samples from 600 B.C. to 600 A.D.. DTA curves of these samples are shown in figure 10. In principle, there is only one curve with completely different characteristics (signed with 5 B.C.) which comes from a mummy's wrapping. The other curves show that the lignin peak decreases with increasing age of the sample. Especially the histochemical investigations lead to the new knowledge that all the pre-Christian samples up to 350 B.C. show a layer of starch between the papyrus sheets, analogous to the old papyri. The younger and the new papyri on the other hand are all manufactured without the aid of a starch binder. This knowledge of the gluing action of starch obviously got lost with the end of the Egyptian dynasties, since all the papyri starting from the Ptolomaic era were manufactured without starch. The wrapping of the mummy is coated on both surfaces with starch. The procedure was to cover the mummy first with a papyrus layer and starch and to wrap it with linen again with addition of starch.

The position or temperature of the DTA peaks may be changed by differences in the manufacturing process. In his work on papyrus, Lucas [14] mentions that the Egyptians impregnated their papyrus sheets with $CaCl_2$ solutions in order to regulate their humidity; that means to avoid any drying out. Figure 11 shows a comparison of DTA curves from untreated and $CaCl_2$-treated papyrus after different times. A gradual shift of the peak onset temperature is obvious; furthermore, the lignin splits up in the samples treated for longer times. This may be explained from the reaction between the carboxyl groups of lignin and the Ca^{2+}-ions, which results in a lignin compound of higher thermal stability. Analytical results [4] of fresh and ancient papyrus are compared in Table 1.

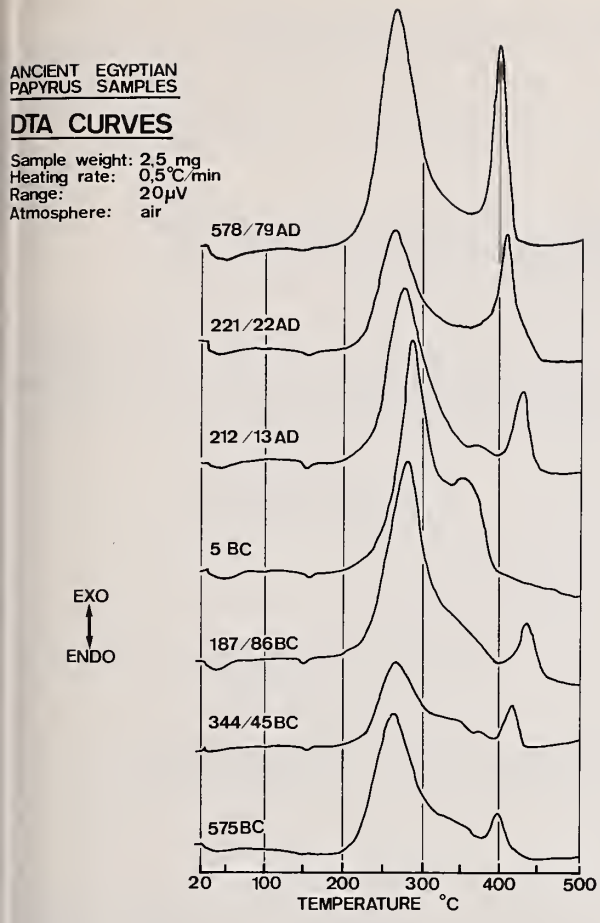

Figure 10. DTA curves of ancient papyri.

Table 1. Analytical Results of Papyrus Samples.

Elements	Ancient Sample % by weight	Fresh Papyrus % by weight
Oxygen	38.56	52.70
Carbon	36.22	40.27
Hydrogen	4.78	4.37
Nitrogen	1.55	0.95
Sulphur	0.55	0.40
Silicon	7.17	0.54
Iron	1.75	trace
Aluminum	4.05	0.009
Calcium	2.64	0.14
Magnesium	0.83	0.07
Sodium	1.43	0.43

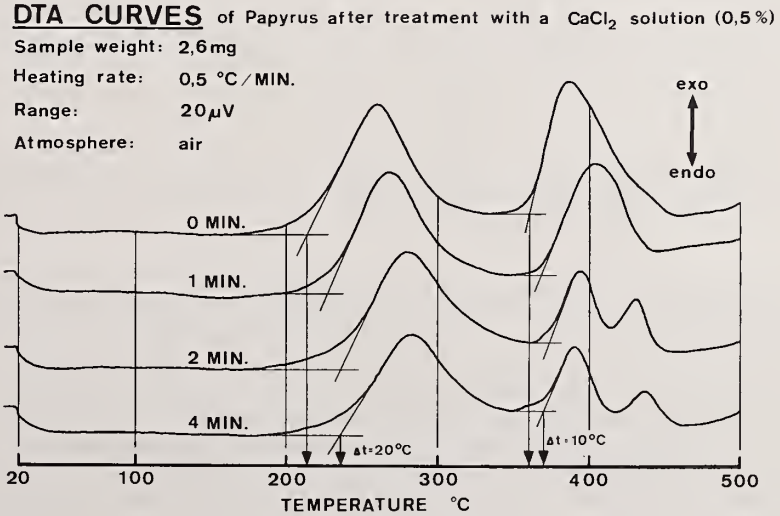

Figure 11. DTA curves of papyrus after treatment with $CaCl_2$.

This splitting of the lignin peak is observed also when papyrus is beaten. In this case a thermally more stable lignin compound is formed by dimerization (figure 12).

> The yellow-brown coloration, which was present in ancient materials, may be due to a higher degree of dimerization of the lignin. These colorations could be simulated in the course of thermomicroscopic investigations on fresh papyrus.
>
> Such papyrus sheets, which were heated for 1 hour at temperatures from 100 to 220 °C, show an increasing intensity of brown coloration. DTA curves on these samples proved that the cellulose peak decreases, whereas the lignin peak remains practically unchanged.

Also, samples irradiated with UV became increasingly brown-colored. The corresponding DTA curves showed changes of the glass transition at 50 °C and of the lignin peak between 400–450 °C, which may be caused by a different degree of condensation of lignin.

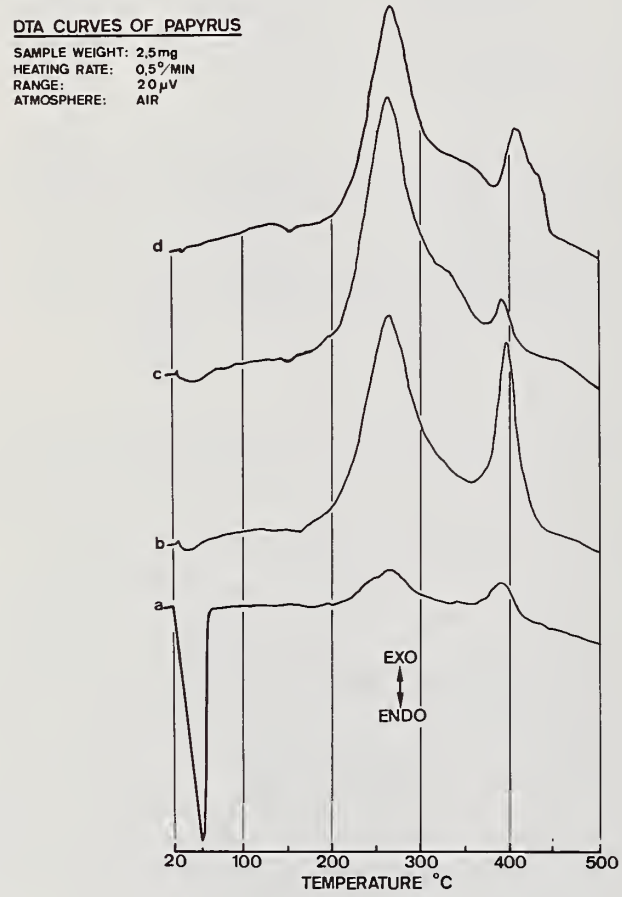

Figure 12. DTA curves of papyrus after different treatment.

The conclusion from these experimental investigations is that thermoanalytical methods like DTA are useful:

- to estimate the rough age of papyri by their content of lignin,
- to distinguish between unbeaten and beaten papyri,
- to prove the treatment with different chemical compounds like $CaCl_2$ which caused shifts of the onset points of the DTA peaks,
- to show any changes in papyrus by fungi, which give additional peaks, e.g., for chitine.

Table 2 is a tentative compilation of various factors which could be used in the differentiation between ancient papyri.

Table 2

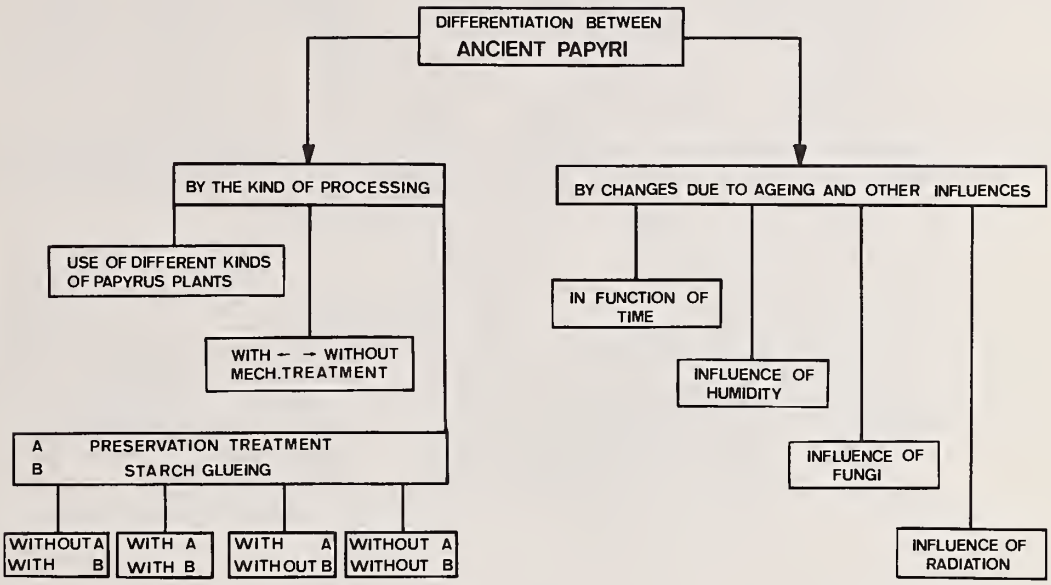

3. Chinese and Japanese Paper Technology

The real paper was invented around 105 A.D. in China where Ts'ai Lung produced the first usable writing material from tree bark and plant fibers, as well as from old rags and fishing nets. Since that time, paper has been in general use all over China.

Later, thanks to the construction of the "Silk Road," the use of paper traveled West, first to Turkestan, and then to the Arabic countries. The manufacturing methods used for the production of paper and silk were jealously guarded secrets which were not revealed to the Arabs until after the battle of Samarkand (in 751 A.D.) by Chinese prisoners of war. In Europe itself, it is virtually certain that the techniques of paper manufacturing were not used until after the time of the crusades, that is to say, in the 12th and 13th century.

Advancing via Korea, the technology of paper manufacturing also arrived in Japan, where the first paper was manufactured around 610 A.D. in Kyoto. Over the centuries the technology of paper manufacturing was constantly refined and modified with respect to the raw materials used in its production.

In this connection the detailed travel descriptions of the German physician Engelbert Kaempfer [8] should be mentioned. In his two-volume work "History and Description of Japan", which was first published in 1779, he also discusses paper manufacturing in Japan. At that time, the Japanese made paper from the bark of the mulberry tree, which was cut in strips, then mixed with ashes and boiled in water (figure 13). This was followed by various cleaning procedures whereby washing played a very important role. The bark prepared in this manner was spread on wooden tables and several labourers then beat the material with hardwood sticks until it could be stirred with water into a kind of pulp. A mixture consisting of rice starch and roots was then added to serve as binder. This Japanese paper is called "Kozo". It is very dense and snow-white. It is still produced today and the dull sheen of its fibrous surface texture is very decorative.

Figure 13. Ancient Japanese paper technology [9].

The purpose of the experimental investigations described here was to use thermoanalytical methods in order to compare old historic papers with modern paper of today, as well as to determine and account for any differences in their thermal behaviour. For this, it was necessary to test also the raw materials of Far Eastern paper manufacturing, such as bamboo, mulberry bark, Gampi Shi, and Mitsumata. For the DTA investigations of East Asiatic paper, we have used at first several sheets of present-day Japanese paper. Figure 14 shows the comparison between the DTA curves of the bark fibers of Mitsumata and Gampi and those of various types of paper made with these fibers. The similarity is obvious: at just below 300 °C, the main peak (cellulose) occurs; the lignin peaks (about 350–450 °C) are differentiated and show splitting because of the varying interlacing of the lignin.

The DTA curves in Figure 15 show one of the papers made from bamboo pulp, "to shi", called "Chinese paper", which was also used by Japanese. The curves of the Japanese Heian and Kamakura paper samples are more similar to the DTA curves of bamboo than those of the Kozo or Mitsumata papers. The curves have a peak of about 400 °C in addition to the regular cellulose and lignin peaks.

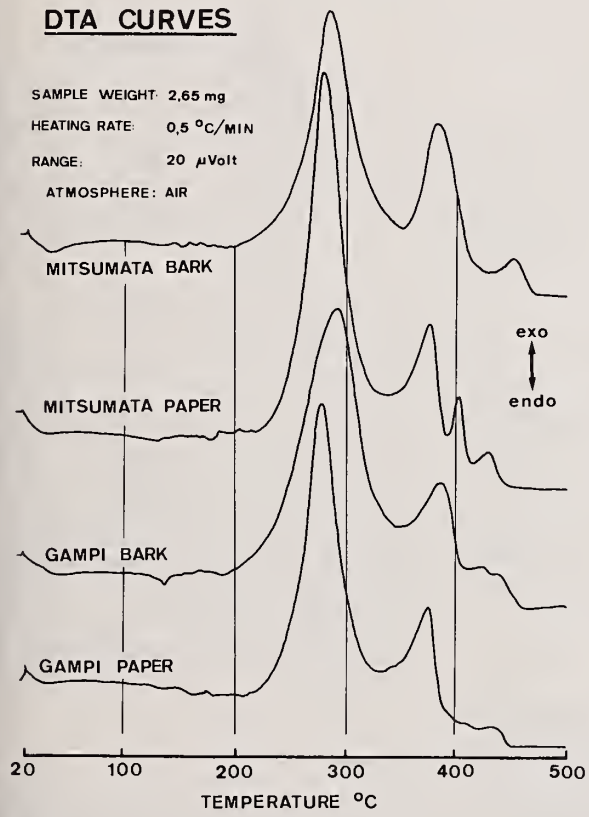

Figure 14. DTA curves of different kinds of Gampi and Mitsumata.

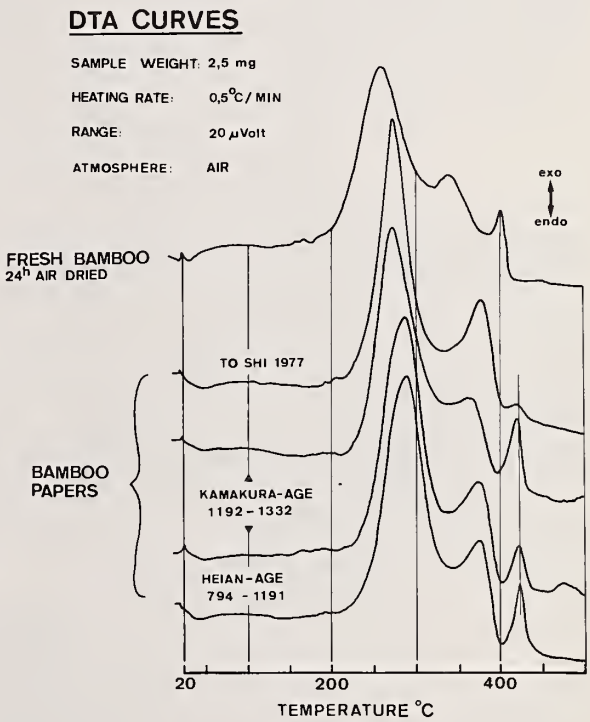

Figure 15. DTA curves of new and ancient bamboo papers.

It is interesting that all these peaks are shifted to lower temperatures for the fresh bamboo samples as compared to the old and new bamboo papers, an observation which was also made when comparing DTA curves of fresh papyrus and papyrus paper. From these results it can be assumed that bamboo has been used for the production of old Japanese paper.

When comparing figure 16 with the DTA curve of the Chinese Song paper, a certain similarity between the DTA curves of the old Chinese paper and those of the bamboo paper can be noted. Possibly the bamboo fiber was used in those days to manufacture paper. For the Tang dynasty paper no correlation or similarity with the other papers could be found.

Kozo paper, which is the main paper today, has been also investigated; the DTA curves are shown in figure 17. Here also the similarity between raw bark, raw paper, bleached bark, and art paper is obvious. The paper making process has the main effect on the lignin peak. None of the investigated ancient Japanese papers had any similarity with the curves which we measured for the Kozo paper samples. Generally, it was observed that various present-day and old East Asia paper grades show certain similarities but also characteristic differences.

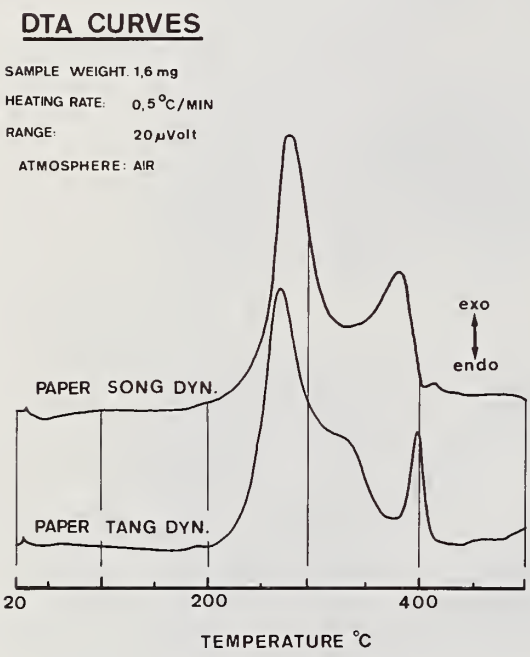

Figure 16. DTA curves of ancient Chinese papers.

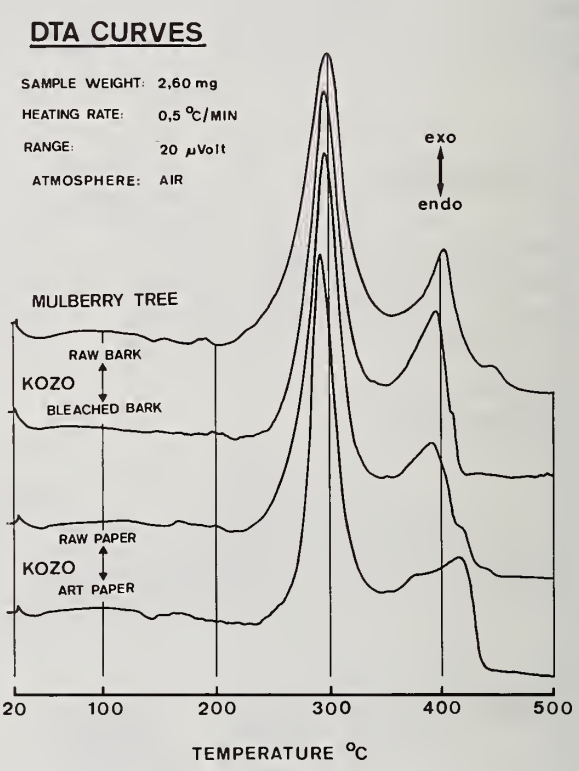

Figure 17. DTA curves of different kinds of Kozo.

4. Paper of the Maya and Aztec Cultures

The story of primitive American papermaking [12] and its place in the Aztec and Maya civilizations is still somewhat obscure and contradictory. Of the thousands upon thousands of paper sheets and paper rolls today, there exist only three complete Maya codices (the Dresdensis, the Peresianus, the Tro-Cortesianus), and scarcely more than a score of Aztec codex fragments. In their search for a smooth, easily handled material for writing, the Mayas discovered that their barkcloth tunics could be used also as a surface for their hieroglyphic symbols. After this discovery, bark-cloth tunics ceased to be used exclusively to cover bodies; they had evolved into paper. This paper was called huum by the Mayas, a "paper" far superior both in texture and durability to Egyptian papyrus. The Mayas made these hieroglyphic charts for centuries, even through the period of decline. Table 3 shows a chronological chart of the Mexican and Mayan history. When Maya civilization revived in the tenth century the Mayas had already begun to fold their huun-paper into book form. During this period they produced a sacred almanac of forty-five pages still in existence and known as the Codex Dresdensis. This remarkable polychromic book was written somewhere between 900 and 1100 A.D.

Table 3

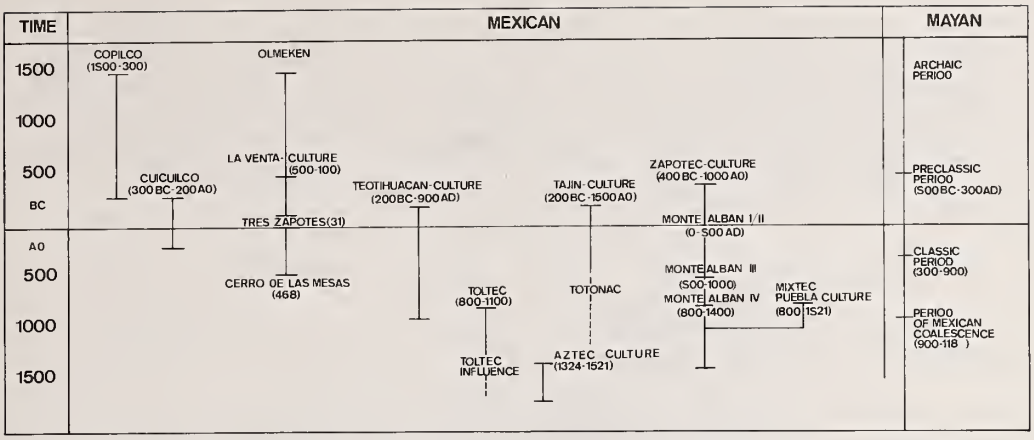

The Toltecs assimilated and improved the Mayan techniques of papermaking and writing. In the seventh century they finished the encyclopedic Teoamoxtili, a "divine book" compiled at Tula in the year 660 by the astrologer, Huematzin. Yet they too, like the Mayas before them, went into eclipse and the Aztec nation appeared between 1100 and 1300 on the cultural horizon. Under their sway, much of Middle America was systemized. Trade and conquest, an inseparable union, expanded together; tribute was levied upon conquered tribes. To keep a record of all this called for precisely written tribute-lists. And so there was an insistent demand for paper as in no other primitive American civilization.

The paper of the Aztecs was made from the bast fibers of the amatl-tree; not in a single fragment the paper was made from any other substance than the wild fig tree. Neither the Mayas nor Aztecs made paper from the maguey agave [13]. Examination disclosed that the fibers of the Maya codices – which were made from wild fig trees of the tierra caliente – differed in their histology from those taken from the Aztec codices, prepared from the bast fibers of the fig trees and the tierra fria. It is then obvious that the paper of the Mayas came from the species in their own lowland areas, while that of the Aztec fragments was always from those that grew on the plateau and hillsides. Comparative study of processes and techniques lead to the conclusion that the Mayas preceded the Aztecs. The Aztecs improved the Maya methods. In order to create a non-blotting surface, they used stone, flat iron-shaped planches which, when heated and pressed upon the paper, closed the pores, and gave it "surface", which is more or less the same technique the European papermakers used during the Renaissance in their burnishing, by means of an agate-stone.

Figure 18. Itzama the highest Mayan God, also the God of writing.

For the thermoanalytical studies we had the opportunity to examine original paper material from a fragment of the Codex of Huamantla. This fragment is kept in the Antropological Museum in Mexico-City. It is the only one from six fragments which is described in the literature. The other fragments were acquired by Alexander von Humboldt and are today in the state library of Berlin. Figure 19 shows the DTA curves of this Codex Huamantla paper and of a recent Mexican paper produced by the Otomi [10] Indians (Otomi village San Pueblito in the Sierra Madre). All three curves show the splitting of the DTA peaks into the cellulose peak and the lignin peak during the oxidative decomposition. Especially the white Otomi paper made from ficus padifolia shows a close resemblance in its DTA curve to that of the Codex Huamantla paper. This justifies the assumption that the latter was also made from the wild fig tree and not from agave fibers which show a somewhat different DTA curve.

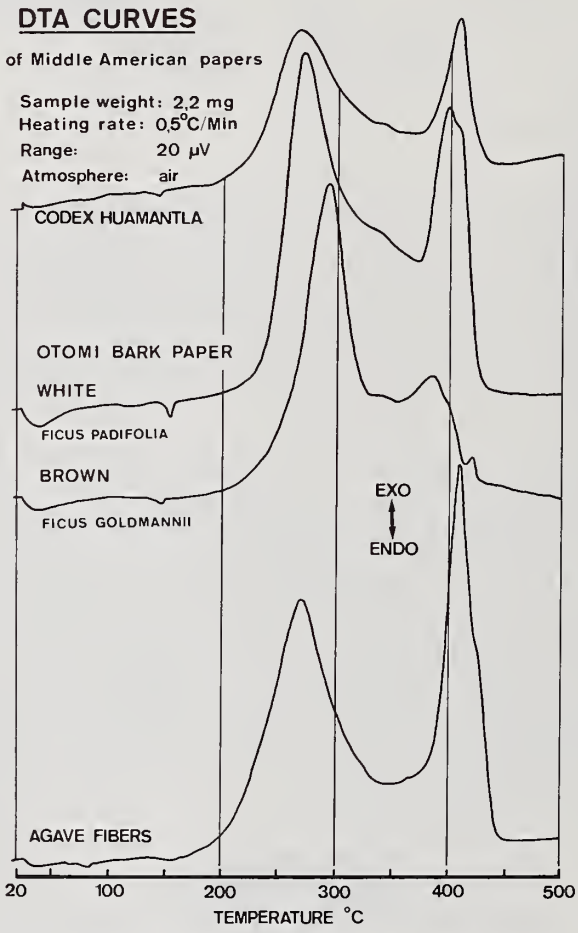

Figure 19. DTA curves, some central American papers.

The small peak at approximately 150 °C is found in all obviously mechanically treated (i.e., the beaten ones) papers. It is probably caused by the destroying of the high molecular compounds into shortchain molecules. It is known that the Otomi Indians also use a mechanical treatment with a wooden or stony beater in the production of their paper. The DTA curve of agave fibers is somewhat similar to that of the Codex Mendoza II paper.

5. Conclusion

The thermoanalytical investigations described in the present paper were a first trial to prove their suitability and informative value in the identification, dating and evaluation of production methods of ancient paper materials. The results obtained so far show that it is possible, in some cases, to distinguish between the different kinds of papers at least qualitatively and to gain some insight into the ancient paper technologies.

References

[1] Simpson, W. K., The literature of ancient Egypt, New Haven and London, Yale University Press, 346 (1977).

[2] Pliny, Natural History, translation by H. Rackham, Loeb Classical Library, London (1952).

[3] Ragab, H., A new theory brought forward about the adhesion of papyrus strips, 14th International Congress of Paper Historical Manchester (1978).

[4] Basile, C., Conservation of Paintings and the Graphic Arts, Lisbon Congress 1972, IIC, London, 901 (1972).

[5] Hussein, M. A., Vom Papyrus zum Codex, Sueddeutscher Verlag, Muenchen (1972).

[6] Ebers, G., Papyrus Ebers, Leipzig, Verlag von Wilhelm Engelmann, (1875).

[7] Erman, A., Die Maerchen des Papyrus Westcar, Berlin, W. Spemann (1890).

[8] Kaempfer, E., Geschichte und Beschreibung von Japan, Stuttgart, F. A. Brockhaus, 1964 (English edition 1728).

[9] Narita, K., A life of Ts'ai Lun and Japanese papermaking, Tokyo Paper Museum (1976).

[10] Sandermann, W., Papiergeschichte 20, 11 (1970).

[11] Glass, J. B., Catalogo de la Coleccion de Codices, Museo National de Antropologia, Mexico (1964).

[12] Hagen, W. von, The Aztec and Maya Papermakers, New York, Hacker Art Books (1977).

[13] Schwede, R., Ueber das Papier der Maya Codices, Dresden, Verlag von Richard Bertling (1912).

[14] Lucas, A., Ancient Egyptian Materials and Industries, Third edition, Arnold, London, 548 (1959).

PAPER TECHNOLOGY FROM EGYPTIAN, CHINESE AND MAYAN CULTURE

RAPPORTEUR'S COMMENTS BY

E. A. Turi
Allied Chemical Corporation
Corporate Research Center
P.O. Box 1021R
Morristown, N.J. 07960

Dr. Wiedemann's lecture reported some of the results of his very valuable pioneering research.

The author took his audience back to the ancient history, and increased their interest to learn from the past.

His lecture was not only a contribution to archeology and history, but also presented a new unique application area for thermal analysis. The author used this technique as a method to determine the age of the papyrus to identify its source and evaluate its "manufacturing" process.

During the discussion period the speaker indicated that he saw no evidence that these cultures, which were separated geographically by immense distances, had an influence on each other in the ancient art of papyrus making. His work constitutes on one hand a unique combination of scientific knowledge and technical expertise, and on the other a very exciting excursion to the ancient Egyptian, Chinese, and Mayan art and culture. It is hoped that Dr. Wiedemann will not only continue his archeological discoveries with the refined methods of thermal analysis, but his research will also inspire other scientists to follow his initiative.

National Bureau of Standards Special Publication 580. Proceedings of the Workshop on the State-of-the-Art of Thermal Analysis held at NBS, Gaithersburg, MD, May 21-22, 1979. (Issued May 1980)

RECENT INSTRUMENTAL DEVELOPMENTS

W. W. Wendlandt

Department of Chemistry
University of Houston
Houston, Texas 77004

Abstract

A survey was made of the thermal analysis (TA) techniques that were used in the six latest volumes of Thermochimica Acta and the Journal of Thermal Analysis. The most widely used techniques are thermogravimetry (TG), differential thermal analysis (DTA), and differential scanning calorimetry (DSC); these techniques account for over 50 percent of the experimental data in a total of 465 technical articles. Rather surprisingly, high temperature x-ray diffraction accounted for about 4 percent of the experimental techniques. New TA techniques discussed include concurrent DTA, EC, and TG using commercial equipment, and the thermophotometry of coordination compounds.

Contents

I. Introduction

According to the ICTA [1][1], thermal analysis is a group of techniques in which some physical property of a substance and/or its reaction product(s) is measured as a function of temperature while the substance is subjected to a controlled temperature program. With this definition, a large number of techniques fall into the classification of thermal analysis. Physical properties measured, as shown in Table 1, include mass, temperature, enthalpy, dimensions, optical characteristics, electrical characteristics, and so on.

[1]Figures in brackets indicate the literature references at the end of this paper.

Perhaps a more illustrative view can be seen in the figure proposed by Kambe [2], as shown in figure 1. The thermal analysis technique is given in the outer circle, while the inner circle defines the measured physical property.

Table 1. Classification of thermal analysis techniques [1].

Measured Property	Principle Techniques
Mass	Thermogravimetry Isobaric mass-change determination Evolved gas detection Evolved gas analysis Emanation thermal analysis
Temperature	Heating curve determination Differential thermal analysis
Enthalpy	Differential scanning calorimetry
Dimensions	Thermodilatometry
Mechanical characteristics	Thermomechanical analysis Dynamic thermomechanometry
Acoustic characteristics	Thermosonimetry Thermoacoustimetry
Optical characteristics	Thermoptometry
Electrical characteristics	Thermoelectrometry
Magnetic characteristics	Thermomagnetometry

The three most widely used thermal analysis techniques are those involving mass, temperature, and enthalpy changes. Indeed, as presented in Part II of this paper, these techniques account for over 50 percent of the experimental data that is published in the two thermal analysis journals. A noticeable trend that is observed, however, involves the use of many well known analytical techniques to complement or supplement thermal analysis studies. Indeed, if the physical parameters of these techniques are measured as a function of temperature, they constitute still other thermal analysis techniques.

2. What TA Techniques Are used Today?

The Techniques used in analytical instrumentation are big business. According to a study by Frost and Sullivan [3], the market for analytical instrumentation will triple over the next ten years. In a recent survey, they predict an overall U.S. market of $2.3 billion by 1987, up from $760 million in 1977. They also predict a "total revolution" in design of instruments; microprocessor-based technology is expected to rapidly replace older instruments during the next five year, in some techniques. New individual instruments are to be self-contained and capable of data analysis, reduction, display, and capture. It should become possible to interface all of the instruments in a laboratory. The report also says that emphasis will be more on applying existing technology than on pushing the limits of the art. Also, it predicts a marketing shift from an emphasis on instruments to a concentration on applications.

American Laboratory [4] polled a sample of those who attended the Pittsburgh conference with regard to anticipated instrumentation budgets and purchase plans of their organizations. For thermal analysis equipment, 103 (30.6%) indicated that they now have such instrumentation in use, while 49 (14.6%) predicted future use in some application area. The projected growth for 1979 was 47.6 percent; this compares with an average projected growth of 20.5 percent for all analytical instrumentation techniques.

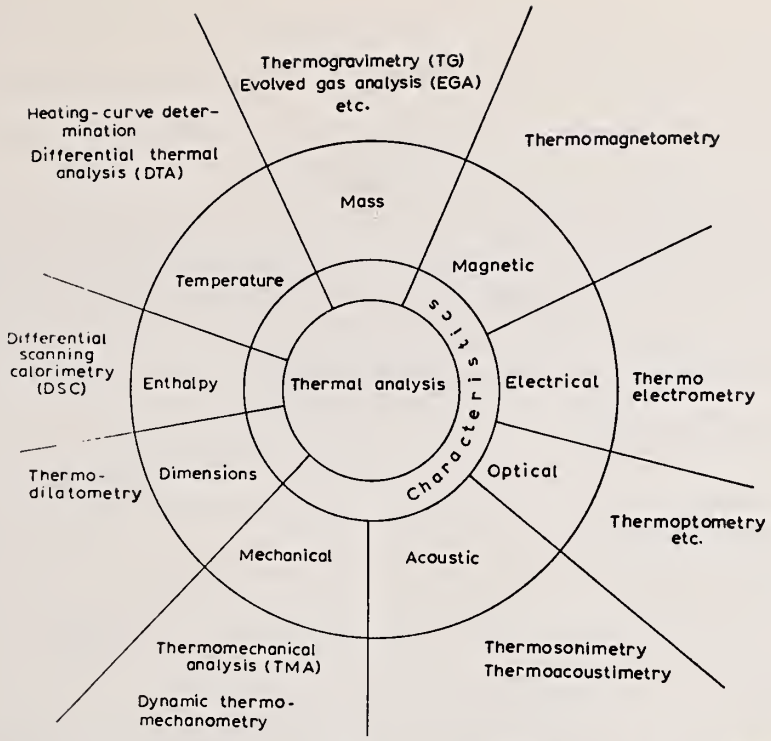

Figure 1. Classification of ICTA techniques as given by Kambe [2].

A survey is reported here of the thermal analysis (TA) techniques that are currently in use, based upon investigations reported in the two leading TA journals. The techniques and their percentage of use are shown in Table 2 and figures 2 and 3.

Table 2. Techniques used in thermal analysis.

		Percentage	
		TCA	JTA
1.	TG (Isothermal)	29.1	22.0
2.	DTA	16.7	26.2
3.	DSC	6.8	6.8
4.	DTG	6.2	4.5
5.	X-ray, H.T.	4.6	4.2
6.	MS (MTA)	2.8	1.1
7.	Elec. properties	2.2	1.4
8.	EGD-EGA	1.9	3.1
9.	TMA (dilatometry)	1.9	1.1
10.	Derivatography (MOM)	1	13.2
11.	Miscellaneous TA	18.5	13.3
12.	Calorimetry, all types	8.7	2.8
13.	Total Number of papers in survey	220	245

References: TCA Volumes 24-29 (1978-1979);
JTA Volumes 8-13 (1975-1978).

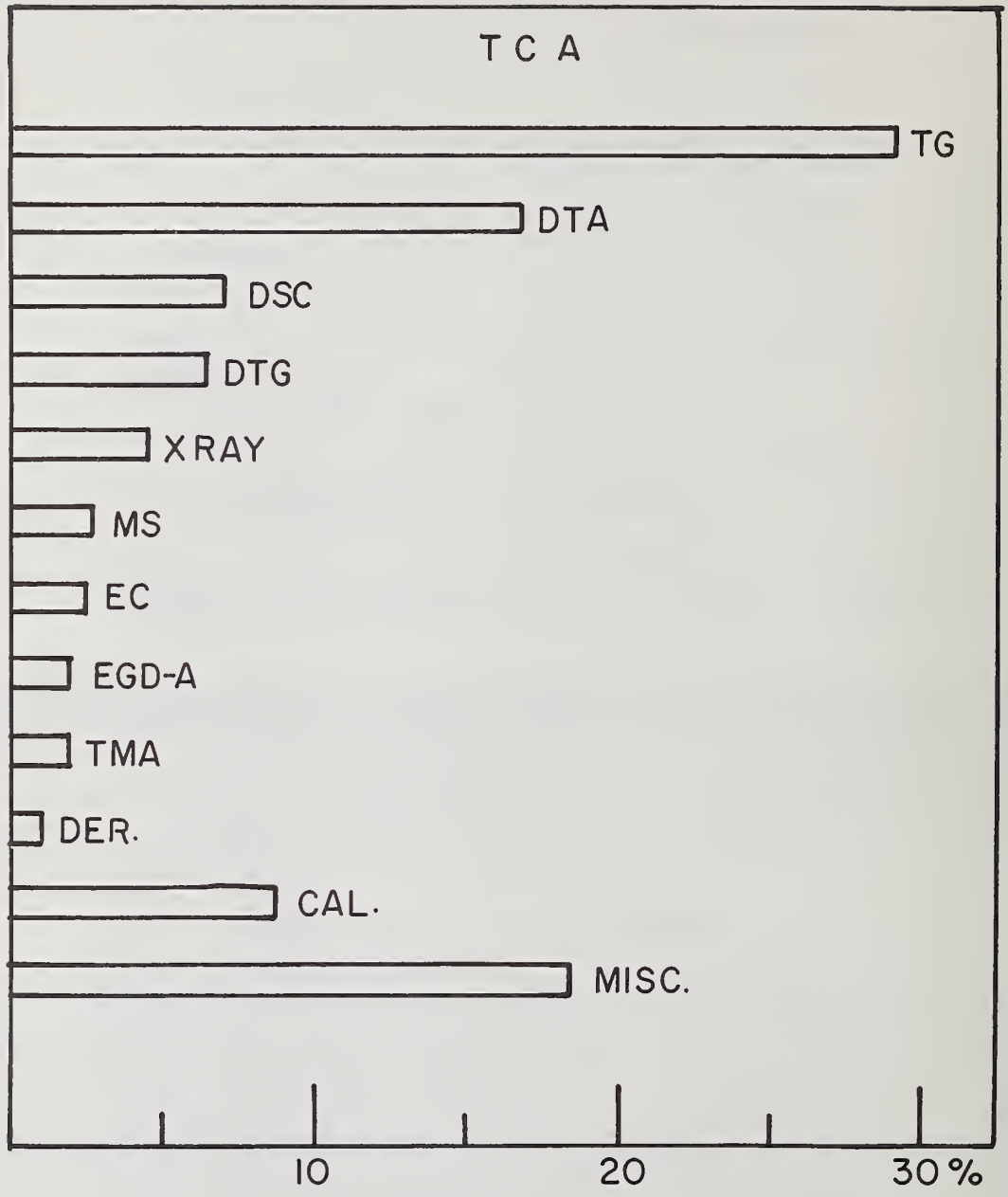

Figure 2. Use of TA techniques reported in TCA volumes 24-29.

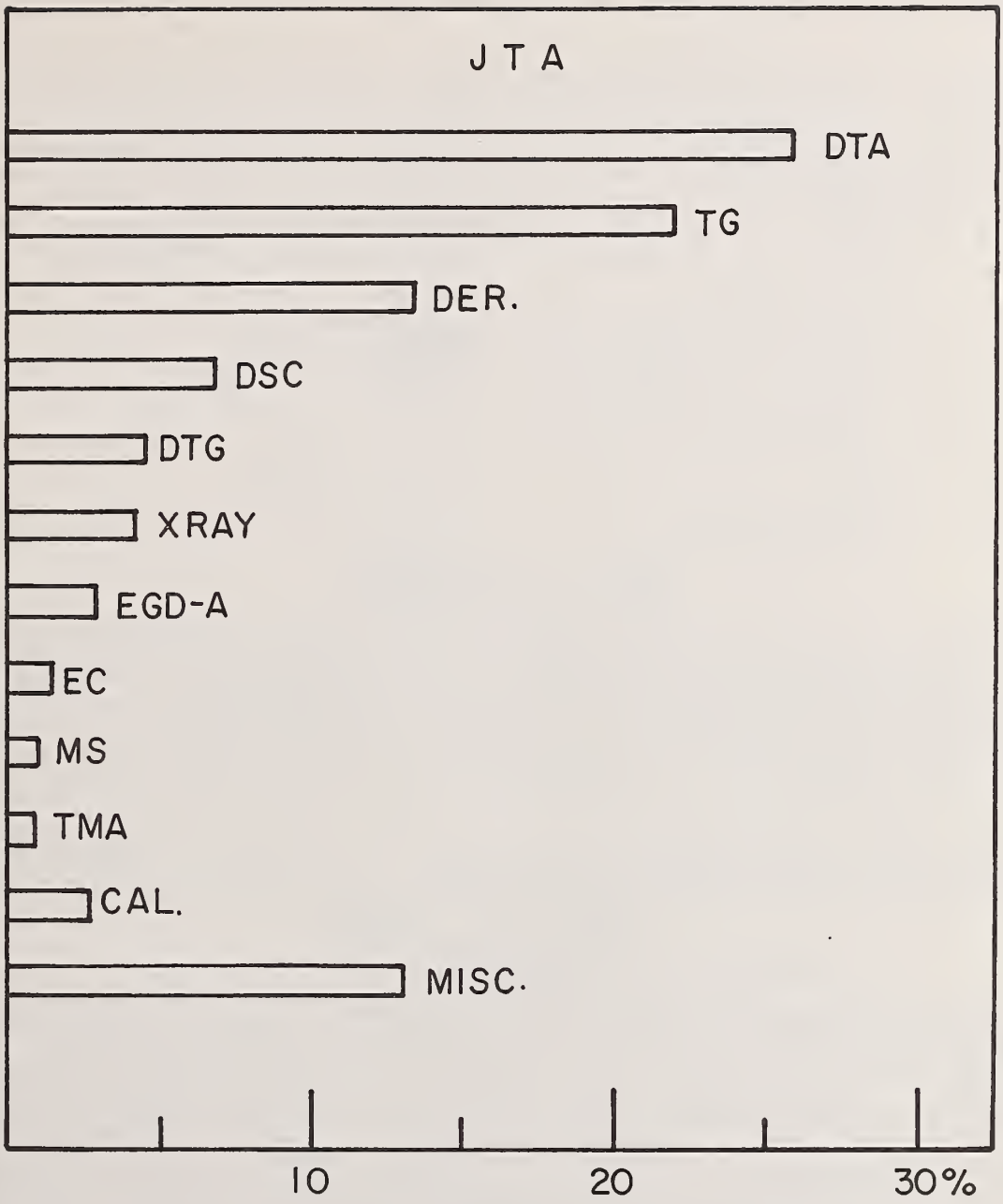

Figure 3. Use of TA techniques reported in JTA volumes 8-13.

The six latest volumes of Thermochimica Acta (TCA) (Volumes 24-29) and the Journal of Thermal Analysis (JTA) (Volumes 8-13) were used in the survey, with similar use reported of certain TA techniques. For TCA, thermogravimetry (TG), both dynamic and isothermal, was the most widely used technique (29.1%), followed by differential thermal analysis (DTA) (16.7%) and differential scanning calorimetry (DSC) (6.8%). Of the other TA techniques, rather surprisingly, high temperature x-ray diffraction accounted for 4.6 percent of current use. The other "major" techniques were mass spectrometry (all types) (2.8%), evolved gas detection (EGD) and analysis (EGA) (1.9%), electrical properties (2.2%) and

thermomechanical analysis (TMA) (1.9%). The miscellaneous TA techniques cited, which were 18.5 percent of the total, consisted of numerous instruments employed in a dynamic temperature mode. Most of these techniques are listed in Table 3.

Table 3. Some miscellaneous TA techniques found in survey.

Light Scattering	GC
Temperature Jump	pH Titration
ESR	EMF
Magnetic Susceptability	Spectrophotometry, Visible, IR
H.T. Microscopy	Density
Thermosonimetry	Diffuse Reflectance
Auger Elecron Spectro.	Thermometric Titrimetry
Temperature Profile Anal.	Torsional Braid Anal.
Thermal Optical Anal.	Mossbauer Spectro.
SEM	Isothermal Compress.
Thermoluminescence	Organoparticulate Anal.
Vapor Pressure	Plus others. . .

For JTA, the most widely used TA technique is DTA (26.2%), followed by TG (22.0%). Both of these techniques would be increased if Derivatography (13.2% was broken down into TG, DTA, and DTG modes. Rather surprisingly, the use of DSC (6.8%) was the same as in the TCA survey. Again, high temperature x-ray diffraction (4.2%) led the other "major" TA techniques, followed by EGD-EGA (3.1%), electrical properties (1.4%), MS (1.1%), and TMA (1.1%). The increased use of Derivatography is, of course, expected, since the instrument is manufactured in Hungary and is widely used there and in Eastern European countries.

This informal survey points out that of 465 papers reported in these two journals, TG DTA, and DSC are the most widely used of all of the TA techniques. They account for 53-55 percent of all of the TA techniques used, a result which is not really very surprising.

3. Concurrent DTA, EC, and TG Using Commercial TA Equipment

The use of simultaneous thermal analysis techniques is today a well-established procedure in thermal analysis. Simultaneous measurements, such as TG-DTG, TG-DTA, TG-DTG-DTA, TG-DTA-EGD, and so on, are easily made, using commercially available equipment from several manufacturers. The advantages of this approach over simple technique measurements are numerous, with the most important being (a) timesaving convenience of two or more measurements at the same time; (b) exposure of the sample to identical conditions of furnace atmosphere and temperature environment; (c) identical sample characteristics, such as packing density, particle size, surface area, and so on; and (d) preparation and instrument loading of a single, rather than multiple samples. There are, as expected, some disadvantages of simultaneous techniques also, the most important of which is that certain thermal analysis techniques require different conditions of furnace heating rates or sample characteristics for optimum results. However, the advantages of the simultaneous measurement technique almost always outweigh the disadvantages so that this approach is widely used in many areas of thermal analysis.

Wendlandt [5] has previously described the modification of commercial TA equipment for concurrent TA measurements. The distinction between simultaneous and concurrent measurements is that the former employs multiple technique measurements on a single sample, while the latter uses an individual sample for each technique employed. As might be expected, the latter approach is easier to carry out in modified commercially available equipment, hence its use in this investigation.

a) Sample probes

The sample probes for the concurrent DTA-TG and EC-TG measurements are shown in figure 4.

Two sample probes are employed: probe A for DTA-TG measurements and probe B for EC-TG measurements. The sample probe is inserted into the outboard end of the furnace tube (see figure 5) and positioned so that the sample holder is located as close as possible to the thermobalance sample container. The DTA sample probe consists of two Inconel cups, each 6 mm in diameter by 1 mm in height, to which is spot-welded the chromel and alumel thermocouple wires. These wires are contained in a 3 mm diameter 4hole ceramic insulator tube whose length in the furnace may be adjusted by a set-screw on the machined

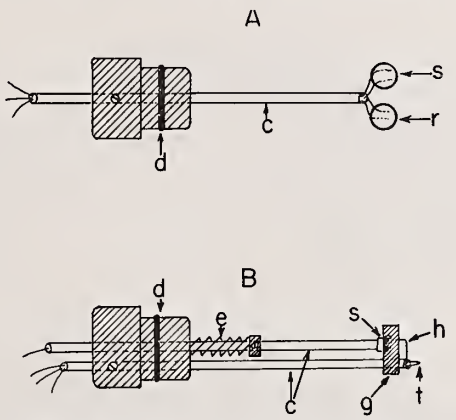

Figure 4. Sample probes for (A) DTA and (B) electrothermal measurements; c, ceramic insulator tubes; d, O-ring; e, spring; r, reference sample holder; s, sample holder; t, thermocouple; g, sample block; and h, contact wire.

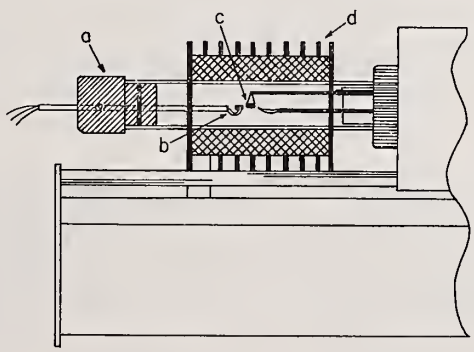

Figure 5. Sample probe configuration in thermobalance a, DTA sample probe; b, DTA sample holder; c, TC sample holder; and d, furnace.

aluminum holder. This holder, which is inserted in the furnace tube, is held firmly in place by the "O"-ring. The electrothermal probe consists of two ceramic insulator tubes, the lower one of which contains a cavity which holds a 6-mm diameter gold cup. The sample is placed in the gold cup and is held in place by the spring-loaded upper ceramic rod, which is capped on the end with a platinum metal disk. Electrical contact with the sample is provided by the wire attached to the gold cup and the wire spot-welded to the spring-loaded platinum disk. The overall length of the probe within the furnace chamber can be adjusted by means of a small set screw on the machined aluminum holder.

The positioning of the sample probe into the thermobalance furnace is shown in figure 5.

The furnace tube hose coupling is cut off and the tube extended about 2.5 cm so that the aluminum holder of the probe can be inserted into the furnace chamber. A tight fit is provided by the rubber "O"-ring, which is fitted in a machined groove in the holder. A small hole is drilled in the holder to permit the effluent gases to be discharged into the atmosphere.

b) TG-DTA System

A schematic diagram of the TG-DTA system is illustrated in figure 6.

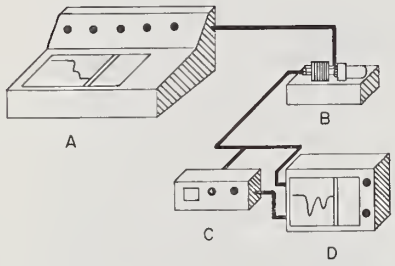

Figure 6. TG-EC system: A, DuPont control console; B, DuPont thermobalance; C, microvolt amplifier; and D, X-Y plotter.

The system components consist of the following components: (A) the DuPont Model 900 control console; (B) a DuPont Model 950 thermobalance; (C) a Leeds and Northrup Model 9835B microvolt amplifier; and (D) a Hewlett-Packard Model 7035B X-Y function plotter. Mass-change data is obtained on the control console plotter while the DTA curve is recorded on the outboard plotter. The temperature drive for both recorders is obtained from two separate thermocouples; one is located near the thermobalance sample container and the other is part of the DTA sample probe.

c) TG-EC System

A schematic diagram of the TG-EC system is illustrated in figure 7.

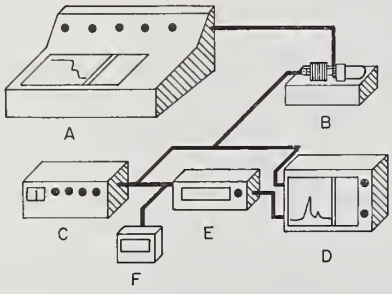

Figure 7. TG-EC system: A, Dupont control console; B, DuPont thermobalance; C, Heath oscillator; D, X-Y plotter; E; digital multimeter; and F, frequency counter.

The system components consist of the following: (A) DuPont Model 900 control console; (B) DuPont 950 thermobalance; (C) Heath Model 1G-1B variable frequency oscillator; (D) Hewlett-Packard Model 7035B X-Y function plotter; (E) Keithley Model 171 digital multimeter; and (F) Southwest Technical Products frequency counter. As in the case of the TG-DTA probe, the temperature drive on both of the recorders is obtained from two separate thermocouples. The mass-change curve is recorded on the DuPont control console while the EC (ac current) is recorded on the Hewlett-Packard X-Y plotter.

4. Concurrent TG-DTA measurements Using a Cahn Balance

Wendlandt [6] has also recently described the conversion of a Cahn Electrobalance for concurrent TG-DTA measurements. This type of balance, due to its sensitive suspension, cannot contain sample and reference thermocouple wires attached to the balance beam, thus it is not possible to determine T_s and T_r on one sample.

a) TG-DTA Apparatus

A schematic diagram of the furnace and sample holder is shown in figure 8.

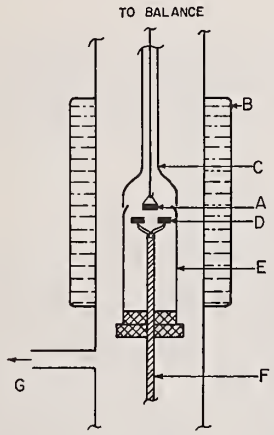

Figure 8. Schematic diagram of furnace and sample holder for TG-DTA measurements: A, TG sample holder; B, furnace; C, TG baffle; D, DTA samples and reference holders; E, DTA baffle; F, ceramic support rod; and G, gas exit tube.

The sample for TG measurements is placed in container A, while that for DTA measurements is held in one of the identical containers at D. As in the DuPont thermobalance [6], the DTA probe is attached to the bottom of the furnace tube and can be easily removed for sample loading and removal. Considerable recorder curve noise is present unless the area around both the samples is properly baffled to prevent extraneous air currents in the furnace chamber. The TG sample is enclosed by baffle C, which is constructed of Pyrex glass, while the DTA baffle E is a tube made from nickel metal foil. For a controlled furnace atmosphere, such as dry nitrogen, gas flow is through the balance chamber, down the inside of baffles C and E, and out exit tube G.

The balance employed was a Cahn Model RG Electrobalance (not shown in figure 8), although other similar balances could be used. A simple tube furnace was constructed from a Vycor tube (2.5 cm in diameter) wound with a Nichrome wire resistance element. The TG and DTA curves were multiplexed on a single X-Y plotter using a Donlee Laboratory electronic switch. Both functions were recorded versus the sample temperature, T_s, as detected by the DTA sample thermocouple.

b) DTA Baseline Compensator Circuit

With a DTA apparatus such as this, there are always difficulties relating to the sloping baseline of the DTA curve. This problem was first noticed by Baxter [7] using the DuPont DSC cell and solved by employing a simple voltage divider circuit. This circuit was modified for use in this DTA apparatus, as shown in figure 9. The resistance values

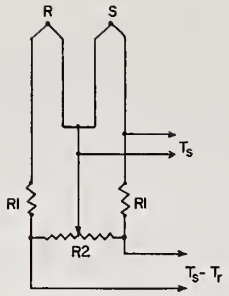

Figure 9. DTA baseline compensation circuit.
R1 = 15; R2 = 200,
10-turn potentiometer.

are not critical but should be within ±50 percent of the values cited. Adjustment of the 10-turn resistor, R2, will change the slope of the baseline either in a positive or negative direction. It is adjusted until the baseline remains flat over the temperature range of interest (usually 25 to 500 °C).

5. The Thermophotometry of Some Coordination Compounds

The light emission or thermophotometry [1] of Alathon [8], various other polymers [9], and of miscellaneous substances [10], has been studied by various detection devices in this laboratory since about 1970. It is inferred from the previous investigation of polymers that the initial light emission in all atmospheres is the result of oxyluminescence associated with the formation of hydroperoxide radical intermediates. Subsequent light emission in air and oxygen also manifests oxyluminescence although a weaker phenomenon, noted as chemiluminescence, was observed in nitrogen atmospheres. Except for 66 Nylon, no correlation was observed between light emission and melting. It was noted that there was a clear relationship between the observed light emission of the polymer and its thermal degradation.

The use of light emission techniques to detect ignition temperatures of various substances was investigated by Collins and Wendlandt [10]. Ignition temperatures, as used by these authors, referred to the temperature at which the first light emission, due to the combustion of the sample, was detected. It was found that the major instrumental factor which affects the ignition temperature was the sample heating rate. Generally, as the heating rate increased, the ignition temperature increased according to an approximately linear relationship. Some substances were observed to char without ignition if the heating rate was too slow, thus, fast heating rates, usually above 50 °C min^{-1}, were recommended.

It is well known [11] that transition metal coordination compounds containing vigorous oxidizing groups in the ionization sphere and reducing ligands such as ammonia or amines in the coordination sphere dissociate very rapidly on heating. In certain cases, the thermal dissociation reaction is of explosive violence suggesting their use as detonators or explosives for various applications. In most cases the rapid thermal dissociation of these compounds has been mainly investigated by the thermal analysis techniques of TG, DTA, and DSC. The highly exothermic nature of these reactions results in rather spectacular DTA and DSC curves using small (1 or 2 mg) quantities of samples. With TG, the ensuing rapid dissociation reaction yields an almost vertical displacement of the curve on the mass-loss axis. Since these vigorous thermal dissociation reactions should be accompanied by light emission, the technique of thermophotometry is immediately suggested as another means for their investigation.

a) Apparatus

Collins and Wendlandt [10] have previously described an appparatus to detect the ignition temperatures of various materials. It consisted of a Vycor tube furnace in which a photomultiplier (PMT) tube was attached to one end via a Pyrex glass window. Any light emission by the sample, which would be indicative of ignition, was detected by the PMT and recorded as a function of temperature on a X-Y plotter. Controlled static or flowing gaseous atmosphere could be maintained in the furnace chamber.

A more sensitive light detection system using a photon counter was employed in an apparatus described by Wynne and Wendlandt [8]. The PMT was mounted directly on the glass plate cover of the sample holder enclosure of the Perkin-Elmer DSC-1B calorimeter. Using this arrangement, the DSC curve as well as the light emission curve could be recorded simultaneously.

Neither of the above systems could be used very satisfactorily under reduced pressures (<760 mm Hg). A new apparatus, which incorporated this feature as well as others, was designed and constructed and is described here.

The thermophotometry apparatus is illustrated schematically in figures 10 and 11.

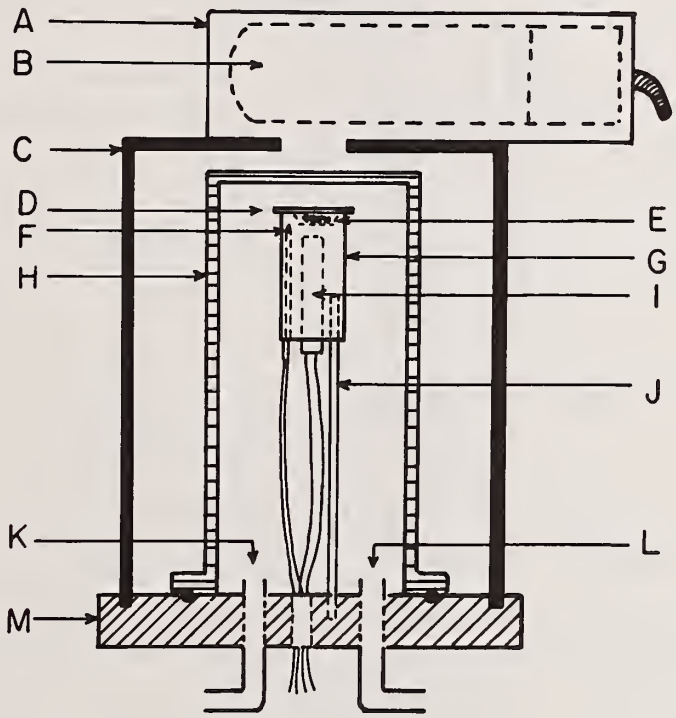

Figure 10. Schematic diagram of furnace and enclosure.

A. Photomultiplier tube housing
B. Photomultiplier tube (1P28)
C. Aluminum enclosure
D. Cover glass
E. Sample chamber
F. Sample thermocouple
G. Aluminum furnace
H. Glass enclosure
I. Heater cartridge
J. Ceramic support rod
K. Gas inlet port
L. Gas outlet port
M. Aluminum base

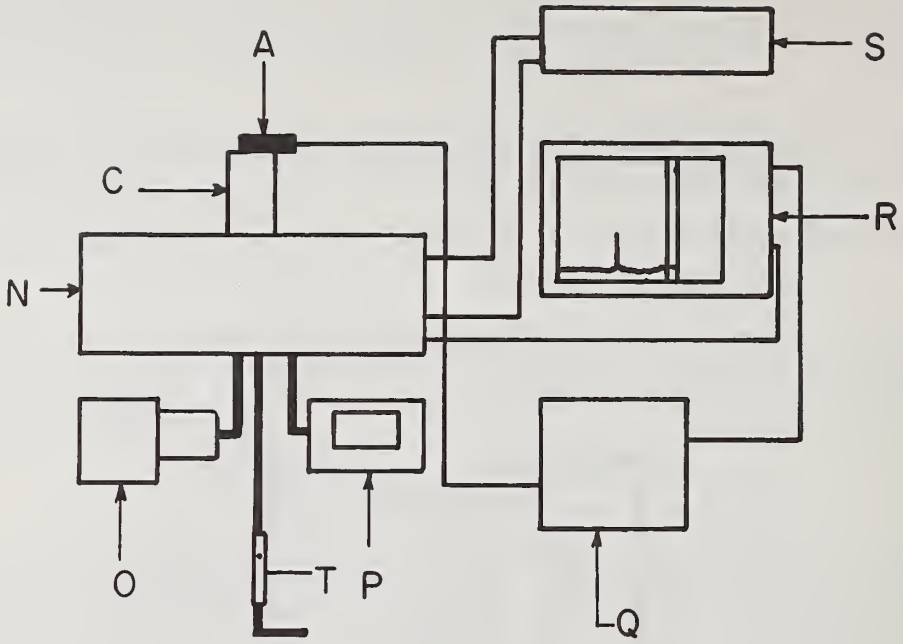

Figure 11. Schematic diagram of apparatus

A. Photomultiplier tube housing
C. Furnace enclosure
N. Cabinet
O. Vacuum pump
P. Digital manometer
Q. Photometer
R. X-Y plotter
S. Temperature programmer
T. Flowmeter

The cylindrical furnace, G, 18 mm by 30 mm, was heated by a small stainless steel heater cartridge of 50-watt capacity. It was supported by a 3.0 mm in diameter ceramic rod, which was attached to an aluminum base. The sample was contained in a 1.0 mm by 7.0 mm in diameter disposable aluminum crucible. To prevent spattering by the sample on the Pyrex glass enclosure, H, a circular microscope coverglass (15 mm) was placed on the top of the furnace. Temperature of the furnace and sample was detected by a Chromel-Alumel thermocouple, F, which was positioned as near as possible to the sample cavity in the furnace. The glass enclosure was covered by a light-tight metal cylinder, C, which contained the 1P28 PMT, B, and enclosure A.

The furnace chamber could be flooded with various gaseous atmospheres as well as operated at reduced pressures via the two inlet and outlet ports, K and L.

The PMT signal was produced by the photometer, Q (American Instrument Co., Silver Spring, MD) whose output was recorded on the Y-axis of an X-Y plotter, R (Model 7035B, Hewlett-Packard Corp., Pasadena, CA). Furnace temperature, as detected by thermocouple F, was recorded on the X-axis. Pump, O, was used to evacuate the furance chamber whose

pressure could be determined using the digital manometer, P (Model CD23, Validyne, Northridge, CA). Temperature programmer, S (Model TP-2000, Theall Eng. Co., Oxford, PA) was used to program the furnace at heating rates from 0.1 to 100.0 °C min. $^{-1}$.

b) Light Emission of Certain Compounds

The thermophotometric (light emission) curves of some coordination compounds that exhibited this phenomena are illustrated in figure 12.

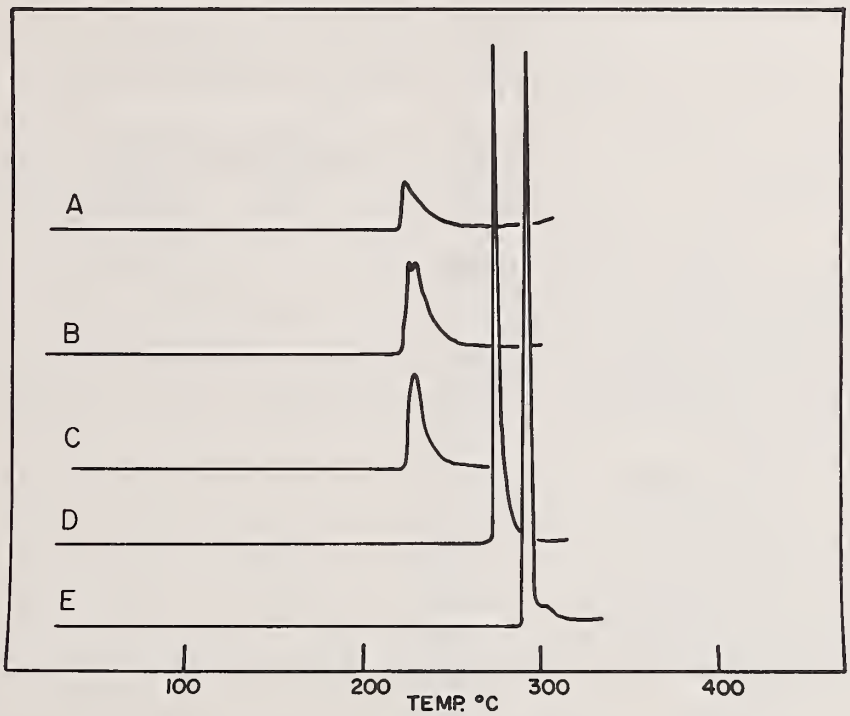

Figure 12. Light emission curves of some coordination compounds

A. α-cis$[Co(trien)(NO_2)_2]Cl$
B. $[Co\ dien\ (NO_3)_3]$
C. $[Co\ dien\ NH_3(NO_2)_2]Cl$
D. cis-$[Co(en)_2(NO_2)_2]NO_3$
E. $[Co(NH_3)_4en](NO_3)_3$

Preliminary studies of about fifty compounds, all containing reducing and oxidizing ligands, showed that sixteen of them exhibited some light emission during their decomposition reaction. These sixteen compounds, as listed in Table 3, featured various amounts of light emission. Some compounds gave pronounced peaks in the curve, which often went off the recorder chart scale, while others, using the identical photometric sensitivity, gave only a small peak. The peaks in the curves, with the exception of $[Cr(NH_3)_5NO_2](NO_3)_2$, all appeared in the temperature range between 200 to 300 °C. Although not investigated, the position of the light emission with respect to the temperature axis is probably dependent on the furnace heating rate as are other thermal analysis data.

For the cobalt(III) compounds investigated, light emission during dissociation is linked with the presence of a carbon containing ligand such as en, dien, trien, and so on. Compounds that contained only ammonia ligands, such as $[Co(NH_3)_6](NO_3)_3$, $NH_4[Co(NH_3)_2NO_2$ oxalate], $[Co(NH_3)_4(NO_3)_4(NO_3)_2]NO_3$, $[Co(NH_3)_4CO_3]NO_3$, and so on, did not exhibit light emission. However, compounds containing ammonia and one or more of the carbon containing

ligands mentioned previously generally did exhibit light emission, such as $[Co(mal)(NH_3)_4]NO_3 \cdot 6H_2O$, [Co dien $NH_3(NO_2)_2$]Cl, $[CO(NH_3)_4en](NO_3)_3$, and so on. The oxidizing group in most cases was either the nitrate (NO_3^-) or nitrate (NO_2^-) ion. Several nickel(II), rhodium (III) and platinum(II) compounds investigated also did not exhibit light emission during their dissociation reactions, although neither did their en analogs, $[Ni(en)_3](NO_3)_2$ and $[Rh(en)_2Cl_2]NO_3$, for example. On the other hand, the chromium(III) ammine compounds, $[Cr(NH_3)_5NO_2](NO_3)_2$ and $[Cr(NH_3)_5NO_3](NO_3)_2 \cdot NH_4NO_3$, did exhibit light emission. No en compounds were investigated, so the presence of a carbon containing compound on the light emission properties could be ascertained.

Table 3. Light Emission of Some Coordination Compounds

	COMPOUND	Light Emission Peak Temperature °C	Small	Medium	Large
1.	$[Co(NH_3)_4\ en](NO_3)_3$	290			X
2.	$[Co(dien)(NH_3)(NO_3)_2]Cl$	225	X		
3.	cis-$[Co(en)_2(NO_2)_2]NO_3$	272			X
4.	α-cis-$[Co(trien)(NO_2)_2]Cl$	220	X		
5.	$[Co(dien)(NO_3)_3]$	222	X		
6.	cis-$[Co(en)_2(NO_3)_2]NO_3$	265			X
7.	trans-$[Co(en)_2Cl_2]NO_3$	205	X		
8.	$[Co(dien)Cl(NO_2)_2]$	230	X		
9.	trans-$[Co(en)_2(NO_3)_2]NO_3$	250			X
10.	$[Co(^{OH}_{OH}>Co(en)_2)_3](NO_3)_6$	240		X	
11.	$[Co(en)_3](NO_3)_3$	290			X
12.	$[Co(mal)(NH_3)_4]NO_3 \cdot 6H_2O$	240			X
13.	$Na[Co(acac)_2(NO_2)_2]$	215			X
14.	$[Co(en)_3](ClO_4)_3$	282			X
15.	$[Cr(NH_3)_5NO_2](NO_3)_2$	190			X
16.	$[Cr(NH_3)_5NO_3](NO_3)_2 \cdot NH_4NO_3$	210			X

Abbreviations employed: en = ethylenediamine; trien = triaminotriethylamine; dien = diethylenetriamine; acac = acetylacetone; mal = malonate.

The beginning temperature for the light emissions of the compounds shown in figure 12 and others are given in Table 3. Most of the light emission curve peaks were quite narrow excepte for those compounds containing the dien ligand.

The support of this work by the Robert A. Welch Foundation of Houston, Texas, is gratefully acknowledged.

6. References

[1] Lombardi, G., For Better Thermal Analysis, ICTA, Rome, Italy (1977).

[2] Kambe, H., Thermochim. Acta 26, 209 (1978).

[3] Anon., Optical Spectra, Dec., 14 (1978).

[4] Anon., American Lab., Jan., 108 (1979).

[5] Wendlandt, W. W., Thermochim. Acta 26, 19 (1978).

[6] Wendlandt, W. W., Thermochim. Acta 30, 361 (1979).

[7] Baxter, R. A., in Thermal Analysis, Schwenker, R. F., and Garn, P. D. (eds.) Academic Press, New York, Vol. 1, 65 (1969).

[8] Wynne, A. M., and Wendlandt, W. W., Thermochim. Acta 14, 61 (1976).

[9] Wynne, A. M., and Wendlandt, W. W., Thermochim. Acta 13, 393 (1975).

10] Collins, L. W., and Wendlandt, W. W., Thermochim. Acta 7, 201 (1973).

11] Wendlandt, W. W., and Smith, J. P., The Thermal Properties of Transition – Metal Ammine Complexes, Elsevier, Amsterdam, 49 (1967).

RECENT INSTRUMENTAL DEVELOPMENTS

RAPPORTEUR'S COMMENTS BY

Pronoy K. Chatterjee
Personal Products
A Johnson & Johnson Company
Milltown, N.J. 08850

Dr. Wendlandt, in his first part of the talk, presented a brief review on recent developments on thermal analysis. His review was based on 465 articles published in recent volumes of Thermochimica Acta (TCA) and Journal of Thermal Analysis (JTA) and some statistics published elsewhere. It is encouraging to note that in 10 years the thermoanalysis instrument market will triple its size; from 76 million dollars in 1977 to 2.3 billion dollars by 1987. The major development in this area will be based on the incorporation of the rapidly developing microprocessor – technology and instruments interphasing techniques. Regarding the applications, thermogravimetry and differential thermal analysis still appear to be more popular than any other technique. Interestingly enough, Dr. Wendlandt's review indicates that there is a diminishing trend of the popularity of DSC technique since 1975-1976 when it reached to a peak. Certainly, DSC is still a more precise quantitative tool than DTA and in many cases DSC offers more accurate fundamental thermodynamic information. If Dr. Wendlandt's review is generally true in all fields, one would wonder if this decreasing popularity of DSC is an effect of the current trend of diminution of the fundamental research in industries as well as in the academic field. Dr. Wendlandt also noted that high temperature x-ray diffraction technique has been widely referred in recent publications.

Simultaneous and concurrent thermoanalytical techniques have special value in analytical laboratories. In the former case, different thermal properties are measured on single substance, and in the latter case, different samples are used under the same environmental conditions. Two concurrent thermoanalysis techniques, thermogravimetry-differential thermal analysis and thermogravimetry-electrothermal analysis developed by Dr. Wendlandt and his associates, were reviewed. For those techniques new probes have been designed to adapt in both DuPont and Cahn thermobalances. The most appealing aspect of this development is that only simple modifications are required on commercial equipment to perform the concurrent measurements.

A thermophotometry technique, where light emission is measured as a function of temperature, has been applied in Dr. Wendlandt's laboratory to investigate thermal dissociation reaction of highly oxidizable metal coordinate compounds. I guess, this technique will be uniquely suited for other applications also, such as accelerated aging studies on polymers or thermal degradation of polymers. However, the success in those areas would depend upon the light detection sensitivity.

Dr. Wendlandt concluded his review by citing three other specific developments published recently. Those are: (1) a new differential thermal analysis technique, where the temperature was raised at 2 °C per minute by a step method for studying phase equilibria, (2) a new temperature programming device, and (3) an emanation thermal analysis method to study the radioactive gas diffusion.

The presentation by Dr. Wendlandt was extremely informative and we hope to see soon a publication with detailed information on new techniques. However, I feel that a comprehensive review on new thermoanalytical techniques should not be based on publications in two journals only. Papers published in other international journals also contain many new and innovative techniques. New thermoanalytical techniques to characterize polymers are usually published in the polymer journals. Consequently, Dr. Wendlandt missed many new techniques in his recent review which are published in journals other than Thermochimica Acta or Journal of Thermal Analysis. Among those techniques, thermoacoustimetry, a new technique for thermal conductivity measurement, thermomechanical spectrometry (TMS) and thermoluminescence are just a few such samples.

National Bureau of Standards Special Publication 580. Proceedings of the Workshop on the State-of-the-Art of Thermal Analysis held at NBS, Gaithersburg, MD, May 21-22, 1979. (Issued May 1980)

THERMOGRAVIMERIC MEASUREMENTS AT HIGH PRESSURES

Nelson C. Gardner, Joseph J. Leto, Sunggyu Lee, and John C. Angus

Chemical Engineering Department
Case Western Reserve University
Cleveland, Ohio 44106

Abstract

Significant advances have been made in the last decade in vacuum microbalance technology, particularly with regard to ultra-high vacuum and nanogram capabilities. However, thermogravimetric measurements at high pressures and temperatures, in regimes of importance to commercial processes, have received much less attention. In this paper, we review the principal techniques that have been used at these conditions and discuss their inherent problems.

Most prior thermobalances for use at high pressure have employed a hanging sample basket within a pressure containment vessel. The devices differed principally in the means of heating and the mass transducer used.

We have employed a novel means for obtaining thermogravimetric kinetic data, viz., the entire reactor plus contents are weighed during the course of a run. A 130 kg reactor (300 lb) with thin-walled flexible gas lines and thermocouples attached is suspended from a large balance. The balance has a sample capacity of 0.5 kg (1 lb) and an inherent sensitivity of 10 mg which is diminished by about 50 mg per attached line. The experimental design permits the entire reacting gas stream to be passed through the sample bed. Control over the fluid mechanical regime is therefore possible allowing elimination of external mass transfer effects, operation as a true differential bed reactor and permitting measurement of meaningful product gas compositions.

The thermobalance has been designed to operate at temperatures to 1370 °K (2000 °F) at pressures as high as 100 atm. This covers the operating range of many practical chemical processes.

Introduction

Many practical chemical processes operate at elevated temperatures and pressures. The recent escalation of both energy and capital costs makes it even more important to achieve optimal design and understanding of these processes. Systematic design and optimization rely on models which ultimately are based on experimental data. Extrapolation of laboratory chemical kinetic measurements done at subatmospheric pressures in unrealistic fluid mechanical regimes cannot be done with confidence. There is, therefore, an increasing need for laboratory scale instruments which can provide accurate kinetic measurements at realistic process conditions of temperature, pressure, chemical environment and fluid mechanical regime. In this paper we discuss several approaches to this problem, including a novel hanging reactor thermobalance.

This paper will be limited to reactions involving a change in weight of a solid phase. This class of reactions includes a large number of very practical, large scale chemical processes. Among these are:

Coal Gasification. The gasification of coal is a complex and poorly understood phenomenon which, depending on the conditions, can involve chemical reaction rate control, mass transfer rate control, or heat transfer rate control. Typical reactions encountered in coal gasification include the water gas reaction,

$$C + H_2O = CO + H_2$$

direct hydrogenation

$$C + 2H_2 = CH_4$$

and the Boudouard reaction

$$CO_2 + C = 2CO.$$

At low temperatures, in the presence of suitable catalysts, some direct formation of methane from water and coal is possible.

$$2C + 2H_2O = CO_2 + CH_4.$$

All of these reactions are conveniently studied using gravimetric techniques.

Some other reactions of importance in coal gasification are not easily studied in conventional gravimetric apparatus because they are too rapid. These would include coal combustion

$$C + O_2 = CO_2$$

$$C + \frac{1}{2}O_2 = CO$$

and the early stages of coal pyrolysis.

Calcination Reactions. The simple calcination of limestone

$$CaCO_3 = CaO + CO_2$$

or the half calcination of dolomite

$$[CaCO_3 \cdot MgCO_3] = [CaCO_3 \cdot MgO] + CO_2$$

are industrially important reactions. The cyclic calcination and subsequent reformation of carbonates can be used as a means of heat transfer and plays an important role in some coal gasification processes, e.g., the CO_2 acceptor process. The overall stoichiometry, using half calcined dolomite, $[CaCO_3 \cdot MgO]$, may be represented as:

$$[CaCO_3 \cdot MgO] = [CaO \cdot MgO] + CO_2$$

$$[CaO \cdot MgO] + CO_2 = [CaCO_3 \cdot MgO].$$

These processes are conveniently studied using gravimetric techniques.

Sulfur Capture. A large number of solid reagents have been proposed for the capture of sulfur containing species derived from coal combustion. These reactions can take place during combustion, e.g., fluidized bed combustion, or post combustion, e.g., sulfur dioxide scrubbers. The reaction generally involves capture of the acidic SO_2 by a basic compound such as limestone or dolomite. A typical stoichiometry in an oxidizing environment can be represented by

$$SO_2 + CaCO_3 + \frac{1}{2}O_2 = CaSO_4 + CO_2.$$

In a reducing atmosphere the sulfur appears as H_2S. A stoichiometry for H_2S capture by half calcined dolomite is

$$[CaCO_3 \cdot MgO] + H_2S = [CaS \cdot MgO] + H_2O + CO_2.$$

Thermogravimetric techniques can also be used to study the reaction between iron sulfide and sulfur dioxide, a reaction which has been proposed as a method for hot stack gas clean-up.

$$3FeS + 2SO_2 = Fe_3O_4 + \frac{5}{2}S_2.$$

Carbon Deposition. The deposition of carbon from high temperature hydrocarbon streams is a poorly understood process. Reactions of this type often play a role in the deactivation of catalysts through the formation of a carbonaceous deposit. Carbon deposition from hydrocarbons also is a means of producing pyrolytic graphite and has been used as a means for growing diamond at low pressures.

Oxidation and Other Reactions. The slow formation of oxide films and metals is amenable to study by gravimetric means. Other reactions of metallurgical importance such as nitriding and carburizing may also be studied this way.

The reduction of metal ores, e.g., by hydrogen, is another type of reaction that can be investigated by gravimetric techniques.

$$Fe_2O_3 + 3H_2 = 2Fe + 3H_2O.$$

Prior Gravimetric Measurements at High Pressure

Very significant advances in vacuum microbalance technology have been made in the last decade, particularly with respect to ultra-high vacuum and nanogram capabilities. Thermogravimetric measurements at high temperatures and pressures, in regimes of importance to commercial processes, have received much less attention. In this section we will briefly review some of the main approaches that have been taken. A comprehensive listing of past efforts has been compiled by Dobner et al. [1][1].

Hanging Basket Thermobalance. The most common means for performing thermogravimetric measurements is to suspend a small basket or pan containing the sample into the high temperature, high pressure environment. The balance mechanism is contained within the high pressure environment, but isolated from the high temperature and corrosive gases by baffles, cooling plates, and sometimes by a counterflow of inert purge gas. An early version of such a device was developed at the Institute of Gas Technology by Feldkirchner and Johnson [2] for study of iron ore reduction and coal gasification.

This basic device was later modified by Gardner, Samuels, and Wilks [3] to provide faster turn-around time and more rapid sample introduction. In this device, shown in figure 1, the sample is suspended from a single beam balance arm of a Statham model UC-3 mass transducer with a capacity of six grams. The sample is lowered from a protective dip tube into the reaction zone at rates that can be varied from 1 to 10 cm/sec. When the sample is lowered sufficiently to be in the isothermal region of the reactive zone, the hangdown wire engages the balance arm, initiating the mass measurement, and the windlass is stopped. The sample is exposed to the reactant gases for only a few seconds before mass measurements are taken. The device is designed to operate isothermally up to 1100 °C and 136 atm. The unit has been successfully used with both H_2 and steam as the reactant gasification gases. This same instrument was also used at Battelle Laboratories for coal gasification studies [4].

[1]Figures in brackets indicate the literature references at the end of this paper.

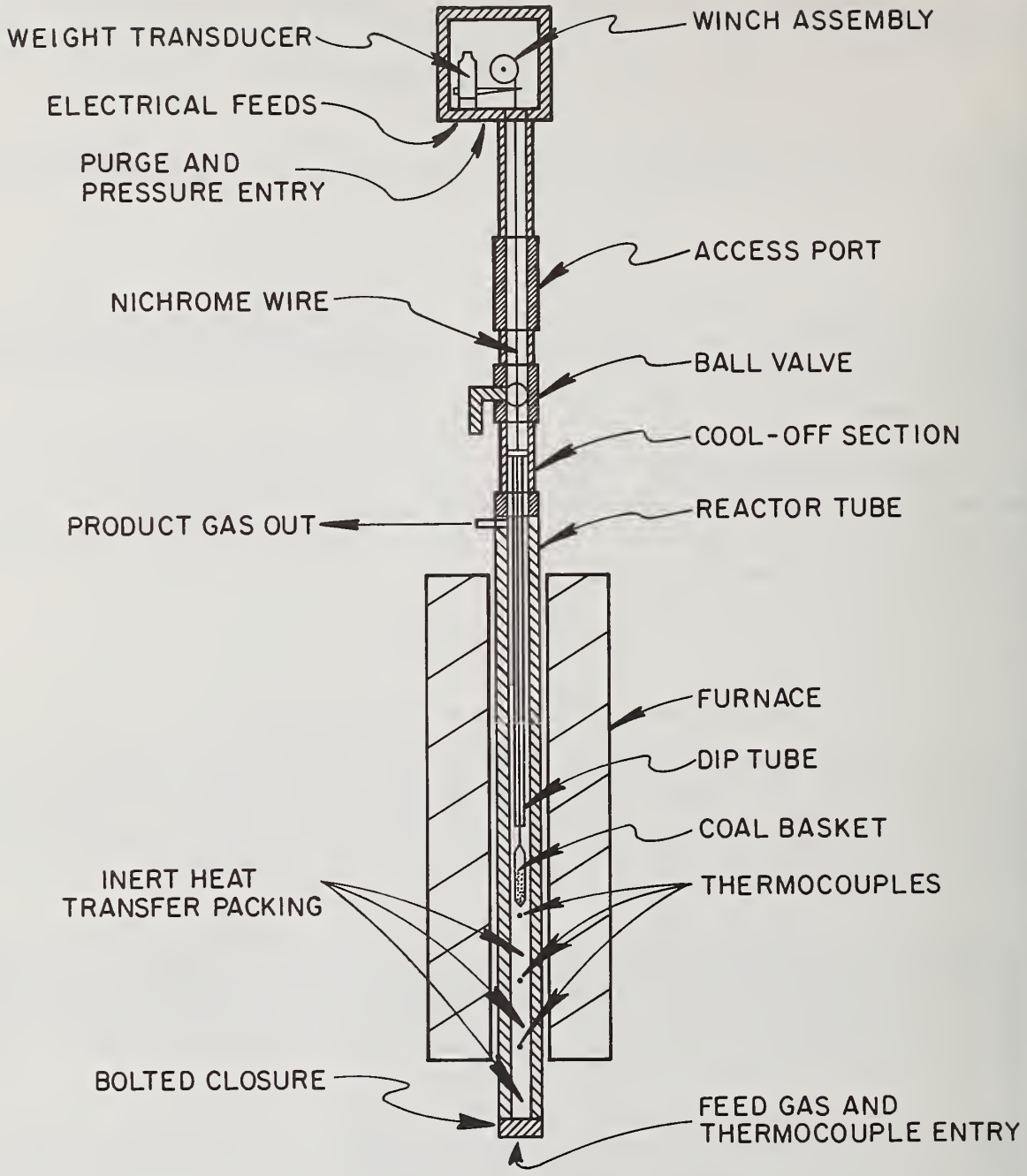

Figure 1. Hanging basket reactor schematic.

Modifications of duPont Thermogravimetric Analyzer. Several workers [1,5] have successfully modified the duPont 950 and 951 Thermogravimetric Analyzers for use at high temperatures and pressures. Dobner et al. [1] describe such an apparatus, which is designed to operate up to 30 atm and 1100 °C, with corrosive atmospheres, and with steam partial pressures up to 20 atm. The balance mechanism is at the reactor pressure, but isolated from the high temperatures and hot gases with a pancake cooling coil and a purge flow of cold nitrogen. As in all hanging basket configurations, it is not possible to place a thermocouple directly in the sample. This can lead to significant errors in the estimate of the sample temperature if the thermocouple is bathed in a gas stream of a different temperature

or if it "sees" hot radiative surfaces. Dobner and his co-workers paid a great deal of attention to this problem of accurate temperature measurement.

Li and Rogan [5] modified the duPont 951 for operation at pressures to 60 atm and temperatures to 1100 °C with corrosive gases such as hydrogen sulfide and hydrogen.

Cold Wall Thermobalance. A somewhat different approach was taken by Forgac and Angus [6]. A Perkin Elmer Model AM-1 Microbalance was enclosed in a cold walled high pressure vessel. This device is shown in figure 2. Because of the cold wall construction and the use of induction rather than resistance heating, significantly higher temperatures can be reached. Runs with temperatures of 1360 °C and pressures of 70 atm were routinely made. Design calculations indicate temperatures of 1700 °C at pressures of 136 atm of hydrogen are feasible. A disadvantage of a cold wall device is, of course, that condensable gases cannot be used. The use of thermocouples was avoided by making temperature measurements with a two-color pyrometer focussed directly on the sample. This thermobalance was used to study the onset of carbon deposition from methane/hydrogen mixtures at near equilibrium conditions.

Limitations of Prior Thermogravimetric Techniques

The devices described in the prior section basically provide measurements of sample mass versus time over a wide range of temperatures, pressures, and overall gas phase compositions. This information is very useful, difficult to achieve, and cannot be discounted. However, there are several serious deficiencies with these devices which limit their use in many important process-related applications. These limitations arise from one basic feature of their design, viz., the suspension of a sample basket or pan in the reacting environment. This basic design element introduces several serious problems.

First, the fluid mechanical regime in the immediate vicinity of the sample is difficult, if not impossible, to control. The major part of the reactant gases bypass the sample. One cannot, therefore, simply increase gas flow rates to reduce external mass transfer resistance for particulate samples. Furthermore, changes in gas flow rates, or convective cells, directly influence the mass measurements in unpredictable ways [1,6].

Secondly, the reactant gases that bypass the sample make it impossible to measure meaningful product gas compositions. The bulk of the gas leaving a typical thermobalance has never been near the solid sample. This means that the entire arsenal of kinetic techniques based on product gas analysis cannot be used. These thermobalances cannot be operated as either well defined differential or integral bed reactors. Virtually all of the kinetic analysis must be made on the basis of the mass changes alone.

In many situations one is very interested in the product gas distribution as well. For example, in catalyzed coal gasification studies, one is not only interested in the rate of mass loss, but also the fraction of methane produced directly in the gasification step. In the experiments of Gardner et al. [3], the excess steam bypassing the hanging basket sample shifted and reformed the exit gas composition so it was virtually all CO_2 and H_2, no matter what the gasification conditions were.

Thirdly, accurate temperature measurements are difficult. One cannot introduce a thermocouple directly into the sample because it will seriously perturb the mass measurement. One can avoid this problem by using optical pyrometry [6]. However, most thermobalance configurations do not permit an optical path to the sample.

Fourth, the introduction of the sample into the heated zone is a difficult problem with conventional thermobalance systems. In some cases, the time for sample heat up is governed by the thermal inertia of the entire furnace and reactor [5] and can be several minutes in duration. In other cases [3,4] provision is made for more rapid introduction by lowering the sample basket. In this case the time can be reduced to several seconds. Ideally, however, one would wish to introduce the sample sufficiently rapidly so the heat-up time is governed only by the thermal inertia of the individual particle. This is the situation in some industrial practice.

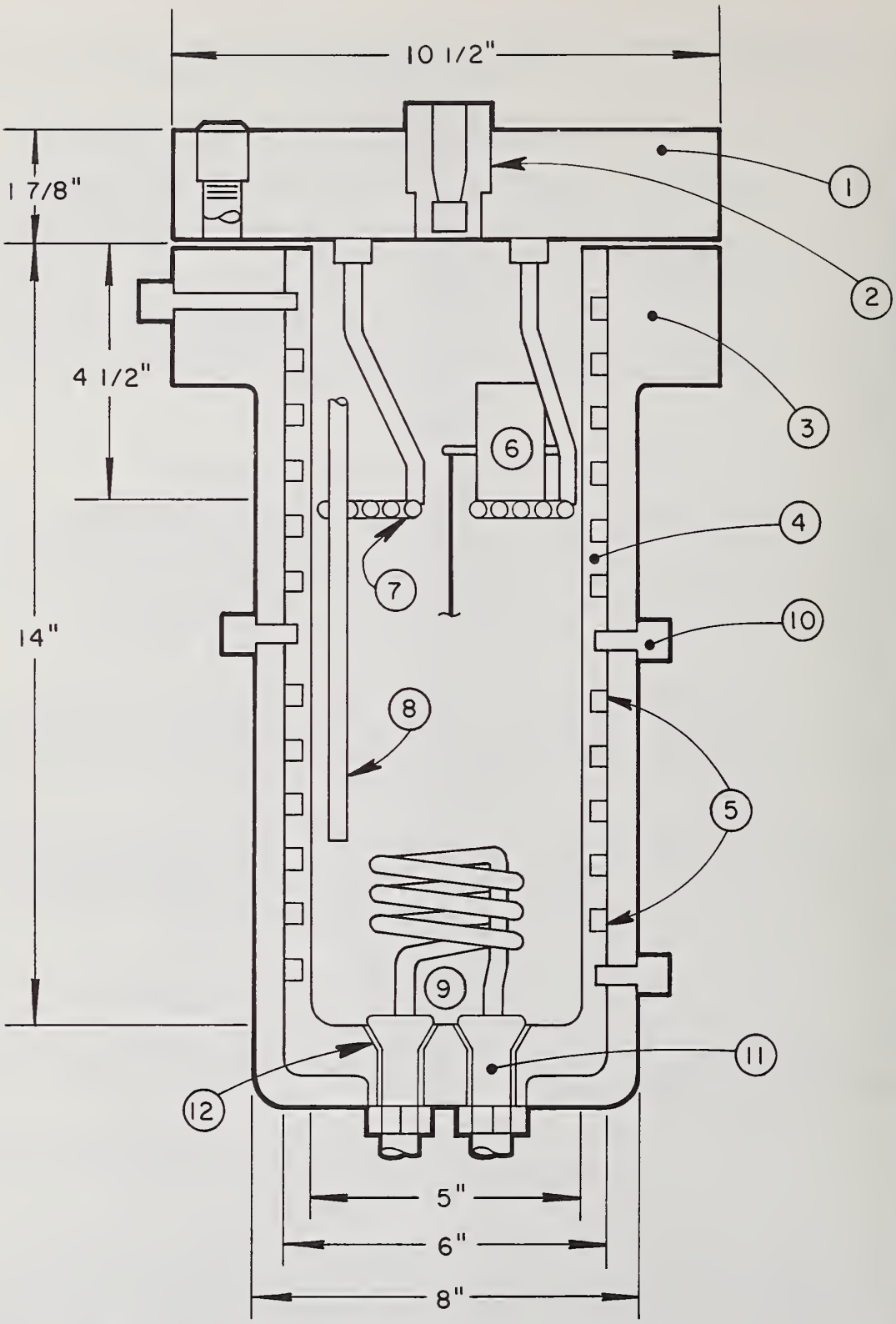

Figure 2. Cold wall high-pressure thermobalance. 1) lid, 2) viewing port, 3) 316 stainless steel outer shell, 4) A286 inner steel liner, 5) cooling water grooves, 6) electronic balance, 7) water cooled plate, 8) gas inlet tube (top portion through lid not shown), 9) induction heating coil, 10) water cooling inlet, 11) Be-Cu insert, 12) Teflon liner.

Design Philosophy of Hanging Reactor Thermobalance

The considerations outlined in the previous section led us to consider an unconventional approach. Instead of weighing a small sample basket within the reactor, we decided to weigh the entire reactor during the course of the reaction. We are aware of one other instance in whch an entire large reactor (incinerator) was weighed for taking kinetic data [7].

There are several difficulties with this approach, the first being the necessity of weighing the reactor with all gas lines and thermocouple wires attached. Furthermore, it is necessary to have a balance with high sensitivity at large loads.

There are several critical advantages to weighing the entire reactor plus contents. First, the entire reactant gas stream passes through the sample bed, i.e., there is no bypassing around the sample. This means that the fluid mechanical regime and external mass transfer processes can be controlled. The fluid mechanics in the bed can be made to more closely simulate the situation in large scale reactors. (It may even be possible to operate small fluidized beds in the new reactor.)

Secondly, because the entire gas stream goes through the sample, the device can be operated as a true differential or integral bed reactor. Chemical analyses of the product gases can be related to the chemical processes taking place in the bed. The well developed means of mathematical analysis of such reactors can be applied.

Thirdly, thermocouples can be placed directly in the sample bed, permitting much more accurate temperature measurements during the course of chemical reactions.

Fourth, certain errors inherent in conventional thermobalances are not present in the externally weighed device. (However, certain other errors unique to the new device are encountered.) There are no drag forces from forced convection or convective cells acting on a sample pan. Convective cells outside the heated reactor do influence the weight but are rather easy to control. Bouyancy corrections, in the normal sense, are absent. However, because the entire reactor plus all of its contents are weighed, an equivalent correction must be made to account for changes in the amount of gas in the reactor.

Hanging Reactor Thermobalance

General Design Criteria and Balance Selection. The size of the reactor was limited by the maximum capacity of an available balance that had the required sensitivity. In order to minimize wall effects and to allow for the eventual possibility of running with fluidized beds, a large sample size was desired.

The largest capacity balance within our economic limitations was the Voland Model HCE-100G, beam balance. In essence this device is a very large, very sensitive version of a conventional laboratory beam balance used in analytical chemistry. The device is contained in its own walk-in chamber 2.29 m (7'6") high, 0.71 m (2'4") deep, and 1.83 m (6') wide. The specifications of the balance are given in Table 1.

Table 1. Balance Specifications: Voland Model HCE-100G.

Design Capacity:	100 Kg on each pan
Sensitivity:	10 mg at full load
Precision:	20 mg
Damping:	magnetic eddy current
Arrestment:	single lever for beam and pan arrest

In operation the load is tared off to within one pound. Mass changes are monitored by a force transducer touching one balance beam arm. Deflections of the beam arm, directly related to mass, are detected as an electrical signal from the force transducer. This procedure reduced the full load beam deflection to 0.635 mm (.025 in.).

Reactor Vessel Design. The size of the reactor vessel was limited by the load which would cause inelastic deformation of the balance beam. By eliminating the large sample pan on the sample size of the balance and after discussions with the manufacturer, the allowed reactor weight was set at 136 kg (300 lbs).

The primary factor determining the overall reactor weight is the wall thickness and the size of the flange for the reactor closure. These in turn are determined by the desired internal reactor volume (sample size), the operating conditions of temperature and pressure, and the mechanical properties of the material of construction at the operating conditions. The maximum sample size was chosen to be approximately one pound, which, assuming a bulk density of solid reactant of .72 g/cm (45 lbs/ft^3), leads to a reactor internal volume of 620 cm^3 (.022 ft^3). The design limits of temperature and pressure were fixed at 1370 °K and 100 atm. These requirements cannot be met within the weight limitations using conventional materials of construction. In order to minimize wall thickness and flange size, an alloy with excellent high temperature creep properties, as well as good chemical resistance to steam, oxidizing and reducing environments, alkali and sulfur containing species is required. The final materials choice was Inconel 617, a high nickel/chromium non-ferrous alloy. To increase the corrosion resistance of the alloy, an aluminum/chromium diffusion coating was applied to all the reactor surfaces.

The hanging reactor system is shown schematically in figure 3. The closure at the bottom permits access to the inside of the reactor and provides for entry of thermocouple and the gas inlet line. A more detailed description of the reactor with engineering drawings is given in reference [8].

Sample Loading. In order to provide rapid loading of particulate samples, a gas transport injection system was used. The sample was first fluidized in a 316 stainless steel chamber directly above the reactor chamber. A small pressure differential is established across a 2.54 cm (1") ball valve separating the reactor and the injection chamber. The ball valve is opened and the solid sample blown into the reactor. A 300 gram, 200 mesh, coal char sample can be injected into the pressurized, hot reactor within three seconds using this procedure.

To remove a sample from the reactor, the reverse procedure is used. The unreacted solid sample is blown out of the reactor into the upper chamber with a high pressure stream of nitrogen.

Gas Lines. Gas lines are attached to the reactor to feed the inlet reactant gases and to remove the product gases. These lines are made of 0.312 cm (1/8") thin walled stainless steel high pressure tubing. The tubing is wound into floppy helical coils to minimize the forces acting on the reactor. Similar gas lines are also attached to the injector to permit fluidization of the sample before injection. There is a loss in sensitivity of approximately 0.050 g for each of these gas lines attached to the reactor.

Data Acquisition and Control. The hanging reactor thermobalance is sufficiently complex that a computer based data acquisition and control system was used. This system was based on a Hewlett-Packard 3000 minicomputer and used microprocessors to serve as the communication link between the experiment and the computer. A simplified flow chart of this system is shown in figure 4.

The HP 3000 minicomputer serves as the host computer; control algorithms are stored and data manipulation carried out here.

The shared variable processor is based on the Motorola 6800 chip. It acts as the communication link between the host computer, the terminal, the device control processor, and the data storage unit.

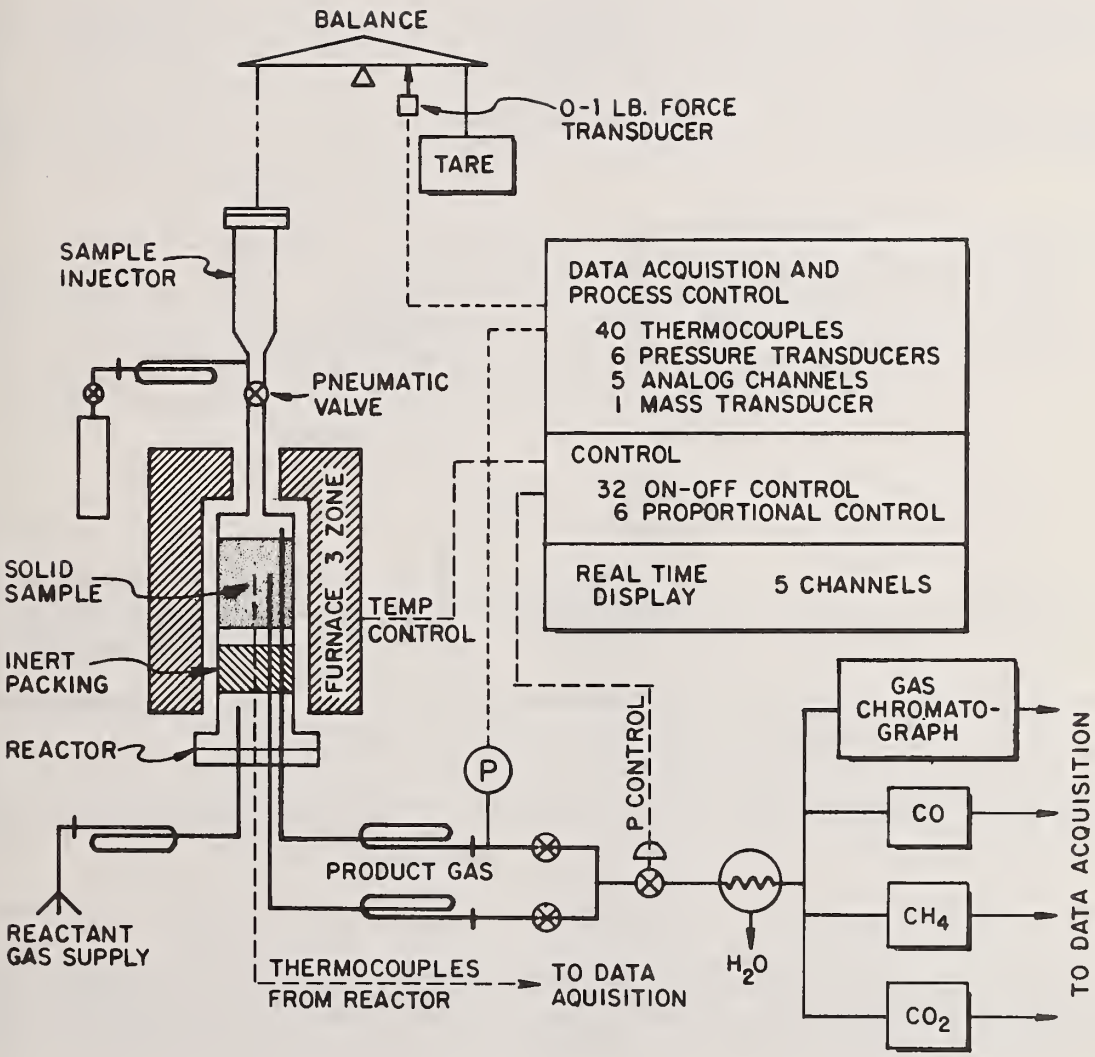

Figure 3. Schematic of Hanging Reactor Thermobalance.

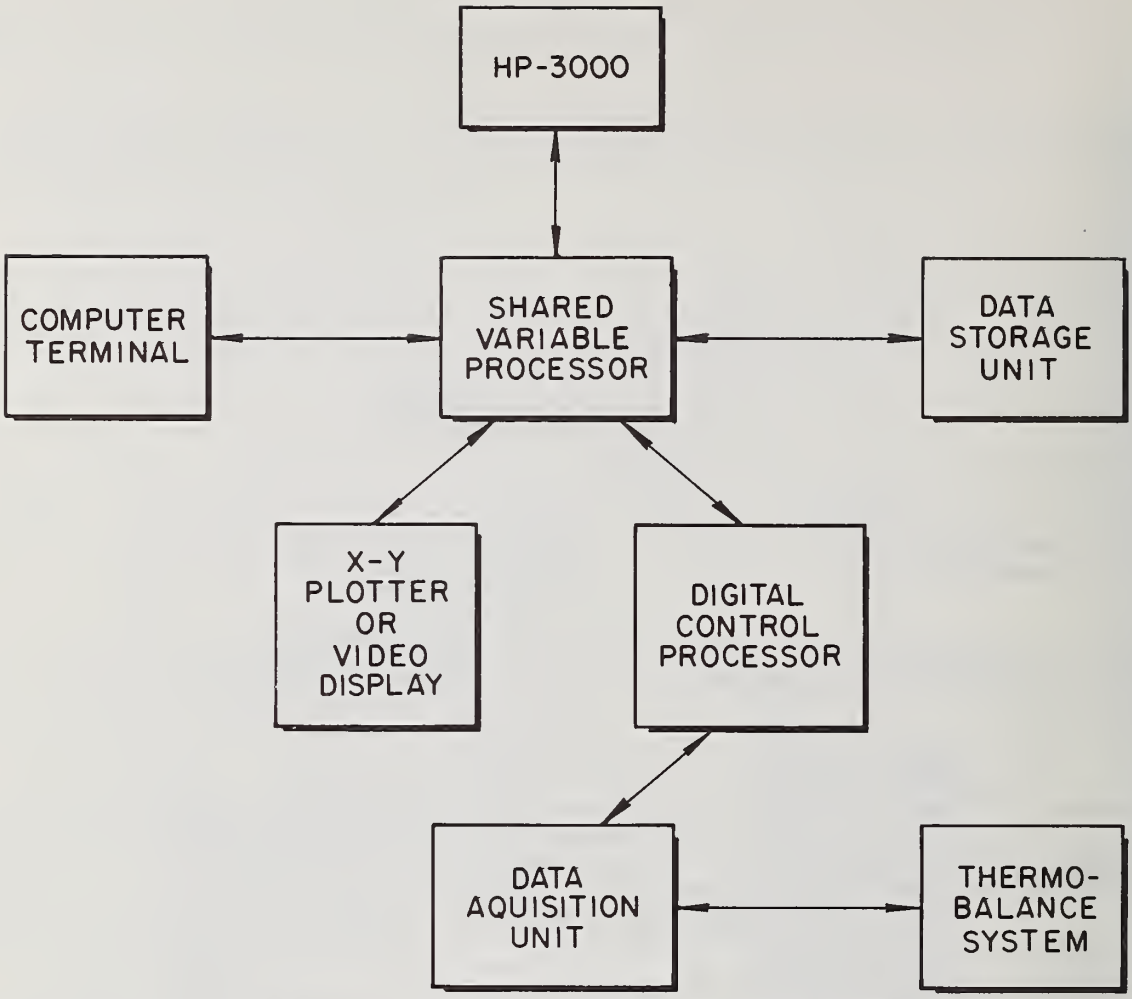

Figure 4. Data acquisition and control system.

The data acquisition unit serves as an interface between the thermobalance and the device control processor. Multiplexing and signal conditioning take place here.

The operator enters commands and queries through the computer terminal. The terminal and the X-Y plotter provide a real time display of various system variables.

All of the computer software for the data acquisition and control is written in APL (A Programming Language). Details of the design and philosophy of the computer system have been published elsewhere [9].

Operating Characteristics of Hanging Reactor Thermobalance

Basic Measurement. It should be emphasized that the actual parameter being measured is the force exerted by the hanging reactor on the beam balance. In most cases changes in this force are directly and closely related to changes in the sample mass; however, there are errors and corrections which can be important in certain circumstances.

First, if there is a significant change in the vertical component of the momentum of the gases passing through the reactor, the momentum change will appear as a force exerted on the beam balance. In the present reactor configuration, gases enter and leave the

weighed portion of the reactor normal to the support cable and therefore changes in velocity do not effect the observations. Even when the gases do not enter horizontally, the magnitude of the momentum effects, $v\frac{dM}{dt}$, is usually much less than the sample weight, Mg.

When momentum effects are negligible, the measurement basically provides the total mass balance about the reactor. (Note that for a closed reactor, no feed or exit lines, there would be no change measured whatsoever.) Measured changes in mass therefore reflect not only changes in the mass of the solid sample, but also changes in the mass of the gas contained within the reactor. Therefore, there are several sources of error unique to the hanging reactor thermobalance which must be considered.

Sources of Error. Because one is weighing not only the solid sample, but the gases contained within the reactor, fluctuations in temperature and pressure are immediately reflected as changes in the measured mass. This effect is obviously most pronounced at high gas densities. For example, for a gas phase containing CO_2 at 773 °K and 68 atm (1000 psi), a fluctuation of 0.068 atm (1 psi) causes an apparent mass change of about .02 grams in the present system. A temperature fluctuation of 1 °C at these conditions causes an apparent mass fluctuation of about .04 grams. If pressure and temperature control are not maintained within a range of about 1.76 atm (20 psi) or 10 °C, they will start to significantly perturb the measured mass.

Another effect, related to a bouyancy correction, is caused by the changing sample volume as reaction proceeds. In a gasification experiment, for example, the volume of solid decreases and this volume is occupied by the gas phase. The apparent mass change of the sample is therefore always less than the measured mass change. The magnitude of this effect depends on the relative densities of the solid and gas phases. This error is usually small, but can become appreciable at high gas densities. The relationship between the observed mass change, $\Delta M'$, and the actual mass change, ΔM, is just

$$\Delta M' = \Delta M \left[1 - \frac{\rho_{gas}}{\rho_{solid}}\right] . \qquad (1)$$

For a solid with a density of 1 g/cm^3 and a gas phase with a density of .024 g/cm^3, i.e., CO_2 at 34 atm (500 psi) and 500 °C, the ratio $\Delta M'/\Delta M$ is .976.

Effects of Residence Time. A unique feature of the hanging reactor thermobalance is the influence of gas phase residence time and residence time distribution on the mass versus time trace. This arises from the fact that gas phase species are weighed as long as they are in the reactor. For example, consider the simple situation where a solid is gasified by a reaction having the same number of moles of reactant and product gases. For example:

$$FeS + H_2 = Fe + H_2S.$$

The H_2S formed in the reaction is weighed until it leaves the reactor. If the reactor has a plug flow residence time distribution, the mass changes will be observed after a delay equal to the gas residence time in that portion of the reactor downstream of the sample. In this simple situation the mass vs. time trace is simply delayed but not distorted.

If there is a distribution of residence times for the gaseous products, the situation becomes more complex. There is a loss of resolution in the mass versus time trace. The magnitude of this effect depends on the details of the residence time distribution; however, the maximum loss of resolution should be on the order of the average residence time itself. In the present reactor configuration, the gas residence time in the upper part of the reactor was typically from several seconds to tens of seconds.

Still further complications arise when the numbers of gaseous reactant and product molecules are not the same. For example, consider the reaction

$$C + CO_2 = 2CO.$$

In this case the flux of gas phase molecules downstream from the reactant bed is greater than that upstream of the bed. If one has perfect pressure and temperature control, the total number of molecules in the gas phase will be essentially constant with time (excluding the effects of diminishing sample size mentioned earlier). To illustrate the problem consider the simple reaction

$$aA_g + bB_s = cC_g + dD_s$$

where A and C are gas phase species, B and D are solid phase species. In general $a \neq c$. The reaction rate, $d\xi/dt$, defined per mole of solid reactant is

$$-\frac{d\xi}{dt} = \frac{1}{b}\frac{dN_b}{dt} \tag{2}$$

Applying the restriction of constant number of moles in the gas phase one easily finds

$$\dot{N}_{1A} - \dot{N}_{2A} = \dot{N}_{2C} + (a-c)\frac{d\xi}{dt} \tag{3}$$

where $\dot{N}_{1A}$ and $\dot{N}_{2A}$ are the inlet and exit flow rates of A, respectively, and $\dot{N}_{2C}$ the exit flow rate of C. It is assumed there is no product C in the feed.

The overall mass balance, taken about the entire reactor, gives

$$\frac{dM}{dt} = (\dot{N}_{1A} - \dot{N}_{2A})\,M_A - \dot{N}_{2C}M_C \tag{4}$$

where M_A and M_C are the molecular weights. Combining one obtains

$$\frac{dM}{dt} = \dot{N}_{2C}\,[M_A - M_C] + (a-c)\left(\frac{d\xi}{dt}\right) M_A. \tag{5}$$

For the most simple case of $a = c$, the second term on the RHS vanishes. Also, in this case, if there is plug flow through the reactor

$$\dot{N}_{2C} = c\left(\frac{d\xi}{dt}\right)_{(t-\tau)} \tag{6}$$

where τ is the residence time downstream from the bed. We have, therefore,

$$\frac{dM}{dt} = c(M_A - M_C)\left(\frac{d\xi}{dt}\right)_{(t-\tau)}. \tag{7}$$

In other words, the measured mass is just equal to the change in mass of the sample, but delayed by a time τ.

For $a \neq c$, the mass balance contains another term. However, if we assume $d\xi/dt$ is constant, and again assume a plug flow reactor we immediately obtain

$$\frac{dM}{dt} = [aM_A - cM_C] \left(\frac{d\xi}{dt}\right). \tag{8}$$

There is, therefore, no error in this case.

If, however, $d\xi/dt$ varies with time, which is the normal situation, we have for a plug flow reactor

$$\dot{N}_{2C}(t) = c \left(\frac{d\xi}{dt}\right)_{t-\tau} \tag{9}$$

where τ is the downstream residence time. We have in this case

$$\frac{dM}{dt} = [aM_A \left(\frac{d\xi}{dt}\right)_t - cM_C \left(\frac{d\xi}{dt}\right)_{t-\tau}] \tag{10}$$

$$+ [\left(\frac{d\xi}{dt}\right)_{t-\tau} - \left(\frac{d\xi}{dt}\right)_t] cM_A.$$

Significant errors will occur when the second term on the right hand side is on the same order of magnitude of the "true" rate of change of sample mass $[aM_A - cM_C] \frac{d\xi}{dt}$. In other words when

$$\left| \frac{\left(\frac{d\xi}{dt}\right)_{t-\tau}}{\left(\frac{d\xi}{dt}\right)_t} - 1 \right| = \text{Order} \left| \frac{a}{c} - \frac{M_C}{M_A} \right| \tag{11}$$

Suppose we are dealing with the reaction

$$CO_2 + C = 2CO$$

for which $a = 1$, $c = 2$, $M_A = 44$, $M_C = 28$. The criterion becomes

$$\frac{\left(\frac{d\xi}{dt}\right)_{t-\tau}}{\left(\frac{d\xi}{dt}\right)_t} - 1 = \text{Order } (0.14) \tag{12}$$

For this reaction, therefore, if the rate of reaction changes by 14 percent within one residence time, very serious errors will be introduced.

Further reflection will show that the mass trace will also be influenced by the details of the response characteristics of the pressure control valve.

Response Time and Mass Sensitivity. The response of the instrument to changes in load was of great concern. Examples of the measured mass versus time trace for instantaneous changes in load are shown in figure 5. The device acts, not unexpectedly, as a damped harmonic mechanical oscillator. The frequency of the oscillations are 1.13 cps, and the time constant for decay of the oscillation is about 10 seconds. Although instantaneous changes in weight are unlikely in practice they can, in principle, be accounted for by appropriate signal averaging if a rapid enough data rate is achieved.

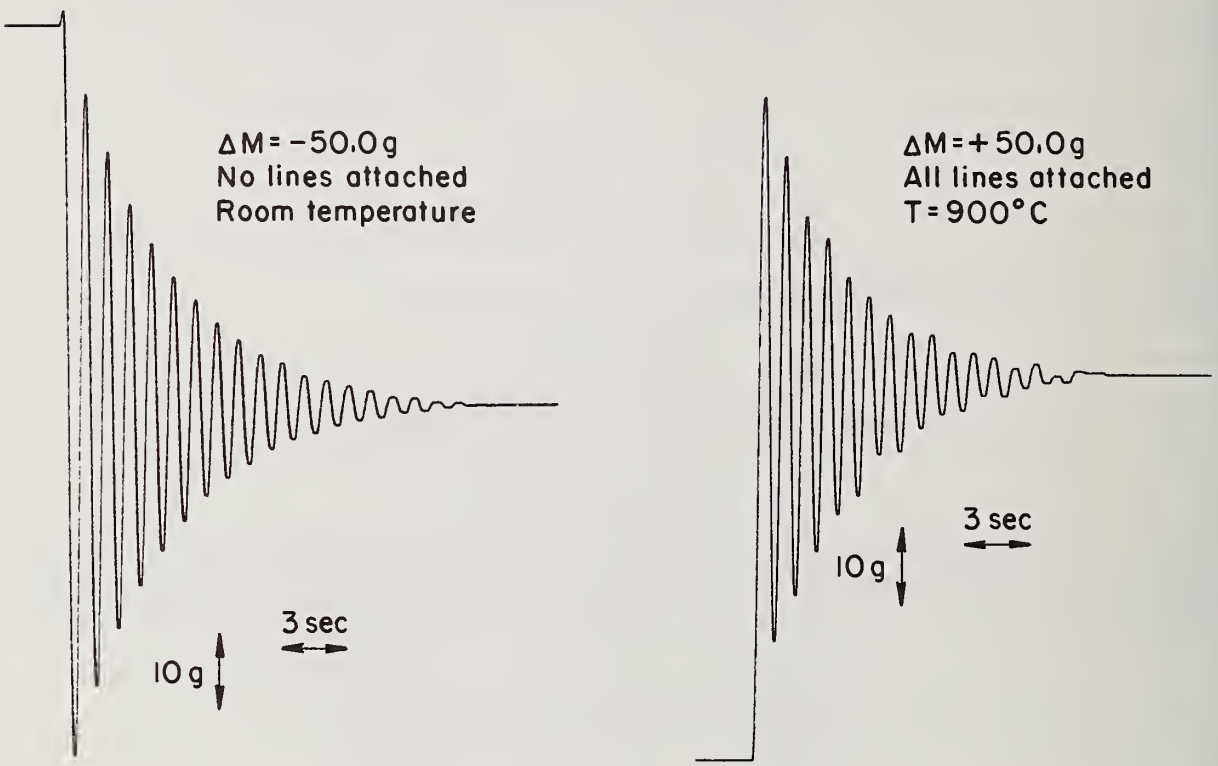

Figure 5. Hanging balance response to abrupt mass change.

The hanging reactor has more than adequate mass sensitivity for our coal gasification studies. changes in mass of approximately 0.5 gram can be detected with all gas and thermocouple lines attached.

Signal to Noise Ratio. The mass versus time trace contains some noise, especially when operating at high temperature. Some of this was traced to thermal convection currents acting on the outside of the reactor. These were reduced by appropriate baffling. In addition, steady state air flow past the reactor arising from forced ventilation of small room within which the reactor was contained caused signal noise and a steady state apparent mass shift of up to three grams. This effect was eliminated when the ventilation was stopped. Other sources of noise arise from building vibrations transmitted to the reactor through the coiled gas lines and from electrical fluctuations in the power supplies and electronic circuitry.

Example Run. An example of data taken on the hanging reactor balance is shown in figure 6. A sample of coal char derived from a Montana Rosebud coal was 62.0 percent fixed carbon, 10.3 percent volatiles, 1.2 percent moisture and the remainder nonvolatiles. Three sample injections are shown in the figure, A, B, and C. The increase in mass leading up to point A resulted from pressurization of the injector. At point A the injector was

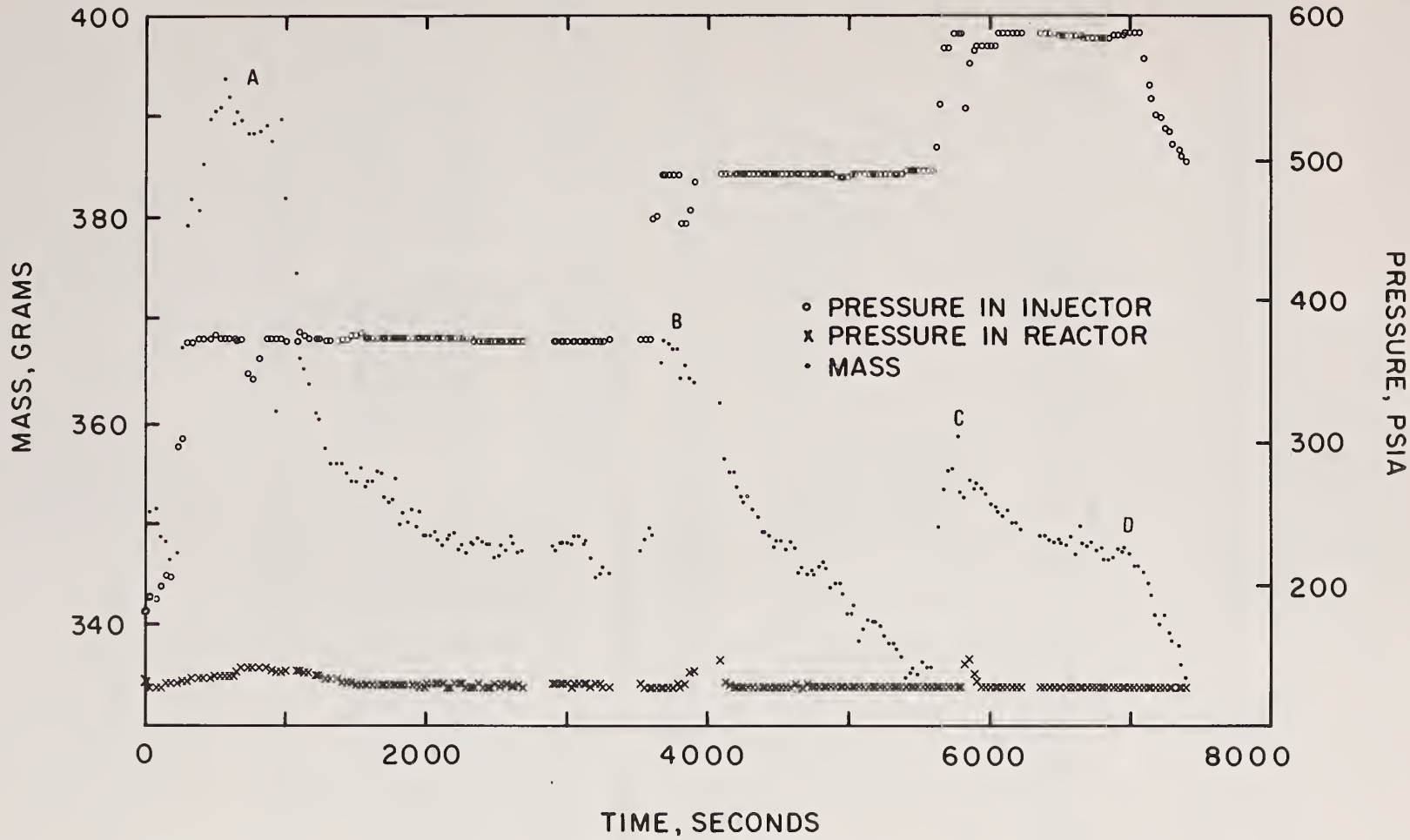

Figure 6. Gasification run of Montana rosebud char.

opened, admitting the sample to the reactor. The mass loss resulting from gasification is shown between points A and B. At point B, the injector was pressurized again, resulting in a mass increase. Additional sample was admitted to the reactor, and the mass loss was recorded between B and C. Point C reflects another pressurization and injection cycle. At D the injector was depressurized, resulting in a mass loss.

Summary. Our work thus far has not revealed any serious operational problems in the use of a hanging reactor thermobalance for kinetic studies at temperatures and pressures regimes typical of industrial processes. With recognization and correction of the major sources of error, the balance is capable of providing thermogravimetric data good to 0.1 to 1.0 percent of the full scale weight change.

The financial support of the Department of Energy under contract E(49-18) 2368 is gratefully acknowledged. The following colleagues played important roles in developing various aspects of the instrument: Dr. Robert V. Edwards, Mr. Jake Fornaro, Mr. Frank Kocjancic, Mr. Frank Kucera, Dr. J. A. Mann, Jr., Mr. Shahram Mobasser, Mr. Steve Shine, Mr. Chi-Kang Tien, and Mr. Robert Williams.

References

[1] Dobner, S., Kan, G., Graff, R. A., and Squires, A. M., Thermochimica Acta, 16, 215 (1976).

[2] Feldkirchner, H. L. and Johnson, J. L., Rev. Sci. Insti. 39, 1227 (1968).

[3] Gardner, N., Samuels, E., and Wilks, K., ACS Advances in Chemistry Series, Number 131, "Coal Gasification", 1974.

[4] Chauhan, S. P., Feldman, H. F., Stambaugh, L. E. P., and Oxley, J. N., ACS Division of Fuel Chem. Preprints, 20, 207 (1975).

[5] Li, Kun and Rogan, F. H., Thermochimica Acta, 26, 185 (1978).

[6] Forgac, J. M. and Angus, J. C., Industrial and Engineering Chemistry Fundamentals, 18, 416 (1979).

[7] Howard, J. B., MIT, private communication.

[8] Angus, J. C., Gardner, N. C., Leto, J. J., Williams, R. J., Shine, S. M., and Tien, C. K., "Study of Coal Reactivities", annual report for ERDA contract E(49-18) 2368, FE-2368-4, June 1977.

[9] Mann, Jr., J. A. and Edwards, R. V., et al., ACS Symposium Series, 57, 41 (1977).

THERMOGRAVIMETRIC MEASUREMENTS AT HIGH PRESSURES

RAPPORTEUR'S COMMENTS BY

Charles M. Guttman
National Bureau of Standards
National Measurement Laboratory
Washington, D.C. 20234

The problems of Thermogravimetry are well known if not well documented. Difficulty in interpretation of results is only overshadowed by the difficulty of various competent investigators in different laboratories to get experimental agreement on the same sample. Yet the technique is of great significance in studies of a variety of important chemical processes.

The authors review some important chemical industry processes at high pressures which are amenable to study by thermogravimetric analysis. Of particular interest was their discussion of the coal gasification problem. They then offer a brief but interesting review of previously used thermogravimetric methods.

In the section III, entitled "Limitations of Prior Thermogravimetric Techniques," they critique the previous methods offering a general listing of the some serious problems. This list deserves repeat here since almost all thermogravimetric methods suffer these limitations.

(1) The fluid mechanical regime in the immediate vicinity of the sample is difficult to control. The major part of the reactant gases bypass the sample.

(2) The reactant gases that bypass the sample make it impossible to measure meaningful product gas compositions.

(3) Temperature measurements are difficult if not impossible. One cannot introduce a thermocouple directly into the sample because it will seriously perturb the mass measurement.

(4) The introduction of the sample into the heated zone is a difficult problem with conventional thermobalance systems.

These limitations are common to almost all thermogravimetric analysis, and are often the cause of disagreements amongst investigators.

The authors try to avoid these limitations by redesigning their thermogravimetric device. In their systems the entire reaction vessel is weighed.

The design of the 300-pound thermobalance is interesting. The authors description of the testing and analysis of the response of the system too should be looked at. It is careful enough to show both the possibilities and flaws of the system.

I only wish the authors had given a more detailed analysis of a system for which the chemistry is relatively well known so we could have seen the interaction of the various instrumental effort they describe at the end of their paper.

National Bureau of Standards Special Publication 580. Proceedings of the Workshop on the State-of-the-Art of Thermal Analysis held at NBS, Gaithersburg, MD, May 21-22, 1979. (Issued May 1980)

POSTER PRESENTATIONS

The abstracts describing the poster presentations are given below. The posters were put on display early to enable participants to study them. During a scheduled part of the poster session, one of the authors was present to respond to questions.

Pilip S. Gill and J. D. Lear, E. I. Dupont de Nemours & Co., Inc., Instrument Products, Wilmington, Delaware 19898

A New Data System for Dynamic Mechanical Analysis Application

The state of the art of Dynamic Mechanical Analysis has made great advances over the past few years with the development of automated and temperature programmed instruments. The technology has continued to advance with the utilization of microcomputer techniques to permit data storage and data analysis to provide rapid calculation and reporting of the basic viscoelastic measurements.

This paper describes the use of such an automated Dynamic Mechanical Analysis System for determination of modulus, damping and tan delta properties of materials as a function of temperature. Experimental data is stored on floppy discs at maximum sensitivity in an eight million bit memory. This data can be subsequently played back or analyzed to provide quantitative values for modulus and damping in the desired parameters.

Examples of the use of this system will be described in the areas of polmer composite materials, and materials possessing damping characteristics which influence specific end use properties (examples include impact resistance and sound dampening).

K. Takamizawa and F. E. Karasz, Polymer Science & Engineering Department, University of Massachusetts, Amherst, Massachusetts 01003

Application of High Pressure DTA to Study Glass Transition Phenomena in Polystyrene under High Pressure

A high pressure DTA instrument with inside heating block type is reported which is capable of operation in the pressure range up to 700 MPa and at temperatures from 250 to 600 K. Under these conditions DTA measurements can be carried out at a wide range of heating and cooling rates. In this instrument permits measurement of small ΔT signals even with a heating block located inside the high pressure vessel.

The glass transition behavior of polystyrene under hydrostatic pressure was studied with this instrument. The change in $\Delta(\Delta T)$ could be observed for polystyrene samples as small as 8 mg at heating and cooling rates of 5 to 40 K/min. The relation between the glass transition temperature and pressure for polystyrene up to 630 MPa was determined. One characteristic feature of DTA measurements for glass transition under high pressure is that the $\Delta(\Delta T)$ signal does not decrease substantially with increasing pressure. The present DTA instrument, having dynamic features, is applicable to the study in various fields of high pressure phenomena.

P. N. Adler, R. J. DeIasi, and J. M. Papazian, Research Department, Grumman Aerospace Corp., Bethpage, New York 11714

Differential Scanning Calorimetry for Microstructural Characterization of Aluminum Alloys

Differential scanning calorimetry (DSC) and transmission electron microscopy (TEM) were used to characterize the matrix precipitate structure of the high strength and overaged tempers of three 7000 series aluminum alloys. Excellent consistency exists between the DSC results, based on the dissolution behavior of existing precipitates, and TEM observations. Each of the observed endothermic or exothermic reactions that occurred over the 20 to 500 °C temperature range was ascribed to the dissolution or formation of specific precipitates. The dissolution of each matrix phase, i.e., GP zones, η and η^1, can be characterized by a distinguishable dissolution temperature, dissolution enthalpy, activation energy, and activation entropy. The values of activation energy and activation entropy for the dissolution of the initial matrix precipitate of these phases indicate that the relative stability of the matrix precipitates is primarily influenced by the entropy rather than the energy term. Aluminum alloys 2024 and 6061 were also characterized using DSC and found to display qualitatively similar behavior.

T. P. Danaher, Perkin-Elmer Corporation, Norwalk, Connecticut 06856

The Role of Thermal Analysis in Evaluating and Characterizing Thermoplastics

The method of using analytical instrumentation to explore new development areas and to routinely characterize manufactured products has been well proven. This area of instrumentation, as can be evidenced by almost weekly news updates, is in a constant stream of improvement. Automation and data handling capabilities can be considered standard, rather than an option. The field of Thermal Analysis is certainly no exception to this increasing technological advancement.

Many of the applications of thermal analysis are so well accepted that they have become routine in laboratories. These include the determination of melting points, percent crystallinity, glass transition temperatures, blend and copolymer composition, analysis of fillers, percent purity, and the evaluation of thermal stability among many others. One especially interesting area is that of engineering thermoplastics. This area has grown tremendously in recent years, as has the role of thermal analysis in this field.

In the session, the advancements and role of thermal analysis will be discussed as an analytical tool for the dynamic, growing thermoplastics field. Particular areas of discussion will be the quality control of thermoplastics, the characterization of these plastics in the electrical and automotive fields, and an overview of the developments in instrumentation for performing the analytical tests required. Included, of course, for review, will be charts and slide reproductions of actual instrumentation scans.

J. Michael Boyle, Mettler Instrument Corporation, Hightstown, New Jersey 08520

Introduction to Simultaneous TG and DSC

Heat Flow Differential Scanning Calorimetry (DSC) and Thermogravimetry (TG) can be conducted simultaneously in the latest addition to the Mettler thermal line, TA2000C. Because it is so easy to operate, the TA2000C substantially reduces the time needed for operator training. The simplicity of this system provides other important advantages: operator mistakes are prevented and error-free operation is assured from the very beginning. At the same time, lengthy and cumbersome calibrations are eliminated. This greatly improves the reliability of analytical work. Thanks to these features, the TA2000C is particularly well suited for high quality single sample and routine analyses.

N. K. Kaushik and Shyam Kumar, Department of Chemistry, University of Delhi, Delhi-110007 India

Synthesis, Characterization, and Thermal Studies of Bis[N-(Ethyl, m-Tolyl) Dithiocarbamato] Zn(II) and Cd(II)

Bis[N-(ethyl, m-tolyl) dithiocarbamato] Zn(II) and Cd(II) have been synthesized by the reaction of sodium N-(ethyl, m-tolyl) dithiocarbamate with zinc sulphate and cadmium acetate in aqueous medium, respectively. Molecular weight, conductance and infrared studies point out that these complexes are monomeric non-electrolytes in which the dithiocarbamate ligand is bidentate. Therefore, a coordination number of four may be assigned to zinc(II) and cadmium(II) in their respective complexes. Electronic spectra of these complexes have also been obtained. Magnetic measurement of these complexes reveals their diamagnetic character.

The TG and DTG curves of these complexes have been obtained in O_2 and N_2 atmosphere. Both these complexes in N_2 atmosphere show two-step decomposition. The first decomposition step corresponds to the formation of their respective thiocyanates, whereas the second decomposition step corresponds to their respective sulphides. In O_2 atmosphere, the Zn(II) complex shows only two decomposition steps, first corresponding to the formation of cadmium thiocyanate, second to cadmium sulphate, and the third to the mixture of cadmium sulphate and oxide. Kinetic parameters such as order of reaction and activation energy have been calculated for the first step decomposition reaction in N_2 and O_2 of both complexes by employing the Coats and Redfern, as well as the Rreeman and Carroll method. It is found that the results by both methods are in good agreement.

A. M. Abdel Rehim, Mineral Technology Laboratory, Geology Department, Alexandria University, Alexandria, Egypt

Derivative Study of Sintering of Corundum with Ammonium Fluoride

The present work deals with a derivative study of the influence of ammonium fluoride on the thermal behavior of corundum using a derivatograph. Fluorination of corundum was found to take place in three distinct steps with the formation of aluminum fluoride. The products of sintering were identified microscopically and by using a Siemens Crystalloflex diffractometer. The DTA curves (using corundum and aluminum fluoride mixes of ration 1:1) indicate the formation of ammonium aluminum hexafluoride $(NH_4)_3AlF_6$ at 120 °C by endothermic reaction. The sharp endothermic peak at 150 °C may represent the decomposition of ammonium aluminum hexafluoride with the formation of ammonium aluminum tetrafluoride NH_4AlF_4. The endothermic peak at 300 °C may represent the dissociation of ammonium aluminum tetrafluoride with the formation of aluminum fluoride. These reactions are accompanied by large weight loss (TG), corresponding to the evolution of ammonia, hydrogen fluoride and water vapors.

James H. Baird
W. R. Grace & Co.
7379 Route 32
Columbia, MD 21044

William R. Bandi
U. S. Steel Research
125 Jamison Lane
Monroeville, PA 15146

James E. Bennett
Bell Telephone Laboratories, Inc.
6200 E. Broad Street
Columbus, OH 43213

David W. Brazier
Dunlop Research Centre
Sheridan Park Research Community
Mississauga, Ontario L5K 1Z8
CANADA

Ray Brown
U. S. Bureau of Mines
4900 LaSalle Road
Avondale, MD 20782

Jean C. Buck
Betz Labs, Inc.
Somerton Road
Trevose, PA 19047

Pronoy K. Chatterjee
Personal Products Company

Jen Chiu
Du Pont Co.
1007 S. Hilton Road
Wilmington, DE 19803

William E. Clark
General Motors - Delco Products
P.O. Box 230
Rochester, NY 14601

Steven Dallek
Naval Surface Weapons Center
Code R-33
White Oak
Silver Spring, MD 20910

Thomas P. Danaher
Perkin-Elmer Corp.
15 Firstfield Road
Gaithersburg, MD 21044

David Daugherty
Research Triangle Institute
P.O. Box 12194
Research Triangle Park, NC 27709

Judy F. R. Dixon
Western Electric Co., Inc.
2500 Broenig Hwy.
Dept. 8860
Baltimore, MD 21224

Herbert D. Dixon
U. S. Environmental Protection Agency
Building 048
Beltsville Agriculture Research
Center - West
Beltsville, MD 20705

David Dollimore
University of Salford
Salford
ENGLAND

Susan M. Dyszel
U. S. Customs Service
Technical Services Division
1301 Constitution Ave., N.W.
Washington, D.C. 20229

Howard Elbaum
ARRADCOM
DRADAR-QAC-E
Aberdeen Proving Ground, MD 21010

Barbara L. Fabricant
Owens-Corning Fiberglas
Technical Center
P.O. Box 415
Granville, OH 43023

Mari-Catherine Fischer
U. S. Army Meradcom
Material Tech Lab
Ft. Belvoir, VA 22060

H. E. Francis
University of Kentucky
Lexington, KY 40506

Carl R. Foltz
Armstrong Cork Co.
2500 Columbia Ave.
Lancaster, PA 17604

Joseph H. Flynn
National Bureau of Standards
Bldg. 224, Rm B318
Washington, D.C. 20234

Nelson C. Gardiner
Case Western Reserve Univ.
Cleveland, OH 44106

Paul Garn
University of Akron
Chemistry Dept.
Akron, OH 44235

Philip S. Gill
Du Pont Instrument Products
Concord Plaza/Quillen Bldg.
Wilmington, DE 19898

Augustus R. Glasgow, Jr.
EPA - Pesticides Reference
Standards Section
4116 Hamilton Street
Hyattsville, MD 20781

Susan A. Grigorian
Ford Motor Company
15000 Century Drive
Dearborn, MI 48121

Betty L. Goldman
U. S. Pharmacopeia
12601 Twinbrook Parkway
Rockville, MD 20852

John W. Goodrum
Georgia Tech
312 Hinman Bldg.
Atlanta, GA 30332

Charles M. Guttman
National Bureau of Standards
Washington, D.C. 20234

Bengt Haglund
Burns, Lobato and Adams
Sandaikab, Box 12612
Stockholm
SWEDEN

J. Walter Hamill
Smith Kline & French Labs
P.O. Box 7929
Philadelphia, PA 19101

Ileana Isern
IBM
Box 1328, Dept. 24X, Bldg. 032-001
Boco Raton, FL 33432

Masayuki Iwasaki
University of Massachusetts
Amherst, MA 01002

Bruce Johnson
E. I. Dupont
Plastic Products & Resin Dept.
E269/209
Wilmington, DE 19898

Joseph Jordan
Penn State University
University Park, PA 16802

Michael D. Judd
European Space Technology Centre
Zwarteweg 62
Noordwijk
Netherlands

Horst G. Langer
Dow Chem. Co.
Box 400
Commonwealth Road
Wayland, MA 01778

Gilbert F. Lee
Naval Surface Weapons Center
White Oak Laboratory
Silver Spring, MD 20901

S. Yen Lee
Harry Diamond Laboratories
Dept. of the Army
2800 Powder Mill Rd.
Adelphi, MD 20783

Eugene Levy
Chemical Data Systems, Inc.
R.D. #2, Box 74
Oxford, PA 19363

Bernie Lipman
Bureau of Printing &
Engraving
14th & C Streets, S.W.
Washington, D.C. 20228

Calvin M. Love
Monsanto Research Corp.
P.O. Box 32
Miamisburg, OH 45342

H. G. McAdie
Ontario Research Foundation
Sheridan Park
Mississauga, Ontario
CANADA

Warren A. McAllister
Burroughs Wellcome Co.
P.O. Box 1887
Greenville, NC 27834

M. C. McClendon
Western Electric
Richmond, VA 23231

R. A. McDonald
The Dow Chemical Co.
Thermal Research, 1707 Bldg.
Midland, MI 48640

Richard B. McGriff
Xerox Corp.
800 Phillips Road, Bldg. 139
Webster, NY 14619

Joseph Mackey
National Bureau of Standards
Washington, D.C. 20234

Patricia McMahon
Gillette Research Institute
1413 Research Blvd.
Rockville, MD 20850

Ross T. Marano
Marche Instruments, Inc.
1009 Southwood Dr.
Waco, TX 76710

Anthony L. Maurer
Owens-Corning Fiberglas Corp.
Technical Center, P.O. Box 415
Granville, OH 43023

John J. Maurer
Exxon Research & Engineering Co.
P.O. Box 45
Linden, NJ 07036

Donald S. Medrick
Anaconda Industries
Wire & Cable Div.
245 Freight Street
Waterburg, CT 06720

Oscar Menis
National Bureau of Standards
Washington, D.C. 20234

Richard E. Meyers
Bureau of Alcohol, Tobacco,
and Firearms
1401 Research Blvd.
Rockville, MD 20850

Bernard Miller
Textile Research Institute
Princeton, NJ 08540

Stephen P. Molnar
Armco, Inc.
Middletown, OH 45043

W. Charles Montgomery
E. I. DuPont de Nemours & Co.
6725 Blanche Drive
Lorton, VA 22079

K. C. Moore
University of Kentucky
Lexington, KY 40206

Cornelius B. Murphy
Xerox Corp.
42 Clarkes Crossing
Fairport, NY 14450

W. R. Ott
Rutgers Univ.
Piscataway, NJ 08854

John M. Papazian
Grumman Aerospace Corp.
ADI - 26
Bethpage, NY 11714

Arvin E. Pasto
ORNL
P.O. Box X
Oak Ridge, TN 37830

Harald Pfaffenberger
Netzsch Brothers, Inc.
119 Pickering Way
Lionsville, PA 19353

Aly Mohamed Abdel Rehim
Alexandria Univ.
Faculty of Science
18 Baliana St.
Morarram Bey, Alexandria
EGYPT

Jean Ronquerol
Centre de Thermodynamique
et de Microcalorimetrie
Marseille 13003
FRANCE

Raymond J. Shuba
Marshall R & D Laboratory
3500 Grays Ferry Ave.
Philadelphia, PA 19146

Stephen D. Skrovanek
Bethlehem Steel Corporation
Homer Research Laboratories
Bethlehem, PA 18016

L. M. Steckel
Union Carbide Corporation
Nuclear Division
P.O. Box Y, Bldg. 9995, MS 1
Oak Ridge, TN 37830

Merrion D. Spruill
E. I. du Pont de Nemours & Co., Inc.
P.O. Box 800
Kinston, NC 28501

Al Stratton
Witco Chemical Corp.
Rte 268
Petrolia, PA 16050

Kanichiro Takamizawa
Polymer Science & Engineering
Department
University of Massachusetts
Amherst, MA 01003

Stephen Teed
IBM
East Fishkill
D/339 Bldg. 300-41C
Hopewell Junction, NY 12533

Kailas D. Thakker
The United States Pharmacopeia
12601 Twinbrook Parkway
Rockville, MD 20852

Wing Tsang
National Bureau of Standards
Washington, D.C. 20234

Edith A. Turi
Allied Chemical
Corporate Research Center
P.O. Box 1021R
Morristown, NJ 07960

Nancy Ulerich
Westinghouse R&D
1310 Beulah Road
Pittsburgh, PA 15235

☆ U.S. GOVERNMENT PRINTING OFICE :1980 O—323-805

Robert B. Vetrecin
Ethicon, Inc.
Rt 22
Somerville, NJ 08876

Patrick Waldrop
Naval Weapons Station
NEDED, Cod 505
Yorktown, VA 23691

James A. Walker
National Bureau of Standards
Washington, D.C. 20234

Norman Weberg
Library of Congress
Thomas Jefferson Bldg.
Rm G1008
Washington, D.C. 20540

Wesley Wendlandt
University of Houston
Houston, TX 77004

Hans G. Wiedemann
Oriental Institute of the
University of Zurich
Zurich
SWITZERLAND

NBS-114A (REV. 9-78)

U.S. DEPT. OF COMM. BIBLIOGRAPHIC DATA SHEET	1. PUBLICATION OR REPORT NO. NBS SP 580	2. Gov't. Accession No.	3. Recipient's Accession No.

4. TITLE AND SUBTITLE

The State-of-the-Art of Thermal Analysis
Proceedings of a Workshop held at the National Bureau of Standards, Gaithersburg, MD May 21-22, 1979

5. Publication Date

August 1980

6. Performing Organization Code

7. AUTHOR(S)

Oscar Menis, Harry L. Rook and Paul D. Garn, editors

8. Performing Organ. Report No.

9. PERFORMING ORGANIZATION NAME AND ADDRESS

NATIONAL BUREAU OF STANDARDS
DEPARTMENT OF COMMERCE
WASHINGTON, DC 20234

10. Project/Task/Work Unit No.

11. Contract/Grant No.

12. SPONSORING ORGANIZATION NAME AND COMPLETE ADDRESS *(Street, City, State, ZIP)*

Same as above

13. Type of Report & Period Covered

Final

14. Sponsoring Agency Code

15. SUPPLEMENTARY NOTES

Library of Congress Catalog Card Number: 80-600099

☐ Document describes a computer program; SF-185, FIPS Software Summary, is attached.

16. ABSTRACT *(A 200-word or less factual summary of most significant information. If document includes a significant bibliography or literature survey, mention it here.)*

A workshop on the State-of-the Art of Thermal Analysis was held at the National Bureau of Standards, May 21-22, 1979. This volume contains the texts of the invited lectures with summaries by the rapporteurs. Topics covered include the variety of uses of thermal analysis in industrial processing, such as the measurement of the temperature coefficients needed for pilot plant design in the chemical industry, quality control and product testing in the rubber industry, a review of instrumental developments, descriptions of enthalpimetry, high pressure thermogravimetry using large samples, reports on polymer ignition, energy conservation in ceramic processing, industrial adsorbents, coordination compounds, and studies of ancient paper technology. Also, a poster session was provided for contributed presentation; these included a dynamic mechanical analysis system, high pressure DTA to study glass transitions, aluminum alloy microstructure, characterization of thermoplastics, and simultaneous thermogravimetry and differential scanning calorimetry. Abstracts of the poster presentations are included.

17. KEY WORDS *(six to twelve entries; alphabetical order; capitalize only the first letter of the first key word unless a proper name; separated by semicolons)*

Adsorbents; chemical processing; coordination compounds; enthalpimetry; glass processing; instrumentation; paper technology; polymer ignition; rubber processing; thermal analysis; thermogravimetry

18. AVAILABILITY

☒ Unlimited

☐ For Official Distribution. Do Not Release to NTIS

☐ Order From Sup. of Doc., U.S. Government Printing Office, Washington, DC 20402.

☐ Order From National Technical Information Service (NTIS), Springfield, VA. 22161

19. SECURITY CLASS (THIS REPORT)	21. NO. OF PRINTED PAGES
UNCLASSIFIED	265
20. SECURITY CLASS (THIS PAGE)	**22. Price**
UNCLASSIFIED	$7.00

USCOMM-DC

NBS TECHNICAL PUBLICATIONS

PERIODICALS

JOURNAL OF RESEARCH—The Journal of Research of the National Bureau of Standards reports NBS research and development in those disciplines of the physical and engineering sciences in which the Bureau is active. These include physics, chemistry, engineering, mathematics, and computer sciences. Papers cover a broad range of subjects, with major emphasis on measurement methodology and the basic technology underlying standardization. Also included from time to time are survey articles on topics closely related to the Bureau's technical and scientific programs. As a special service to subscribers each issue contains complete citations to all recent Bureau publications in both NBS and non-NBS media. Issued six times a year. Annual subscription: domestic $13; foreign $16.25. Single copy, $3 domestic; $3.75 foreign.

NOTE: The Journal was formerly published in two sections: Section A "Physics and Chemistry" and Section B "Mathematical Sciences."

DIMENSIONS/NBS—This monthly magazine is published to inform scientists, engineers, business and industry leaders, teachers, students, and consumers of the latest advances in science and technology, with primary emphasis on work at NBS. The magazine highlights and reviews such issues as energy research, fire protection, building technology, metric conversion, pollution abatement, health and safety, and consumer product performance. In addition, it reports the results of Bureau programs in measurement standards and techniques, properties of matter and materials, engineering standards and services, instrumentation, and automatic data processing. Annual subscription: domestic $11; foreign $13.75.

NONPERIODICALS

Monographs—Major contributions to the technical literature on various subjects related to the Bureau's scientific and technical activities.

Handbooks—Recommended codes of engineering and industrial practice (including safety codes) developed in cooperation with interested industries, professional organizations, and regulatory bodies.

Special Publications—Include proceedings of conferences sponsored by NBS, NBS annual reports, and other special publications appropriate to this grouping such as wall charts, pocket cards, and bibliographies.

Applied Mathematics Series—Mathematical tables, manuals, and studies of special interest to physicists, engineers, chemists, biologists, mathematicians, computer programmers, and others engaged in scientific and technical work.

National Standard Reference Data Series—Provides quantitative data on the physical and chemical properties of materials, compiled from the world's literature and critically evaluated. Developed under a worldwide program coordinated by NBS under the authority of the National Standard Data Act (Public Law 90-396).

NOTE: The principal publication outlet for the foregoing data is the Journal of Physical and Chemical Reference Data (JPCRD) published quarterly for NBS by the American Chemical Society (ACS) and the American Institute of Physics (AIP). Subscriptions, reprints, and supplements available from ACS, 1155 Sixteenth St., NW, Washington, DC 20056.

Building Science Series—Disseminates technical information developed at the Bureau on building materials, components, systems, and whole structures. The series presents research results, test methods, and performance criteria related to the structural and environmental functio ınd the durability and safety characteristics of building ele. its and systems.

Technical Notes—Studies or reports which are complete in themselves but restrictive in their treatment of a subject. Analogous to monographs but not so comprehensive in scope or definitive in treatment of the subject area. Often serve as a vehicle for final reports of work performed at NBS under the sponsorship of other government agencies.

Voluntary Product Standards—Developed under procedures published by the Department of Commerce in Part 10, Title 15, of the Code of Federal Regulations. The standards establish nationally recognized requirements for products, and provide all concerned interests with a basis for common understanding of the characteristics of the products. NBS administers this program as a supplement to the activities of the private sector standardizing organizations.

Consumer Information Series—Practical information, based on NBS research and experience, covering areas of interest to the consumer. Easily understandable language and illustrations provide useful background knowledge for shopping in today's technological marketplace.

Order the **above** *NBS publications from: Superintendent of Documents, Government Printing Office, Washington, DC 20402.*

Order the **following** *NBS publications—FIPS and NBSIR's—from the National Technical Information Services, Springfield, VA 22161.*

Federal Information Processing Standards Publications (FIPS PUB)—Publications in this series collectively constitute the Federal Information Processing Standards Register. The Register serves as the official source of information in the Federal Government regarding standards issued by NBS pursuant to the Federal Property and Administrative Services Act of 1949 as amended, Public Law 89-306 (79 Stat. 1127), and as implemented by Executive Order 11717 (38 FR 12315, dated May 11, 1973) and Part 6 of Title 15 CFR (Code of Federal Regulations).

NBS Interagency Reports (NBSIR)—A special series of interim or final reports on work performed by NBS for outside sponsors (both government and non-government). In general, initial distribution is handled by the sponsor; public distribution is by the National Technical Information Services, Springfield, VA 22161, in paper copy or microfiche form.

BIBLIOGRAPHIC SUBSCRIPTION SERVICES

The following current-awareness and literature-survey bibliographies are issued periodically by the Bureau:

Cryogenic Data Center Current Awareness Service. A literature survey issued biweekly. Annual subscription: domestic $25; foreign $30.

Liquefied Natural Gas. A literature survey issued quarterly. Annual subscription: $20.

Superconducting Devices and Materials. A literature survey issued quarterly. Annual subscription: $30. Please send subscription orders and remittances for the preceding bibliographic services to the National Bureau of Standards, Cryogenic Data Center (736) Boulder, CO 80303.

U.S. DEPARTMENT OF COMMERCE
National Bureau of Standards
Washington, D.C. 20234

OFFICIAL BUSINESS

Penalty for Private Use, $300

POSTAGE AND FEES PAID
U.S. DEPARTMENT OF COMMERCE
COM-215

SPECIAL FOURTH-CLASS RATE
BOOK